

## Nonlinear FE analysis of shear behaviour in reinforced concrete

### Modelling of shear panel tests

Master's Thesis in the International Master's Programme Structural Engineering

MANUEL MARTIN

Department of Civil and Environmental Engineering

*Division of Structural Engineering*

*Concrete Structures*

CHALMERS UNIVERSITY OF TECHNOLOGY

Göteborg, Sweden 2007

Master's Thesis 2007:46



MASTER'S THESIS 2007

# Nonlinear FE analysis of shear behaviour in reinforced concrete

Modelling of shear panel tests

Master's Thesis in the International Master's Programme Structural Engineering

MANUEL MARTIN

Department of Civil and Environmental Engineering  
*Division of Structural Engineering*  
*Concrete Structures*

CHALMERS UNIVERSITY OF TECHNOLOGY

Göteborg, Sweden 2007

Nonlinear FE analysis of shear behaviour in reinforced concrete

Modelling of shear panel tests

Master's Thesis in International Master's Programme Structural Engineering

MANUEL MARTIN

© MANUEL MARTIN 2007

Master's Thesis 2007

Department of Civil and Environmental Engineering

Division of *Structural Engineering*

Concrete Structures

Chalmers University of Technology

SE-412 96 Göteborg

Sweden

Telephone: + 46 (0)31-772 1000

Cover:

Figure 4.1, Shear stress-strain curve for the A3 model with crack pattern and shear deformation at certain stages, for detailed information; see Section 5.2.1.

Chalmers repro services / Department of Civil and Environmental Engineering  
Göteborg, Sweden 2007

## Nonlinear FE analysis of shear behaviour in reinforced concrete

### Modelling of shear panel tests

Master's Thesis in the International Master's Programme Structural Engineering

MANUEL MARTIN

Department of Civil and Environmental Engineering

Division of *Structural Engineering*

Concrete Structures

Chalmers University of Technology

### ABSTRACT

Nowadays, non-linear FE analysis can be used to prove the load carrying capacity of bridges where normal stresses and bending govern the failure modes. However, non-linear FE methods used for proving capacity of bridges governed by shear and torsion failure modes need to be verified. A project team was setup at Chalmers to investigate and to improve analysis methods to predict the shear capacity of bridges using non linear FE analysis and to establish guidelines for design and assessment of prestressed concrete bridges with respect to shear and torsion. At Chalmers, nonlinear FE analyses have been previously performed to predict and simulate shear behaviour and shear failure modes using shell elements with embedded reinforcements and tension softening property of concrete. Results were compared with experimental results such as shear panel tests conducted at University of Houston by Pang and Hsu (1992) and at University of Toronto by Vecchio and Collins (1986). In the project presented here, a detailed model of an interior unit of a shear panel was made. The model incorporated a bond-slip relationship between reinforcement and concrete, hardening of the reinforcement, tension softening property of the concrete and bending stiffness of the reinforcement. The model was loaded with a pure shear load in a deformation controlled process.

The model was built up by plane stress elements for the concrete and beam elements for reinforcement, which enabled the possibility to capture the dowel action of the reinforcement at a crack interface. Structural interface elements were used to incorporate the bond-slip phenomenon between concrete and reinforcement. At first, simple tension analysis was performed using the model to verify the proper function of the constituents of the model, such as the bond-slip phenomenon, the tension stiffening and the hardening of the reinforcement. In the shear analyses appropriate boundary conditions were applied to the model to enable the model to behave like an interior unit of a shear panel when loaded in shear. Six models were made to study the effects in shear capacity: three with symmetrical reinforcement ratio and another three with asymmetrical reinforcement ratio. The results from the FE analyses were compared with the experimental results of the shear panel tests conducted at Houston by Pang and Hsu. The results from the FE analyses corresponded well with the experimental results; it was shown that a small interior unit of a structure can be successfully modelled using appropriate boundary conditions. The results showed that the shear behaviour of reinforced concrete structures can be simulated through detailed analysis. Dowel action of reinforcement at a crack interface was captured.

Key words: shear stress, shear strain, bond-slip, dowel action, tension stiffening, loading beam system, dummy elements, boundary conditions.



# Contents

ABSTRACT	I
CONTENTS	III
PREFACE	VII
NOTATIONS	VIII
1 INTRODUCTION	1
1.1 Background	1
1.2 Purpose	1
1.3 Modelling and Evaluation	2
2 SHEAR IN REINFORCED CONCRETE STRUCTURES	3
2.1 Shear Behaviour of Reinforced Concrete	3
2.2 Shear Modes of Failure of RC member	3
2.2.1 Shear Sliding failure	4
2.2.2 Web Shear Compression failure	5
2.3 Components of Shear Resistance in Concrete structures	6
2.3.1 Shear Reinforcement	6
2.3.2 Concrete Contribution	6
2.4 Previous research conducted to investigate shear in reinforced concrete	11
2.5 Analytical models for the calculation of the shear capacity	11
2.5.1 Truss models	11
2.5.2 Models predicting the nonlinear response in shear	12
3 SHEAR PANEL TEST	20
3.1 General description of the shear panels	20
3.1.1 Measurement of the applied stress	22
3.1.2 Measurement of Strains	23
4 FINITE ELEMENT MODELLING AND ANALYSIS	24
4.1 General	24
4.2 FE Model	25
4.2.1 Geometry and mesh	25
4.2.2 Element types used for concrete	26
4.2.3 Element types used for reinforcement	28
4.2.4 Element types used for the representation of bond-slip phenomenon	31
4.2.5 Material and Physical properties	34
4.3 Verification of the model	38
4.3.1 General description	38
4.3.2 FE model for the verification analyses	39
4.3.3 Material and Physical properties	40

4.3.4	Boundary conditions	40
4.3.5	Application of prescribed deformation	40
4.3.6	Results from the verification analyses	40
4.3.7	Conclusion	48
4.4	Analyses of shear panel tests	50
4.4.1	Loading beam system	50
4.4.2	Connection between the model and the loading system	53
4.4.3	Boundary conditions for the model	54
5	RESULTS OF THE SHEAR ANALYSES	61
5.1	Calculation of shear stress and shear strain values	61
5.2	Panel A3	63
5.2.1	Crack Pattern and Shear deformation	65
5.2.2	Bond-slip relation for reinforcement L1	68
5.2.3	Moments in the reinforcement L1	69
5.2.4	Deformation of the edges of the model	72
5.3	Panel A2	73
5.3.1	Crack pattern and shear deformation	74
5.4	Panel A4	75
5.4.1	Crack pattern and shear deformation	76
5.5	Panel B2	77
5.5.1	Crack pattern and shear deformation	78
5.6	Panel B1	80
5.6.1	Crack Pattern and shear deformation	81
5.7	Panel B4	83
5.7.1	Crack pattern and shear deformation	84
6	CONCLUSION	86
6.1	General conclusion	86
6.2	Drawbacks	86
6.3	Suggestions for future work	87
7	REFERENCES	89
	APPENDIX A: TENSION ANALYSES USING LOWER ORDER ELEMENTS	91
	APPENDIX B: TENSION ANALYSES USING HIGHER ORDER ELEMENTS	106
	APPENDIX C: HAND CALCULATION FOR VERIFICATION ANALYSES	121
	APPENDIX D: BATCH FILE (*.BAT FILE) USED FOR THE GENERATION OF THE INPUT FILE.	123
	APPENDIX E: BATCH FILE (*.BAT) USED FOR THE EXTRACTION OF THE RESULTS FROM THE POSTPROCESSOR.	134
	APPENDIX F: INPUT DATA FILE (*.DAT FILE)	165
	APPENDIX G: COMMAND FILE (*.COM FILE)	192

APPENDIX H: MAT LAB FILES AND MATH CAD FILE	196
APPENDIX I: BOND – SLIP CURVE DATA	202
APPENDIX J: LOADING BEAM SYSTEM	203



## Preface

The project was done at the department of Structural Engineering, Chalmers University of Technology, Göteborg, Sweden; to satisfy the requirements to complete the International Master's program Structural Engineering successfully. The project was supervised by Tech. Lic. Helén Broo and examined by Assistant Professor. Mario Plos. The working period was from December 2006 to May 2007. The project was a part of a research work done by a team at the division of concrete structures at Chalmers to establish general guidelines for design and assessment of prestressed concrete bridges with respect to shear and torsion and to improve the nonlinear analyses methods for the structural assessment of bridges. The project was done using DIANA 9.1 FE analyses package.

I am thankful to my supervisor and examiner for their continuous supervision and guidance during the working period without which the project would have not been a success. I thank Associate Professor. Karin Lundgren for her suggestions and expertise which helped me to steer the project towards success. I also thank everyone at the Concrete division for all their suggestions and assistance.

I am grateful to my parents and sister for their unconditional love and support, without which my stay in Sweden would have not been possible. I thank my friends and colleagues who have made my stay in Sweden a pleasant memory. Last but never the least; I am grateful to my almighty for all his blessings and greatness.

Gothenburg, Sweden, May 2007

Manuel Martin

# Notations

## Roman upper case letters

$S$	First moment of area
$V_i$	Contribution from inclined compressive or tensile resultant or inclined tendon force
$E_c$	Modulus of Elasticity of concrete
$E_s$	Modulus of Elasticity of reinforcement
$E_p$	Plastic modulus
$G_f$	Fracture energy of concrete
$A_{sx}$	Cross sectional area of the longitudinal reinforcement
$A_{sy}$	Cross sectional area of the transversal reinforcement
$A_p$	Cross sectional area of prestressed steel
$V_{c,cr}$	Shear force causing web shear crack
$V$	Shear force
$N$	Axial force
$B$	Parameter taking the reinforcement ratio and concrete tensile strength into account
$I$	Moment of Inertia
$P$	Prestressing force

## Roman lower case letters

$z$	Internal lever arm
$f_{ct}$	Tensile strength of concrete
$b_w$	Breadth of web
$f_{cd}$	Design compressive strength of concrete
$f_{ck}$	Characteristic compressive strength of concrete
$s$	Spacing of reinforcement

$f_{cc}$	Peak compressive stress
$f_{cc2}$	Maximum concrete compressive stress
$f_l$	Yield stress of longitudinal reinforcement
$f_t$	Yield stress of transversal reinforcement
$d$	Depth of the beam

### **Greek letters**

$\sigma_1$	Principal tensile stress
$\sigma_2$	Principal compressive strength
$\theta$	Angle between the cracks and the reinforcement
$\varepsilon_x$	Average longitudinal strains
$\varepsilon_y$	Average transversal strains
$\varepsilon_2$	Average strain in principal compression direction
$\rho$	Density of the material
$\varepsilon_h$	upper yield strain
$\tau$	Shear stress
$\gamma$	Shear strain in micro strains
$\xi, \eta, \zeta$	Local coordinate system in an element
$\sigma_{sx}$	Strength of longitudinal reinforcement
$\sigma_{sy}$	Strength of transversal reinforcement
$\sigma_p$	Strength of prestressed steel
$\varepsilon_1$	Average principal tensile strain
$\varepsilon'_{cc}$	Strain at peak compressive stress
$\varepsilon_{sx}$	Average longitudinal strain
$\varepsilon_{sy}$	Average transversal strain
$\varepsilon_{cx}$	Average concrete strain in longitudinal direction
$\varepsilon_{cy}$	Average concrete strain in transversal direction

$\varepsilon_x$	Average strain in longitudinal direction
$\varepsilon_y$	Average strain in transversal direction
$\sigma_{c1}$	Principal tensile strain in concrete
$\sigma_{c2}$	Principal compressive strain in concrete
$\rho_x$	Reinforcement ratio in x direction
$\rho_y$	Reinforcement ratio in y direction
$\alpha$	Angle between the direction of the concrete principal compressive stress direction and direction of longitudinal steel, rotating angle
$\alpha_2$	Angle between the principal compressive stress direction and longitudinal steel direction
$\beta$	Angle between the principal compressive direction and longitudinal steel direction
$\zeta$	Softening coefficient taking the Poisson ration into account
$\varepsilon_n$	Average yield strain of steel bars embedded in concrete at the beginning of yielding
$\sigma_l$	Stress in longitudinal reinforcement
$\sigma_t$	Stress in transversal reinforcement
$\tau^c_{21}$	Shear stress in concrete in principal directions
$\varepsilon^c_1$	Strain in concrete in principal direction 1
$\varepsilon^c_2$	Strain in concrete in principal direction 2
$\tau_{lt}$	Shear stress in the structural unit
$\varepsilon_s$	Strain in reinforcement steel
$\sigma_x$	Stress in the x direction
$\sigma_y$	Stress in the y direction
$\varphi_z$	Rotational displacement about the local z axis

### Abbreviations

Lrein Elements of Longitudinal reinforcement

Trein Elements of transversal reinforcement

L1 nodes of longitudinal reinforcement 1  
L2 nodes of longitudinal reinforcement 2  
T1 nodes of transversal reinforcement 1  
T2 nodes of transversal reinforcement 2  
CLL1 concrete nodes under longitudinal reinforcement 1  
CLL2 concrete nodes under longitudinal reinforcement 2  
CTL1 concrete nodes under transversal reinforcement 1  
CTL2 concrete nodes under transversal reinforcement 2  
Ledge concrete nodes along the left edge  
Redge concrete nodes along the right edge  
Tedge concrete nodes along the top edge  
Bedge concrete nodes along bottom edge



# 1 INTRODUCTION

## 1.1 Background

In the past decades many bridges were strengthened or replaced since their reliability could not be proven based on the conventional structural assessments made. Nowadays, non-linear FE analysis can be used to prove the load carrying capacity of bridges where normal stresses and bending govern the failure. However, for many bridges the capacity is being limited due to shear and torsion. A project team has been setup at Chalmers to investigate the behaviour of prestressed concrete bridges in shear and torsion. The aim of the project is to establish general guidelines for design and assessment of prestressed concrete bridges with respect to shear and torsion and to improve the analysis methods for structural assessment of bridges.

In the non-linear FE analyses done by Broo (2007 a & b), shear behaviour and shear failure modes were simulated successfully. A secondary aim of the work was to determine the most important parameters for the modelling to enable better prediction of shear capacity. In the work, a prestressed box beam, a four point bending beam and shear panels tested at Houston and Toronto were modelled. In the models, 4-node curved shell elements with embedded reinforcement were used. For the tensile behaviour of concrete, the relation presented by Hordijk taking the fracture energy of plain concrete into account, was compared with the relationship used in Modified Compression Field Theory (MCFT); Broo (2007 a & b). The latter relationship includes the contribution from tension softening, tension stiffening, dowel action and shear friction at crack interface. It was shown that the shear capacity was predicted conservatively compared to experimental results by taking into consideration only the fracture energy of concrete. On the other hand, if the relation according to MCFT was used, the capacity was overestimated in many cases. However, if the shear contribution from phenomena such as tension stiffening, dowel action and aggregate interlock were included in the model along with the relationship based on fracture energy; the prediction of shear capacity will be better when compared with experimental results.

This necessitates a further detailed modelling technique leading to this Master's project titled '**Nonlinear FE analysis of shear behaviour in reinforced concrete**'. In the Master's project shear panels tested at University of Houston were modelled more in detail in order to improve the knowledge regarding how contributions due to tension stiffening and dowel action can be taken into account.

## 1.2 Purpose

In this master's project, the non-linear finite element method (FEM) was used to obtain a better understanding of the shear behaviour of reinforced concrete. Detailed FE models were used to study the possibilities to predict various effects influencing the shear response. Results from the FE analyses were compared with experimental results. If possible, the influence from effects such as dowel action, tension stiffening, tension softening and friction due to aggregate interlocking was to be quantified. Another objective of the study was to evaluate the possibility to perform detailed

analysis of a part of a shear panel and to determine how such a detailed cut-out can be modelled with respect to boundary conditions and loading.

From now on in this report, the master's project will be referred to as the project, and the shear panel tests conducted at University of Houston by Pang and Hsu (1992) will be referred to as the tests.

### **1.3 Modelling and Evaluation**

The main task of the project was to model shear panel tests and to perform non-linear analyses of their response. Pure shear loads were applied on the shear panels.

2D models were created based on the tests by varying the following parameters:

- Change of diameter of the reinforcements.
- Providing reinforcements of different diameter in longitudinal and transversal directions.

## 2 Shear in Reinforced Concrete Structures

### 2.1 Shear Behaviour of Reinforced Concrete

Behaviour of reinforced concrete before cracking is isotropic and stresses are carried equally by concrete domain and reinforcements. First crack appears after principal tensile stress ( $\sigma_1$ ) violated the condition  $\sigma_1 < f_{ct}$  where  $f_{ct}$  is the concrete tensile strength; after first crack has appeared stresses vary nonlinearly in the member and behaviour of the member is anisotropic. Redistribution of stresses occurs within the member between concrete domain and reinforcements to attain equilibrium. Presence of longitudinal reinforcement, transverse shear reinforcement or friction along crack plane is needed to satisfy the new equilibrium condition.

In uncracked state the maximum shear stress is at the shear centre and the shear stress is zero at the edges of the member, the bending stress varies linearly being zero at the neutral axis and maximum at edges; see Figure 2.1(a). In cracked state the shear stress and bending stress vary as shown; see Figure 2.1(b). For members subjected to shear loading cracks are inclined to the axis of the member because of inclination of principal tensile stress with longitudinal axis of the member.

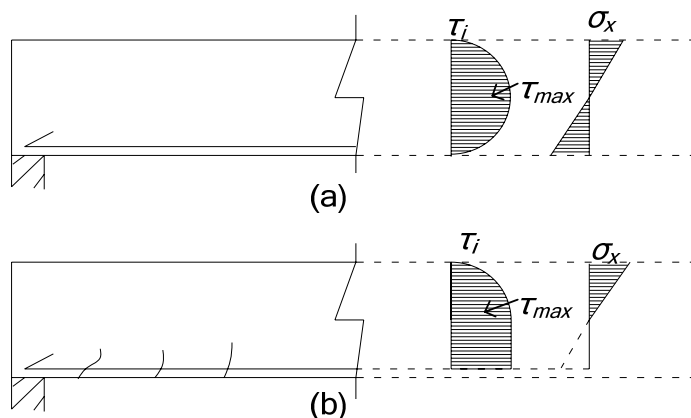


Figure 2.1 Shear stress and bending stress distribution in a cross section before and after cracking

For the members subjected to pure shear loading having isotropic physical properties i.e. same reinforcement ratio in both directions with same properties, inclination of cracks is at an angle of  $45^\circ$  to the axis of the member, this fact can be rendered to the orientation of principal tensile stress ( $\sigma_1$ ) to the axis of the member.

### 2.2 Shear Modes of Failure of RC member

Failure of a structure in shear happens in any of the following modes:

- Shear sliding failure
- Web shear compression failure

## 2.2.1 Shear Sliding failure

When a member is subjected to flexure, flexural cracks due to influence of bending stresses appear when condition for cracking is satisfied; see Figure 2.2. As the loading increases flexural cracks change orientation and incline to the axis of the member due to influence of shear stresses. A web shear crack; see Figure 2.3 appears at the shear centre i.e. the web part of a member where principal tensile stress is equal to  $f_{ct}$ . In the case of prestressed concrete members such as hollow core slabs which are not provided with transverse reinforcement a direct web shear tension failure is obtained. This type of cracking phenomenon leads to a brittle failure of the member and hence considered to be a governing shear failure mode in prestressed concrete members without shear reinforcements. Prestressed concrete members mostly have longer spans and slender webs and hence prone to risk of web shear cracks predominantly than flexural shear cracks.

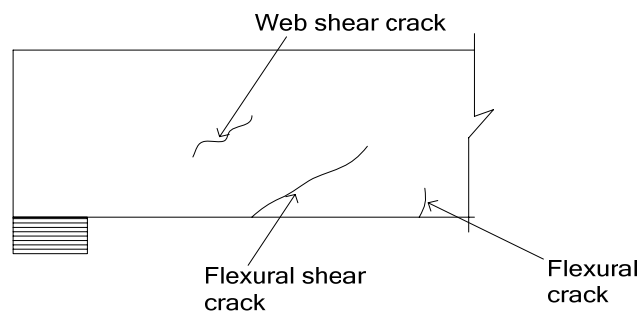


Figure 2.2 Different types of cracks

The shear force that causes a web shear crack  $V_{c,cr}$  can be calculated according to equation; Engström (2005)

$$V_{c,cr} = \frac{I \cdot b_w}{S} f_{ct} \quad (2.1)$$

The shear failure can be obtained by a sliding phenomenon along the face of the crack after the disintegration of the resistance offered especially by the aggregate interlock, dowel action and other modes of resistance; see Section 2.3. This type of failure constitutes the lower limit of the shear capacity of RC members; the failure is accompanied by sliding of the two faces along the crack plane; see Figure 2.3

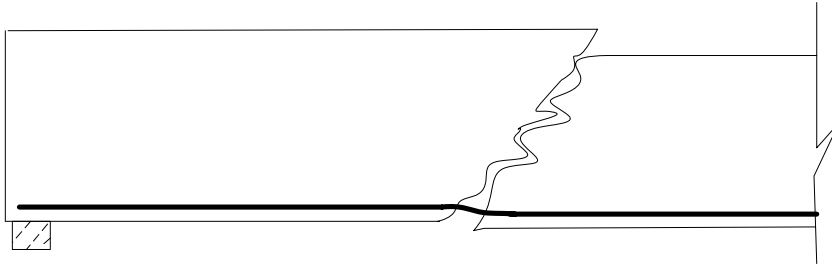


Figure 2.3 Shear sliding failure

## 2.2.2 Web Shear Compression failure

When external load is increased after cracking, to attain equilibrium principal compressive stress ( $\sigma_2$ ) increases acting along the concrete compressive struts that are between cracks, when more amount of shear reinforcements are provided compressive stress in the struts increases and leads to crushing of concrete in the struts resulting in web shear compression failure; see Figure 2.4 . This type of failure is considered as the upper limit of shear capacity of a RC member leading to following design condition in the case of vertical shear reinforcement provision; Engström (2005)

$$V_{sd} - V_i \leq \frac{1}{2} \nu \cdot f_{cd} \cdot b_w \cdot 0.9d \quad (2.2)$$

$$\nu = 0.7 - \frac{f_{ck}}{200} \text{ not smaller than } 0.5 \quad (2.3)$$

Where  $\nu \cdot f_{cd}$  is the effective compressive strength

$V_i$  is the contribution from inclined compressive or tensile resultant or inclined tendon force.

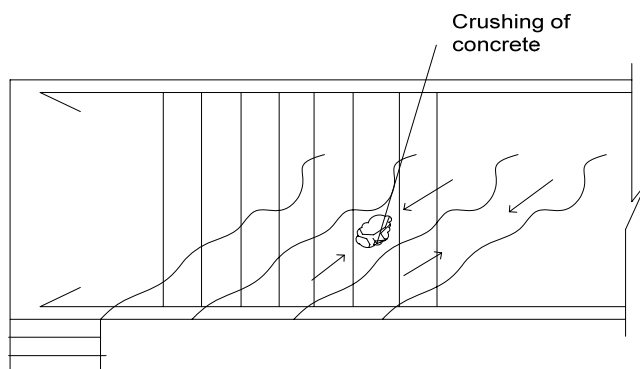


Figure 2.4 Web shear compression failure

## 2.3 Components of Shear Resistance in Concrete structures

Shear loads are resisted by the following phenomena in reinforced concrete structures

- Shear reinforcement
- Concrete contribution
  - Diagonal compressive struts between cracks
  - Dowel action of reinforcement
  - Friction due to the aggregate interlock at crack interface
  - Tension stiffening provided by reinforcement
  - Tension softening of concrete
  - Compressive zone in concrete or any external prestressing force.

At a crack location, local forces normal to the crack plane are resisted by axial stress developed in reinforcing bars at the crack plane; which is transferred to concrete between cracks through bond stress over a transfer length or bond length. The tensile stresses are entirely carried by the reinforcing bar at an open crack plane. The local forces parallel to the crack plane are resisted by the dowel action of reinforcement, and aggregate interlock.

Compressive stress developed due to aggregate interlocking at the crack plane called as dilatancy stress and stresses due to dowel action are defined along the crack plane; Soltani *et al* (2005).

### 2.3.1 Shear Reinforcement

Transverse reinforcements in a structure act as shear reinforcement preventing the failure of the member in shear after the cracking has occurred in concrete. Transverse shear reinforcements carry a major part of the shear load after cracking of the concrete domain. In the early 20<sup>th</sup> century the shear reinforcement was the part which was said to carry the entire shear load; truss models and variable inclination strut model used in EC2; CEN/TC250/SC2 (2004) provide design procedure where shear reinforcements are very important in carrying the shear load.

### 2.3.2 Concrete Contribution

#### 2.3.2.1 Diagonal compressive struts between the cracks

After the cracking, concrete is split into series of struts which act as the compressive members of the truss system to carry the shear load. The concrete struts have compressive strength lesser than the concrete cube compressive strength due to the presence of transverse splitting tensile stresses in the struts caused by the bond stress between the reinforcement and the concrete; see Figure 2.5

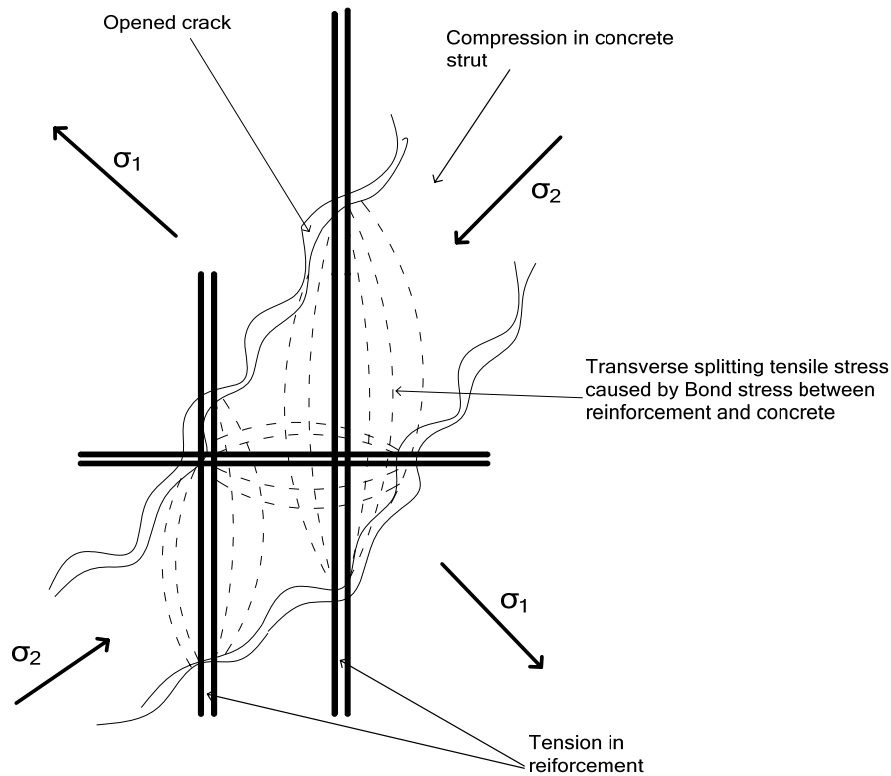


Figure 2.5 Splitting tensile stress reducing the crushing capacity of concrete strut

### 2.3.2.2 Dowel action

Dowel action of reinforcement bars is the bending of reinforcement bar at a crack plane. The dowel force in a bar is the force resisting the transversal displacement or the slipping of two segments along a crack interface, the dowel action of a rebar acts like a bridge keeping the segments of the splitted member intact. Dowel action can comprise of bending, shear or kinking of the bar; FIB (1999); see Figure 2.6.

The kinking of the bar is a phenomenon that can occur when plastic hinges have formed in the reinforcement at both the sides of a crack. This type of mechanism is possible when the member undergoes very large shear displacements only; FIB (1999). The dowel stress in longitudinal reinforcement is dependant on transverse rigidity and strength of the longitudinal reinforcement; Razaqpur *et al* (2004).

The bending of a rebar occurs at crack plane due to the difference in direction of the principal tensile stress and direction of reinforcement. The bending of reinforcement causes deterioration of the bond between rebar and concrete at vicinity of the crack leading to flaking of concrete at the side where reinforcement is oblique to the crack plane; see Figure 2.7. The flaking of concrete causes an increase in curvature of the rebar at vicinity of the cracks; Soltani *et al* (2005). Influence of the dowel action in the shear capacity can be more appreciated in RC members with less transverse reinforcement as because a greater proportion of applied shear load is resisted by the dowel action of longitudinal reinforcement; He and Kwan (2001).

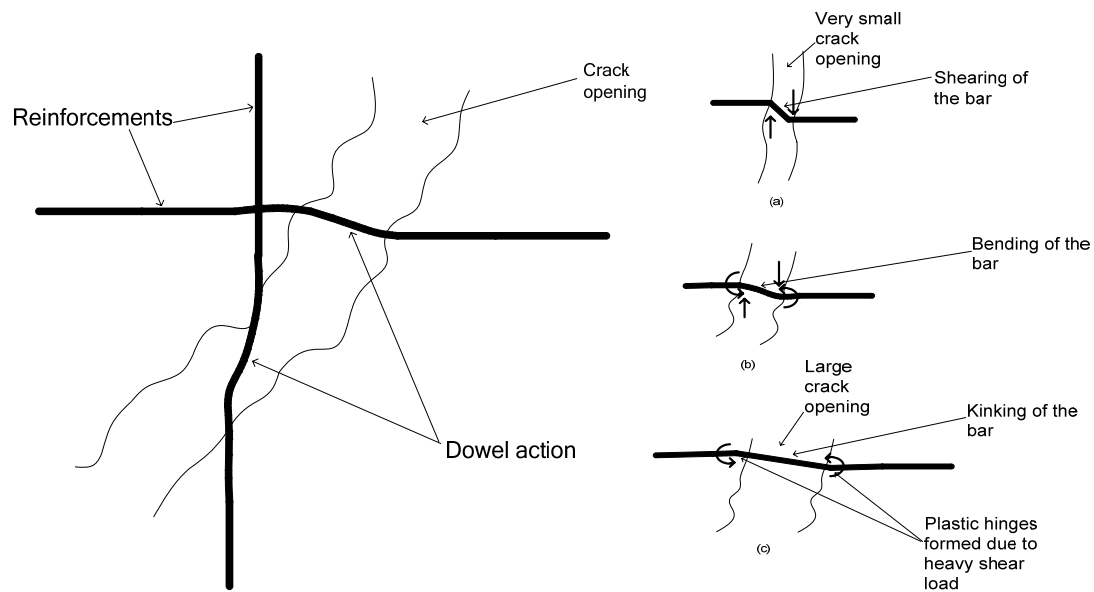


Figure 2.6 Dowel action in reinforcements at a crack opening

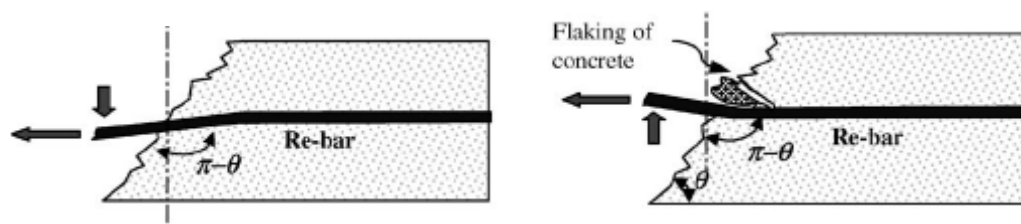


Figure 2.7 Flaking of concrete; Soltani et al (2003)

### 2.3.2.3 Friction due to the aggregate interlock

The “concrete contribution” term is comprised of friction due to aggregate interlock in majority. Roughness of a crack provides frictional resistance to external shearing action; see Figure 2.8. In the case of conventional concrete, strength of cement-sand matrix is lesser than strength of coarse aggregate thus cracks propagate in the matrix around the periphery of coarse aggregate; Pang and Hsu (1992). Frictional resistance is provided by contact points at crack plane; the developed frictional force causes a dilatation effect at crack interface as dilatancy stresses are created normal to crack plane, eventually leading to increase of crack width. When crack width increases; contribution by the aggregate interlock reduces due to loss of contact points along the rough interface of the crack. Friction due to aggregate interlock depends on maximum particle diameter, concrete strength, shear slip and crack width; FIB (1999).

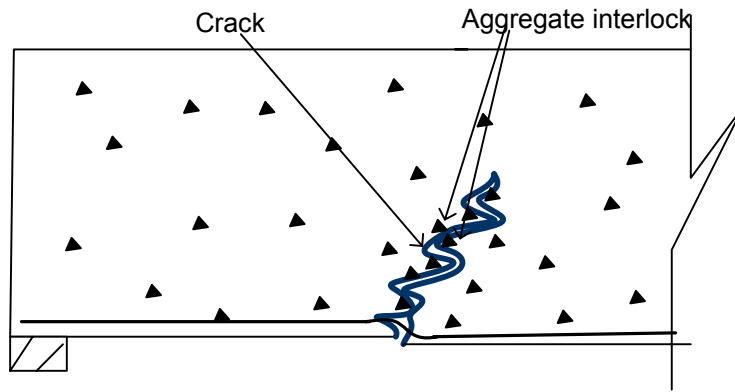


Figure 2.8 Friction due to aggregate interlock at the crack plane

### 2.3.2.4 Tension Softening of concrete

When a crack starts to localize in concrete domain a narrow band of micro cracks are formed prior to a fully developed single crack plane; see Figure 2.9. While localisation of micro cracks occur tensile stress in concrete does not drop to zero immediately as a result concrete shows a softening behaviour in tension. This phenomenon is called tension softening of concrete. Residual tensile stresses are present in cracked concrete for crack width lesser than 0.15mm; Razaqpur *et al* (2004). The contribution of tension softening to the “concrete contribution” term of the shear capacity is mainly realized in the cases of lightly reinforced concrete structures; Soltani *et al* (2003).

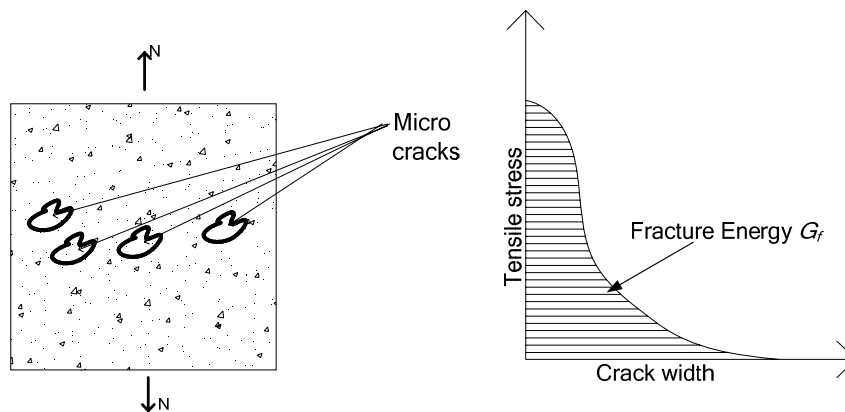


Figure 2.9 Micro cracks formed prior to fully localised crack in a concrete element in tension

### 2.3.2.5 Tension stiffening of reinforcement

The behaviour of the reinforcement embedded in the concrete is different from the bare rebar. A rebar carries entire tensile stress at a crack; away from the crack tensile stress in the rebar is transferred into concrete by development of bond stress between rebar and concrete; see Figure 2.10. After a distance called the bond length, tensile stresses are carried also by uncracked concrete and hence tensile stresses in a rebar are lower when compared with stresses in rebar at crack interface. This phenomenon is called tension stiffening. The tensile stress transfer from a rebar to concrete depends

upon cross sectional size of a rebar, type of rebar and anchorage of the rebar in concrete; Soltani *et al* (2005)

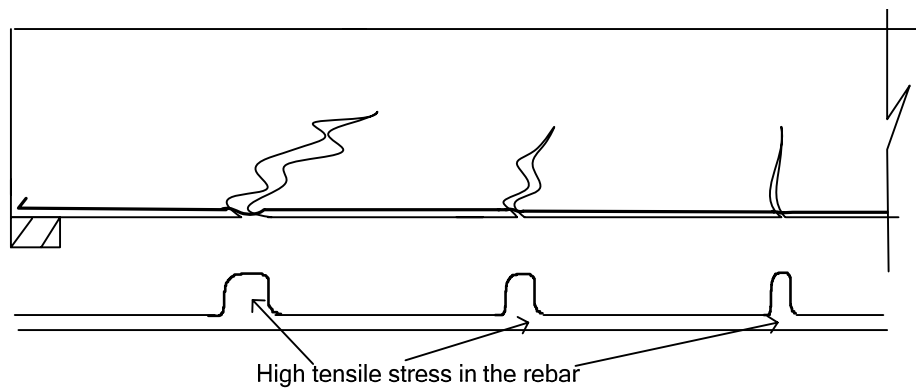


Figure 2.10 Tension stiffening effect in a reinforced concrete structure

### 2.3.2.6 External Prestressing force

The presence of prestressing force or external compressive load provides better rigidity and better shear load carrying capacity. The shear load capacity of these members can be divided into two parts; one resisted by the arch action provided by prestressing force and the other resisted by the beam action of reinforced concrete; see Figure 2.11.

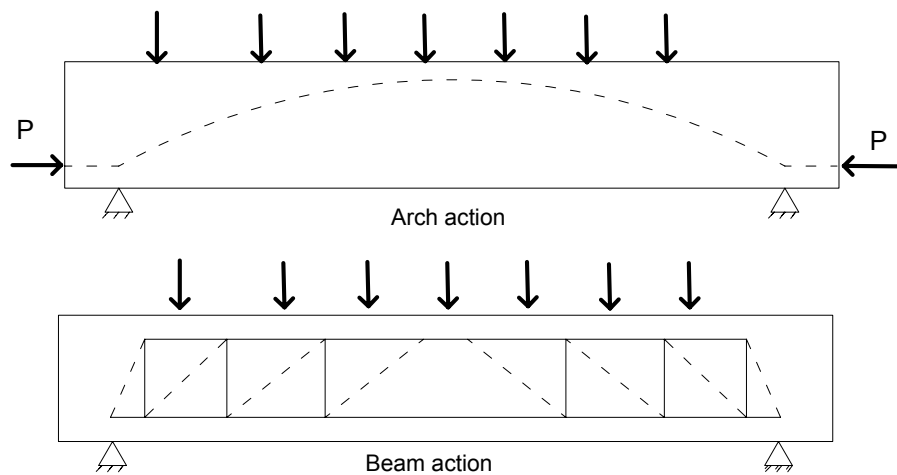


Figure 2.11 Beam and arch action in prestressed concrete structures

### 2.3.2.7 Compression in the compressive zone

The compression zone in a beam acts as a barrier preventing the easy propagation of the crack in a member and hence provides a better shear carrying capacity or delays the shear failure of the member. The crack tends to change direction due the influence of the compression field in the compressive zone; see Figure 2.12

Crack propagating in horizontal direction due to the influence of the compressive zone

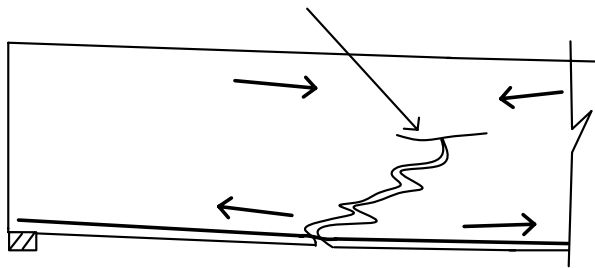


Figure 2.12 Influence of compressive zone in reinforced concrete structures

## 2.4 Previous research conducted to investigate shear in reinforced concrete

There are many research work done to investigate the shear behaviour of reinforced concrete structures. In the previous decades various types of models which can possibly depict the nonlinear response in shear of reinforced concrete were proposed. Shear panel tests conducted by Vecchio and Collins to derive the Modified Compression Field Theory (MCFT), see Section 2.5.2.2, Shear panel tests done by Pang and Hsu in Houston to derive Softened truss models such as RA-STM and FA-STM; see Section 2.5.2.3 which have the ability to predict post cracking behaviour of reinforced concrete and facilitate tracking of deformations of RC member throughout the loading process. Research is done in the field of nonlinear FE analysis of reinforced concrete to predict the behaviour of RC members close to reality; many nonlinear FE procedures were created based on smeared crack approach. Localized nonlinear procedures were also devised to predict the shear behaviour of RC members; some of these procedures facilitate the quantification of contribution of various modes of shear resistance; see Section 2.3; Soltani *et al* (2005). Empirical models predicting the shear strength of RC members were also developed using genetic programming methods; Ashour *et al* (2002). Damage models and models based on Plasticity such as Drucker-Prager material model, Mohr-Coulomb material model were also used to predict the behaviour of concrete; Broo (2006).

## 2.5 Analytical models for the calculation of the shear capacity

### 2.5.1 Truss models

In the early decades of 20<sup>th</sup> century the truss model presented by Ritter and Mörsh were used to calculate the ultimate shear capacity. According to the theory, shear force is transferred by diagonal compressive struts inclined at an angle of 45°; see Figure 2.13. Later the truss model was modified to variable inclination strut model in which inclination of compressive concrete struts are based on the minimum energy principles. The variable inclination strut model is the proposed method for calculation of the shear capacity in EC2; CEN/TC250/SC2 (2004). For the structures without shear reinforcements, shear resisted by concrete contribution such as dowel action, tension stiffening, tension softening, compressive zone and aggregate interlock are taken into account based on an empirical formula.

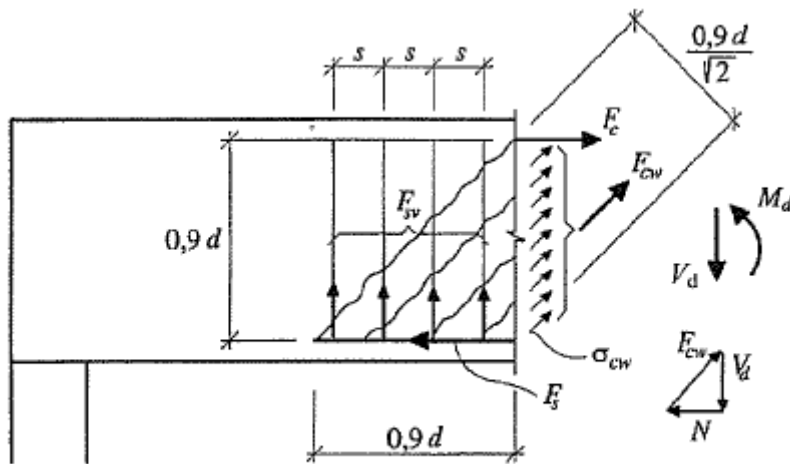


Figure 2.13 Truss model; Broo (2006)

## 2.5.2 Models predicting the nonlinear response in shear

Some of the commonly used models which are capable of predicting the nonlinear response in shear are as follows:

Compression Field Theory, CFT, (Collins)

Modified Compression Field Theory, MCFT, Vecchio and Collins (1986)

Disturbed Stress Field Theory, DSFM, Vecchio (2000b)

Cracked Membrane Model, CMM, Kaufmann and Marti (1998)

Rotating-Angle Softened Truss Model, RA-STM, Pang and Hsu (1995)

Fixed-Angle Softened Truss Model, FA-STM, Pang and Hsu (1996)

Softened Membrane Model, SMM, Hsu and Zhu (2002)

All of the above mentioned models are based on smeared crack concept and use stress equilibrium, strain compatibility and constitutive laws that link stresses to strains to predict shear force for chosen strain. In this report a brief description of some of these models is given as this is not the main task of the report.

### 2.5.2.1 Compression Field Theory, CFT

CFT, Collins and Mitchell (1991) is a smeared rotating crack model in which concrete is assumed not to carry any tensile stress after cracking occurred and shear is carried by diagonal compressive struts which are inclined at an angle  $\theta$

$$\tan^2 \theta = \frac{\varepsilon_x - \varepsilon_2}{\varepsilon_y - \varepsilon_2} \quad (2.4)$$

Where  $\varepsilon_x$  average longitudinal strains

$\varepsilon_y$  average transversal strains

$\varepsilon_2$  average strains in the principal compression direction

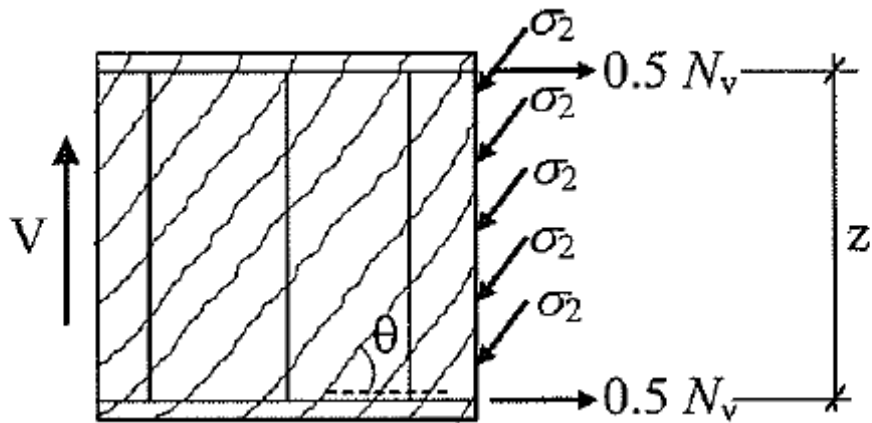


Figure 2.14 Equilibrium condition for a cracked element according to CFT, Broo (2006)

The equilibrium equations are derived from a free body diagram, see Figure 2.14

$$\sigma_2 = \frac{V}{b_w z} \left( \tan \theta + \frac{1}{\tan \theta} \right) \quad (2.5)$$

$$N_V = A_{sx} \sigma_{sx} + A_p \sigma_p = \frac{V}{\tan \theta} \quad (2.6)$$

$$\frac{A_{sv} \sigma_{sv}}{s} = \frac{V}{z} \tan \theta \quad (2.7)$$

Where  $b_w$  is the web thickness

$z$  is the internal lever arm

$A_{sx}$  and  $A_{sy}$  are the cross sectional area of the longitudinal and transversal reinforcement respectively

$A_p$  is the cross sectional area of the prestressed steel

$\sigma_{sx}$   $\sigma_{sy}$   $\sigma_p$  are the strength of the longitudinal, transversal and prestressed reinforcement respectively

$s$  is the spacing of the transversal reinforcement

The constitutive relationship of materials links stresses and strains. Uniaxial stress - strain relationship is adopted for reinforcement. A parabolic function is assumed for the stress-strain relation for cracked concrete in compression

$$\sigma_2 = f_{cc2} \left[ 2 \left( \frac{\varepsilon_2}{\varepsilon'_{cc}} \right) - \left( \frac{\varepsilon_2}{\varepsilon'_{cc}} \right)^2 \right] \quad (2.8)$$

Where  $f_{cc2}$  is the maximum concrete compressive stress which is dependent on  $\varepsilon_1$

$$\frac{f_{cc2}}{f_{cc}} = \frac{1}{0.8 + 170\varepsilon_1} \leq 1.0 \quad (2.9)$$

Where  $f_{cc}$  is the peak compressive stress

$\varepsilon'_{cc}$  is the strain of  $f_{cc}$

$\varepsilon_1$  is the principal tensile strain

In this theory tensile stresses in concrete are neglected, the model gives conservative estimates of shear capacity and overestimates deformations.

### 2.5.2.2 Modified Compression Field Theory, MCFT

The modified compression field theory MCFT by Vecchio and Collins (1986) was developed based on CFT with a modification accounting for the contribution of tensile stresses in cracked concrete. An empirical relationship between average stresses and average strains for concrete in tension is introduced.

The strain deformations between concrete and reinforcement are assumed to be identical i.e. no slip between concrete and reinforcement.

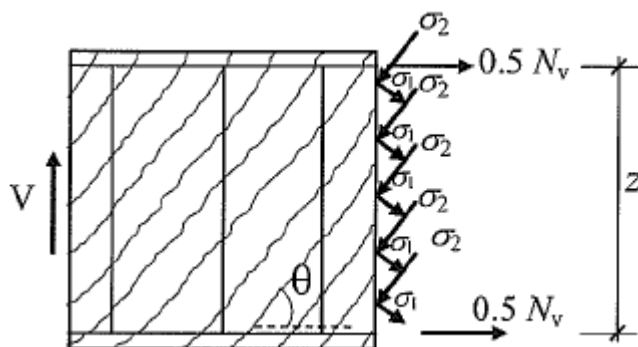


Figure 2.15 Equilibrium for a cracked element according to MCFT; Broo (2006)

The strains in longitudinal direction (x direction) are given by

$$\varepsilon_{sx} = \varepsilon_{cx} = \varepsilon_x$$

and in the transversal direction are given by

$$\varepsilon_{sy} = \varepsilon_{cy} = \varepsilon_y$$

Where  $\varepsilon_{sx}$  and  $\varepsilon_{sy}$  are the average steel strains

$\varepsilon_{cx}$  and  $\varepsilon_{cy}$  are the average concrete strains

$\varepsilon_x$  and  $\varepsilon_y$  are the average strains in the longitudinal and vertical direction respectively.

The strain compatibility relationships are obtained using the Mohr's circle

$$\gamma_{xy} = \frac{2(\varepsilon_x - \varepsilon_2)}{\tan \theta} \quad (2.10)$$

$$\varepsilon_x + \varepsilon_y = \varepsilon_1 + \varepsilon_2 \quad (2.11)$$

$$\tan^2 \theta = \frac{\varepsilon_x - \varepsilon_2}{\varepsilon_y - \varepsilon_2} = \frac{\varepsilon_1 - \varepsilon_y}{\varepsilon_y - \varepsilon_x} = \frac{\varepsilon_x - \varepsilon_2}{\varepsilon_1 - \varepsilon_x} \quad (2.12)$$

Where  $\gamma_{xy}$  is the average shear strain relative to x, y-axis

The equilibrium equations of CFT are modified to take effect of principal tensile stress into consideration.

$$\sigma_2 = \frac{V}{b_w z} \left( \tan \theta + \frac{1}{\tan \theta} \right) - \sigma_1 \quad (2.13)$$

$$N_V = A_{sx} \sigma_{sx} + A_p \sigma_p = \frac{V}{\tan \theta} - \sigma_1 b_w z \quad (2.14)$$

$$\frac{A_{sv} \sigma_{sv}}{s} = \frac{V}{z} \tan \theta - \sigma_1 b_w \quad (2.15)$$

The constitutive relationship for concrete in compression is similar as in CFT which is given by

$$\sigma_2 = f_{cc} \left[ 2 \left( \frac{\varepsilon_2}{\varepsilon'_{cc}} \right) - \left( \frac{\varepsilon_2}{\varepsilon'_{cc}} \right)^2 \right] \quad (2.16)$$

For concrete in tension relationship before cracking is linear

$$\sigma_{c1} = E_c \varepsilon_1 \quad (2.17)$$

After cracking average tensile stress  $\sigma_{c1}$  decrease with increasing values of principal concrete tensile strain,  $\varepsilon_1$ . The relationship suggested after cracking is

$$\sigma_{ct} = \frac{f_{ct}}{1 + \sqrt{500\varepsilon_1}} \quad (2.18)$$

### 2.5.2.3 Softened – Truss Models

The softened truss models were developed by Pang and Hsu (1995) based on the shear panel tests conducted at Houston. A reinforced concrete element exhibits a homogenous behaviour initially and the principal stresses in the element coincide with the external stresses. When the external principal tensile stress ( $\sigma_1$ ) reaches the tensile strength of concrete ( $f_{ct}$ ) a crack appears, on further loading concrete is separated into series of struts along the 2-direction. The angle between the direction of the cracks and the direction of the longitudinal steel ( $l$ -axis) is defined as the fixed angle ( $\alpha_2$ ). When an element is asymmetrically reinforced, the direction of the principal stresses in the concrete after cracking will deviate from the direction of the applied principal stresses. The angle between the direction of the concrete principal compressive stress ( $d$ -axis) and direction of the longitudinal steel ( $l$ -axis) is defined as the rotating angle ( $\alpha$ ). After cracking in an asymmetrically reinforced element and direction of the crack and the direction of the principal compressive stress differs; this difference enables the calculation of the shear stress along the crack plane possible; see Figure 2.16.

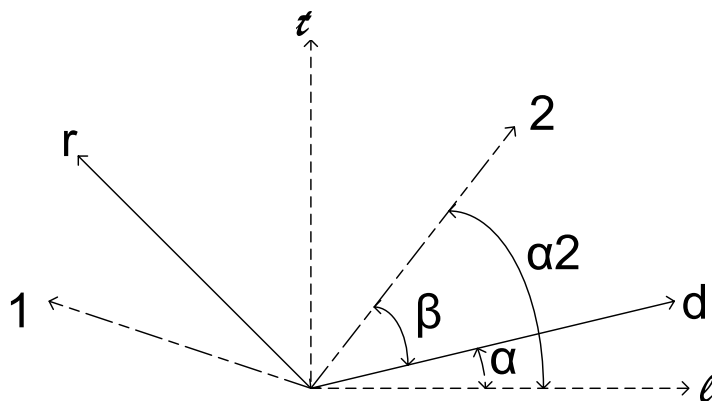


Figure 2.16 Relationship between the coordinates; (Pang and Hsu 1992)

#### Rotating-Angle Softened-Truss Model, RA-STM

RA-STM is a smeared crack rotating model developed by Pang and Hsu (1995). In this model shear stresses along crack plane are not considered. The direction of cracks is assumed to coincide with the direction of principal compressive stress after cracking. This assumption is made to simplify calculations. The model not only facilitates calculation of shear capacity but also deformations throughout the loading history can be predicted.

Shear resistance of reinforced concrete can be divided into two parts. A major part is from steel and a minor part is from concrete which is termed as ‘concrete contribution’. The ‘concrete contribution’ part primarily arises from the shear resistance along crack due to interlock and secondarily by the tension softening property of concrete. Concrete contribution due to aggregate interlock along the crack

cannot be calculated using rotating crack model as because of the assumption of crack rotation with direction of the principal compressive stress.

Equilibrium equations

$$\sigma_x = \sigma_2 \cos^2 \theta + \sigma_1 \sin^2 \theta + \rho_x \sigma_{sx} \quad (2.19)$$

$$\sigma_y = \sigma_2 \sin^2 \theta + \sigma_1 \cos^2 \theta + \rho_y \sigma_{sy} \quad (2.20)$$

$$\tau_{xy} = (\sigma_2 - \sigma_1) \sin \theta \cos \theta \quad (2.21)$$

Where  $\rho_x$  and  $\rho_y$  are the reinforcement ratios in the x and y-direction respectively.

The strain compatibility equations

$$\varepsilon_x = \varepsilon_2 \cos^2 \theta + \varepsilon_1 \sin^2 \theta \quad (2.22)$$

$$\varepsilon_y = \varepsilon_2 \sin^2 \theta + \varepsilon_1 \cos^2 \theta \quad (2.23)$$

$$\tau_{xy} = 2(\varepsilon_2 - \varepsilon_1) \sin \theta \cos \theta \quad (2.24)$$

The relations between average concrete and steel stresses and average concrete and steel strains respectively were determined through full-scale shear panel experiments, Pang and Hsu (1995).

Material constitutive laws

Concrete in compression:

$$\sigma_2 = f_{cc} \left[ 2 \left( \frac{\varepsilon_2}{\zeta \varepsilon'_c} \right) - \left( \frac{\varepsilon_2}{\zeta \varepsilon'_c} \right)^2 \right] \quad \frac{\varepsilon_2}{\zeta \varepsilon'_c} \leq 1 \quad (2.25)$$

$$\sigma_2 = f_{cc} \left[ 1 - \left( \frac{\frac{\varepsilon_2}{\zeta \varepsilon'_c} - 1}{\frac{2}{\zeta} - 1} \right)^2 \right] \quad \frac{\varepsilon_2}{\zeta \varepsilon'_c} > 1 \quad (2.26)$$

Where  $\zeta$  is a softening coefficient taking the Poisson ration into account.

Concrete in tension:

$$\sigma_1 = E_c \varepsilon_1 \quad \varepsilon_1 \leq 0.0008 \quad (2.27)$$

$$\sigma_1 = f_{ct} \left( \frac{0.0008}{\varepsilon_1} \right)^{0.4} \quad \varepsilon_1 \geq 0.0008 \quad (2.28)$$

Reinforcement steel:

$$\sigma_s = E_s \varepsilon_s \quad \varepsilon_s \leq \varepsilon_n \quad (2.29)$$

$$\sigma_s = f'_y = f_y \left[ \left[ 0.91 - 2B \right] + \left( 0.02 + 0.25B \left( \frac{\varepsilon_s}{\varepsilon_y} \right) \right) \right] \quad \varepsilon_s \geq \varepsilon_n \quad (2.30)$$

Where  $B$  is a parameter taking the reinforcement ratio and concrete tensile strength into account

$\varepsilon_n$  is the average yield strain of steel bars embedded in concrete at the beginning of yielding

### Fixed Angle Softened Truss Model, FA-STM

In this model the direction of crack is assumed to be fixed in the direction of principal compressive stress as soon as the first crack develops under the action of principal tensile stress. As the applied external stress increases the direction of principal compressive stress is said to differ from the direction of the crack, this leads to development of shear stresses along the crack. The difference between the direction of crack and principal compressive stress enables calculation of the concrete contribution due to shear resistance along the crack plane.

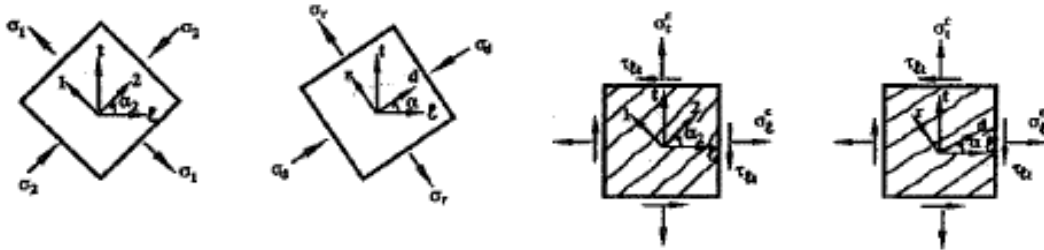


Figure 2.17 In plane stresses in reinforced concrete according to Pang and Hsu (1994)

The average shear stresses and average shear strains relationships used in this model are derived from 10 full-size reinforced concrete panel tests subjected to pure shear loading, Pang and Hsu (1994).

Stress equilibrium equations:

$$\sigma_x = \sigma_2^c \cos^2 \alpha_2 + \sigma_1^c \sin^2 \alpha_2 + \tau_{21}^c 2 \sin \alpha_2 \cos \alpha_2 + \rho_x \sigma_{sx} \quad (2.31)$$

$$\sigma_y = \sigma_2^c \sin^2 \alpha_2 + \sigma_1^c \cos^2 \alpha_2 - \tau_{21}^c 2 \sin \alpha_2 \cos \alpha_2 + \rho_y \sigma_{sy} \quad (2.32)$$

$$\tau_{xy} = (-\sigma_2^c + \sigma_1^c) \sin \alpha_2 \cos \alpha_2 + \tau_{21}^c (\cos^2 \alpha_2 - \sin^2 \alpha_2) \quad (2.33)$$

These equations relate applied stresses to internal stresses of reinforcement and concrete. The fixed angle  $\alpha_2$  is determined from applied stresses.

The strain compatibility equations:

$$\varepsilon_x = \varepsilon_2^c \cos^2 \alpha_2 + \varepsilon_1^c \sin^2 \alpha_2 + \frac{\gamma_{21}}{2} 2 \sin \alpha_2 \cos \alpha_2 \quad (2.34)$$

$$\varepsilon_y = \varepsilon_2^c \sin^2 \alpha_2 + \varepsilon_1^c \cos^2 \alpha_2 + \frac{\gamma_{21}}{2} 2 \sin \alpha_2 \cos \alpha_2 \quad (2.35)$$

$$\frac{\gamma_{xy}}{2} = (-\varepsilon_2^c + \varepsilon_1^c) \sin \alpha_2 \cos \alpha_2 + \frac{\gamma_{21}}{2} (\cos^2 \alpha_2 - \sin^2 \alpha_2) \quad (2.36)$$

Transformation of stresses and strains in cracked concrete from the non-principal 2, 1 coordinate to the x, y-coordinate requires a condition that reinforced concrete should be considered as a continuous material. Calculated stresses and strains are averaged values.

#### Material constitutive models

Material models are same as in RA-STM. In addition FA-STM takes relation between the average shear stresses and average shear strains of concrete into consideration.

Concrete in shear:

$$\tau_{21}^c = \frac{1}{2} [(\sigma_l - \rho_l f_l) - (\sigma_t - \rho_t f_t)] \sin 2\alpha_2 + \tau_{lt} \cos 2\alpha_2 \quad (2.37)$$

Where  $\sigma_l$  is the stress in the longitudinal reinforcement

$\sigma_t$  is the stress in the transverse reinforcement

$f_l$  is the yield stress of the longitudinal reinforcement

$f_t$  is the yield stress of the transverse reinforcement

$\tau_{lt}$  is shear stress in the unit

$\alpha_2$  is the angle fixed angle

## 3 Shear Panel test

### 3.1 General description of the shear panels

Shear panels are subjected to shear stresses called as membrane stresses or in-plane stresses. These types of structures which are subjected to membrane stresses can be found in the box girder bridges, cooling towers, shear walls and deep beams etc; see Figure 3.1.

Shear panels analysed in the project are based on the guidelines and properties of the shear panel tests done at Houston by Pang and Hsu (1992)

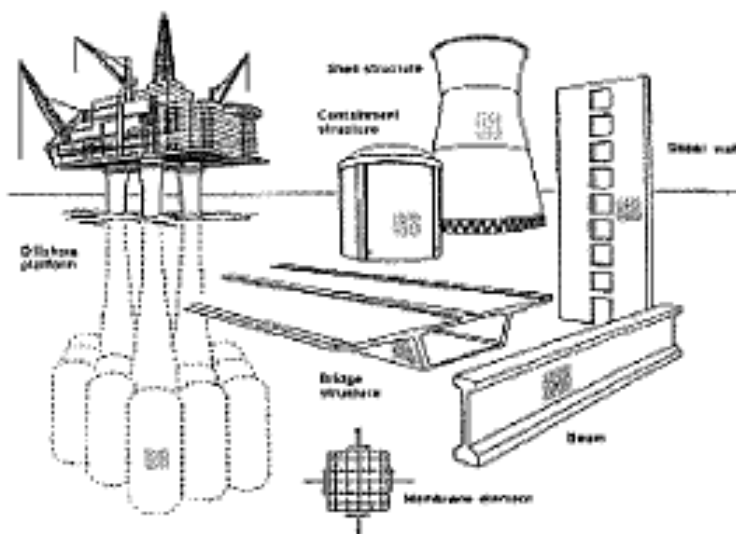


Figure 3.1 Structures subjected to membrane stresses; Vecchio and Collins (1986)

The Houston test panels were of dimensions 1.397 m by 1.397 m and of thickness 0.1778 m; see Figure 3.3. At Houston thirteen panels were tested, they were divided into three groups; group A constituted four panels provided with symmetrical reinforcements, group B constituted six panels provided with asymmetrical reinforcements and group C constituted three panels provided symmetrical reinforcements. Group A and B were subjected to proportional loading and Group C was subjected to sequential loading; see Figure 3.2. The panel tests were used to derive RA-STM and FA-STM; see Section 2.5.2.3 to predict the non-linear behaviour in shear. In this project panels A2, A3, A4, B1, B2 and B4 were analysed and results were compared with the experimental results.

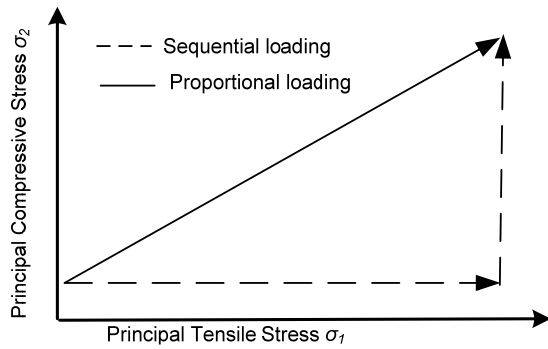


Figure 3.2 Loading types used in the shear panel tests

The reinforcements in the panel were arranged at 45° with respect to the principal loading conditions (1-2 axes); see Figure 3.3. There were two layers of reinforcements in the panel, in each layer the reinforcements were welded to shear keys or anchor units at the edges of the panel to prevent pull out or anchorage failure of the panel. The anchor units of each layer were connected to a yoke. The yoke was connected to a pair of in-plane loading jacks. 40 in-plane loading jacks were used to load the panel; see Figure 3.4. Thirty two pieces of steel plates were placed along the perimeter of the panel to reinforce the edges of the panels. Each pair of reinforcing plates on the two faces was clamped by two bolt-and-anchor devices to the connector yokes. The loads imparted by the jacks on the panel were individually monitored using load cells.

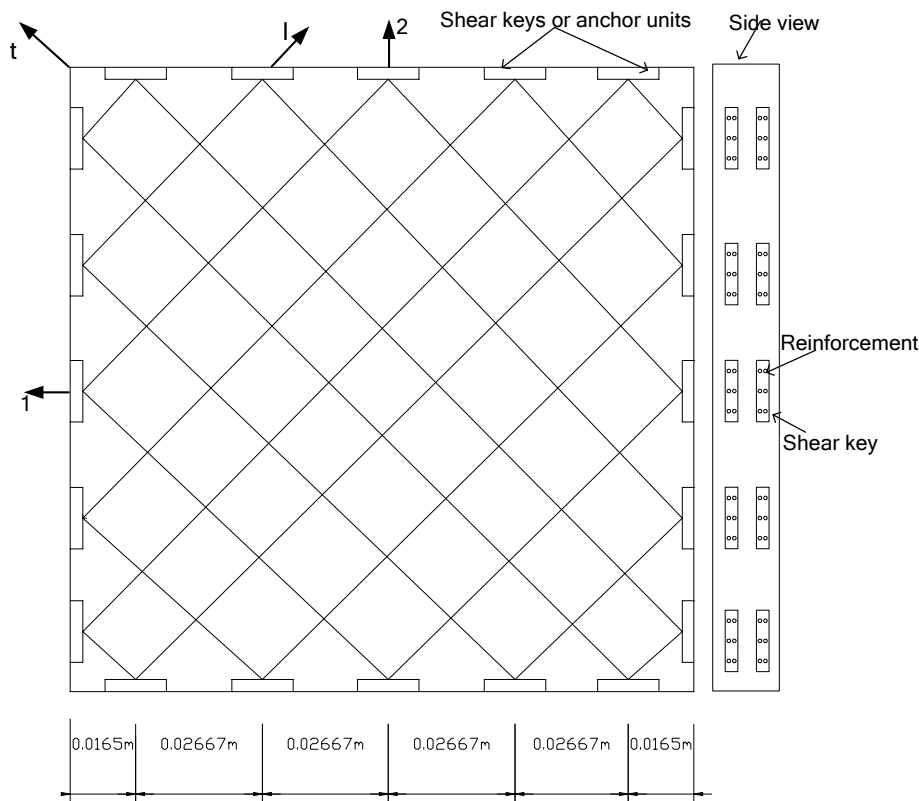


Figure 3.3 Plan view (top side) of the arrangement of the reinforcements in the shear panels

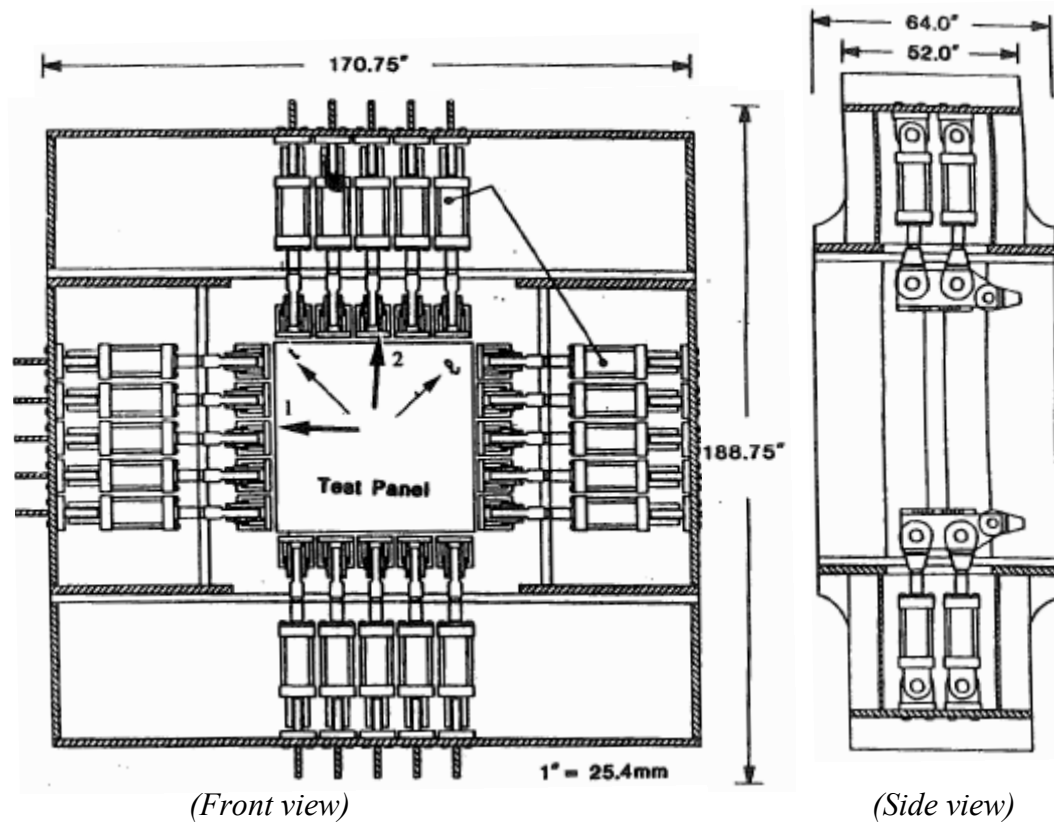


Figure 3.4 Universal panel tester; Pang and Hsu (1992)

### 3.1.1 Measurement of the applied stress

The applied principal stresses,  $\sigma_1$  in the 1-direction and  $\sigma_2$  in the 2-direction were calculated from the loads measured by the load cells; see equation 3.1

$$\begin{aligned}\sigma_1 &= \frac{P_h}{A_c} \\ \sigma_2 &= \frac{P_v}{A_c}\end{aligned}\tag{3.1}$$

Where  $P_h$  and  $P_v$  are the total applied force in the horizontal direction (1 axis) and vertical direction (2 axis) respectively

$A_c$  is the cross sectional area of the panels (1.397 m x 0.1778 m)

The applied normal stresses in  $l$  and  $t$  coordinates were calculated using principal stresses  $\sigma_1$  and  $\sigma_2$ ; see equation 3.2

$$\begin{aligned}\sigma_l &= \sigma_2 \cos^2 \alpha_2 + \sigma_1 \sin^2 \alpha_2 \\ \sigma_t &= \sigma_2 \sin^2 \alpha_2 + \sigma_1 \cos^2 \alpha_2 \\ \tau_{lt} &= (\sigma_1 - \sigma_2) \sin \alpha_2 \cos \alpha_2\end{aligned}\tag{3.2}$$

Where  $\sigma_l$  and  $\sigma_t$  are the applied normal stresses in the  $l$  and  $t$  directions respectively

$\tau_{lt}$  is the applied shear stress in the  $l-t$  coordinates

$\alpha_2$  is the angle between  $2-1$  coordinates and the  $l-t$  coordinates

### 3.1.2 Measurement of Strains

#### 3.1.2.1 LVDT

Sixteen LVDTs were mounted onto the two surfaces of the test panel, forming a "LVDT rosette". Eight LVDTs were used to measure the vertical compressive strains, four on either faces of the panel. Horizontal tensile strains of a test panel were measured using four LVDTs. The diagonal tensile strains in the longitudinal direction and in transverse directions were measured by two LVDTs on each face of the panel; see Figure 3.5

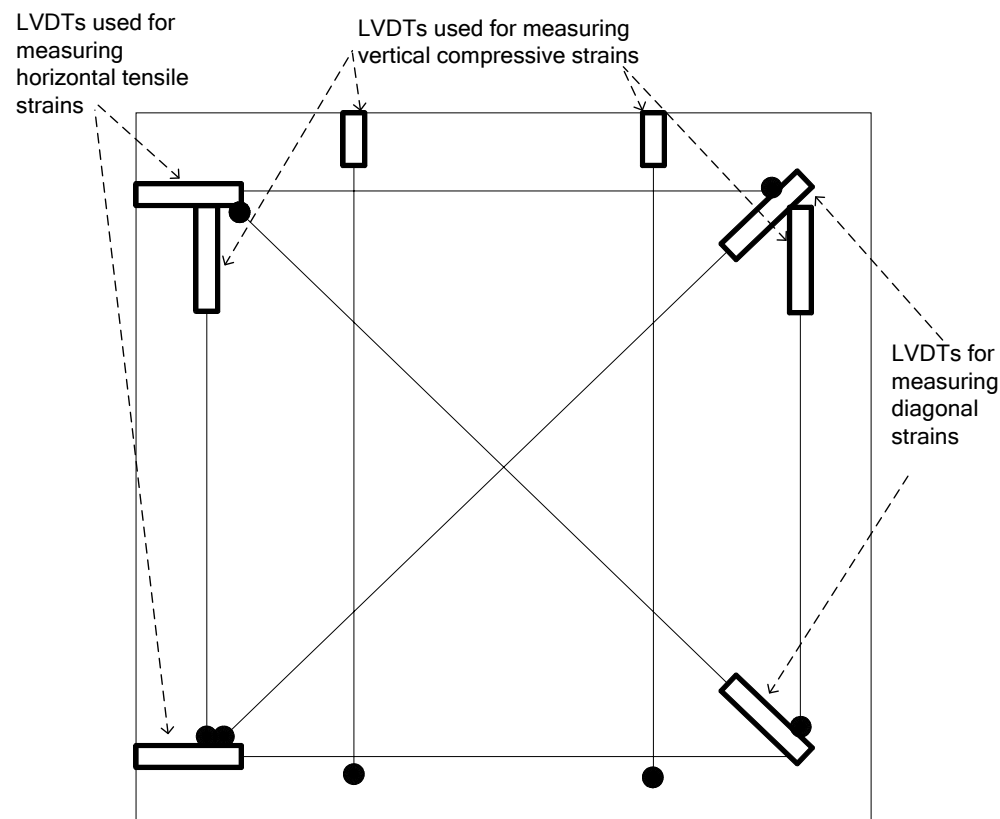


Figure 3.5 Position of LVDTs on the concrete surface (top face); Pang and Hsu (1992)

## 4 Finite Element Modelling and Analysis

### 4.1 General

The created FE model was a small interior unit; see Figure 4.2 of the experimental panel tested at Houston by Pang and Hsu (1992); see Figure 3.3. The shear panels were loaded by tension and compression in orthogonal directions and reinforcements were arranged at angle of  $45^\circ$  to the directions of application of the loads; Figure 3.3.

The FE model was loaded by pure shear load applied along the edges of the model and the reinforcements were arranged in the direction along the x and y axis; see Figure 4.2, due to symmetry half the thickness of the panel was modelled.

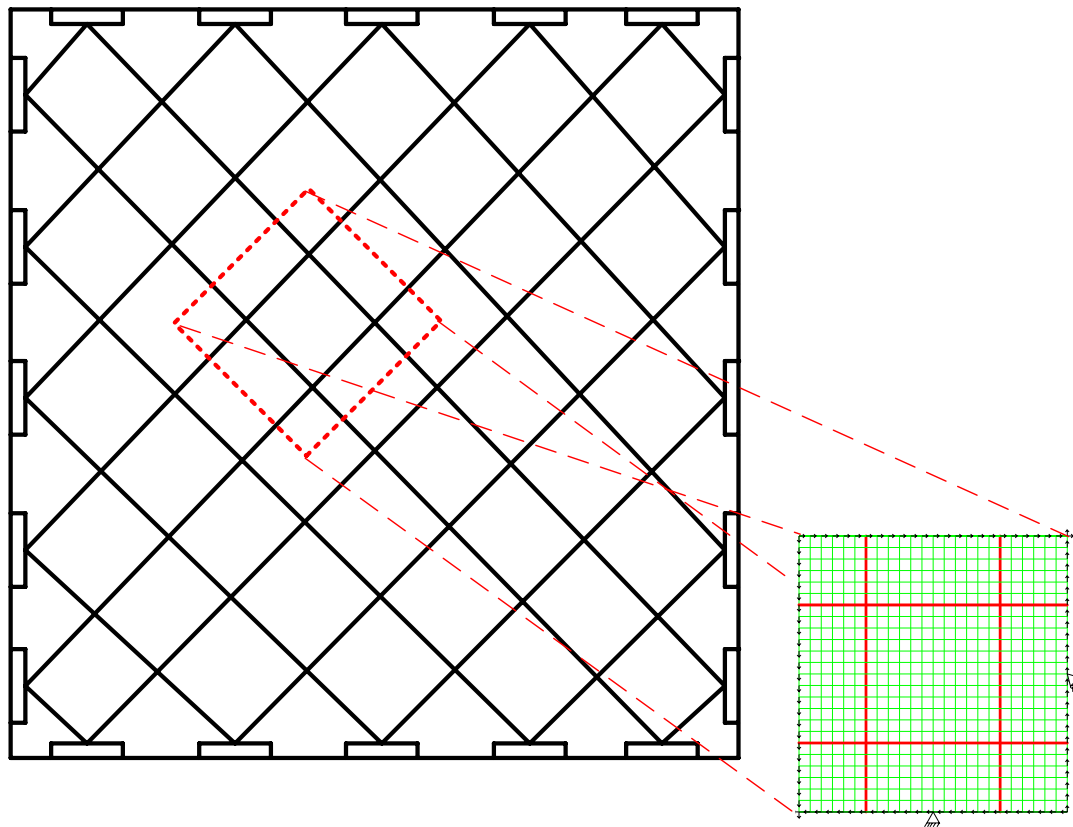


Figure 4.1 Test panel and FE model

Entire analysis was done using DIANA 9.1. The geometry was created in IDIANA pre-processor using a batch-file. The batch-file was created to incorporate easy modification to obtain new models; see Appendix D. The created batch file was called in the pre-processor using the command 'utility read batch filename' and the geometry was created and its properties were assigned. Two files were necessary to run the analyses, which are as follows

*Dat-file*: An input file containing geometrical data, physical, material and other necessary properties; see Appendix F

*Com-file*: A command file containing the commands to run non-linear analyses, specifying the execution of the load cases and commands stating which result data was to be recorded; Appendix G.

At first, the panel type A3 was created. Verification analyses were conducted with higher and lower order elements to choose a proper model for the shear analyses and to make sure the proper function of the model and its constituents such as element types, bond-slip phenomena, reinforcement behaviour etc. A proper model based on the results of the verification was chosen for the shear analyses of the panel; see Section 4.3.7. The same input file was used with required modifications to create different models for the analyses of other shear panels.

## 4.2 FE Model

2D models of shear panels were created and analysed by nonlinear FE analysis method.

### 4.2.1 Geometry and mesh

FE model was a square in geometry with a length of each side measuring 0.3772 m and thickness of the model was 0.0889 m, each element was nearly of size 15.7x15.7 mm; see Figure 4.2

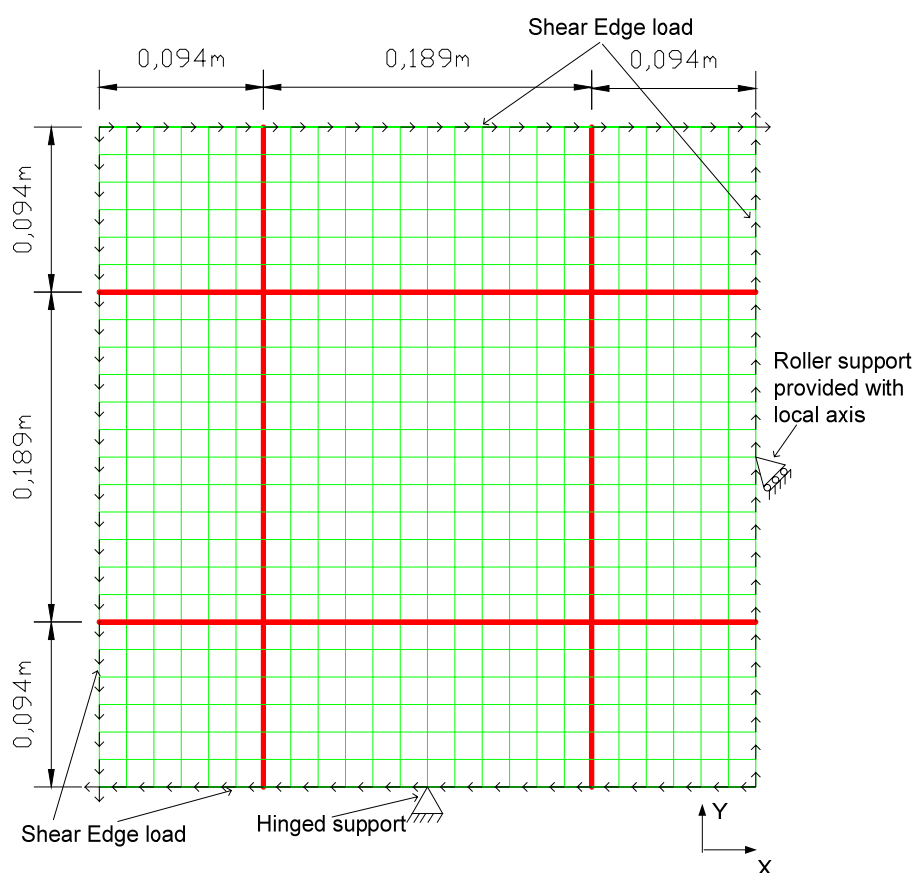


Figure 4.2 FE model

## 4.2.2 Element types used for concrete

The model was not subjected to out of plane bending and hence it is sufficient to use plane stress elements to predict the shear behaviour of the model. For the plane stress elements 2x2 gauss integration scheme was used; see Figure 4.5 and Figure 4.6.

The basic variables of the plane stress elements are  $u_x$  and  $u_y$ ; *TNO Diana manual (2005)*

$$u_e = \begin{Bmatrix} u_x \\ u_y \end{Bmatrix} \quad (4.1)$$

Where  $u_x$  is the displacement in the x direction

$u_y$  is the displacement in the y direction

The deformations of an infinitesimal part of the element; see Figure 4.3 are used by Diana to derive Green-Lagrange strains given by; see equation 4.2; *TNO Diana manual (2005)*

$$\varepsilon = \begin{Bmatrix} \varepsilon_{xx} \\ \varepsilon_{yy} \\ \varepsilon_{zz} \\ \gamma_{xy} \end{Bmatrix} \quad (4.2)$$

Where

$$\varepsilon_{xx} = \frac{\partial u_x}{\partial x}$$

$$\varepsilon_{yy} = \frac{\partial u_y}{\partial y}$$

$$\varepsilon_{zz} = \frac{\nu(\varepsilon_{xx} + \varepsilon_{yy})}{1 - \nu}$$

$$\gamma_{xy} = \frac{\partial u_x}{\partial y} + \frac{\partial u_y}{\partial x}$$

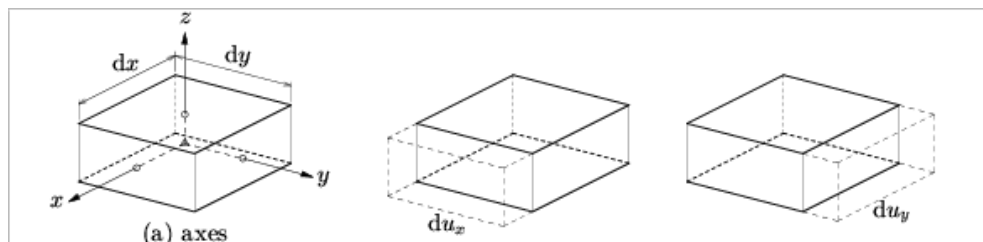


Figure 4.3 Deformations of an infinitesimal part of an element; *TNO Diana manual (2005)*

The Cauchy stresses; see equation (4.3) are derived from the basic strain equation (4.2). The positive direction of the stresses in a cubic unit is shown, Figure 4.4; tensile stress is positive; *TNO Diana manual (2005)*

$$\sigma = \begin{Bmatrix} \sigma_{xx} \\ \sigma_{yy} \\ \sigma_{zz} = 0 \\ \gamma_{xy} = \gamma_{yx} \end{Bmatrix} \quad (4.3)$$

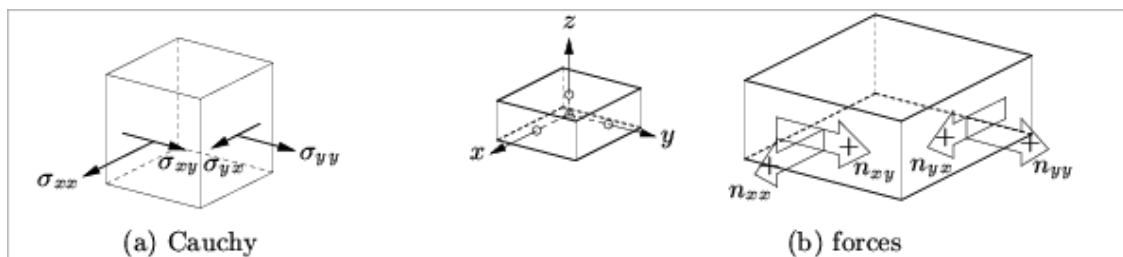


Figure 4.4 Stress in a cubic unit of a plane stress element; *TNO Diana manual (2005)*

#### 4.2.2.1 Q8MEM – 4 node plane stress element

A four node isoparametric element based on linear interpolation was used; see Figure 4.5. The polynomial for the displacements  $u_x$  and  $u_y$  is given by equation 4.4; *TNO Diana manual (2005)*

$$u_i(\varepsilon, \eta) = a_0 + a_1\varepsilon + a_2\eta + a_3\varepsilon\eta \quad (4.4)$$

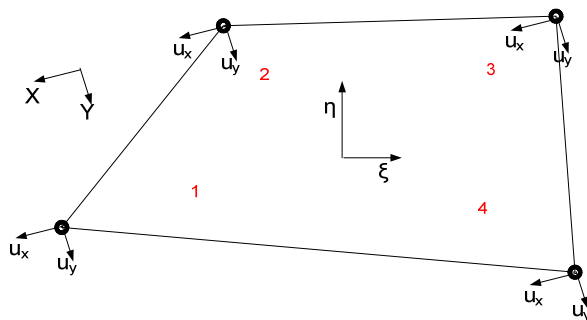


Figure 4.5 Q8MEM isoparametric plane stress element with local axes, variables and arrangement of integration points

#### 4.2.2.2 CQ16M – 8 node plane stress element

An eight node isoparametric element based on quadratic interpolation and Gauss integration; see Figure 4.6. The polynomial used for the calculation of  $u_x$  and  $u_y$  is given by equation 4.5; *TNO Diana Manual (2005)*

$$u_i(\varepsilon, \eta) = a_0 + a_1\varepsilon + a_2\eta + a_3\varepsilon\eta + a_4\varepsilon^2 + a_5\eta^2 + a_6\varepsilon^2\eta + a_7\varepsilon\eta^2 \quad (4.5)$$

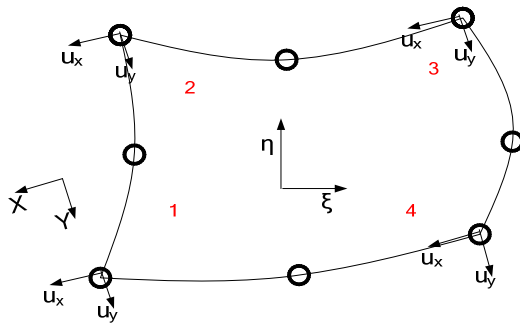


Figure 4.6 CQ16M 8 node isoparametric element with local axes, variables and arrangement of integration points

#### 4.2.3 Element types used for reinforcement

Reinforcements were modelled using beam elements in order to capture the bending of the reinforcements and dowel action phenomenon. For a two dimensional beam element, Diana calculates forces, moments and Cauchy stresses

$$N = \begin{Bmatrix} N_x \\ Q_y \end{Bmatrix} \quad (4.6)$$

$$M = M_z$$

Where  $N_x$  is the normal force in the element

$Q_y$  is the shear force in the element

$M_z$  is the moment about the local z axis

The sign convention for moment is that a positive moment yields a positive stress in the positive area; sign convention of forces is that a positive force yields positive stress; see Figure 4.7 and Figure 4.8. Positive direction of the Cauchy stresses; see Figure 4.8

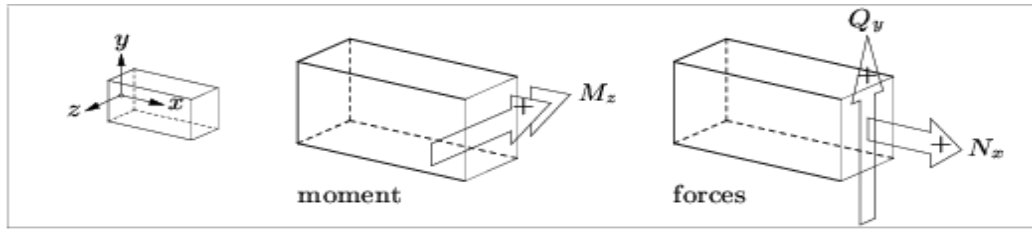


Figure 4.7 Moments and forces with positive direction for a two dimensional beam element; TNO Diana manual (2005)

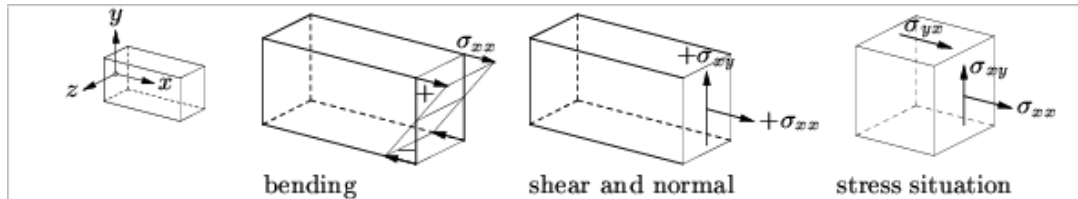


Figure 4.8 Cauchy stresses with the positive directions in a two dimensional beam element; TNO Diana manual (2005)

The variables of a two dimensional beam element  $u_x$  and  $u_y$ ; see equation 4.11 & 4.12; see Figure 4.9; TNO Diana manual (2005)

$$u_e = \begin{Bmatrix} u_x \\ u_y \\ \phi_z \end{Bmatrix} \quad (4.7)$$

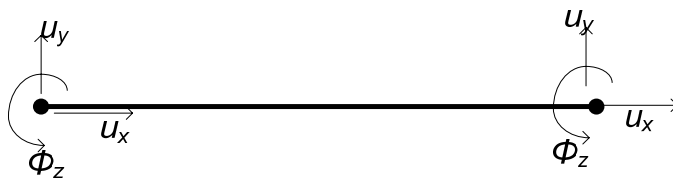


Figure 4.9 Displacements for class II two dimensional beams, L7BEN straight beam; TNO Diana manual (2005)

Diana derives the deformation of an infinitesimal element based on the displacements at the nodes; see Figure 4.9. The positive direction of the deformations; see Figure 4.10. The primary strains are the Green-Lagrange strains given by; see equation 4.8 & 4.9

$$\varepsilon = \begin{Bmatrix} \varepsilon_{xx} \\ \gamma_{xy} \end{Bmatrix} \quad (4.8)$$

Where

$$\begin{aligned}\varepsilon_{xx} &= \frac{du_x}{dx} \\ \gamma_{xy} &= \frac{du_x}{dy} + \frac{du_y}{dx}\end{aligned}\tag{4.9}$$

The primary stress are derived from the strains

$$\sigma = \begin{Bmatrix} \sigma_{xx} \\ \sigma_{xy} \end{Bmatrix}\tag{4.10}$$

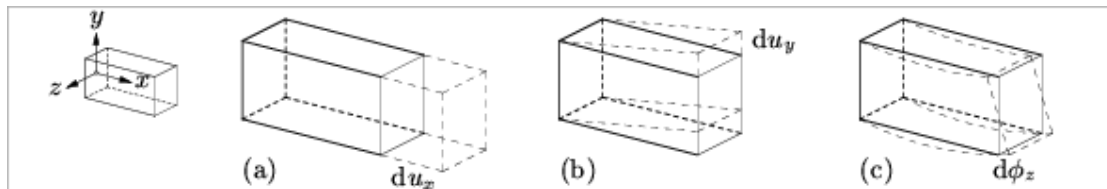


Figure 4.10 Deformations in a two dimensional beam element; TNO Diana manual (2005)

The gauss integration scheme across the cross section for a beam element; see Figure 4.11

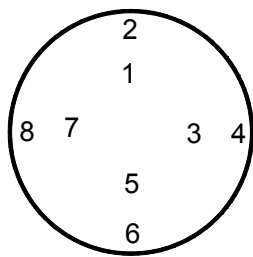


Figure 4.11 Arrangement of integration points in the cross section of the reinforcement

#### 4.2.3.1 L7BEN – straight, 2 node, 2-D beam element

The interpolation polynomials for the displacements can be expressed as; see equation 4.11; *TNO Diana manual (2005)*

$$\begin{aligned} u_x(\xi) &= a_0 + a_1\xi + a_2\xi^2 \\ u_y(\xi) &= b_0 + b_1\xi + b_2\xi^2 + b_3\xi^3 \end{aligned} \quad (4.11)$$

The positive direction of the local axis and configuration of L7BEN element is as shown; see Figure 4.12

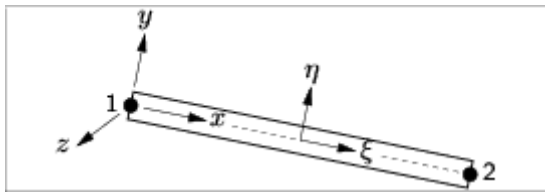


Figure 4.12 L7BEN 2-node straight beam element; *TNO Diana manual (2005)*

#### 4.2.3.2 CL9BE – curved, 3 nodes, 2-D

The interpolation polynomials for the displacements can be expressed as; see equation 4.12; *TNO Diana manual (2005)*

$$\begin{aligned} u_x(\xi) &= a_0 + a_1\xi + a_2\xi^2 \\ u_y(\xi) &= b_0 + b_1\xi + b_2\xi^2 \\ \phi_z(\xi) &= c_0 + c_1\xi + c_2\xi^2 \end{aligned} \quad (4.12)$$

The positive direction of local axis and configuration of CL9BE element is as shown; see Figure 4.13

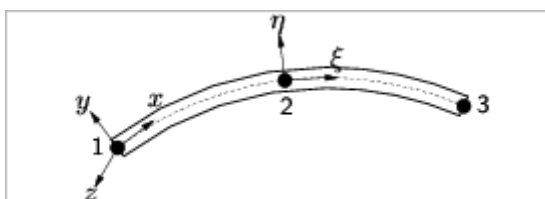


Figure 4.13 CL9BE 3-node curved beam element; *TNO Diana manual (2005)*

#### 4.2.4 Element types used for the representation of bond-slip phenomenon

The interface elements of zero area were created between concrete elements and reinforcement elements to describe the bond-slip relationship. The interface elements used in the analysis were structural interface elements.

The basic variables of structural interface elements are the nodal displacements  $\Delta u_e$ . The derived values are the relative displacements  $\Delta u$  and the tractions  $t$ ; see equation 4.13; see Figure 4.14. The output is given at the integration points. The shear traction is  $t_y$  which is tangential to the interface.

The variables of the two-dimensional structural interface elements; see equation (4.13); see Figure 4.14

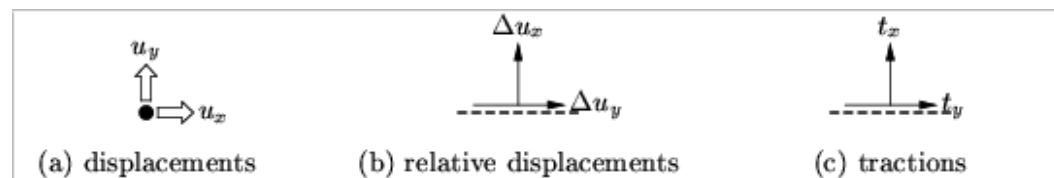


Figure 4.14 Variables of two-dimensional structural interface elements; TNO Diana manual (2005)

$$\begin{aligned}
 u_e &= \begin{Bmatrix} u_x \\ u_y \end{Bmatrix} \\
 \Delta u &= \begin{Bmatrix} \Delta u_x \\ \Delta u_y \end{Bmatrix} \\
 t &= \begin{Bmatrix} t_x \\ t_y \end{Bmatrix}
 \end{aligned} \tag{4.13}$$

#### 4.2.4.1 Slip between concrete and reinforcement

The structural interface elements had to be modified to represent the bond-slip action between reinforcement and concrete. The slip between concrete and reinforcement nodes was allowed along the direction of the reinforcement only; see Figure 4.15. Tying type known as ‘equal’ was used with translational motion along the direction orthogonal to the reinforcement axis being controlled; slip in the orthogonal direction was locked with the concrete nodes as the master and corresponding reinforcement nodes as slave.

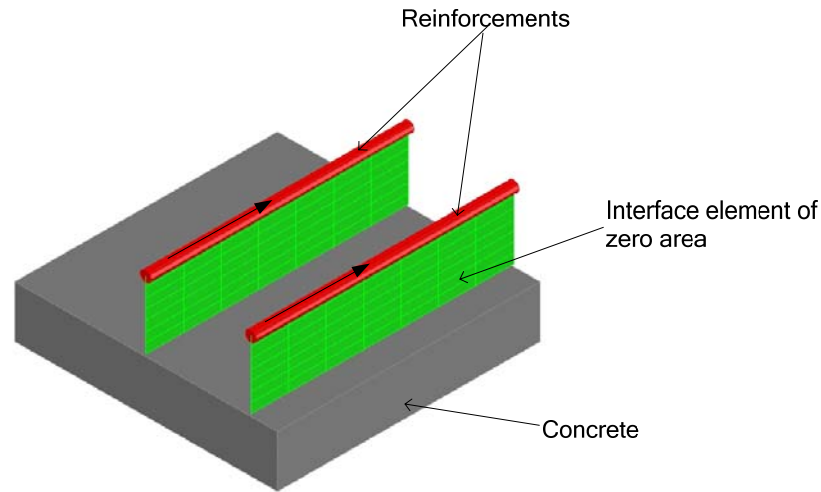


Figure 4.15 Slip between concrete and reinforcement

#### 4.2.4.2 L8IF – 2D line interface elements

The L8IF is a 2+2 node interface element used between two straight lines in a two-dimensional configuration. The element is based on linear interpolation; 3-point Newton-Cotes integration scheme is used; see Figure 4.16. Positive direction of the local axis and configuration of L8IF; see Figure 4.17

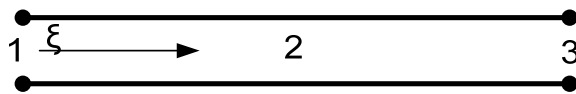


Figure 4.16 Integration scheme for L8IF structural interface element

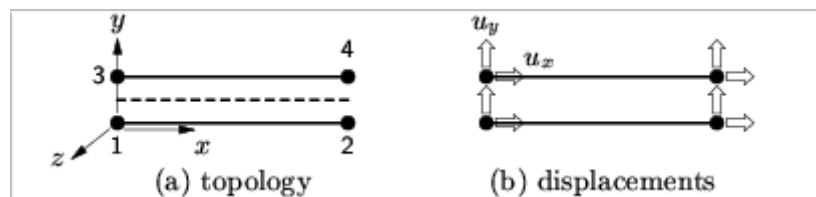


Figure 4.17 Configuration of L8IF interface element; TNO Diana manual (2005)

#### 4.2.4.3 CL12I – 2D interface elements

CL12I is a 3+3 node interface element used between two lines either straight or curved in a two dimensional configuration. The element is based on a quadratic interpolation scheme. 4 point Newton – Cotes integration scheme is used; see Figure 4.18. Positive direction of the local axis and configuration of CL12I; see Figure 4.19

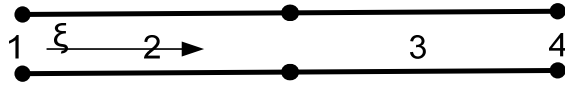


Figure 4.18 Integration scheme for CL12I structural interface element (2005)

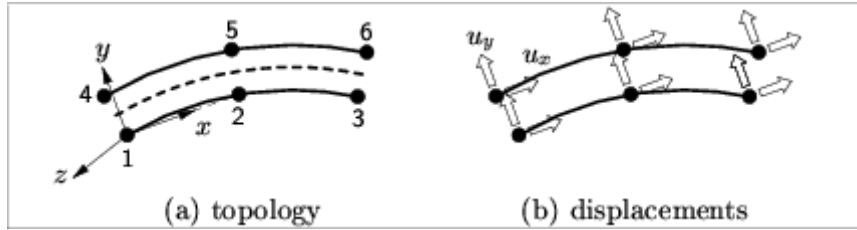


Figure 4.19 Configuration of CL12I interface element; TNO Diana manual (2005)

## 4.2.5 Material and Physical properties

### 4.2.5.1 Concrete

The material data for concrete was assigned based on the material properties of the test panels. Graded limestone aggregate of maximum aggregate size 19mm was used. Compressive strength of concrete  $f_{cm}$  reported in the shear panel tests was used to calculate  $f_{ct}$ ,  $G_f$ ,  $E$ ; CEB (1993).

$$f_{ct} = f_{ctk0,m} \left( \frac{f_{cm}}{f_{ck0} + \Delta f} \right)^{0.6} \quad (4.14)$$

Where  $f_{ct}$  tensile strength of concrete

$$f_{ctk0,m} = 1.80 \text{MPa}$$

$$f_{ck0} = 10 \text{MPa}$$

$$\Delta f = 8 \text{MPa}$$

$$G_f = G_{f0} \left( \frac{f_{cm}}{f_{cm0}} \right)^{0.7} \quad (4.15)$$

Where  $G_f$  is the fracture energy of concrete

$$G_{f0} = 0.025$$

$$f_{cm0} = 10 \text{MPa}$$

$$E_c = E_{c0} \left( \frac{f_{cm}}{f_{cm0}} \right)^{1/3} \quad (4.16)$$

Where  $E_c$  is the modulus of elasticity of concrete

$$E_{c0} = 2.15E+04 \text{ MPa}$$

Table 4.1 Material properties of concrete

Name of the model	A3	A2	A4	B1	B2	B4
Compressive strength (MPa) $f_{cm}$	41.6	41.2	42.4	45.2	44.0	44.7
Tensile strength (MPa) $f_{ct}$	2.98	2.96	3.01	3.13	3.08	3.11
Fracture energy (Nm/m <sup>2</sup> ) $G_f$	67.8	67.4	68.8	71.9	70.6	71.3
Modulus of elasticity (GPa) $E$	34.58	34.47	34.81	35.55	35.24	35.42
Poisson's ratio $\nu$	0.15					
Density (kg/m <sup>3</sup> ) $\rho$	2400					

### The constitutive model for concrete

Concrete was analysed using total strain rotating crack model. The tensile behaviour of concrete i.e. the tension property of concrete was based on the theory proposed by Hordijk *et al* (1986) for nonlinear tension softening of concrete. The compressive behaviour of concrete was modelled based on curve according to Thorenfeldt *et al* (1987). The reduction in the compressive strength of inclined struts subjected to lateral tension is taken into account by a curve based on theory proposed by Vecchio and Collins (1993). The local x axis of concrete elements was oriented in the direction of the global x axis.

#### 4.2.5.2 Reinforcement

The material and geometrical data for reinforcement was according to the panel tests; see Table 4.2, Table 4.3 and Figure 4.20 . Reinforcements used in the panel test were from Stelco steel company, Canada. The reinforcements were low-alloy grade 60 deformed rebars in accordance with ASTM A706; Pang and Hsu (1990)

*Table 4.2 Diameter of reinforcements in the test panels*

Name of the panel	<b>A3</b>	<b>A2</b>	<b>A4</b>	<b>B1</b>	<b>B2</b>	<b>B4</b>
Diameter of longitudinal reinforcement (mm)	20	15	25	15	20	25
Diameter of transverse reinforcement (mm)	20	15	25	10	15	10

*Table 4.3 Material properties of reinforcement of shear panel tests*

Diameter of the Rebar	$E_s$ (GPa)	$f_y$ (MPa)	$\epsilon_y$	$\epsilon_h$	$E_p$ (GPa)	$f_{0.05}$ (Mpa)
10	181.21	444.47	0.0044	::	2.69	578.76
15	192.23	462.32	0.0024	0.0144	3.73	609.08
20	199.81	446.13	0.0022	0.0111	4.60	624.92
25	200.50	469.42	0.0023	0.0073	3.76	629.06

The density of the reinforcements was 7800 Kg/m<sup>3</sup>. The constitutive model for reinforcements was based on the Von Mises yield theory, strain hardening of reinforcement was assigned as material property for the reinforcements; see Appendix H for the mat lab code for the strain hardening input values.

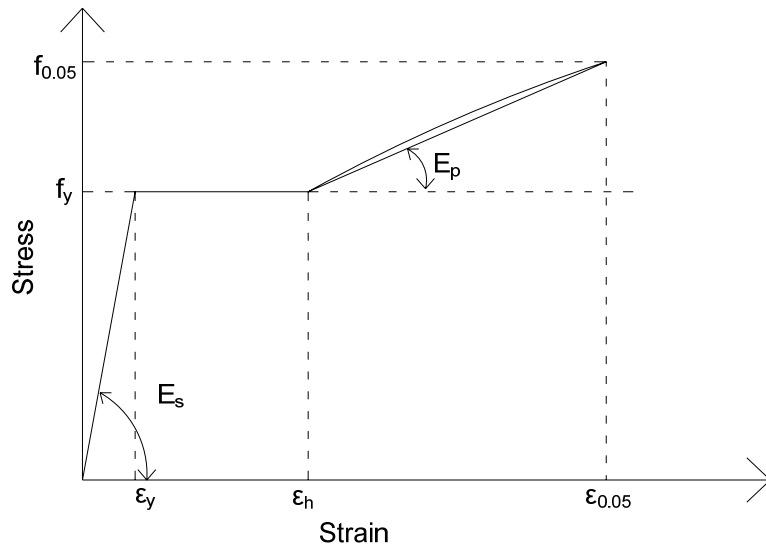


Figure 4.20 Stress strain curve for reinforcement

#### 4.2.5.3 Bond-slip between concrete and reinforcement

The FE model was created with bond slip interaction between reinforcement and concrete. The bond-slip curve for good bond conditions; CEB (1993) was adopted. The circumference of the rebar was assigned as the thickness of the interface elements; see Table 4.4. Bond-slip data for Confined good bond condition was used in the models; see Figure 4.21.

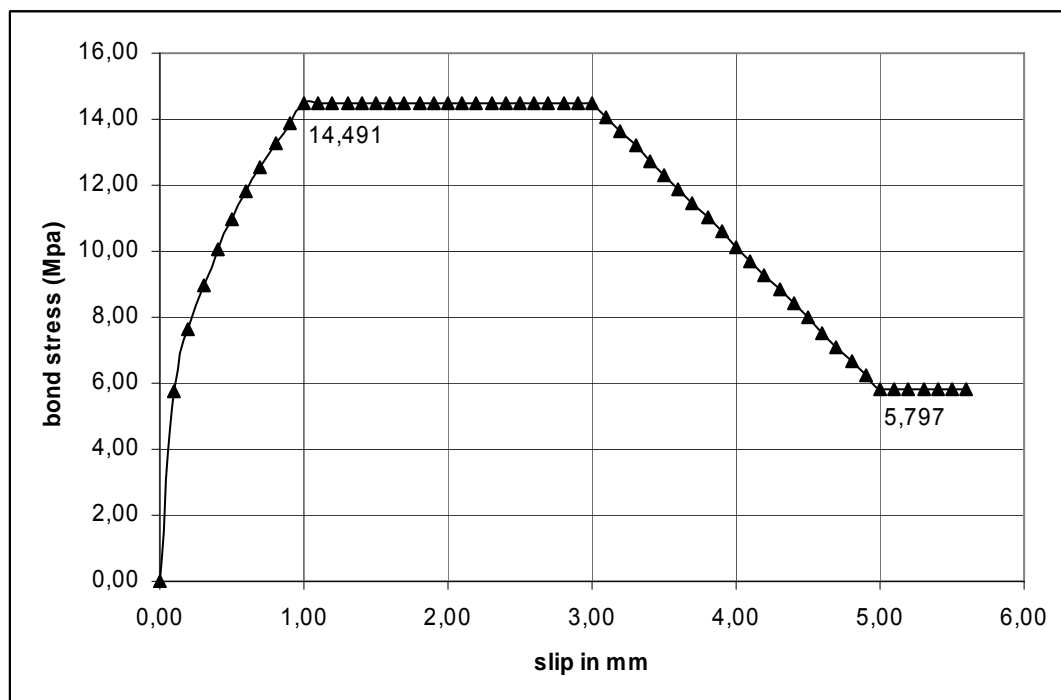


Figure 4.21 Bond-slip curve for Confined good bond conditions

Table 4.4 Thickness of the interface elements

Name of the panel	A3	A2	A4	B1	B2	B4
Thickness of the interface elements in longitudinal direction (*10 <sup>-2</sup> m)	6.283	4.712	7.854	4.712	6.283	7.854
Thickness of the interface elements in transversal direction (*10 <sup>-2</sup> m)	6.283	4.712	7.854	3.142	4.712	3.142

## 4.3 Verification of the model

### 4.3.1 General description

Verification of the model was necessary to confirm the proper function of the model and its constituents such as response of interface elements with bond-slip relationship as an input, hardening phenomenon of the reinforcements etc. Verification of the model was also performed to compare two different types of models one with elements of lower order and another with higher order elements, to find out an appropriate model, which could perform the shear analysis with better accuracy and lower computational time.

The following were the different types of analyses performed:

**Type 1:** Model with lower order elements

**Type 2:** Model with higher order elements

The models had same number of elements and hence the number of nodes in the type 2 models was twice the number of nodes in the type1 models.

The created models were verified by performing a pure tension analyses which was chosen because of its simplicity. Tension analyses were performed by deformation control process. In reality a tested specimen has a weaker part at which micro crack initiates and starts to propagate slowly and finally develops into a full crack when localisation is complete; to consider this in the model, a concrete element was weakened about 10% of the original strength. This was also done to prevent cracking of all elements at one step when the model was loaded. A concrete element at the centre was weakened due to its position being in the middle of the model and hence the forced equilibrium caused due to weakening of the element is symmetrical.

The decision to weaken an element at intersection of reinforcement was made since available concrete area is much lesser at this region compared to any other region.

Also a higher force is transferred from reinforcement to concrete at an intersection through the bond stress when compared to an element at the centre of the panel.

In the two types of models few changes were made to incorporate the following different models

**Type a:** A weakened concrete element at the centre of the model; see Figure 4.22

**Type b:** A weakened concrete element at a point of intersection between the longitudinal and transverse reinforcement; see Figure 4.22

**Type c:** No concrete element weakened

The same FE model was used for each analysis but with minor modifications to suit each case. In this section each analysis is referred by the above numbering; for example type1a, type2a, type1c etc. Results of the analyses were verified with the simple hand calculations; see Appendix C.

### 4.3.2 FE model for the verification analyses

The FE model for the verification; see Figure 4.22 was similar to the model used for shear analyses of panels; see Figure 4.2 but with minor modifications in the model such as boundary conditions and load application. In this section the reinforcements will be referred according to their names; see Figure 4.22

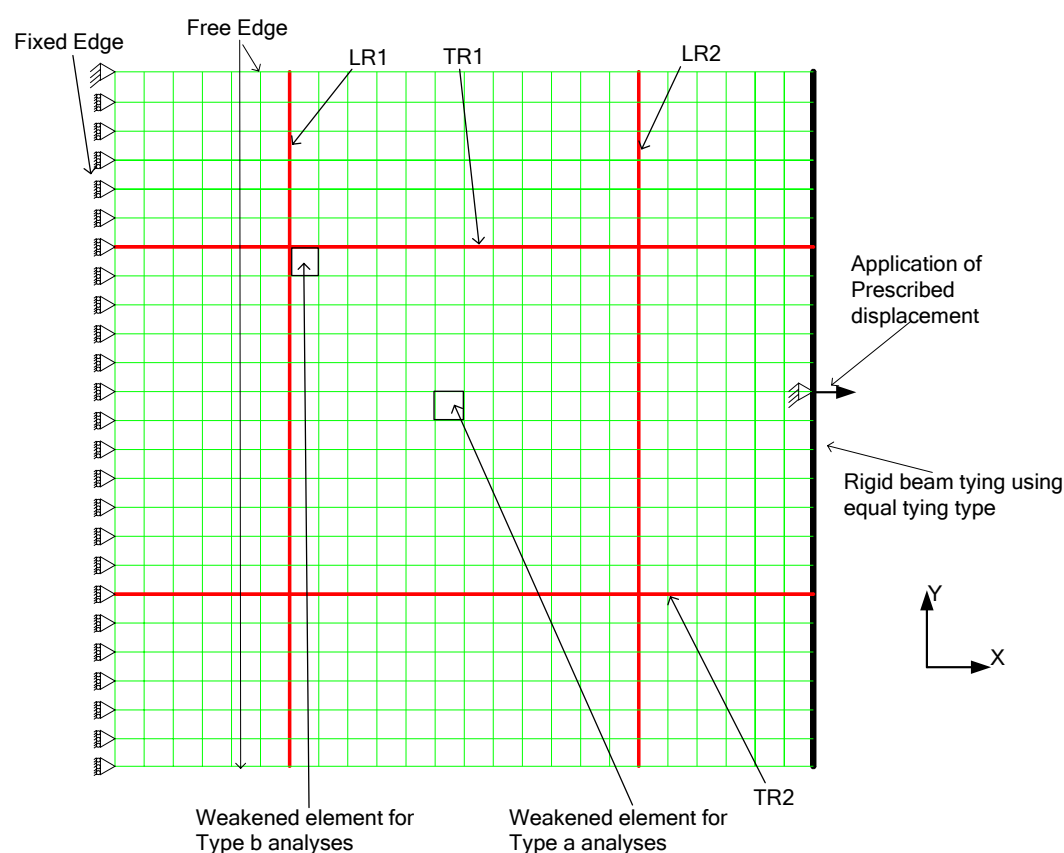


Figure 4.22 FE model for the verification analyses

### **4.3.3 Material and Physical properties**

The material properties and physical properties were the same as the ones used for the A3 panel; see Section 4.2.5

### **4.3.4 Boundary conditions**

The nodes along the left edge were restrained in the direction of application of prescribed deformation and top left corner node was restrained in all directions to prevent rotation of the model; see Figure 4.22

### **4.3.5 Application of prescribed deformation**

The magnitude of prescribed deformation was 0.01 mm per step and total deformation of 6 mm was applied. The deformation was applied at centre node of the right edge. A rigid beam tying was created using the equal tying type along the right edge with centre node being the master node to ensure uniform displacement of right edge of the model.

### **4.3.6 Results from the verification analyses**

All the models behaved similarly but with minor differences at first cracking stage. Before the initiation of micro cracks all the models followed the path of the stage I curve which is the stiffness of plain concrete. After cracking, tension stiffening effect was clearly observed in the models; stiffness of the models after cracking became lesser and lesser due to formation of more cracks and finally before yielding adopted the stiffness of the stage II curve. Crack was initiated at prescribed deformation value of 0.03 mm and the yielding of steel occurred at 0.84 mm in all the models; see Figure 4.23, which were corresponding well with the hand calculations; see Appendix C. Activation of the reinforcements after the occurrence of the first crack was clearly observed, see Figure 4.23 . Based on the results from the verification analyses, a model made of 4 node plane stress elements for concrete with no element weakened and loaded by deformation controlled process was finally suggested for the shear analyses of the panels; see Section 4.3.7 for further understanding.

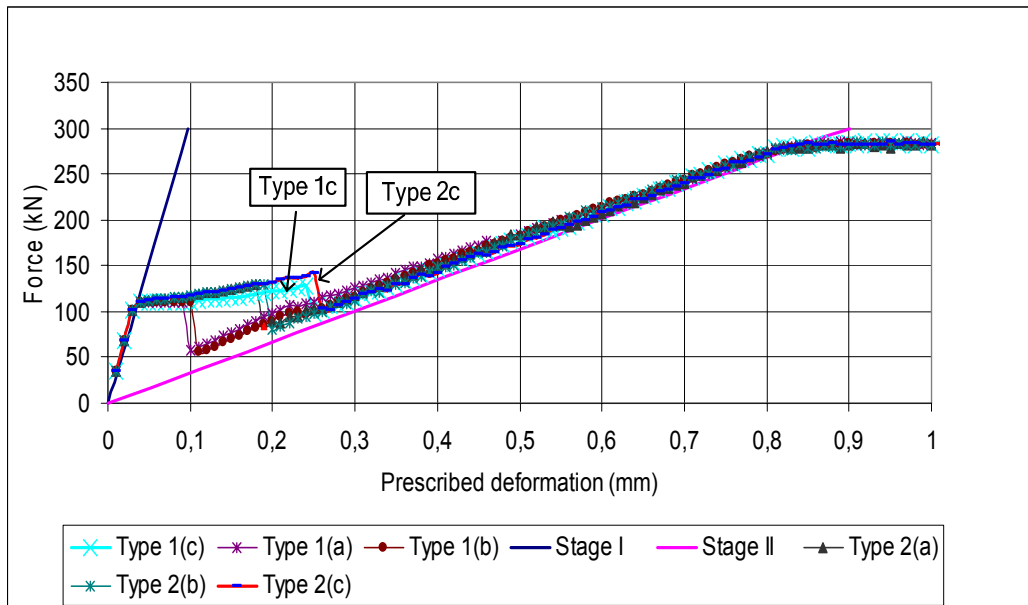


Figure 4.23 Load deformation curves of all models for tension analyses

#### 4.3.6.1 Models with lower order elements, type 1 analyses

Models for type1 analyses were modelled using the following element types

- Concrete – 4 node plane stress elements called as Q8MEM; see Section 4.2.2.1
- Reinforcement – 2 node straight beam elements called as L7BEN; see Section 4.2.3.1
- Bond-slip relationship between concrete and reinforcement – 2+2 node line interface elements called as L8IF; see Section 4.2.4.3

#### Analysis type 1a

First and final stabilised crack pattern at which yielding started; see Figure 4.24. For more details about evolution of crack and propagation, bond stress and slip variation; see Appendix A.

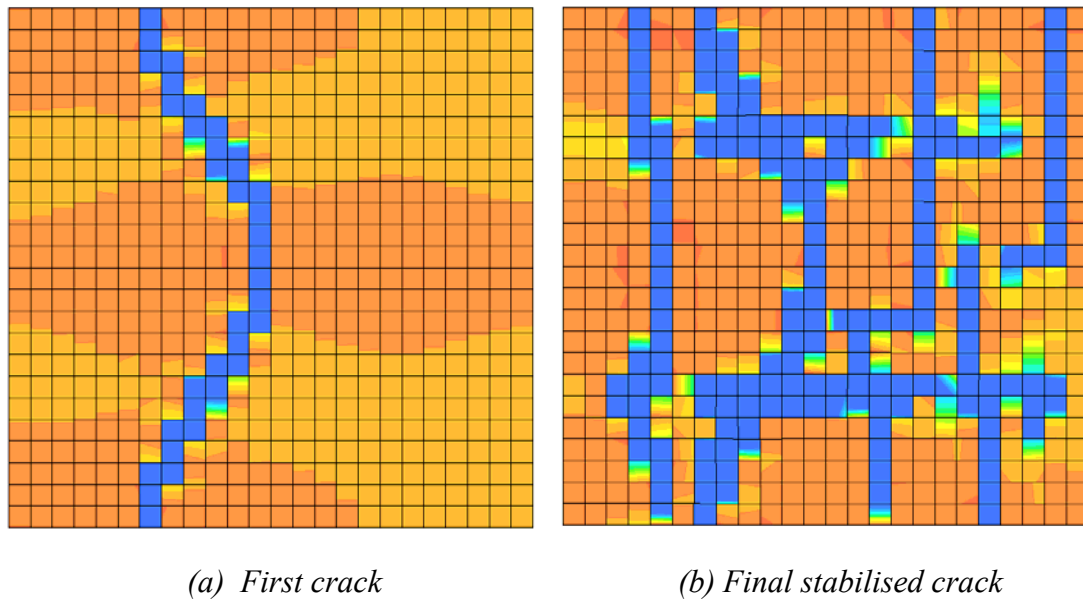
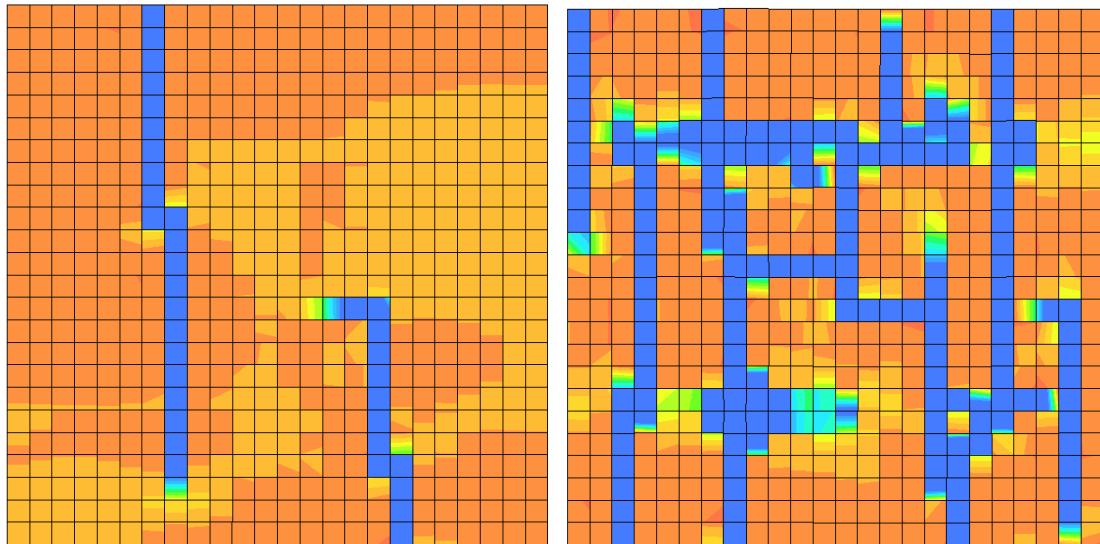


Figure 4.24 Analysis type 1a

When the prescribed deformation was increased, tensile strain in the weakened element and in the elements around reinforcements LR1 and LR2; see Figure 4.22 along the free edges was higher. The reinforcements inhibited the lateral shortening of the model and hence high local stresses in the surrounding concrete elements along the free edges were developed. On further increase in the prescribed deformation, the stress field from the weakened element propagated outwards and the stress field around the reinforcements LR1 and LR2 at the free edges propagated inwards, when meeting the reinforcements TR1 and TR2, see Figure 4.24, the stress field propagating from the free edges was forced to deviate at an angle of  $45^\circ$  due to the influence of the axial force in the reinforcements TR1 and TR2. The first crack in the form of an arc appeared when the stress fields fully localised and connected each other; see Figure 4.24(a). While increasing the prescribed deformation further, more cracks were initiated from the elements surrounding the reinforcements TR1 and TR2 when the axial force in the reinforcements was enough to cause the condition  $\sigma_I = f_{ct}$  in the surrounding concrete elements. After reaching a stabilised condition when no more cracks can appear, the reinforcements started to carry the entire applied force and started to yield; see Figure 4.24(b).

### Analyses type 1b and type 1c

In the type1b, the stress was higher in the concrete elements surrounding reinforcements LR1 and LR2 and in the weakened element; see Figure 4.22. The first crack appeared when the force was sufficient to cause the stress fields to fully localise. The first crack appeared along the reinforcement line LR1; to balance the formation of the first crack, a crack also appeared along the reinforcement LR2; see Figure 4.25(a).

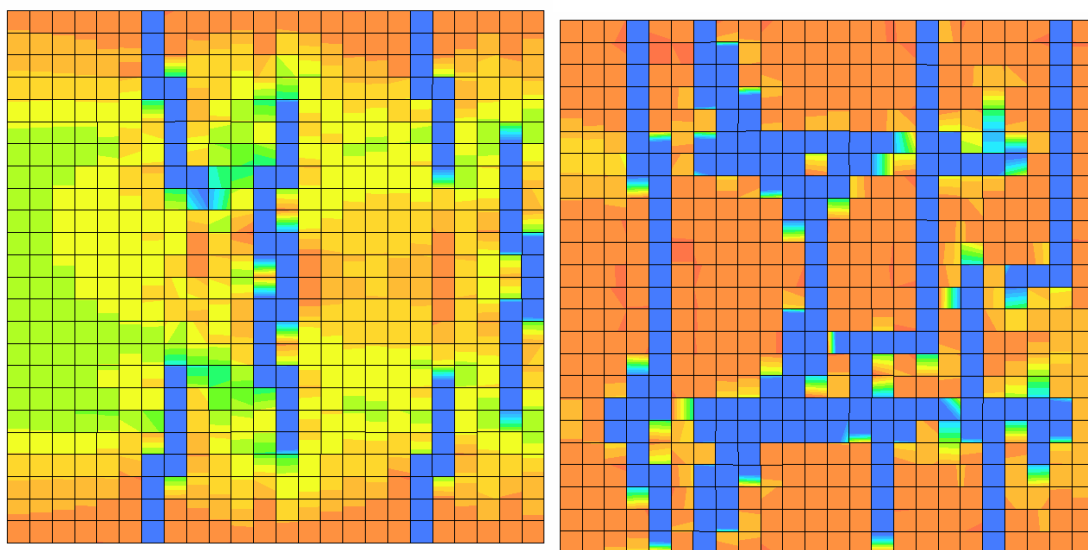


(a) First crack

(b) Final stabilised crack

Figure 4.25 Analysis type 1b

Analysis type 1c was performed to find out whether the model could follow any natural equilibrium path of its own if no element was weakened. A crack pattern was generated due to the influence of transverse reinforcements which prevented the concrete from freely shortening, generating stresses at the free edges. The first crack pattern; see Figure 4.26(a) was almost similar to the first crack pattern of analysis type 1a; see Figure 4.24(a). The stabilised crack pattern at the start of yielding of reinforcement was similar but with marginal difference for all the type 1 analyses. For better understanding; see Appendix A.



(a) First crack

(b) Final stabilised crack

Figure 4.26 Analysis type 1c

## Comparison of type 1 models

Load – deformation curve of analyses type1 when compared were found to be similar except at the point of first cracking stage; see Figure A. 26. The force needed to cause the first visible crack for type1a and type1b analyses was of same magnitude and it happened at nearly the same deformation step, the force needed to cause the first visible crack in analysis type1c was higher and it happened at a higher prescribed deformation value; see Figure A. 26 . The behaviour of all the type 1 models were nearly the same after the first crack appeared; see Figure 4.27. For more detailed comparison; see Appendix A.

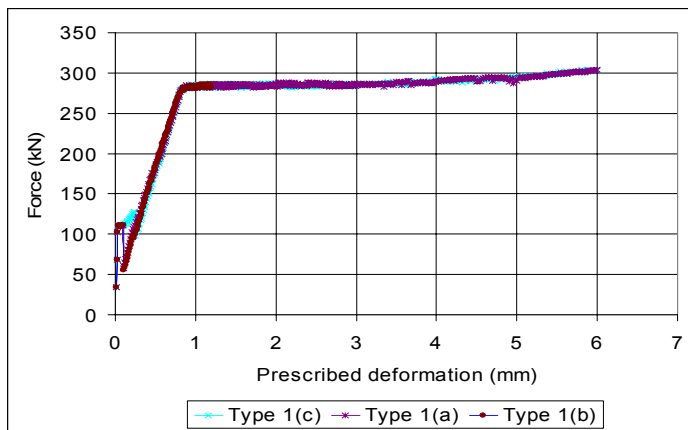


Figure 4.27 Comparison of Load – deformation curve of type 1 analyses

### 4.3.6.2 Models of higher order elements, type 2 analyses

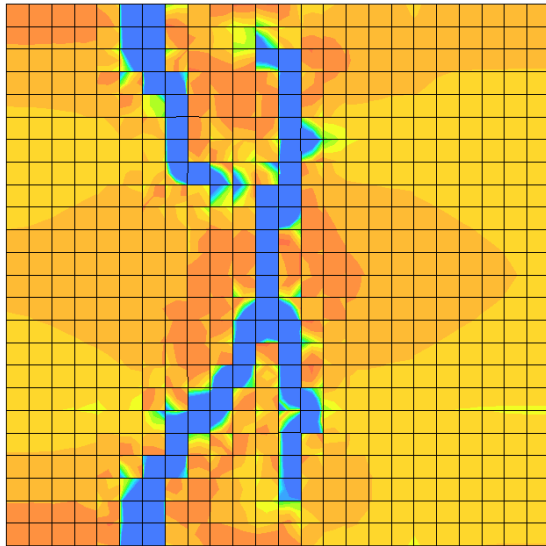
Models with higher order elements were modelled using following type of elements

- Concrete – 8 node plane stress elements (a mid node on each side) called CQ16M; see Section 4.2.2.2
- Reinforcement – 3 node beam elements called CL9BE; see Section 4.2.3.2
- Bond-slip relationship between concrete and reinforcement – 6 node interface element (with a mid node on each side) called CL12I; see Section 4.2.4.3

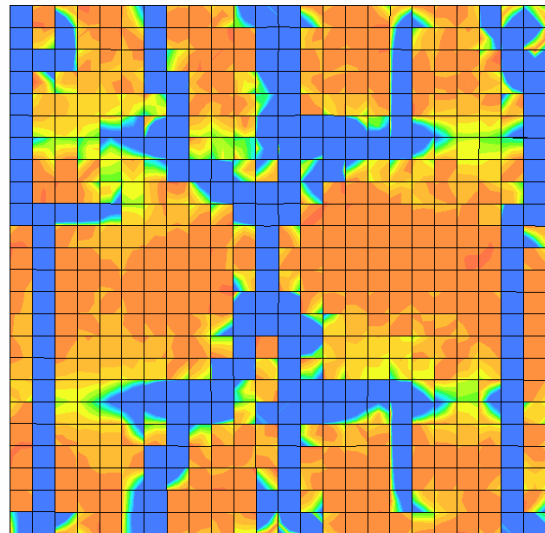
Model had same number of elements as model with lower order elements but with more number of nodes; see Figure 4.22. Analysis type 2a and 2b were performed by weakening the same elements as performed with the analysis type 1a and 1b respectively; see Figure 4.22.

### The first and the final stabilised crack pattern of analyses type2

The crack patterns of analysis type 2 when compared with analysis type 1 were found to be similar. However, the cracks appeared to be smooth in the case of type 2 models due to the presence of more number of nodes per element and since the displacements at the nodes  $u_x$  and  $u_y$  are calculated using a higher order polynomial; see Section 4.2.2.2.

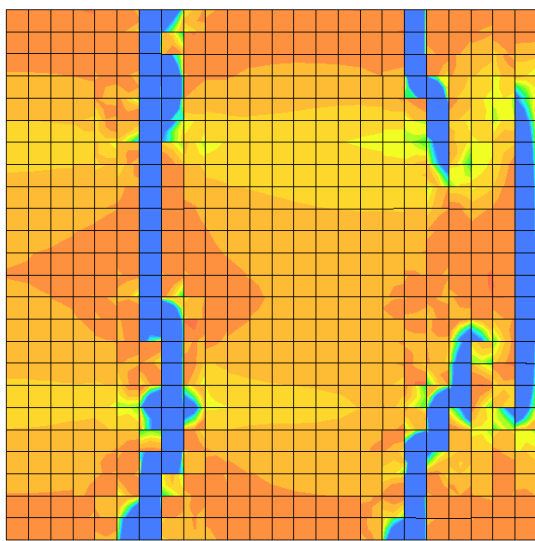


(a) *First crack*

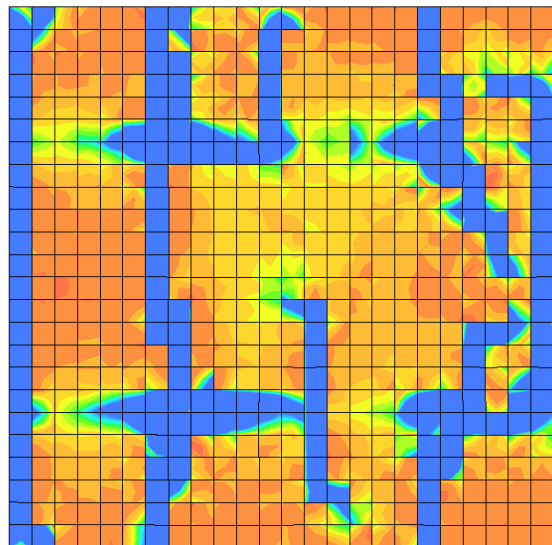


(b) *Final stabilised crack*

Figure 4.28 Analysis type 2a

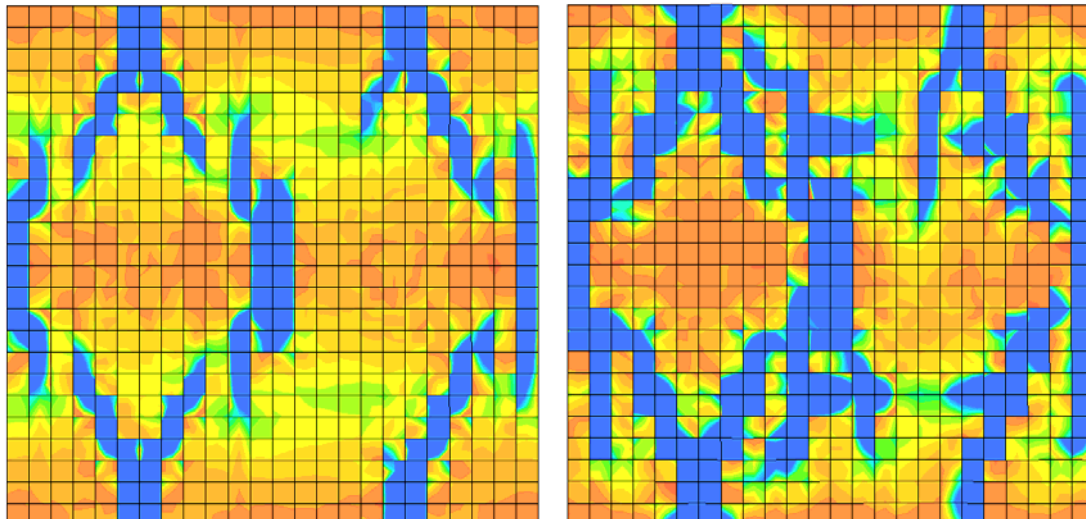


(a) *First crack*



(b) *Final stabilised crack*

Figure 4.29 Analysis type 2b



(a) First crack

(b) Final stabilised crack

Figure 4.30 Analysis type 2c

### Comparison of type 2 analysis

Load – deformation curves of analyses type 2 were similar expect at the first cracking stage; see Figure B 28 and Figure 4.31. For more details see; Appendix B

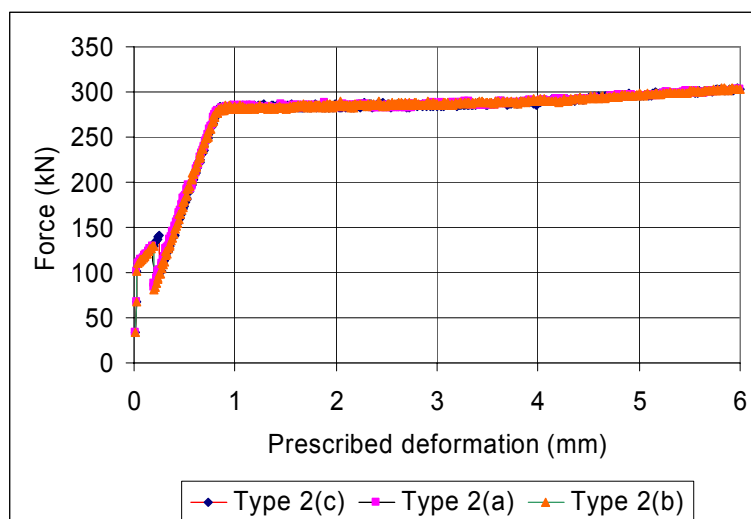


Figure 4.31 Comparison of Load – deformation curve for analysis type 2

In all the models, transformation of the model from stage I to stage II with the slope of the curve changing regularly were the stiffness of the model becomes lesser and lesser due to the formation of new cracks was observed, see Figure 4.23. The slope of stage I curve is the elastic modulus of plain concrete, the slope of the stage II curve is the elastic modulus of bare reinforcing bar.

### 4.3.6.3 Stress in the reinforcement

Due to symmetry, stress in the reinforcement TR1 was only checked; see Figure 4.22. The variation of stress along the reinforcement for analysis type 1c is shown below; see Figure 4.33. When comparing the first and the stabilised crack pattern of analysis type 1c; see Figure 4.26 with the status of the stress in the reinforcement; see Figure 4.33 *particularly (curve 0.25 & 0.84)* it can be inferred that the stress in the reinforcement was higher at the points where concrete was cracked and the reinforcement had to carry entire tensile stress.

The stress strain curve of the reinforcement corresponded well with the material data for reinforcement; see Figure 4.32. The stress strain curve was obtained by processing the data obtained from the stress along the local x axis of the reinforcement and local strain along the local x axis of the reinforcement.

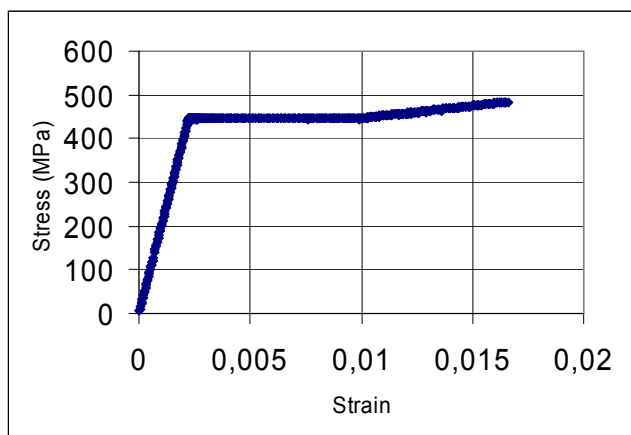


Figure 4.32 Stress – strain curve of reinforcement TR1

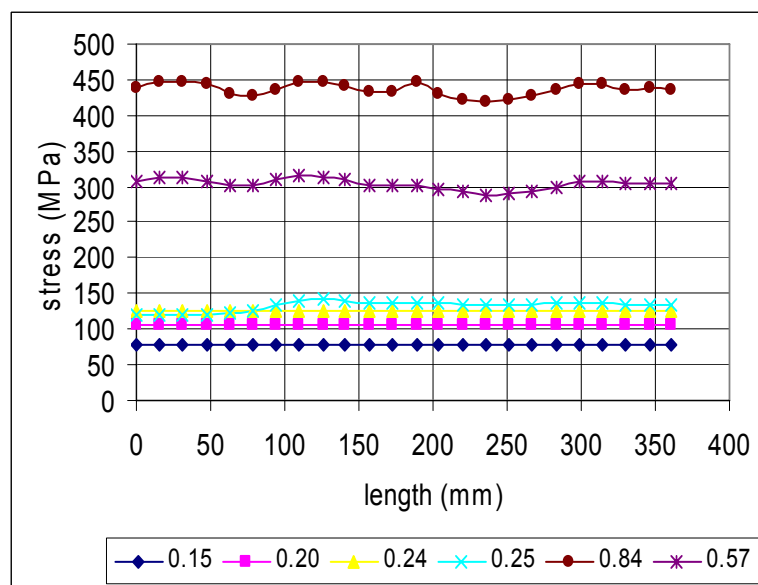


Figure 4.33 Stress variation along TR1 for different prescribed deformation values

## Bond stress and slip variation

The bond stress and slip variation along TR1 reinforcement for analysis type 1c; see Figure 4.34. It can be inferred that the slip in the interface elements were higher at the points where the cracks appeared. The traction stress value was higher at the points where the slip was higher, the values of traction stress matched well with the bond-slip curve values which was the material input for the interface elements. For detailed comparison with crack patterns for every corresponding prescribed deformation stage; see Appendix A.

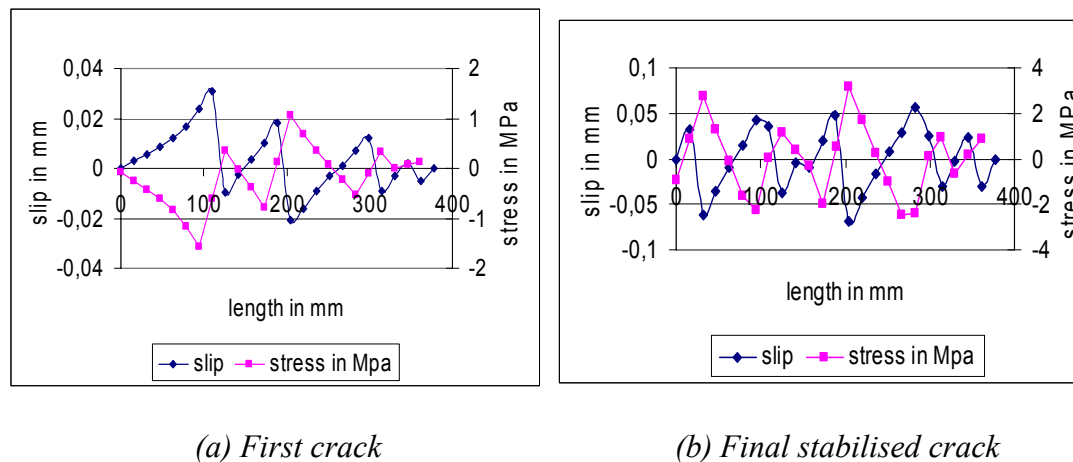


Figure 4.34 Bond stress and slip variation along reinforcement TR1

### 4.3.7 Conclusion

All the models simulated the tension test in a similar manner but with minor differences especially at first cracking stage. For more details; see Appendix B particularly Figure B 28.

When models type 1a, 2a, 1b and 2b were compared with each other it was found that the behaviour of the models were slightly different which was evident from the first crack patterns and the difference in the value of prescribed deformation at which the first crack appeared; but when the models type 1c and 2c were compared it was found that the difference in the behaviour was negligible which was evident from the force and the prescribed deformation at which the first crack appeared; see Figure B 28.

It can be inferred that a model without any element weakened responded in a better and similar manner either when using lower order elements or higher order elements as because the models were allowed to follow their own natural equilibrium.

It was found out that by using the deformation control process the sudden dropping of the curve at the first crack formation was captured. The computational costs and the stability of the solution was much better when compared to the analyses performed using a force control method. While using force control method the drop down in the curve was not possible to be captured after the full localisation of the micro cracks, which was due to the reason that when the force is further increased the process attempts to find an equilibrium of forces which is higher than the natural equilibrium

that could happen in reality and hence the computational cost and the stability of the solution is affected; see Figure 4.35

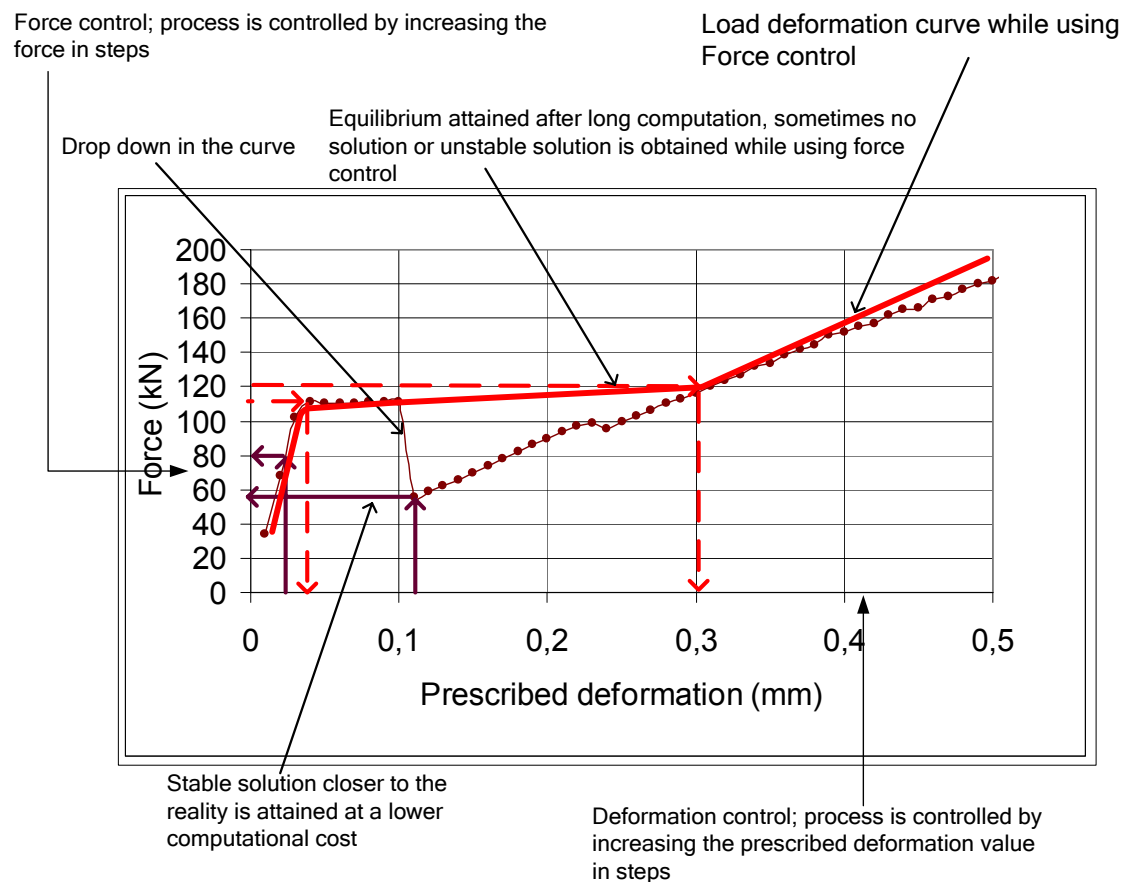


Figure 4.35 Difference in Force control and Deformation control process

The deformation control process used for the verification of the model was easy to implement for models with lower as well as higher order elements.

The deformation control process for the shear analyses of the panels was a complex process and the loads should be distributed in such a way that a uniform shear edge loading was applied along the edges of the model to cause the uniform shear deformation of the model; due to the lack of strong knowledge of how the edge load was distributed to the 8 node plane stress elements, the choice of using a model with higher order elements was not possible.

A choice of using 4 node plane stress elements (lower order elements) without weakening any element and deformation control process was finally suggested for the shear analyses of the panel.

## 4.4 Analyses of shear panel tests

### 4.4.1 Loading beam system

The model was loaded using deformation control method. The model had to be controlled by applying prescribed deformation at one point which would finally apply equal magnitude of force at the nodes along the edges of the panel through a system of beams to cause uniform shear deformation of the panel. The process of application of prescribed deformation at a single point to cause deformation controlled loading on the model also simplifies the shear stress calculation for the model, as because the load-deformation values are extracted at the point of application of prescribed loading only.

The fulcrum point of the beam in the highest level of the beam system was subjected to prescribed displacement. The ends of the beams at the lowest level of the system were connected to the nodes along the edges of the model. The number of levels in the beam system depends upon the number of nodes along the edges of the model. The position of the fulcrum point along the beam was dependant on the amount of reaction force that had to be transferred to the two ends of the beam.

The beam system was made in such a way that the reaction force at the ends of the beams at the lowest level was equal so that each node along the edge was subjected to equal reaction force from the beam system. The corner nodes were loaded with half the magnitude of force in each orthogonal direction so that the total magnitude of force applied at the corner node is equal to the force applied at an interior node along the edge.

It should be noted that the response of the model to the loading using the beam system depends on the stiffness of the model at the nodes which in turn affect the reaction forces at the beam system.

Before the beam system was used for loading the model it was checked to ensure that the reaction force at the ends of the beams in the lowest level of the system was equal; see Appendix J. The beams loading the corner nodes were placed at the next lower level so that half the magnitude of force was applied at the node in each orthogonal direction; see Figure 4.36. Four beams were connected to the two beams at the lowest level and hence had eight ends to load in two orthogonal directions at four corner nodes. For input file for the loading beam system; see Appendix J.

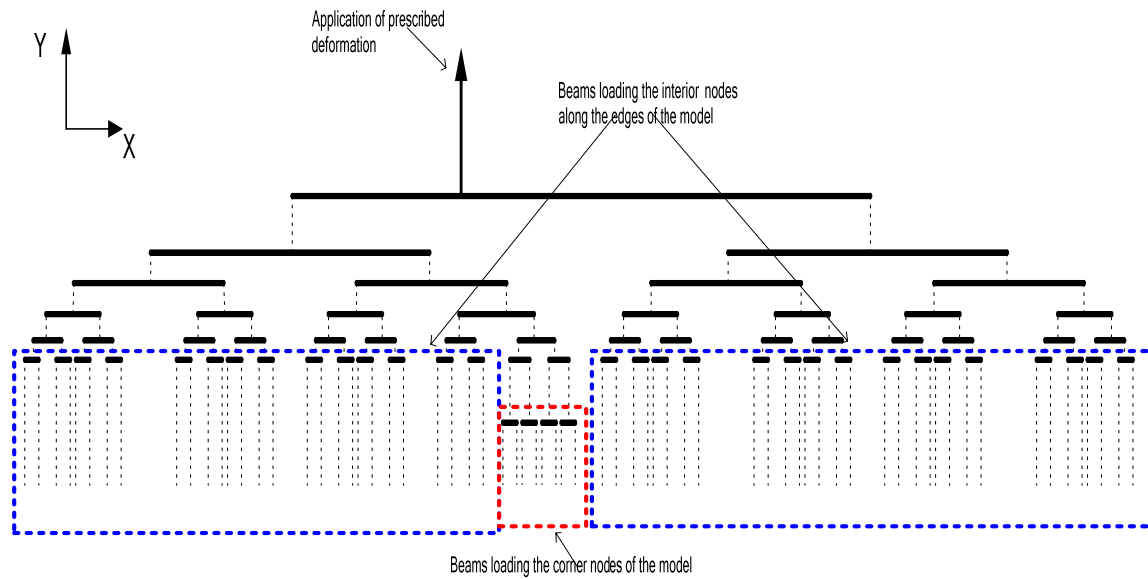


Figure 4.36 Beam system for loading the model

The corner nodes were not directly loaded by the beam system because of the necessity that the corner nodes had to be used as master nodes for specifying a boundary condition; see Section 4.4.3.3. The corner nodes were indirectly loaded by using dummy loading beams which are connected to the corner nodes; see Figure 4.37. The ends of the beam system which were supposed to load the corner nodes were connected to the dummy loading beams and hence indirectly applying the force at the nodes.

The dummy rigid beams, guiders and the beams of the loading beam system were made to be rigid so that the bending of the beams was negligible. The density of the dummy beams and loading system was zero so that they do not affect the model when loading the self weight on the model and to transfer the loads directly to the nodes of the model without any loss of applied force at the loading system. The beams were made rigid by assigning large cross sectional dimension to the beams.

The rigid beams had the following material and physical properties. Modulus of Elasticity was  $200\text{E}+09$ , Poisson's ratio was 0.3, Density was zero and yield value was not assigned to the beams so that they do not yield. The cross section of the beams was a square with a side measuring 1 m and the local z axis was oriented along the direction of the global z axis.

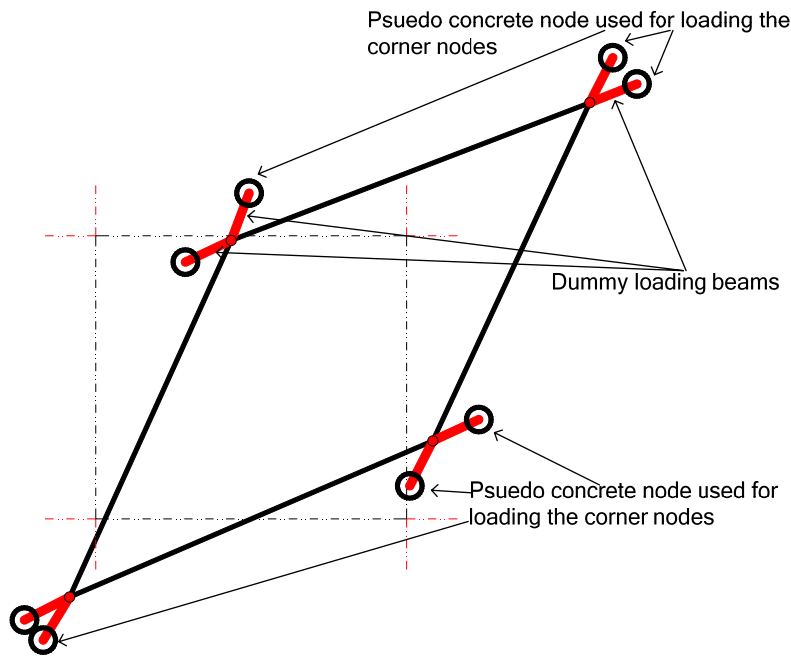


Figure 4.37 Dummy beams loading the corner nodes in orthogonal directions

#### 4.4.1.1 Connection within the loading beam system

The beams in the system were connected to each other using the 'equal' tying type.

Equal tying serves like a rigid beam which displaces the fulcrum point of the beam in the lower level equal to the displacement of the start or the end point of the beam at the immediate higher level to which it was connected; see Figure 4.38.

#### 4.4.1.2 Supports within the beam system

The beam at the highest level was supported in x and y direction in translation at the fulcrum point at which the prescribed deformation was applied. All beams in the loading system had their translational degree of freedom in x direction and rotational degree of freedom about the x axis restricted at the start point; see Figure 4.38.

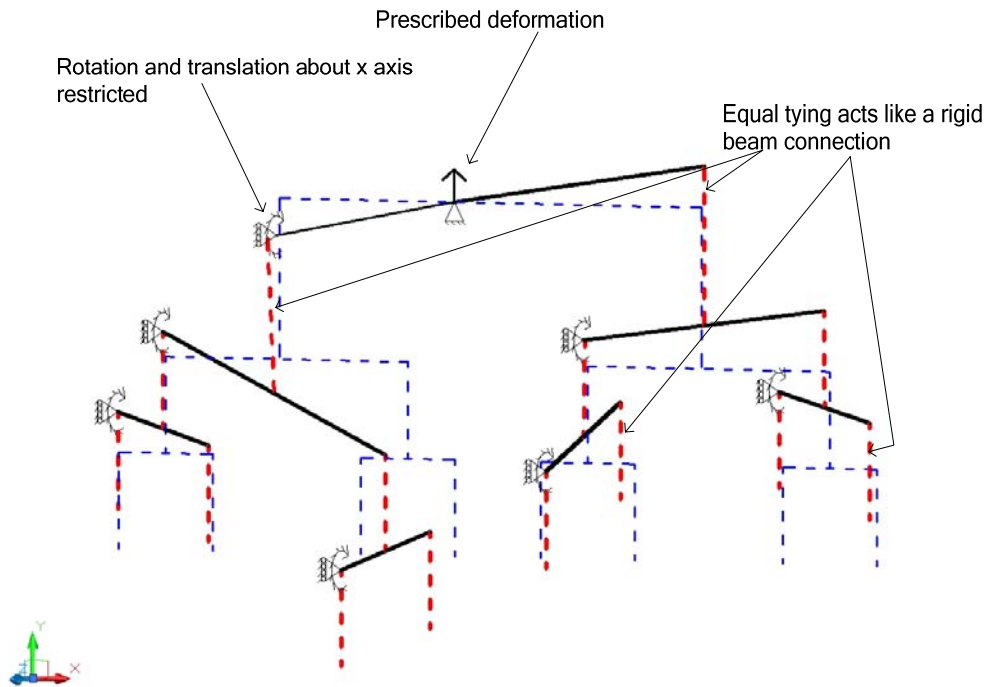


Figure 4.38 Tying and supports within the loading beam system

#### 4.4.2 Connection between the model and the loading system

The loading system and the model were connected to each other using the 'fix' tying type. Fix tying allows translational movement of the beams at the lowest level of the system in the y direction be connected to the nodes along the edges of the model in a direction which will cause the shear deformation of the panel; see Figure 4.39; see Appendix F for syntax.

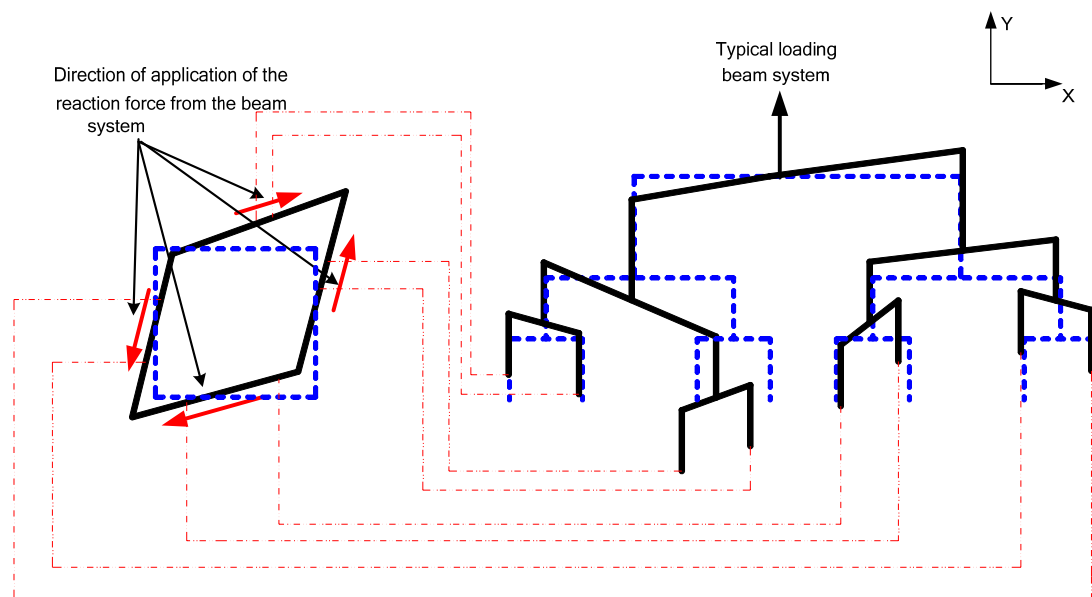


Figure 4.39 Connection between model and loading system using Fix tying

### 4.4.3 Boundary conditions for the model

Boundary conditions formed the paramount concern in the analyses. The model was an interior small unit cut out from a large panel and hence the boundary conditions were to be created with the compatibility of the small unit with the rest of the panel in mind so that the behaviour of the model was the same when compared to other units of the panel; see Figure 4.40, allowing the model to deform like an interior unit the test panels at the same time supported to prevent the rigid body motion.

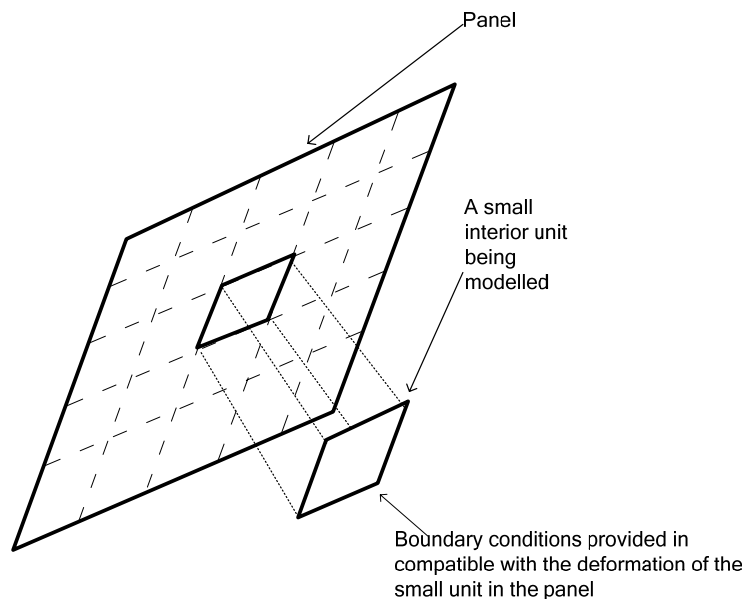


Figure 4.40 Model with respect to the test panel

#### 4.4.3.1 Supports for the model

The model was supported at two points in order to apply the self weight. A hinge support was provided at the midpoint of the bottom edge, the support was restrained in all degrees of freedom except the rotational degree of freedom about the z axis to cause the hinge effect. Second support was provided as a roller support at the midpoint of the right edge allowing the translation of the model along the local x axis inclined at an angle of  $225^\circ$  to the global x axis in the anti-clockwise direction and rotation about the global z axis; all other degrees of freedom were restrained. The support condition was not assigned directly to the model of the panel due to the condition of the edge nodes of the model being a slave to the beam system; see Section 4.4.1. To solve the problem dummy support beams were created with one end of them connected to the actual support node and the other end called as 'pseudo supports' were provided with the support conditions. The local axis was assigned as a property to the pseudo support end along the right edge. The pseudo support end of at the bottom edge had all the degrees of freedom restricted and the pseudo support end at the right edge had the translational degree of freedom along the y direction of the local axis and all rotational degree of freedom restricted; see Figure 4.41. For the properties of dummy support beams; see Section 4.4.1.

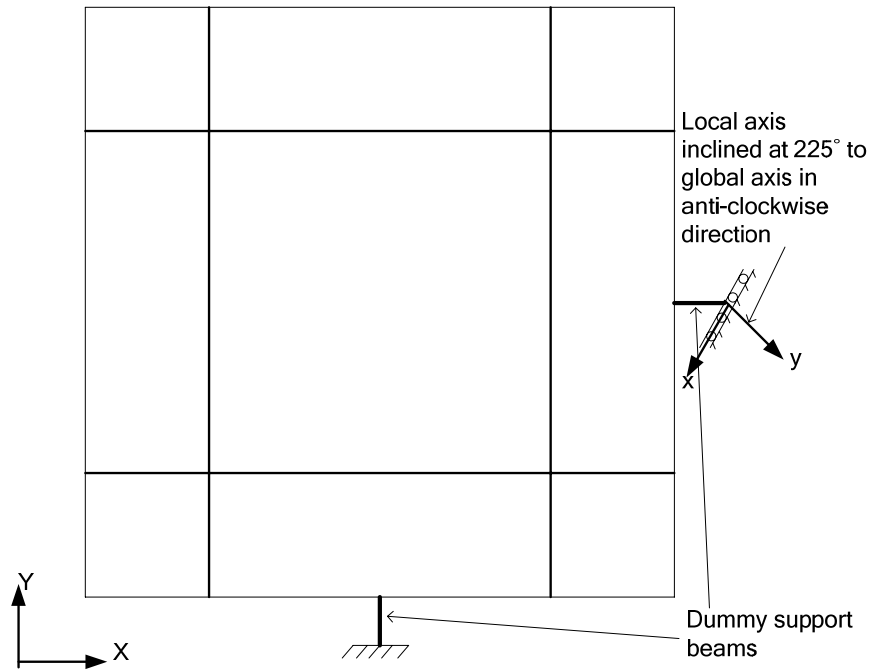


Figure 4.41 Model with rigid support beams

#### 4.4.3.2 Parallel edges

To satisfy the compatible deformation of the model the opposite edges of the model should rotate equally so that they are parallel to each other. The edges were kept parallel by using tying type 'equal' and controlling the rotation about the global z axis. The plane stress element type which was used to model concrete did not have the drilling rotational degree of freedom and hence it was not possible to implement the process directly. To achieve the phenomenon, beam elements with rotational degree of freedom along the axis perpendicular to the main axis of the element were provided along the edges of the model, the dummy edge beams render the rotational degree of freedom to the nodes along the edges of the model. The elements are provided with hinges at the corner of the model to prevent the transfer of moments between the edges and to allow free deformation of the panel at its corners.

The dummy edge beams along the edges of the model rendering the drilling rotational degree of freedom were made in such a way that they act like a very thin elastic thread not hindering the shear deformation of the model. The edge beams were also assigned to have zero density for the same reason as the dummy support beams; refer Section 4.4.1. The edge beams meeting at the corners of the model were provided with hinges at their ends at the corner; see 4.4.3.2.

The dummy edge beams were assigned the following material and physical properties, Modulus of Elasticity was 198.8 GPa, density of the beams was zero, Poisson's ration was 0.3. The cross section of the edges beams was a circle with a diameter of 0.1 mm, the local z axis of the beams were oriented along the direction of the global z axis.

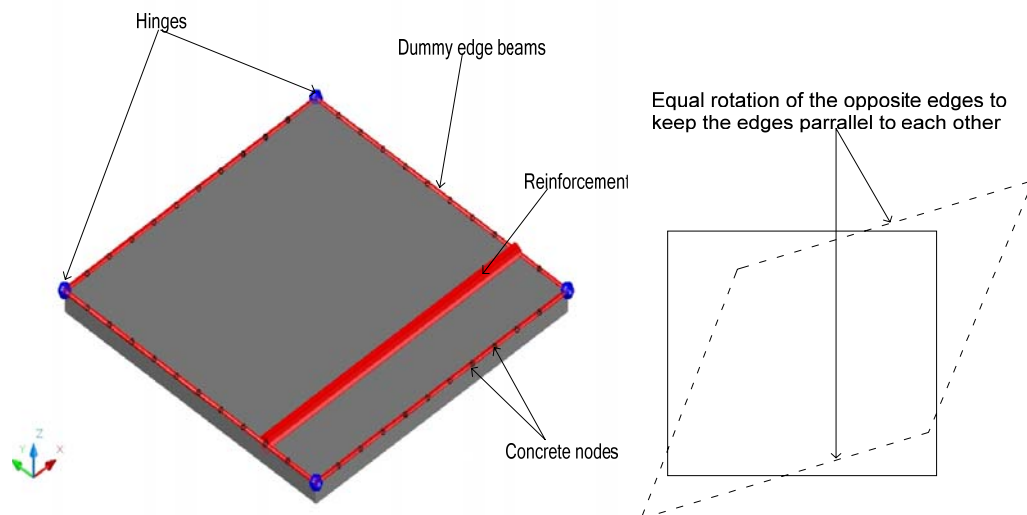


Figure 4.42 Dummy edge beams with hinges at the corners

#### 4.4.3.3 Straight edges

The model should have straight edges to have compatible deformation compared with an interior unit in the test panel. The nodes along the edges of the model should have the translational degree of freedom in the direction perpendicular to the edge controlled, so that they move in a straight line in relation to each other but had unrestricted translational degree of freedom along the edge direction; see Figure 4.43. ‘Between’ tying type was used to implement the phenomenon. In the tying command the corner nodes of the model were the master nodes and the interior nodes of the edges were the slave nodes; see Figure 4.43. ‘Between’ tying allowed the slave nodes to move freely in the direction of the edge but were forced to be in a straight line in relative to the movements of the master node in the direction perpendicular to the edge.

Another option to achieve the phenomenon was by using ‘eccent’ tying type which was much complex to implement because of the necessity of drilling rotational degree of freedom at the master node, to implement the eccent tying dummy beams with rotational degree of freedom along the local z axis of the member were to be used, these dummy beams were attached to the mid points of the edges. Nodes at the midpoints of the edges were the master nodes and the other nodes at the edge were slave nodes controlled in the translational degree of freedom in the direction perpendicular to the edge; see Figure 4.44. The model was rigid and it was not able to predict the shear behaviour of the panel as successful as the between tying type.

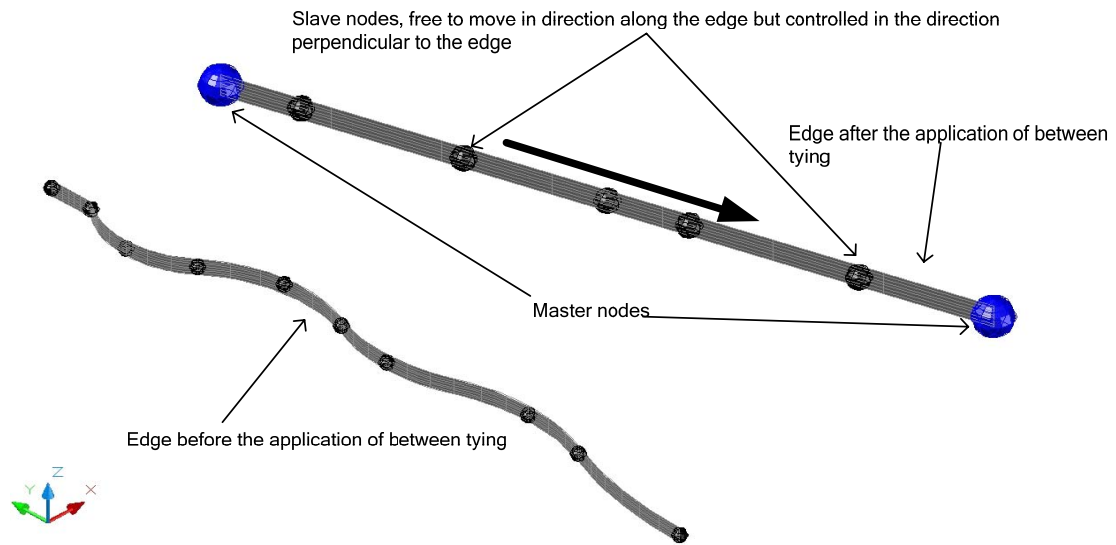


Figure 4.43 Between tying to keep the edge straight

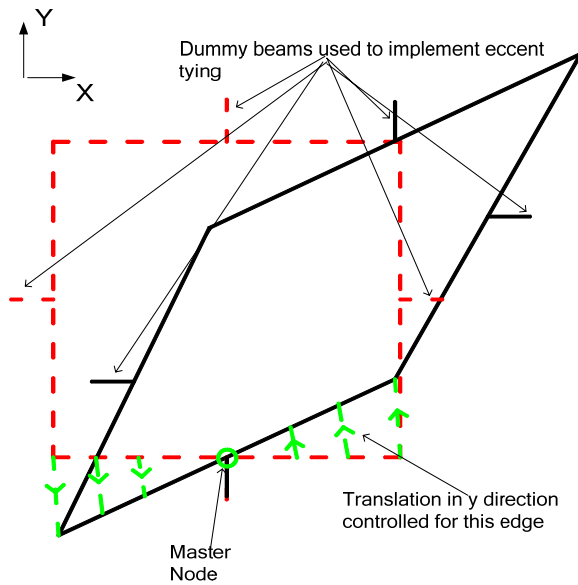


Figure 4.44 Eccent tying to keep the edge straight

#### 4.4.3.4 General connection to prevent the anchorage failure

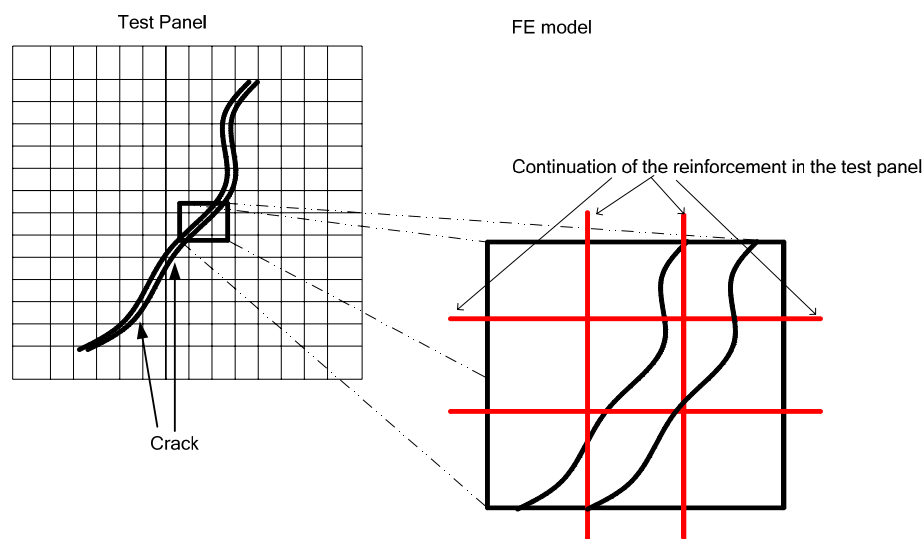


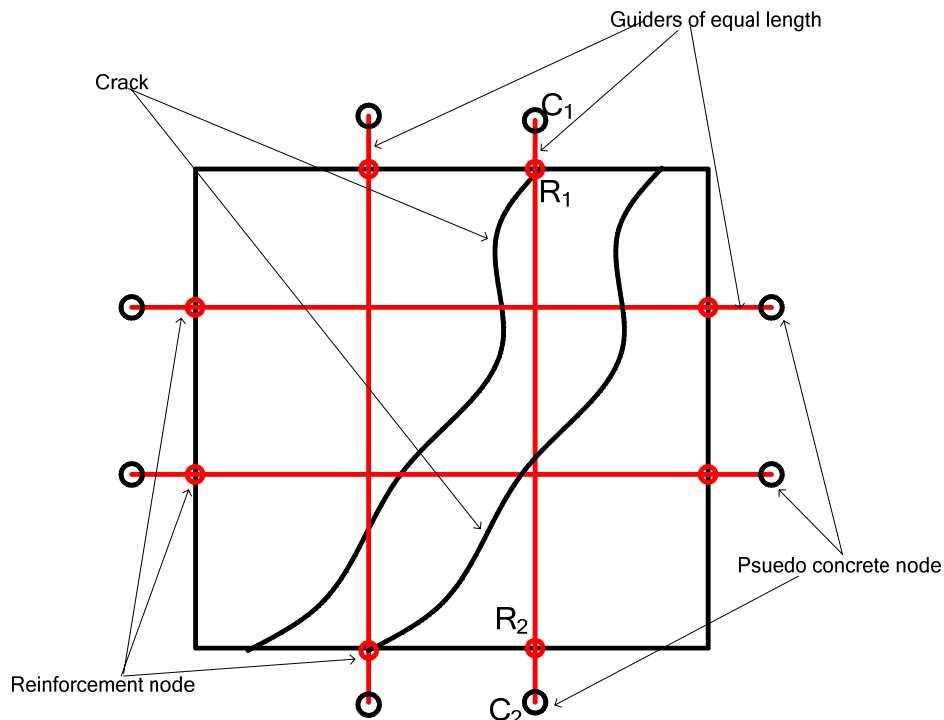
Figure 4.45 Global view of the FE model with the cracks

A general connection was made using the fix tying type in order to prevent the anchorage failure or pull out failure of the reinforcements. The connection was done in correspondence with the continuation of the reinforcement in the test panel beyond the FE model unit; see Figure 4.45. The reinforcements in the test panel were prevented from anchorage failure as they were attached to the shear keys; see Figure 3.3. The general connection was made in such a way that the relative displacements between the concrete and reinforcement nodes along the reinforcement at the edges of the FE unit were equal; see Figure 4.46. The general connection was made between pseudo concrete nodes and corresponding reinforcement nodes; see Figure 4.47. The connection could not be made directly between the concrete node and the corresponding reinforcement node, since the concrete node was a slave to the loading beam system; see Section 4.4.2 and for the 'between' tying type to keep the edge straight; see Section 4.4.3.3

$$C1-R1 = C2 - R2$$

$$R1 = R2 + C1 - C2$$

The equation was implemented using the fix tying; see Appendix F for the syntax.



Relative slip between the concrete (C1) and the reinforcement (R1) nodes = Relative slip between the concrete (C2) and the reinforcement (R2) nodes

*Figure 4.46 General connection between reinforcement and concrete nodes at the edges*

#### **4.4.3.5 Controlled movement of guiders and dummy loaders**

The guiders and the dummy loaders attached to the model were forced to be in position in relative to the edges of the model during the shear deformation process of the model. The dummy loaders should be kept in position otherwise the nodes will not be loaded with the same amount of reaction force as in an interior node; the guiders should be kept in straight line with the concrete node to ensure a similar relative displacement if the general connection was made between the actual concrete node and the reinforcement node. Beams elements were preferred instead of truss elements for the dummy beams and guiders because of the availability of rotational degree of freedom along the axis perpendicular to the main axis of the member in beam elements which was not available in truss elements; the rotational degree of freedom was used to provide controlled movements of the dummy beams and guiders.

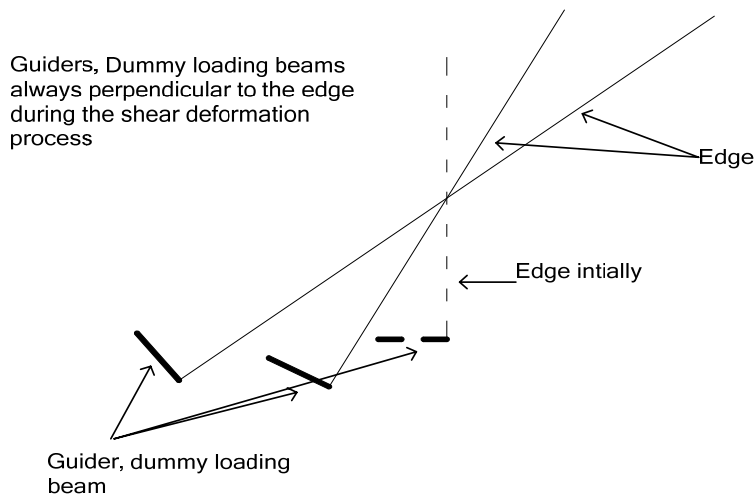
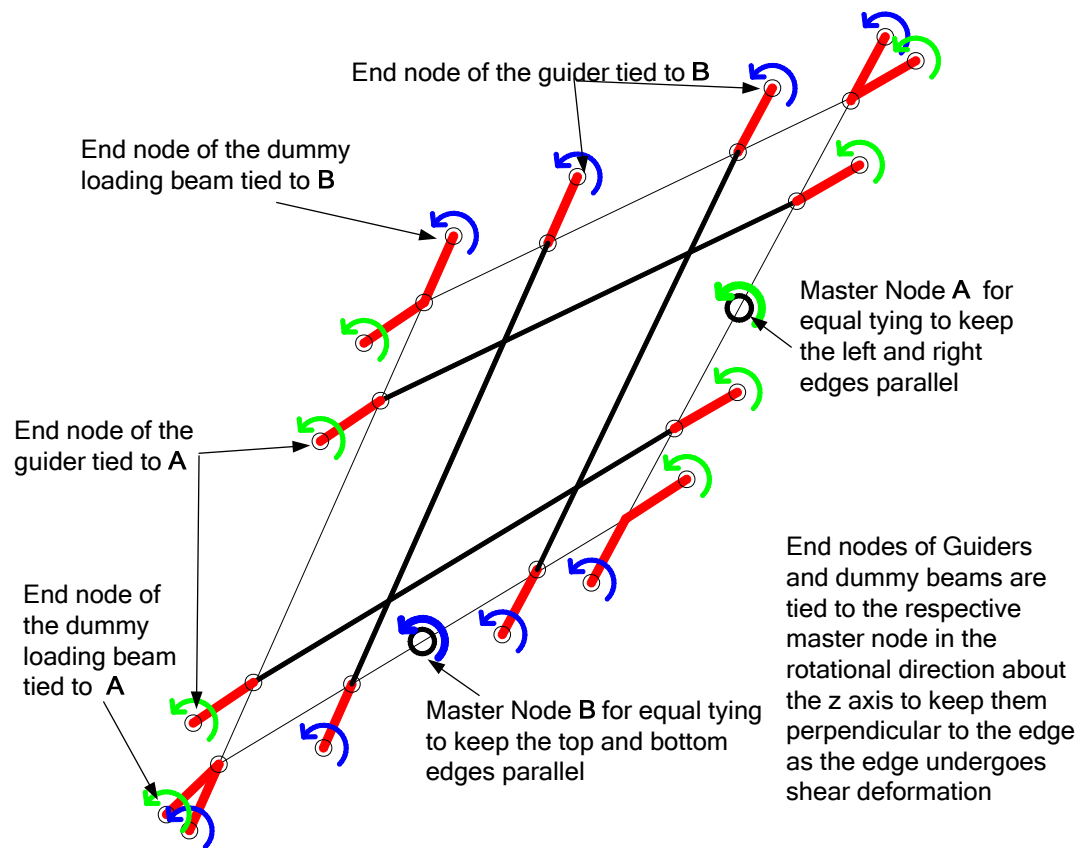


Figure 4.47 Control of the movements of guiders, loading beams

## 5 Results of the shear analyses

In this section the results from analyses of shear panels A2, A3, A4, B1, B2 and B4 are discussed. The shear stress-strain curve of the analyses was compared with the shear stress-strain curve of the panel tests done at Houston by Pang and Hsu (1992). However, since the behaviour in the analyses were similar, detailed results such as bond-slip relationship, dowel action of the reinforcement and bending moments in the reinforcement are discussed for longitudinal reinforcement L1 of the A3 panel only; see Figure 5.1

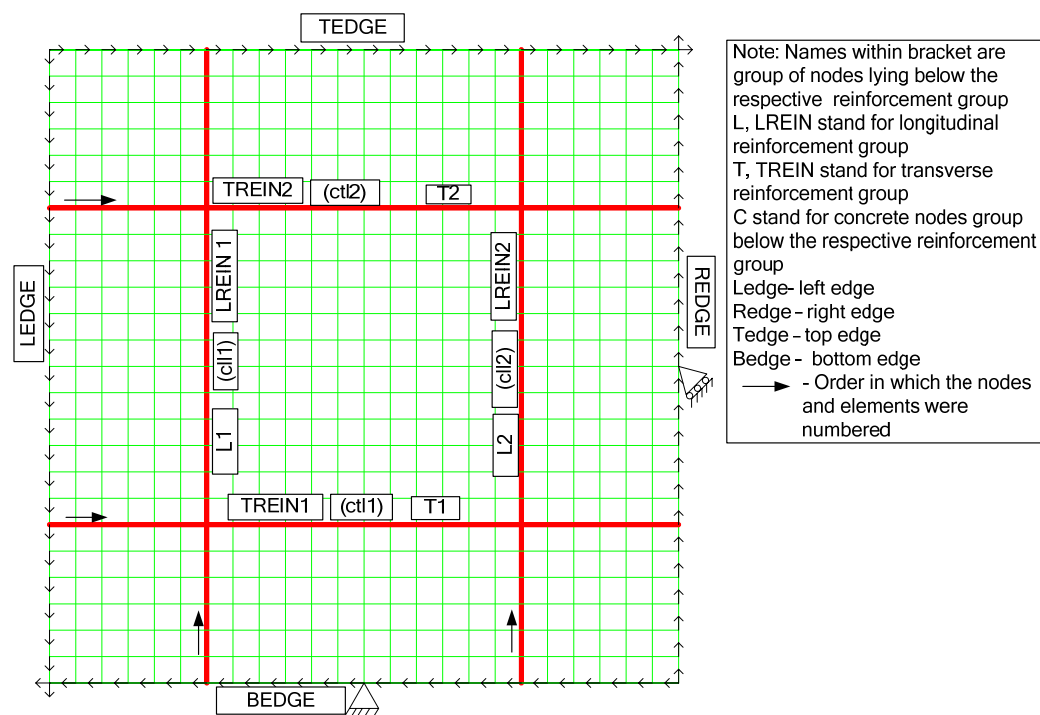


Figure 5.1 Model with abbreviation explanation

### 5.1 Calculation of shear stress and shear strain values

Shear stress values were calculated from the load-deformation values obtained at the loading point in the beam system. The obtained values were divided by four to obtain the shear edge loading at one edge because the beam system was used to load all the four edges simultaneously. The shear stress along the edges was obtained by dividing the shear force values by the area of the edge. The area of the edge was the product of length and thickness of the edge i.e. (0.3772 m x 0.0889 m).

Let  $l$  be the length of the edge

$t$  be the thickness of the model

$F$  be the shear force

$$\tau = \frac{F}{l * t} \quad (5.1)$$

Where  $\tau$  is the shear stress in MPa

Shear strain values were obtained by using the deformation data of four selected nodes; see Figure 5.2 i.e. (nodes 638, 725, 329 and 224). The selected nodes were at equal distance from each other, in this case preferably centre points of the corner grids of the model.

Let  $x$  be the distance between the nodes in horizontal direction

$y$  be the distance between the nodes in the vertical direction

$u$  be the diagonal distance between the nodes

$$\begin{aligned} tdx_1 &= b_x - c_x \text{ mm} \\ tdy_1 &= b_y - c_y \text{ mm} \\ e_1 &= \frac{\sqrt{(x + tdx_1)^2 + (y + tdy_1)^2} - u}{u} * 1000 [\text{‰}] \\ tdx_2 &= a_x - d_x \text{ mm} \\ tdy_2 &= a_y - d_y \text{ mm} \\ e_2 &= \frac{\sqrt{(x + tdx_2)^2 + (y + tdy_2)^2} - u}{u} * 1000 [\text{‰}] \\ \gamma &= \frac{e_1 + e_2}{2} [\text{‰}] \end{aligned} \quad (5.2)$$

Where  $\gamma$  is the shear strain in micro strains [ $\text{‰}$ ]

Note that in this section the shear strain values mentioned are of micro strains [ $\text{‰}$ ].

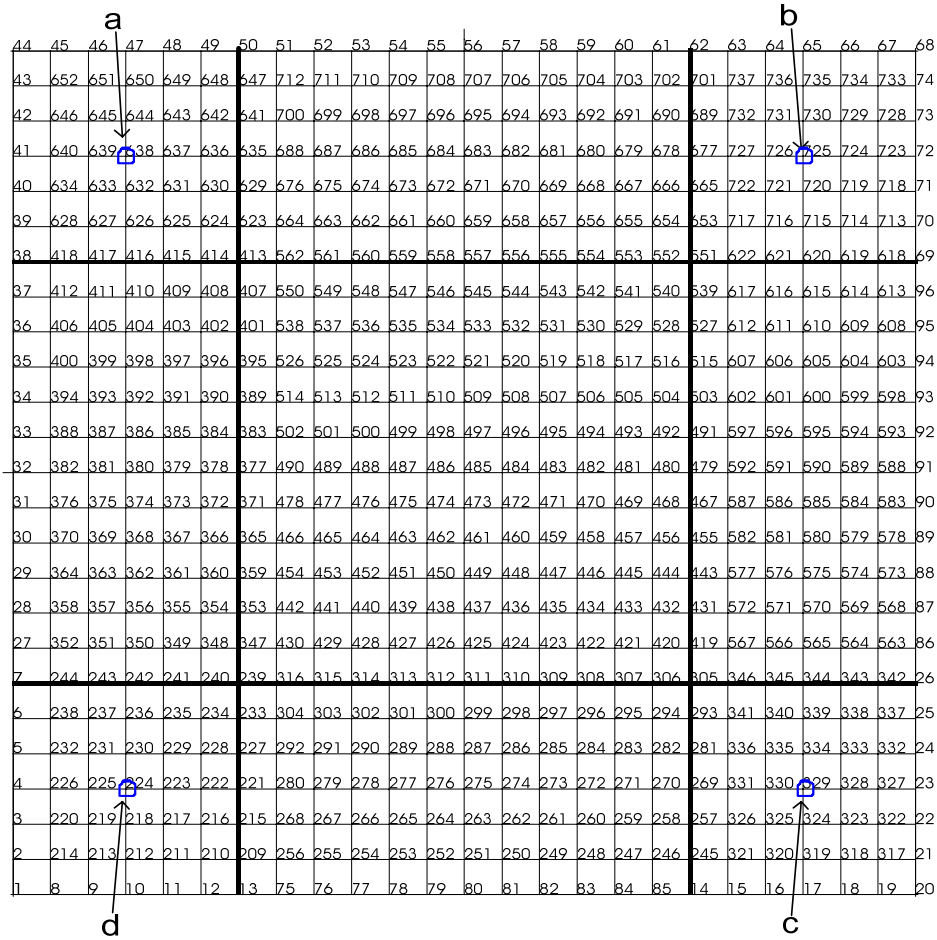
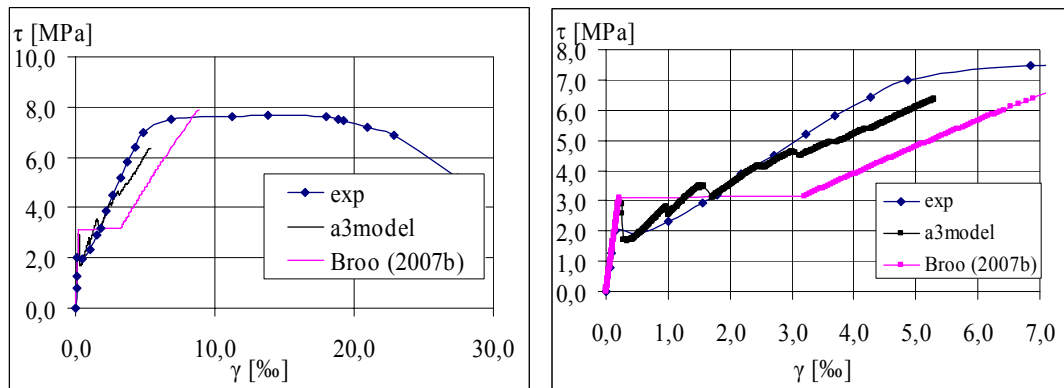


Figure 5.2 Nodes used for the calculation of shear strain values for the loading history

## 5.2 Panel A3

The shear stress-strain curve of the analysis agreed well with the shear stress-strain curve of the test; see Figure 5.3



(i) Overall view

(ii) Closer view

Figure 5.3 Comparison of Shear stress-strain curve for panel A3

Comparing the shear stress-strain curves, the model behaved similar to test panel before cracking, however after cracking the behaviour of the model was less stiff than the test panel. This could be because the shear strength offered by the aggregate interlocking at the crack interface was not taken into account in the model.

The first crack started to form when shear stress reached the tensile strength of the concrete ( $f_{ct} = 2.98\text{MPa}$ ); see Table 4.1. The model was able to capture the drop down in the curve at the point of the first crack; see Figure 5.3(ii); activation of reinforcement after the formation of first crack was clearly evident Figure 5.3(ii). This model with non-linear properties such as bond-slip relationship and loaded by deformation controlled process showed a better behaviour closer to the test; see Figure 5.3 (curve *a3model*) when compared to a model with embedded reinforcement and force controlled loading; see Figure 5.3 (curve *Broo(2007b)*), refer Broo (2007b)

The shear stress strain curve was plotted as long as the deformation of the model was reasonable. After the yielding of reinforcement occurred the deformation of the model started to be irrelevant.

The final relevant deformation of the model was at the prescribed deformation value of 0.577 m which corresponds to a shear strain value 5.3, longitudinal reinforcement L1 had yielded at integration point 2; see Figure 5.4. The legend in the figure; see Figure 5.4 should be read as (reinforcement name, integration point)

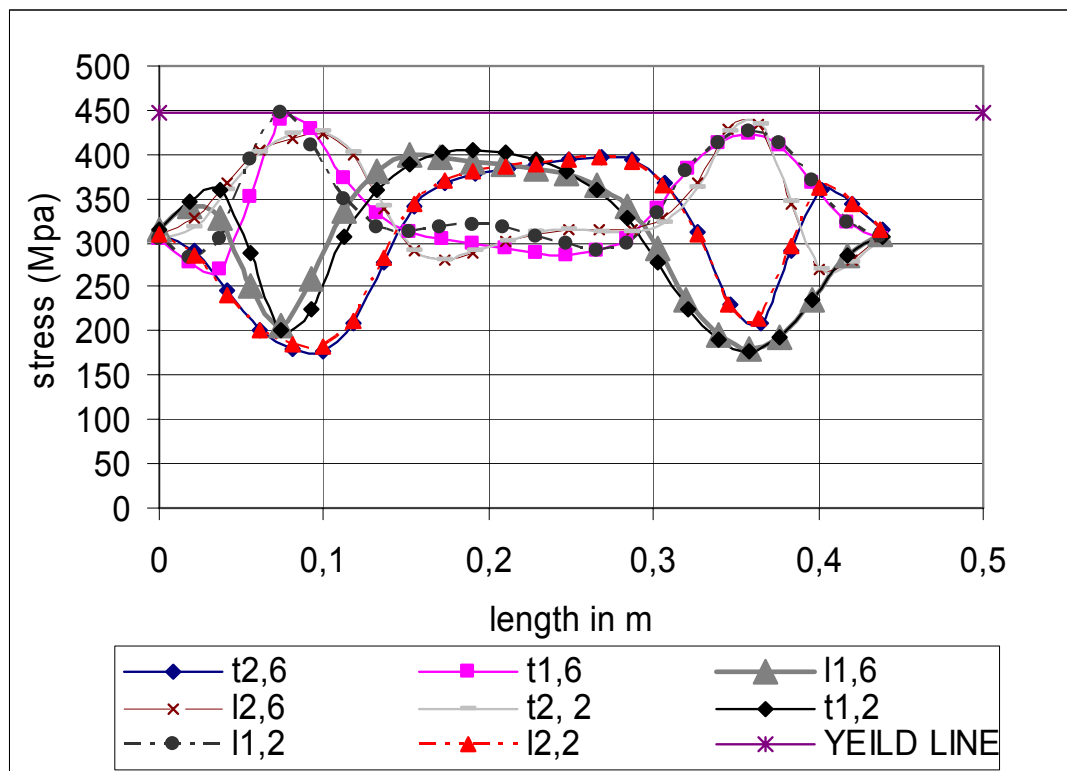
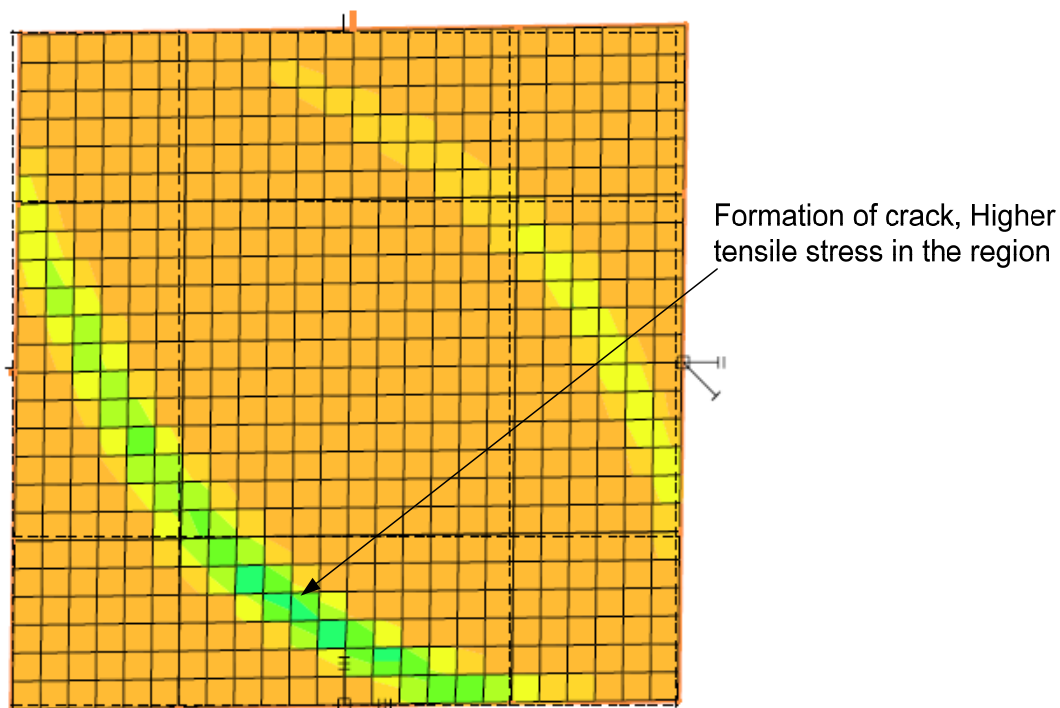


Figure 5.4 Stress in the reinforcement at the final relevant deformed state, shear strain value 5.3

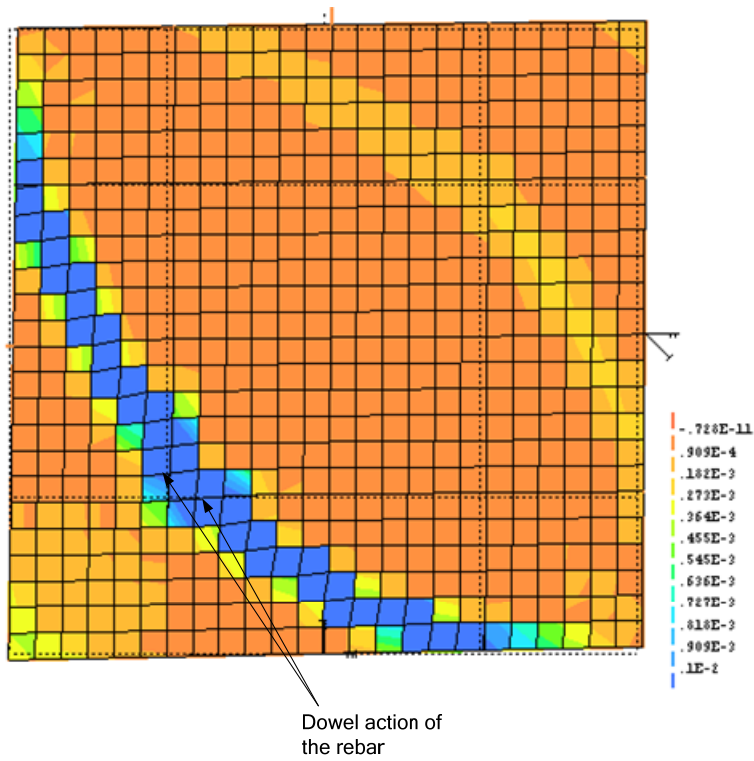
## 5.2.1 Crack Pattern and Shear deformation

In the Figure 5.5(a-f) crack patterns for different shear strain levels are shown. Localisation of micro cracks could be seen before the first fully opened crack appeared at shear strain value 0.276. As the loading increased further, spalling of concrete at the corners was observed. However, the boundary conditions of the model made it possible to load the model with shear edge loading even after the spalling of concrete at the corners. Dowel action in the reinforcements i.e. the bending of the reinforcements at the cracks was clearly visible in the later stages as the crack became wider.

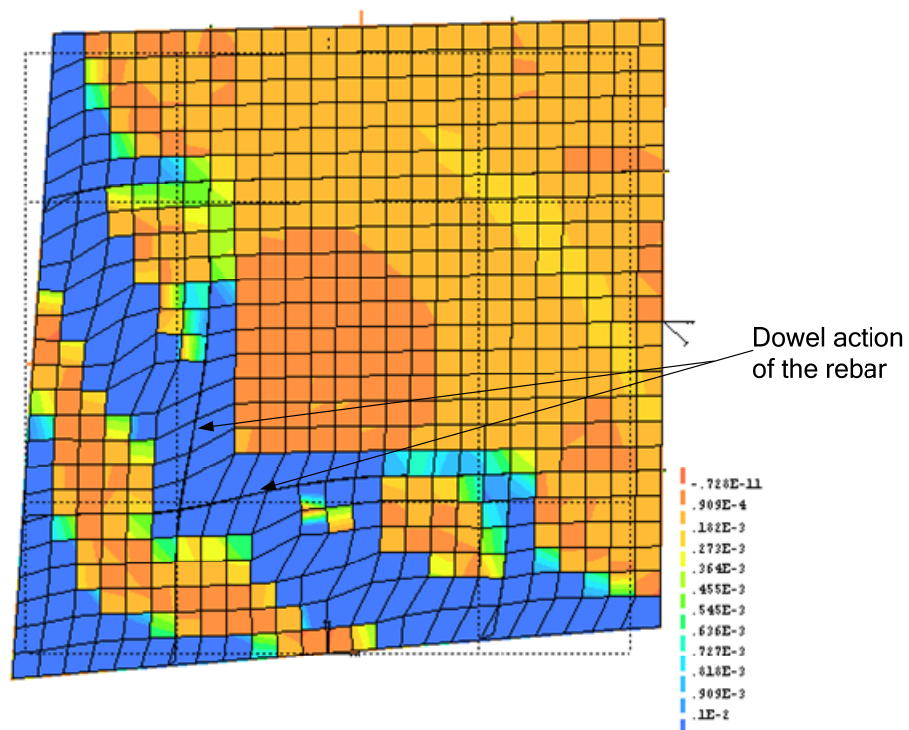
A second fully opened crack was seen at shear strain value 2.484. On further loading, concrete slowly disintegrated and finally the reinforcements were carrying the applied load; the final relevant shear deformation pattern of the model was at shear strain value 5.3 at which the longitudinal reinforcement L1 yielded, after the yielding of the reinforcement the results of the analysis were irrelevant. The scale for the contour plot is as shown; see Figure 5.6.



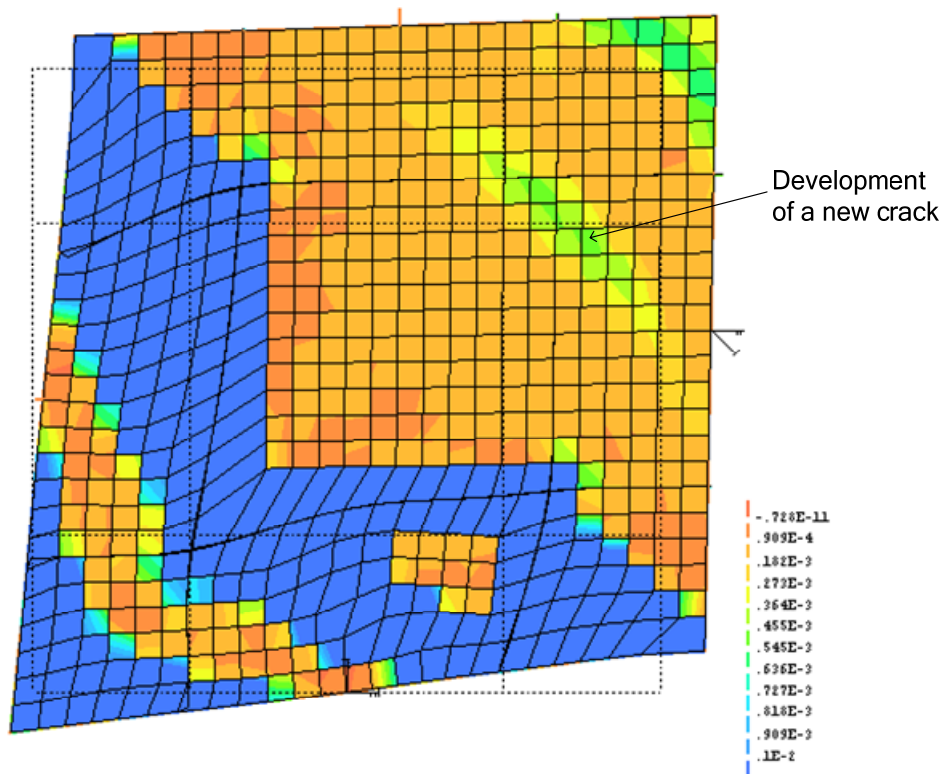
(a) At shear strain value 0.266



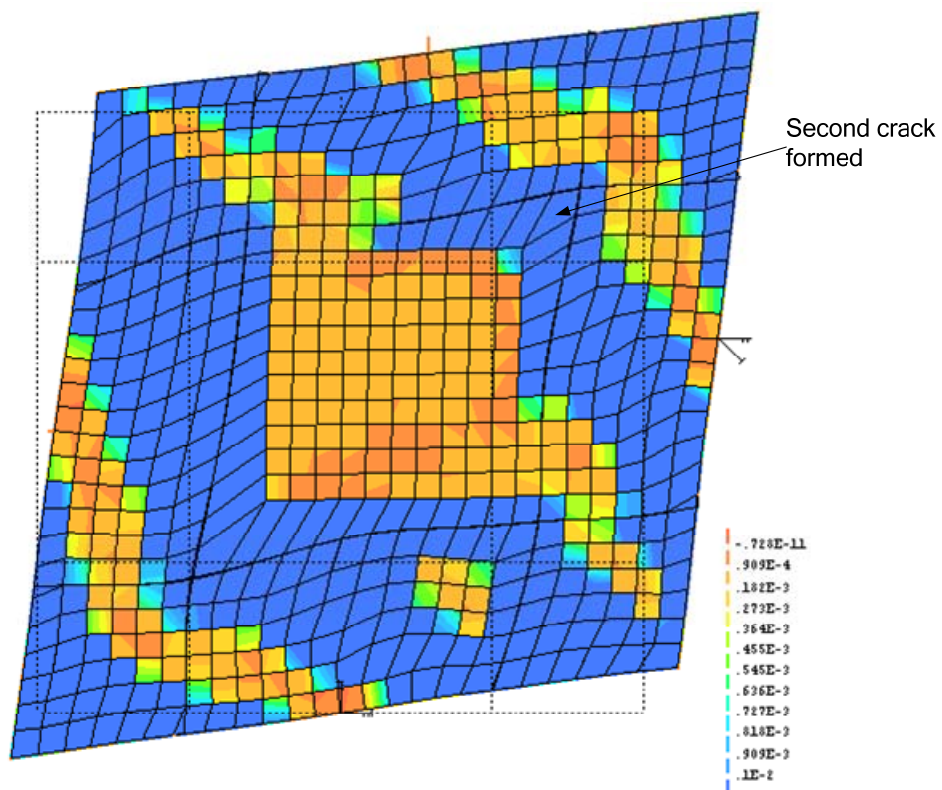
(b) At shear strain value 0.276



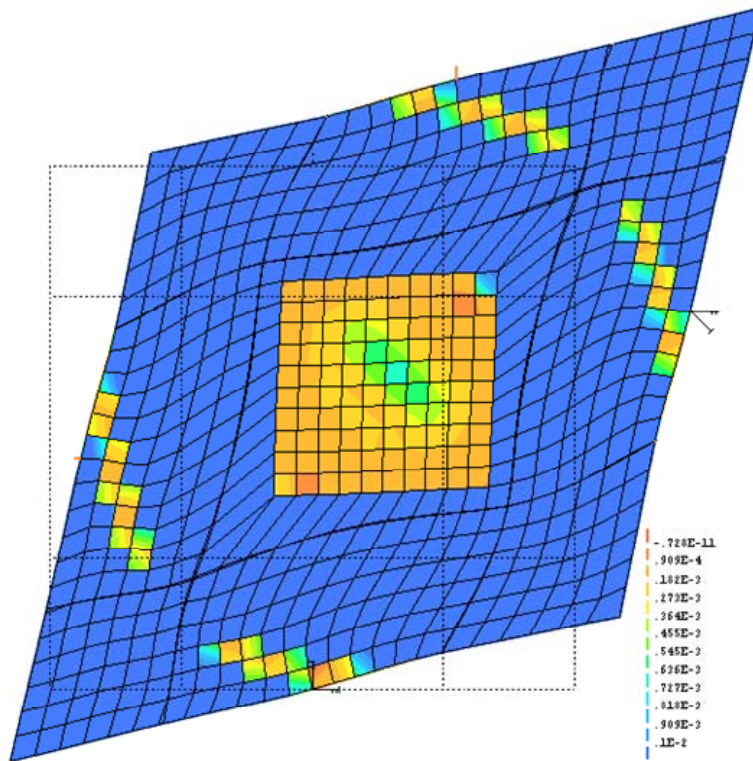
(c) At shear strain value 0.99



(d) At shear strain value 1.565



(e) At shear strain value 2.484



(f) At shear strain value 5.3

Figure 5.5 Shear deformation and crack patterns of A3 model



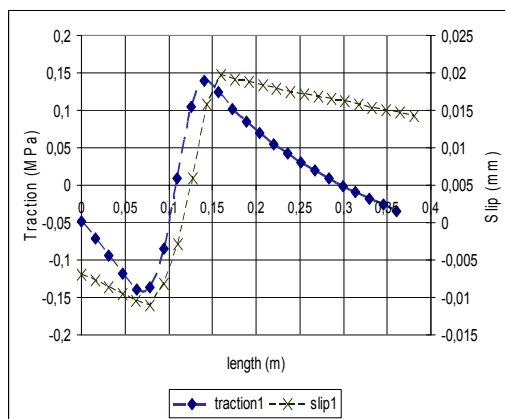
Figure 5.6 Scale for the contour plot of principle tensile strain

## 5.2.2 Bond-slip relation for reinforcement L1

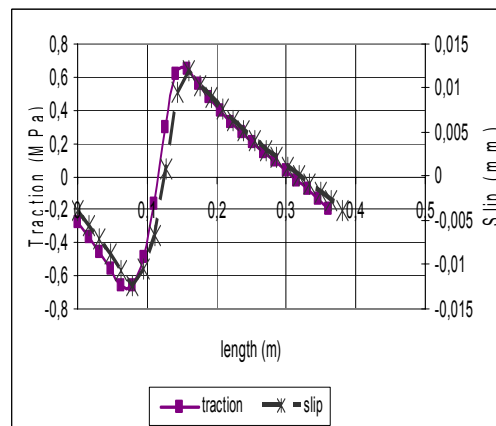
Slip was obtained as the difference between the displacements of concrete nodes and corresponding reinforcement nodes in the direction along the reinforcement. Traction stress was obtained as the traction along the local y direction of the interface element. Stress in the interface elements was higher at points where slip was higher i.e. at the region where crack crossed the reinforcement; see Figure 5.7. The slip and traction

were found to increase for a distance of the crack width and then starts to fall from the point where the concrete was intact to reinforcement. For example the crack appeared between the 6<sup>th</sup> and 10<sup>th</sup> element along reinforcement L1 at the shear strain value 0.276; see Figure 5.5 (b). Comparing the figure with the traction slip curve; see Figure 5.7(i) we can find that slip and traction curve started to increase from the 6<sup>th</sup> dot and then started to fall or reduce from 10<sup>th</sup> dot. Note that each dot in the slip curve represents a node along the reinforcement and each dot in the traction curve represents an element along the reinforcement.

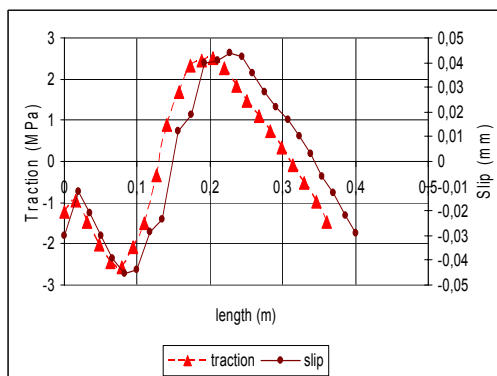
The values of the traction-slip curve matched with the bond-slip curve values for confined good bond conditions according CEB(1993); see Appendix I.



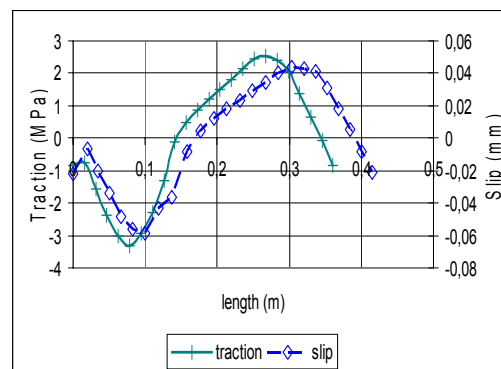
(i) At shear strain value 0.276



(ii) At shear strain value 0.99



(iii) At shear strain value 1.565



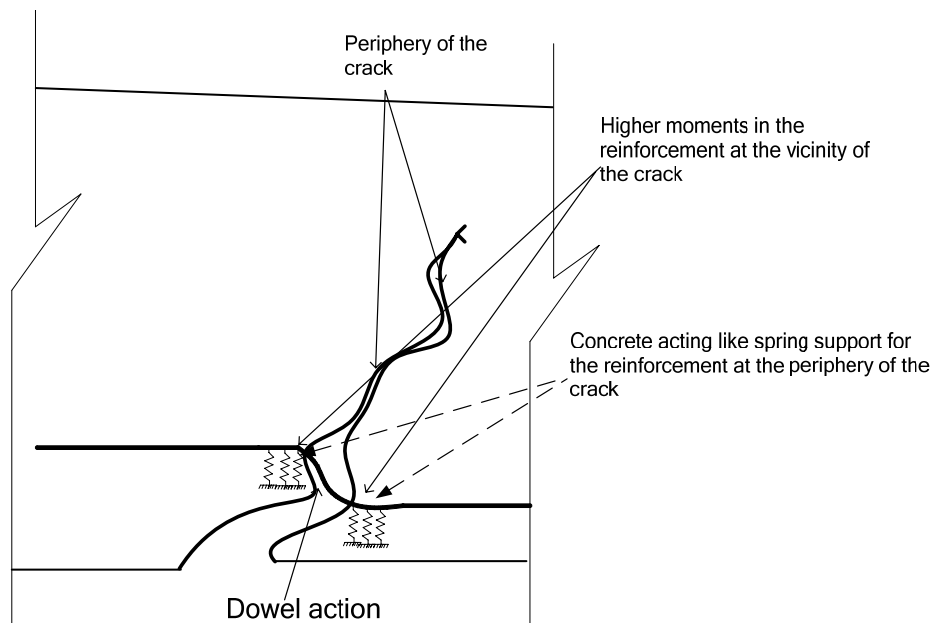
(iv) At shear strain value 2.484

Figure 5.7 Bond-slip curve for reinforcement L1 at different shear strain levels

### 5.2.3 Moments in the reinforcement L1

Distributed moment along the reinforcement was plotted using the moment data along the local z axis of the beam elements. The absolute value of the moment was high at the points where the bending of the reinforcement occurred due to the dowel action at

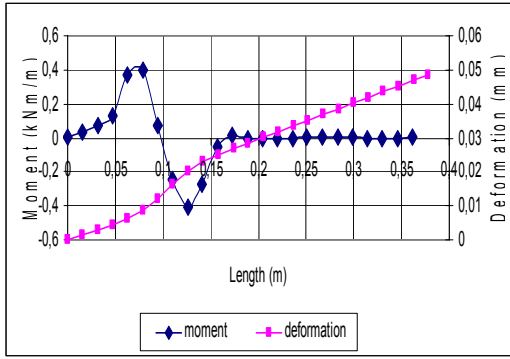
the crack interface. Concrete intact to the reinforcement at the periphery of the crack acts like an elastic spring support resisting the free translational movement of the reinforcement under the action of the shear force at the crack interface and hence the reinforcement bends like a beam holding the two sliding faces together; see Figure 5.8



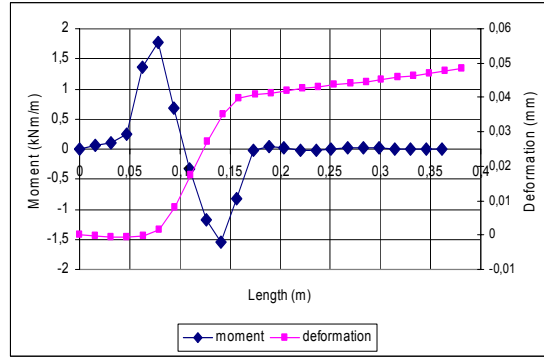
*Figure 5.8 Dowel action of reinforcement*

Relative displacement of the reinforcement in the direction perpendicular to the main axis of the reinforcement was plotted using the relative nodal displacements of the reinforcement nodes with respect to the first node of the reinforcement; see Figure 5.1. The bending of the reinforcement can be clearly seen at the stage of the first crack where a steep increase in the values of the relative displacement is seen; see Figure 5.9(ii). Note that each dot in the moment curve in the figure represents an element along the reinforcement and each dot in the deformation curve denotes a node along the reinforcement; see Figure 5.9.

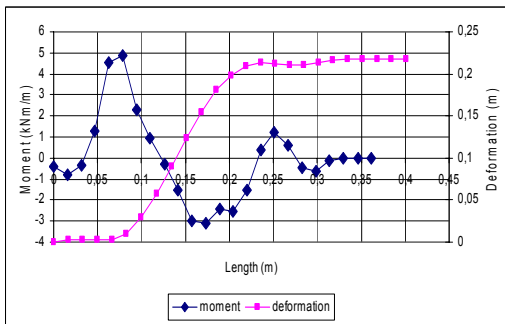
Beam elements made it possible to capture the bending moments in the reinforcement. Bending moment was high in the element closest to the periphery of the crack; it can be clearly seen at the first crack stage and in a few further stages in which concrete was not much deteriorated; see Figure 5.9(ii) and (iii). The values of bending moments increase with the increase in loading which was because of the increase in the shear deformation of the model and shear slip at the crack face; see Figure 5.5. The variation of the moments along the reinforcement L1 at various shear strain levels was as shown; see Figure 5.10.



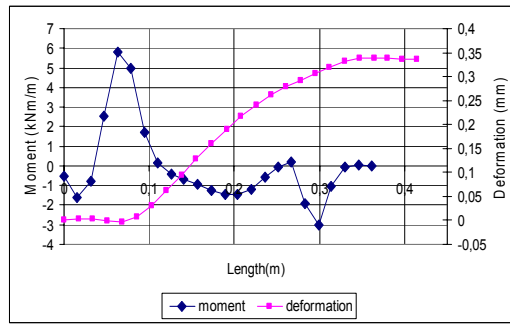
(i) At shear strain value 0.276



(ii) At shear strain value 0.99



(iii) At shear strain value 1.565



(iv) At shear strain value 2.484

Figure 5.9 Moments and bending of the reinforcement L1 at various shear strain levels

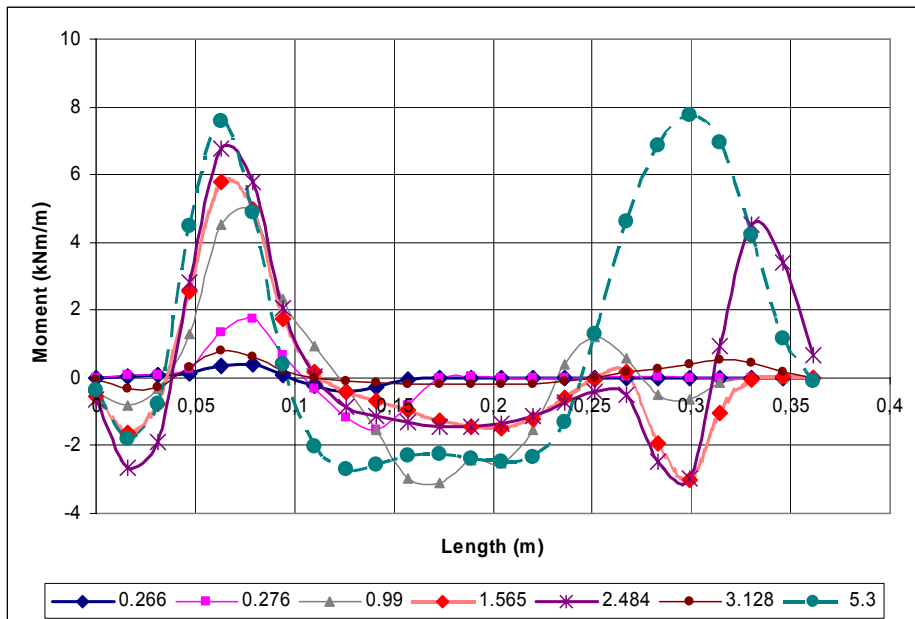
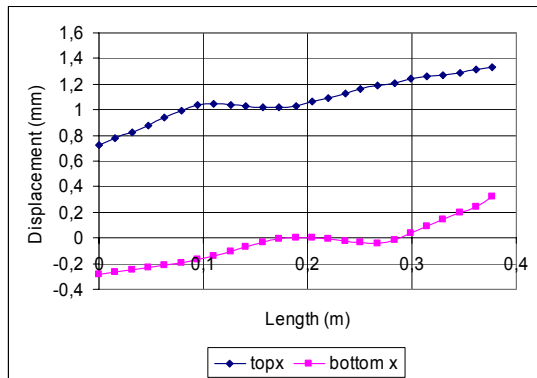


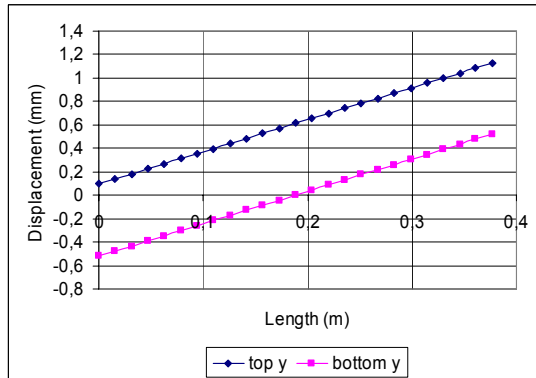
Figure 5.10 Bending moment variation along the reinforcement L1 for various shear strain levels

## 5.2.4 Deformation of the edges of the model

The condition of the edges at the final relevant deformed stage was checked. The applied tying allowed the edges to move in a straight line in the direction perpendicular to the edge; see Figure 5.11 (ii) and (iii); the nodes had the freedom to move unrestricted in along the edge direction, this is evident from the graph; see Figure 5.11 (i) and (iv).

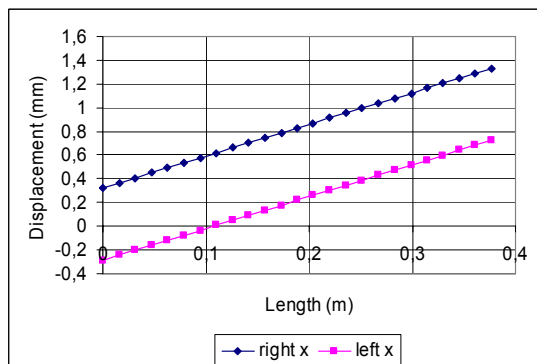


(i) Displacements in x direction

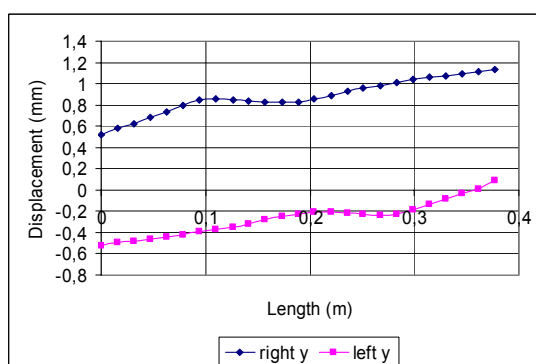


(ii) Displacements in y direction

(a)



(iii) Displacements in x direction



(iv) Displacements in y direction

(b)

Figure 5.11 Displacement of the nodes along the edges of the model (a) top and bottom edge (b) right and left edge, shear strain value 5.3

The edges of the model were parallel to each other. The values of the rotational displacement of the nodes of the opposite edges about global z axis was equal and hence it was evident that the edges were parallel to each other; see Figure 5.12

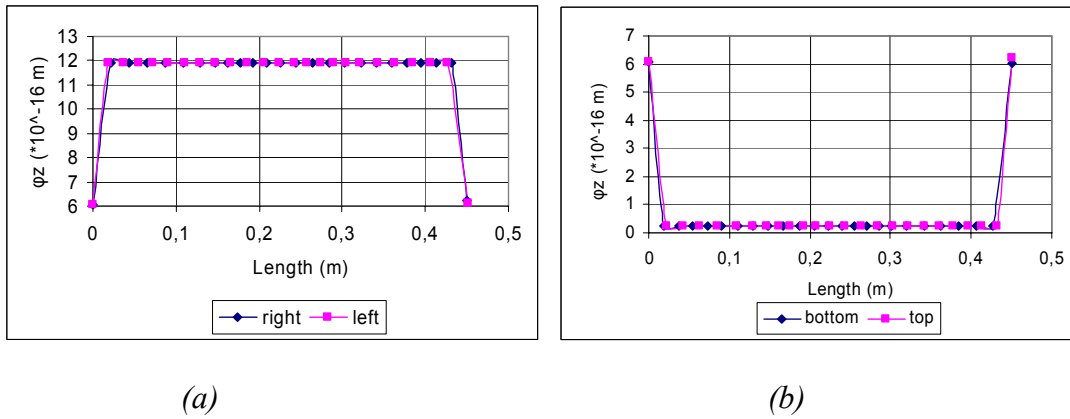


Figure 5.12 Rotational displacement of the edges about global z axis, (a) right and left edge (b) top and bottom edge, shear strain value 5.3

### 5.3 Panel A2

The shear stress-strain curve of the analysis agreed well with the shear stress-strain curve of the test; see Figure 5.13

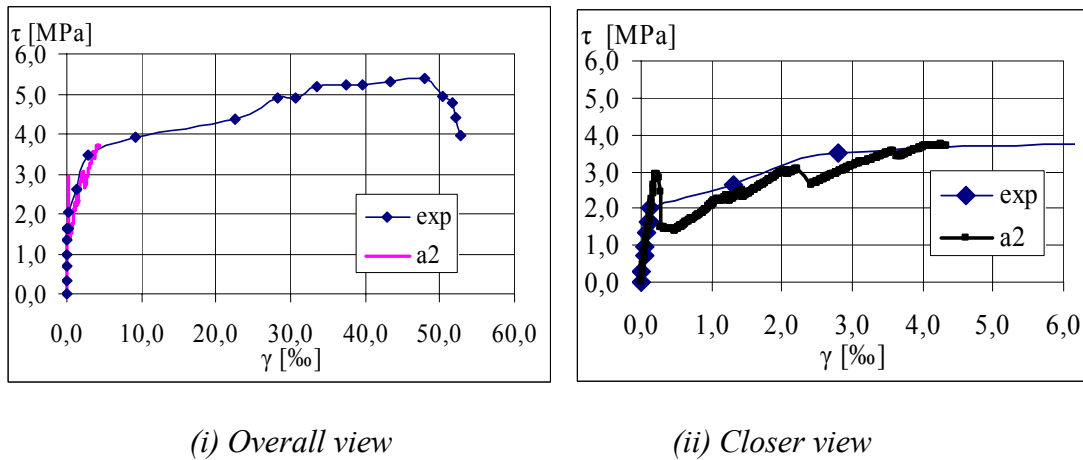


Figure 5.13 Shear stress strain curve for A2 model

The shear stress strain curve was plotted as long as the deformation of the model was reasonable for the applied prescribed deformation values. The model behaved similar like the test panel until the first crack appeared and later after the cracking the behaviour of the model was less stiff compared to the test. This could be due to the reason the aggregate interlock factor was not taken into account in the model. The shear deformation of the model was irrelevant after the reinforcements L1 and T1 yielded. The stress in the reinforcement at the final relevant deformed stage was as shown; see Figure 5.14

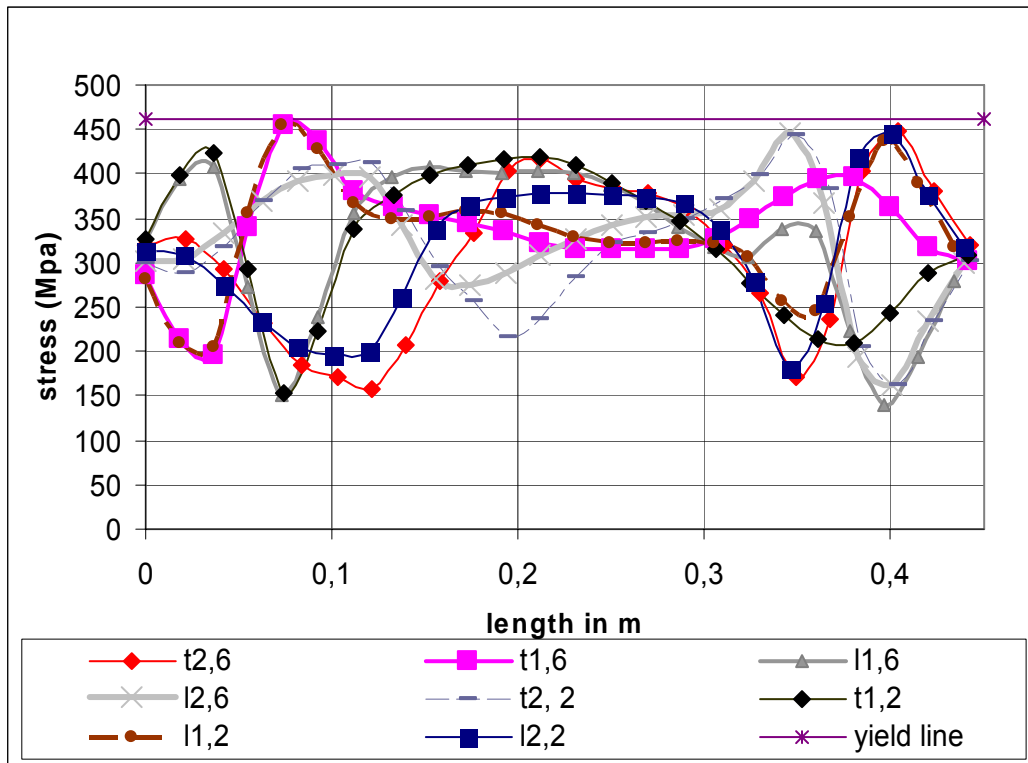
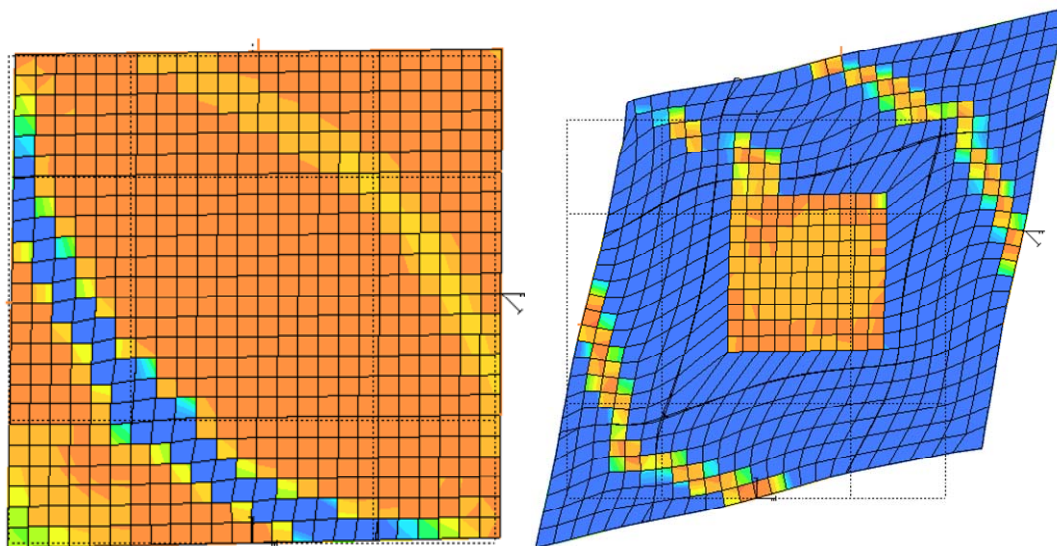


Figure 5.14 Stress in the reinforcements at the final relevant deformed state (shear strain value 4.35)

### 5.3.1 Crack pattern and shear deformation

The crack patterns were similar to the crack patterns of A3 but with minute differences. The first and the final relevant deformed state were as shown; see Figure 5.15 (i) for the first crack stage and (ii) for the last crack stage. The first crack stage occurred at shear strain value 0.28 and final crack stage occurred at shear strain value 4.35. When the final deformed state of panel A3; see Figure 5.5(g) and panel A2; see Figure 5.15 (ii) were compared it can be inferred that the concrete in the panel with higher reinforcement ratio i.e. panel A3 has less amount of concrete left than in the panel with lower reinforcement ratio. This was because the steel yielded in the panel with lower reinforcement ratio and hence the shear deformation of the panel was higher and hence the concrete was not crushed or disintegrated as in the panel with higher reinforcement ratio.



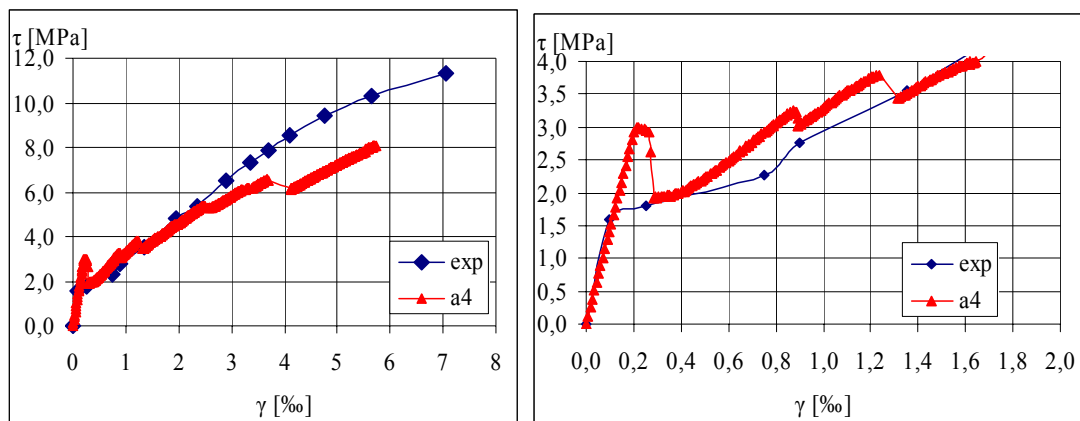
(i) At shear strain value 0.28

(ii) At shear strain value 4.35

Figure 5.15 First and the last crack stage of the A2 model

## 5.4 Panel A4

The shear stress-strain curve of the model agreed well with the shear stress-strain curve of the test; see Figure 5.16.



(i) Overall view

(ii) Closer view

Figure 5.16 Shear stress strain curve for A4 model

The model behaved similar like the test panel until the first crack appeared; after cracking the behaviour of the model was less stiff compared to the test. At the final relevant deformed state the stress in reinforcements; see Figure 5.17 were well below the yield value of the reinforcements; the failure happened in this case due to crushing of concrete or due to much of concrete in the model had deteriorated; see Figure 5.18(ii).

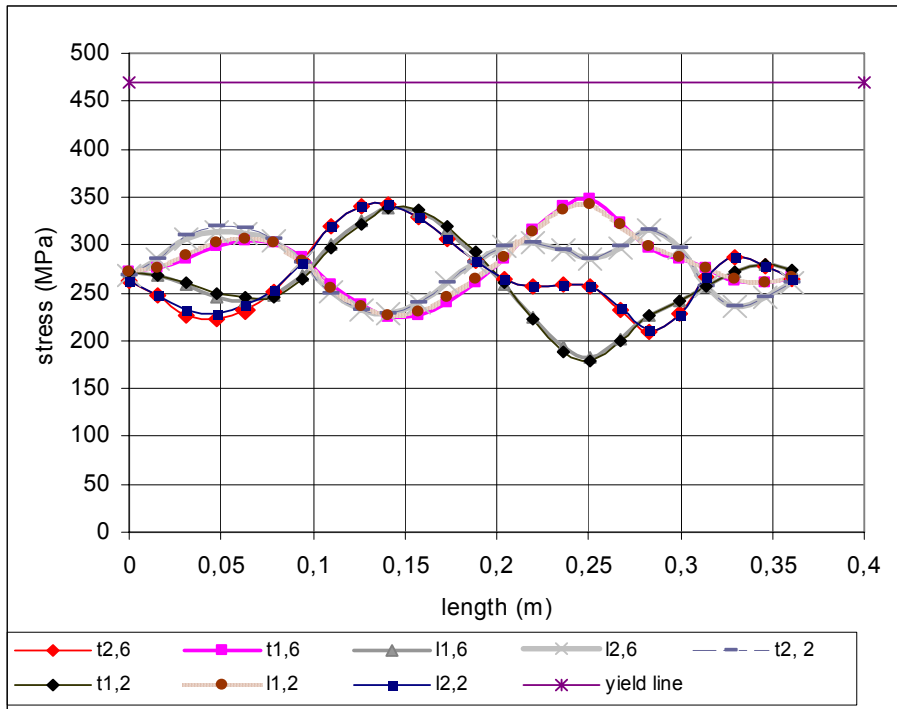
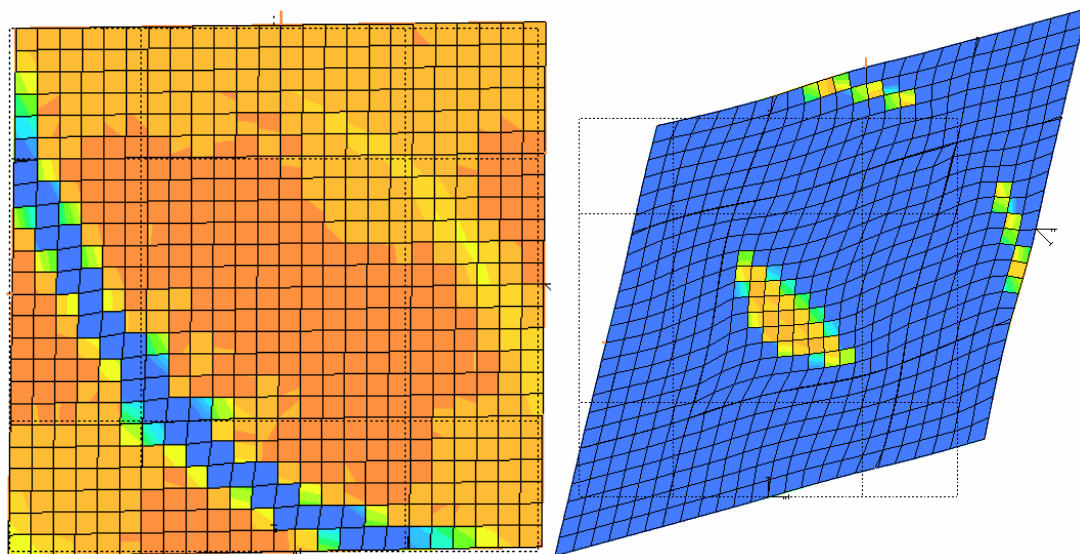


Figure 5.17 Stress in reinforcements at the final relevant deformed state (shear strain value 5.726)

### 5.4.1 Crack pattern and shear deformation



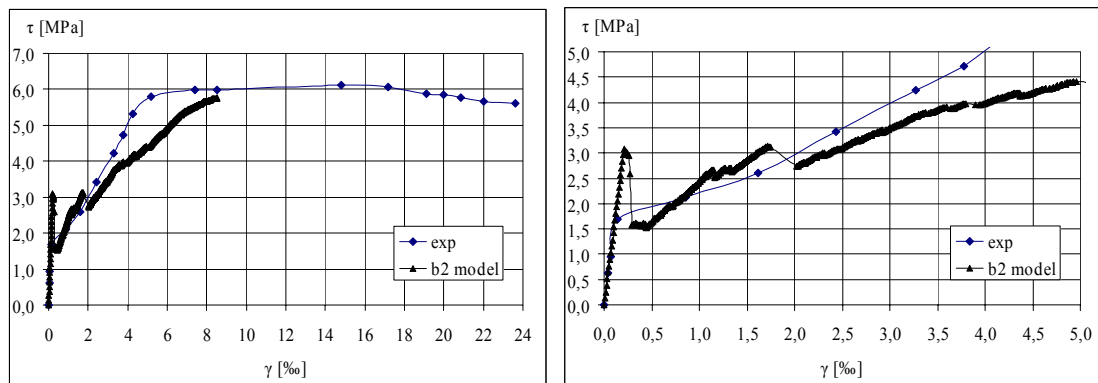
(i) At shear strain value 0.2823

(ii) At shear strain value 5.726

Figure 5.18 First and final relevant deformed state for A4 model

## 5.5 Panel B2

The shear stress-strain curve of the analyses agreed well with the test; see Figure 5.19. The slope of the shear stress strain curve became lesser and started to fall rapidly after the yielding of the transverse reinforcement. However, as soon as the longitudinal reinforcement yielded the shear deformation of the model was irrelevant. The behaviour of the panel was relevant until the longitudinal reinforcement L1 had yielded, before the yielding of the longitudinal reinforcement L1 the transverse reinforcements yielded and were hardening; see Figure 5.20.



(i) Overall view

(ii) Closer view

Figure 5.19 Shear stress strain curve for B2 model

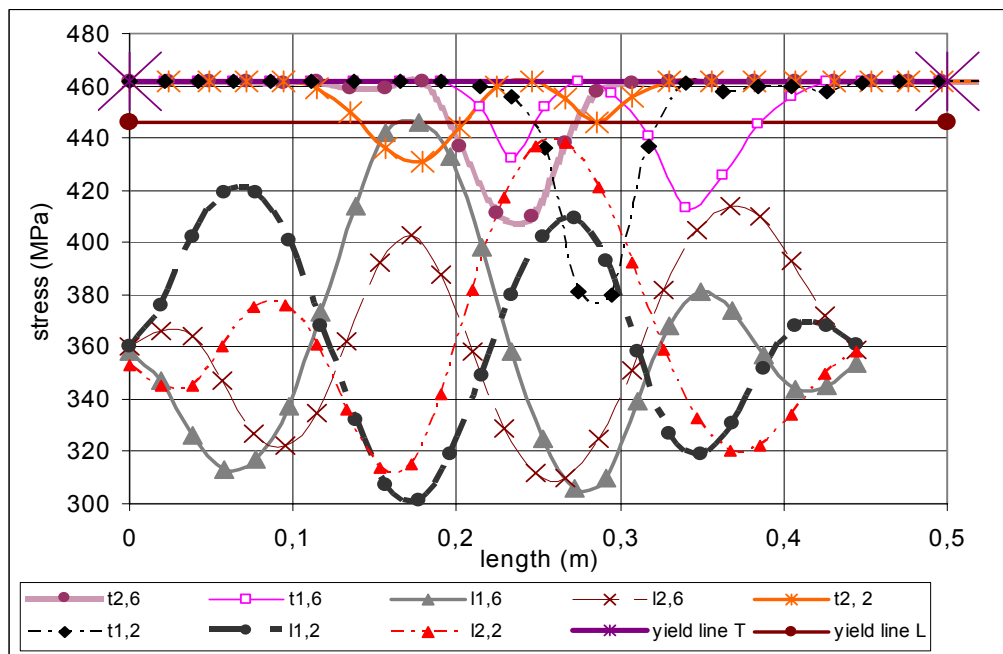
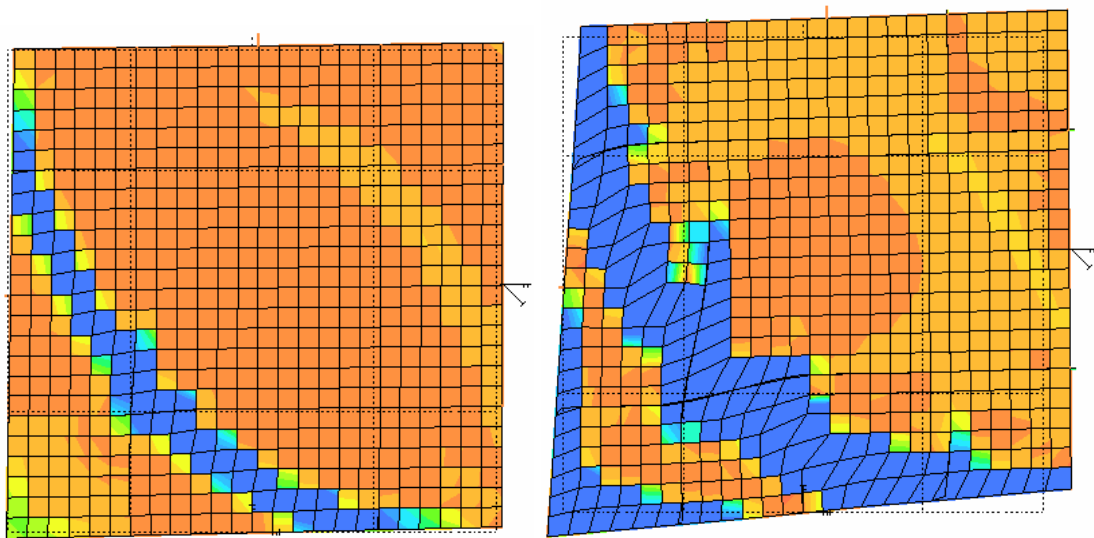


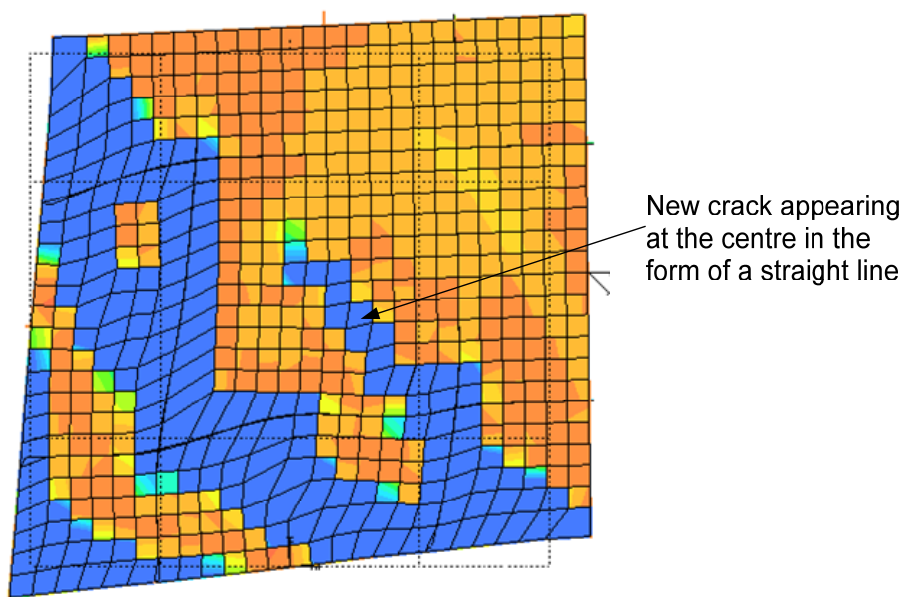
Figure 5.20 Stress in the reinforcement at the final relevant deformed state, shear strain value 8.54

### 5.5.1 Crack pattern and shear deformation

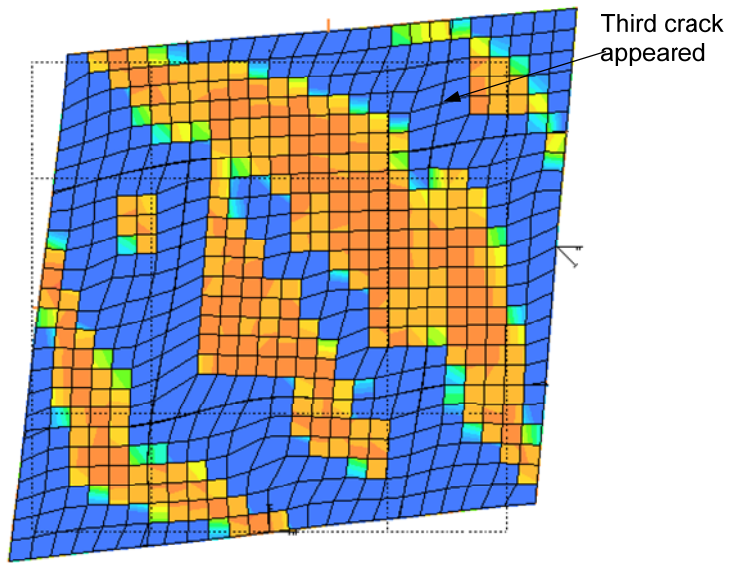
The crack patterns were marginally different when compared with the crack patterns of panels A. The crack patterns of panel B2 at certain important stages are displayed; see Figure 5.21(a-f). The first crack pattern was similar when compared with the rest of the models. However, as the loading was further increased the patterns were different when compared with the crack patterns of panels A. A crack developed at the centre of the model at shear strain value 1.34 which was nearly like a straight line. The third crack developed at shear strain value 2.02, model was able to capture relevant shear deformation of the panel till shear strain value 8.54 when the longitudinal reinforcement L1 started to yield.



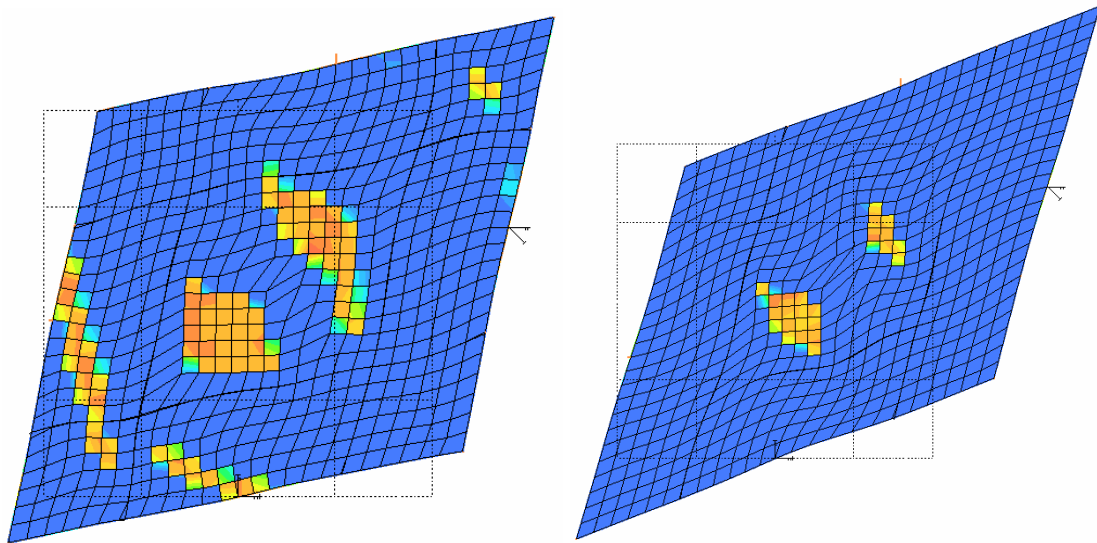
(a) At shear strain value 0.28      (b) At shear strain value 1.0



(c) At shear strain value 1.34, a straight crack formed at the centre of the model



(d) At shear strain value 2.02



(e) At shear strain value 4.5

(f) At shear strain value 8.54

Figure 5.21 Crack pattern and shear deformation of B2 model

The moments in the reinforcement due to dowel action, bond-slip relationship in the interface elements and the movements of the edges were similar to the panels A.

## 5.6 Panel B1

Shear stress-strain curve of the analyses agreed well with the shear stress-strain curve of the test; see Figure 5.22. Shear deformation of the model was relevant till shear strain value 4.29, at this shear strain level longitudinal reinforcement L1 yielded and transverse reinforcements were in their hardening stage; see Figure 5.23. The first crack appeared when the principle tensile stress reached the tensile strength of concrete. When  $\sigma_I=f_{ct}$ , micro cracks started to appear, leading to a first fully developed crack. After the first crack appeared, the behaviour of the model was less stiff compared to the test. The slope of the curve changed rapidly after the yielding of the transverse reinforcements. When loading further the longitudinal reinforcement yielded, the shear deformation of the model was irrelevant after the yielding of the longitudinal reinforcement L1.

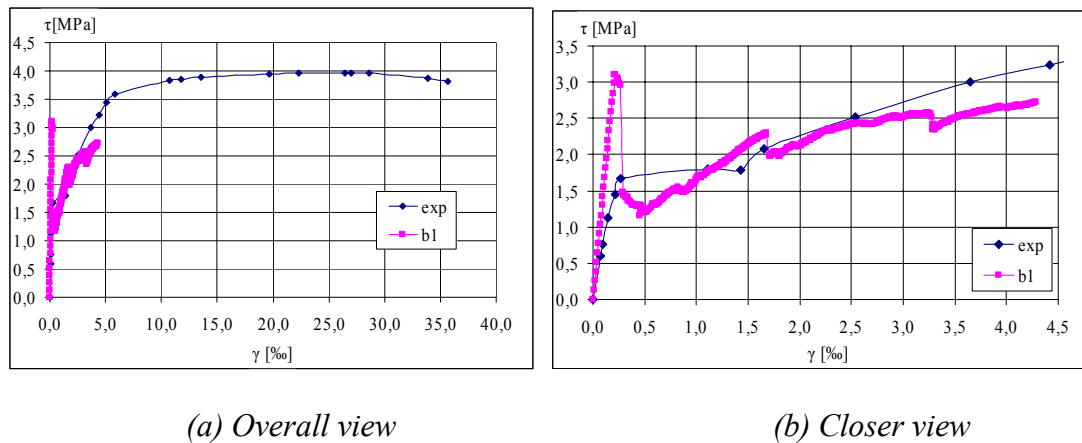


Figure 5.22 Shear stress strain curve for model B1

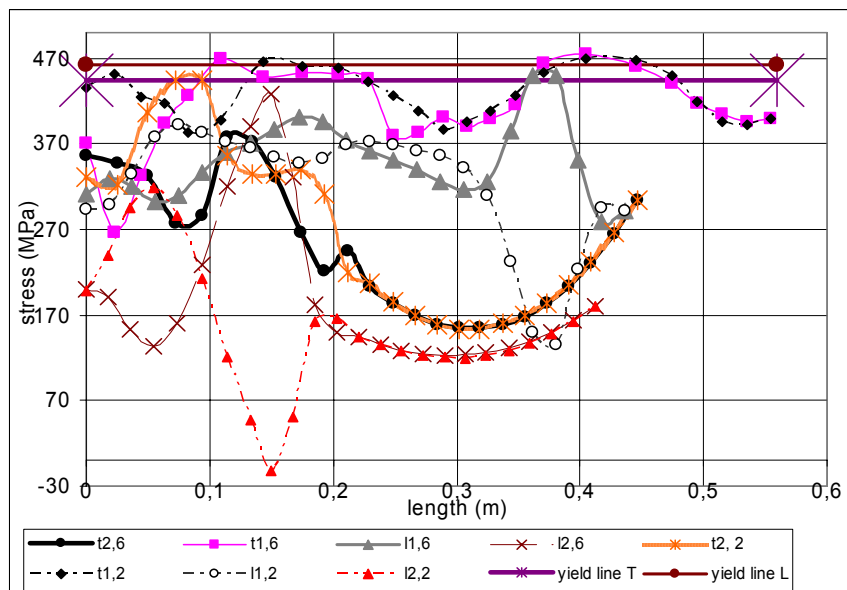


Figure 5.23 Stress in the reinforcements at the final relevant deformed state, shear strain value 4.29

### 5.6.1 Crack Pattern and shear deformation

The crack patterns of the analyses were as shown; see Figure 5.24(a-d). The first crack pattern was similar with the other analyses. The second crack developed more like a straight line as in model B2; see Figure 5.21(c), on further loading the second crack connected with the first crack. When the loading was further increased, the crack increased in its width and no new cracks were formed.

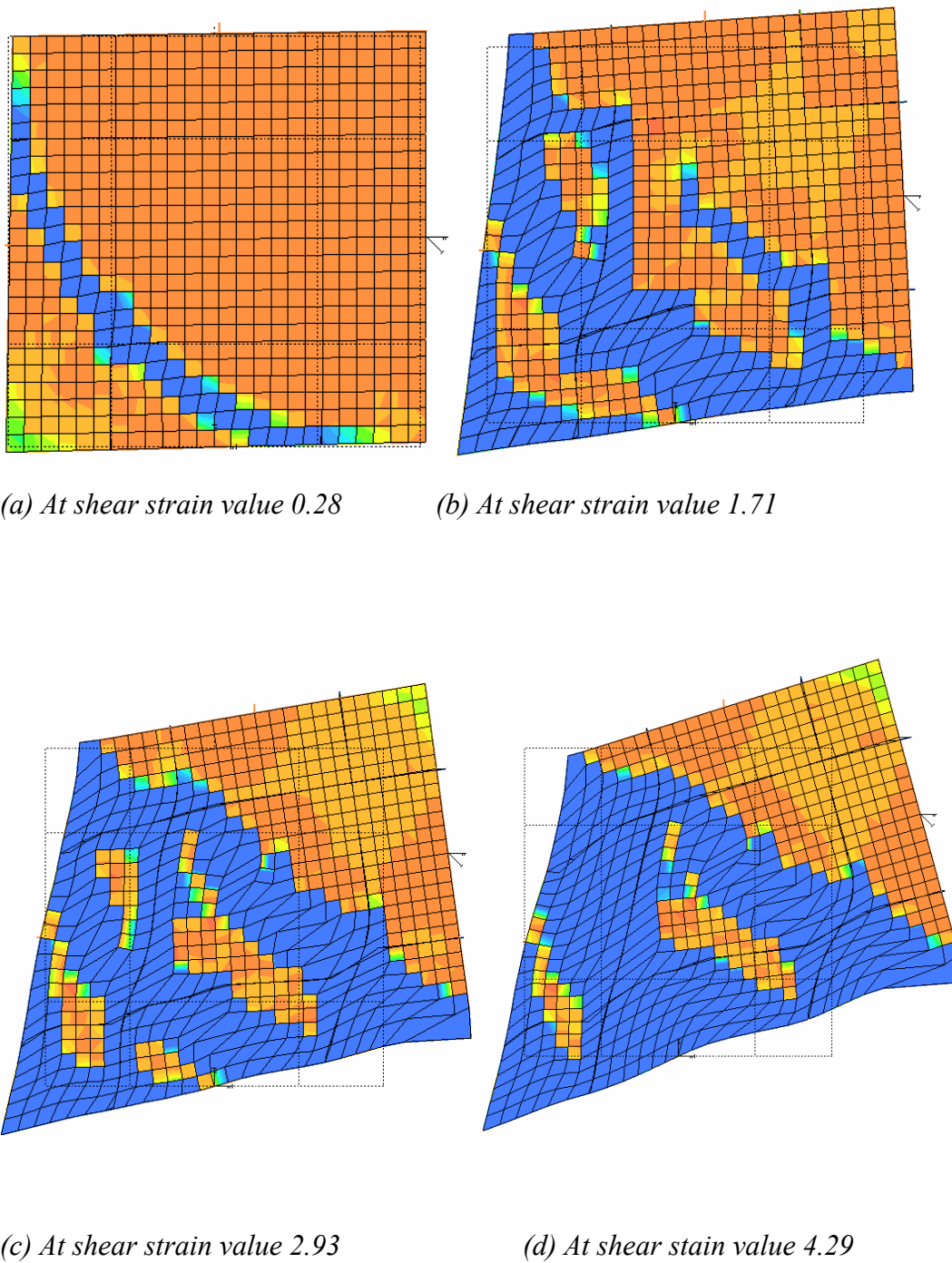
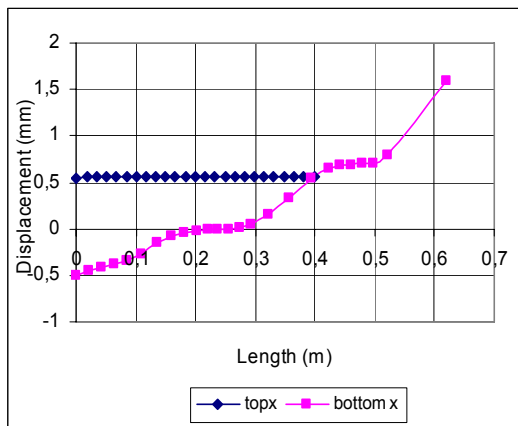


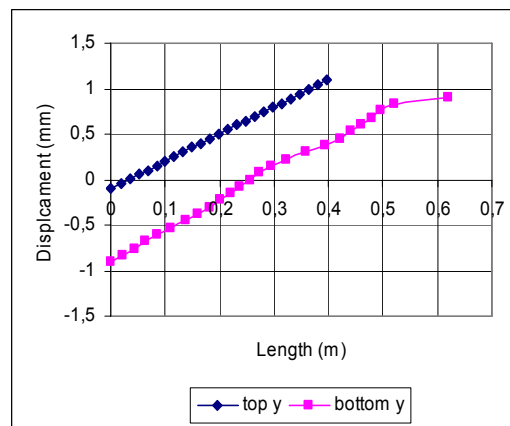
Figure 5.24 Crack pattern and shear deformation of model B1

### 5.6.1.1 Deformation of the edges of the model

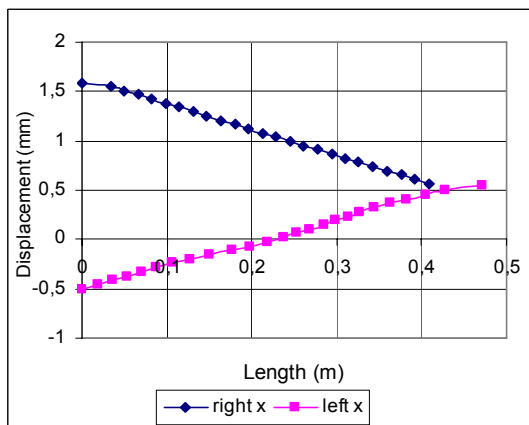
The edges of the model at the final relevant deformed state were not perfectly straight in the direction perpendicular to the edges, the bottom edge was slightly curved at the ends; see Figure 5.25(b) and the same case with the left edge; see Figure 5.25 (c). However the model was capable to simulate the behaviour until the longitudinal reinforcement L1 yielded. The nodes along the edges were allowed to move freely in along the edge direction; see Figure 5.25 (a & d). The rotational displacement of the nodes of the edges about the z axis was equal except for the corner nodes; see Figure 5.26.



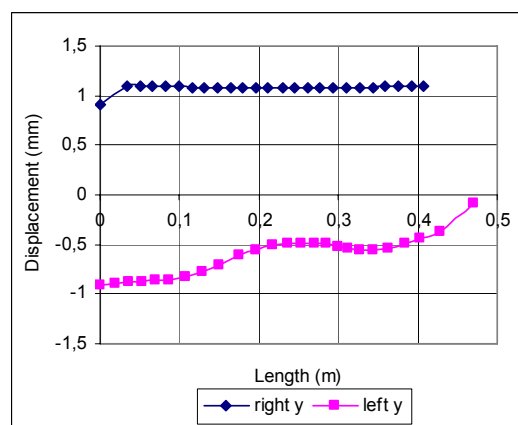
(a) Displacement in x direction



(b) Displacement in y direction

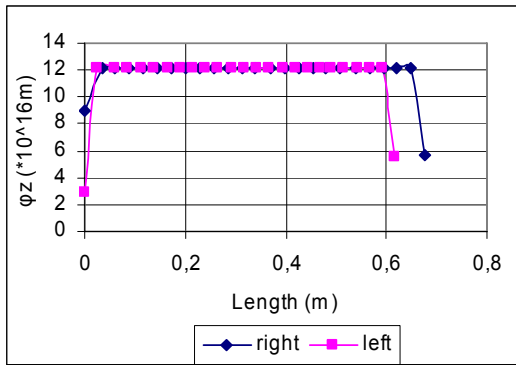


(c) Displacement in x direction

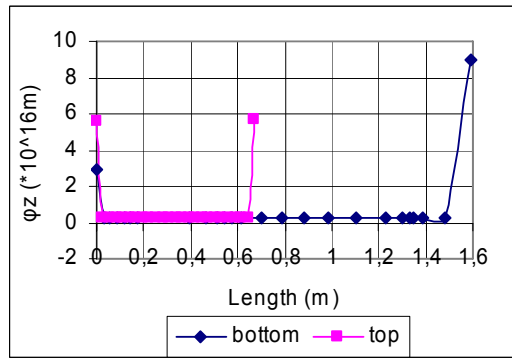


(d) Displacement in y direction

Figure 5.25 Deformation of the edges at the final relevant deformed state, shear strain value 4.29



(i) right and left edge

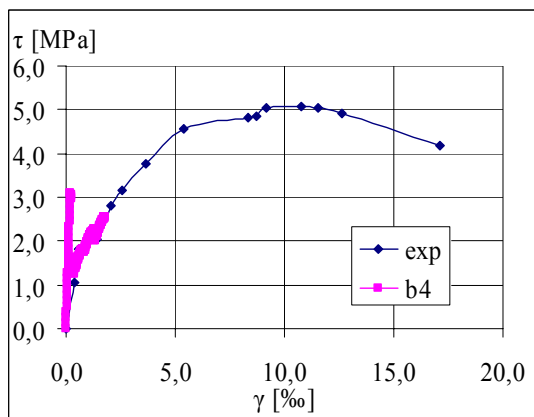


(ii) bottom and top edge

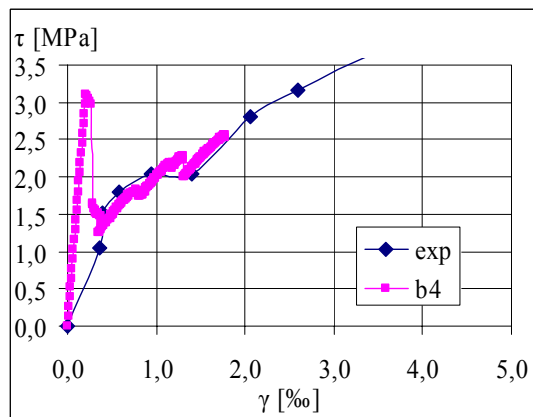
Figure 5.26 Rotational displacement of the edges about global z axis, (a) right and left edge (b) top and bottom edge, shear strain value 4.29

## 5.7 Panel B4

The shear stress-strain curve of the analyses agreed well with the shear stress-strain curve of the test; see Figure 5.27. The model started to exhibit irrelevant deformed shape very early when compared model B2 this may be due to the large difference in the reinforcement ratio of the panel; see Section 4.2.5.2. The stress in the reinforcements at the final relevant deformed state at shear strain value 1.29 was as shown; see Figure 5.28. Colossal difference can be observed in the stress value between longitudinal and transverse reinforcements. In the transverse reinforcements stresses were much higher when compared with the stress in the longitudinal reinforcements. Transverse reinforcement T1 will soon yield within further few stages of loading.



(i) Overall view



(ii) Closer view

Figure 5.27 Shear stress strain curve for B4 model

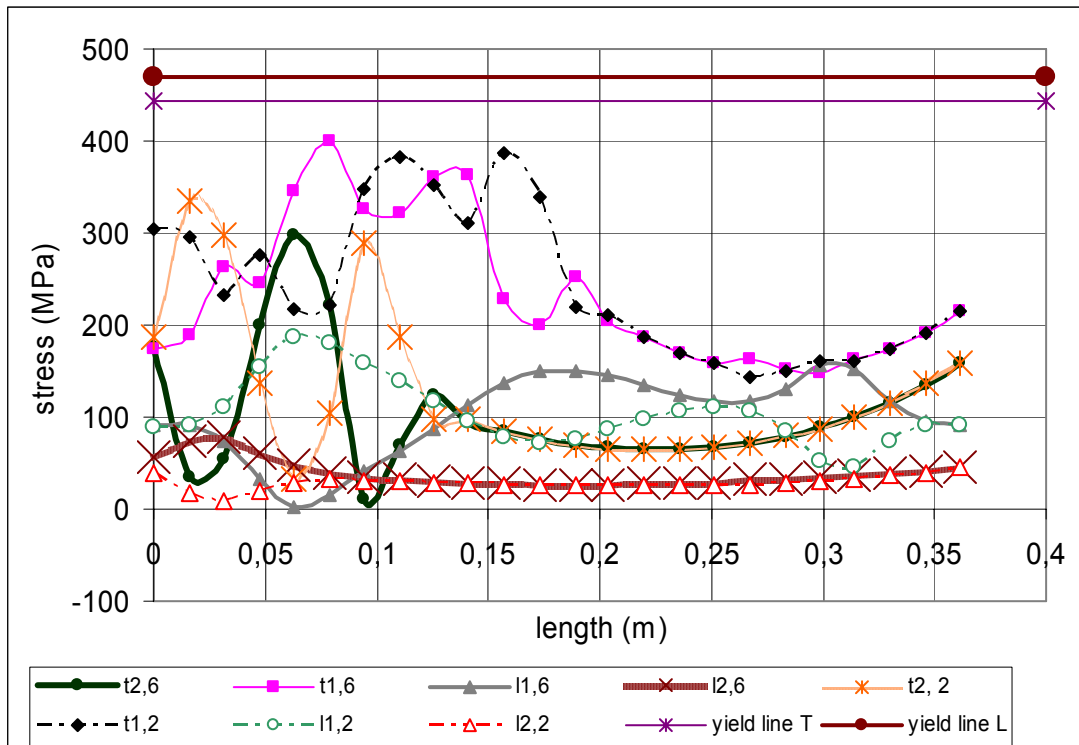
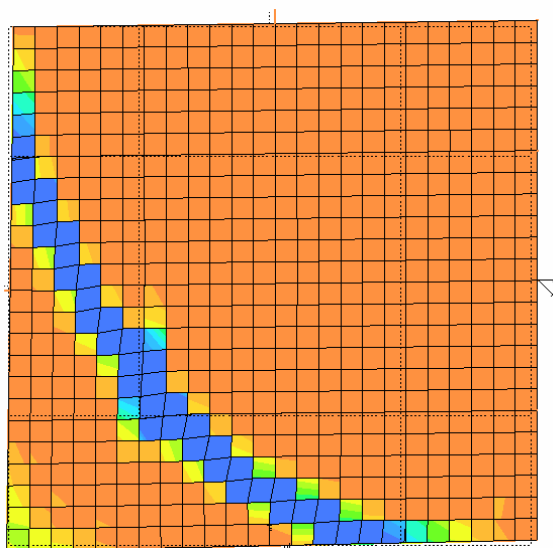


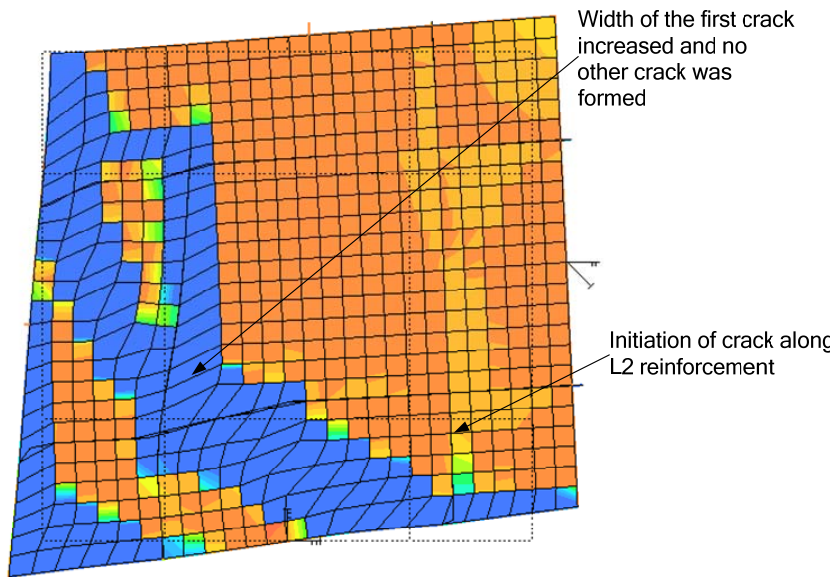
Figure 5.28 Stress in reinforcements for final relevant deformed state, shear strain value 1.29

### 5.7.1 Crack pattern and shear deformation

The first crack pattern; see Figure 5.29 (a) was very similar to the other panels, but the final crack pattern was different when compared with the above discussed models. At the final relevant deformed state there was only a fully developed crack; see Figure 5.29 (b) the first crack developed and increased in width as the loading increased. The crack developed along the longitudinal reinforcement L1 increasing in size.



(a) First crack appeared at shear strain value 0.30



*(b) Final crack pattern at shear strain value 1.29*

*Figure 5.29 Crack pattern and shear deformation of B4 model*

## **6 Conclusion**

### **6.1 General conclusion**

In the project, an interior unit of a shear panel tests conducted at the University of Houston by Pang and Hsu (1992) were modelled. The model was built up by using plane stress elements for concrete, beam elements for reinforcement and structural interface elements to represent the bond-slip phenomenon between concrete and reinforcement. The model was verified by performing simple tension analyses in a deformation controlled process. In the verification analyses, models made of higher and lower order elements were analysed to choose a model which would perform the shear analyses in a better manner and to make sure that the constituents of the model such as the bond-slip relationship in the interface elements, hardening of the reinforcement etc were working properly. It was found that in the deformation controlled process, the drop-down in the load-deformation curve at the first crack stage can be captured and that the analyses were faster and more stable compared to a force controlled process. A model with lower order elements and loaded by a deformation controlled process was selected for shear analyses.

In the shear analyses, six different models corresponding to the six different panel tests A2, A3, A4, B1, B2 and B4 were modelled. A statically determined loading beam system was created to load the model with pure shear load in a deformation controlled process. Prescribed deformation was applied at a loading point in the beam system which transfers the load through the system of beams to the model. Appropriate connections were made between the loading beam system and the model to cause the shear deformation of the model based on the deformation of the loading beam system. The model was provided with appropriate boundary conditions to satisfy the compatibility of the model with the shear deformation of the test panel. Dummy elements were provided when necessary to able to perform the shear analyses successfully.

The shear stress-strain curves of the analyses agreed well with the shear stress-strain curve of the tests. The model was able to capture shear behaviour of the panel tests. Dowel action and bond-slip phenomenon were reflected realistically by the model. It was shown that a small interior part of a structure can be successfully modelled, using appropriate boundary conditions, to simulate the shear behaviour of reinforced concrete.

### **6.2 Drawbacks**

Even though the model was able to predict the shear behaviour in an appropriate manner, the model had some drawbacks. After the first cracking occurred, the behaviour simulated by the model was not perfect when compared to the test, which may be due to the fact that aggregate interlock was not taken into account.

The crack that developed in the analyses, were in the form of a curved shape rather than being fairly straight since they were influenced by the edge effect of the applied boundary conditions. The boundary conditions made the crack to follow a curved path rather than a straight path. The modelled unit was 3.6% of the volume of the original panel; if the dimensions of the modelled unit are increased, the cracks may propagate

more freely with only a marginal influence in the central part from the boundary conditions applied at the edges. The model was functioning very well for the panels with a low reinforcement ratio difference or for panels with similar reinforcement ratio in orthogonal directions. However, for the panels with very large difference in reinforcement ratio, the model was able to predict the behaviour only for a short loading period because the transverse reinforcement yielded at a much earlier stage than the longitudinal reinforcement. On further loading, the analysis resulted in unrealistic response.

### 6.3 Suggestions for future work

The drawbacks of the model can be solved by modelling a larger unit or by modelling the entire panel with its original dimensions and half the thickness. Mesh density is coarse for the outer 4/5<sup>th</sup> of the model and finer for the interior unit in the model. Embedded reinforcements for the coarse part or bond-slip relationship can be applied but with coarse interface elements for the coarse part of the model. Detailed material properties such as bond-slip relationship, hardening of reinforcement and other conditions can be applied to the finer interior unit of the model. Boundary conditions to keep edges straight and make opposite edges to rotate parallel can be applied to the outer boundary of the model; boundary condition for the relative slip between reinforcement and concrete nodes at the edges can be neglected. The loading beam system is now connected to the outer edges of the model and hence the interior unit is now free to deform in its own manner without any boundary control at its periphery.

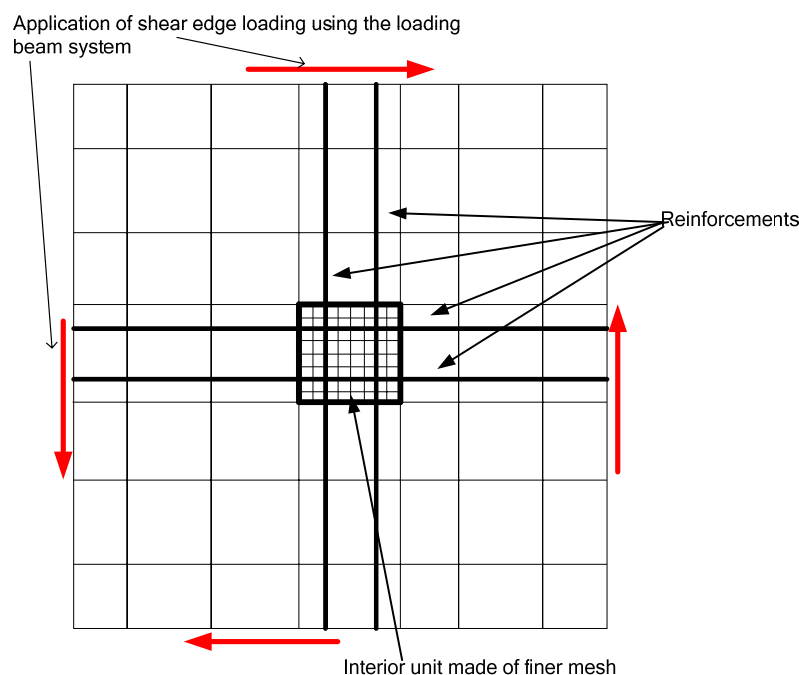


Figure 6.1 Rough sketch of a suggested model for future work

With such an improved model, the following variations can be modelled and the effects of the parameters on shear capacity can be studied.

- Changing the spacing of reinforcement in the model, with symmetrical spacing in orthogonal directions and with asymmetrical spacing in orthogonal directions
- Changing the type of reinforcement i.e. to use hot rolled or cold drawn plain bars and hot rolled ribbed bars in orthogonal directions.
- A welded mesh made of different types of bars such as hot rolled or cold drawn plain bars and hot rolled ribbed bars. A welded mesh can be created by locking the reinforcement nodes at intersections.
- Different material models for the constituents of the model.
- Different element type such as plane stress elements with drilling rotational degree of freedom etc.
- Changing the mesh density but involves additional work due to the changes to be made in the loading beam system, if the model is loaded by deformation control process.
- The aggregate interlock factor can be studied by modelling the crack interface separately using the dilatancy models available in Diana; see TNO Diana manual (2005) particularly Section 9.3.2.2. The crack dilatancy models can be applied at the crack interface represented by interface elements.
- While using the crack dilatancy models the aggregate size can be varied to study the effect of aggregate size in aggregate interlock factor in shear contribution.

A 3-D model can be made for the entire panel using the above mentioned method.

The same changes as mentioned for a 2D model can be implemented.

- The different bond-slip scheme can be used; Confined good bond condition was used in the analysed models of this project.
- The effect of concrete cover can also be studied by varying the concrete cover.

## 7 References

- Ashour A.F, Alovarex L.F. and Toropov V.V. (2003): Empirical modelling of shear strength of RC deep beams by genetic programming. *Computers and Structures*, Vol.81, No.03, 2003, pp.331-338
- Broo H. (2006): *Design and assessment for shear and torsion in prestressed concrete bridges*, Report 2006:2. Department of Civil and Environmental engineering, Chalmers University of Technology, Göteborg, Sweden, 2006, pp.48
- Broo H., Plos M., Lundgren.K and Engström B. (2007a): Reinforced and prestressed concrete beams subjected to shear and torsion. Accepted for publication, 6<sup>th</sup> *International conference on Fracture Mechanics of Concrete and Concrete Structures* (FraMCoS-6)
- Broo H., Plos M., Lundgren K. and Engström B. (2007b): Simulation of shear-type cracking and failure with non-linear finite element method. Accepted for publication in *Magazine of Concrete Research* 2007.
- CEB (1993): *CEB.FIP Model Code 1990*, Bulletin d'Information 213/214, Lausanne, Switzerland, 1993.
- CEN/TC250/SC2 (2004): Eurocode2: *Design of concrete structures Part2: Concrete bridges Design and detailing rules Stage 49*, European Committee for Standardization, Brussels, 2004.
- Collins M.P. and Mitchell D. (1991): *Prestressed Concrete Structures*, Prentice Hall, Englewood Cliffs, New Jersey, 1991.
- Engström B. (2005): *Design and analysis of prestressed concrete structures*, Educational 04:13. Department of Structural Engineering and Mechanics, Chalmers University of Technology, Göteborg, Sweden.
- FIB (1999): *fib Bulletin 1: Structural concrete – Text book on behaviour, design and performance*, vol-1, International federation for Structural concrete (*fib*), Lausanne, Switzerland, 1999, 224 pp.
- He X.G. and Kwan A.K.H. (2001): Modelling dowel action of reinforcement bars for finite element analysis of concrete structures. *Computers and Structures*, Vol.79, No. 01, 2001, pp.595-604
- Hordjik D.A., Cornelissen H.A.W. and Reinhardt H.W. (1986): Experimental determination of crack softening characteristics of normalweight and lightweight concrete. *Heron*, Vol 31, No.2, 1986
- Hsu T.T.C. and Zhu R.R.H. (2002): Softened membrane model for reinforced concrete elements in shear. *ACI Structural Journal*, Vol. 99, No.4, July – August, pp.460-469.
- Kaufmann W. and Marti P. (1998): Structural concrete: Cracked membrane model. *Journal of Structural Engineering*, Vol.124, No.12, pp.1467-1475.

- Pang X. and Hsu T.T.C. (1992): *Constitutive laws of reinforced concrete in shear*, Research report UHCEE92-1. Department of Civil and Environmental engineering, Division of Concrete structures, Houston, Texas, 1992, pp.180
- Pang X.B.D. and Hsu T.T.C. (1995): Behaviour of reinforced concrete membrane elements in shear. *ACI Structural Journal*, Vol. 92, No. 6, November – December, pp. 665-679.
- Pang X.B.D. and Hsu T.T.C. (1996): Fixed angle softened truss model for reinforced concrete. *ACI Structural Journal*, Vol. 93, No. 2, March – April, pp. 197-207.
- Plos M. (2000): *Finite element analyses of reinforced concrete structures*, Compendium 96:14. Department of Structural Engineering and Mechanics, Chalmers University of Technology, Göteborg, Sweden.
- Razaqpur G.A., Isgor B.O., Greenway S. and Selley A. (2004): Concrete contribution to the Shear resistance of Fibre reinforcement polymer reinforced concrete members. *ASCE*, Vol.8, No.5, pp.452-460
- Soltani M., An X. and Maekawa K. (2005): Localized nonlinearity and size-dependant mechanics of in-plane RC element in shear. *Engineering structures*, Vol.27, No.05, 2005, pp.891-908
- Soltani M., An X. and Maekawa K. (2003): Cracking response and local stress characteristics of RC membrane elements reinforced with welded wire mesh. *Cement & Concrete Composites*, Vol. 26, N0.03, 2003. pp.389-404
- TNO 2005. DIANA Finite Element Analysis: User's Manual release 9.1, TNO DIANA BV, Delft, The Netherlands, 2005.
- Thorenfeldt E., Tomaszewicz .A., and Jensen .J.J. (1987): Mechanical properties of high-strength concrete and applications in design. *Proc.Symp.Utilization of High-Strength Concrete*, Stavanger, Norway, 1987.
- Vecchio F.J. (2000b): Distributed Stress Field model for Reinforced concrete: Formulation. *Journal of Structural Engineering*, Vol.126, No.9, September, pp.1070-1077
- Vecchio F.J. and Collins M.P. (1986): The modified compression .field theory for reinforced concrete elements subjected to shear. *Journal of the American Concrete Institute*, Vol.83, No.2, March-April, pp.219-231.
- Vecchio F.J. and Collins M.P. (1993): Compression response of cracked reinforced concrete. *Journal of Structural engineering*, Vol.119, No. 12, (1993), pp. 3590-3610.

# APPENDIX A: Tension analyses using lower order elements

## Analysis Type 1a

The first visible crack was observed at prescribed deformation value of 0.1 mm.

The crack initiated at deformation value 0.03 mm; see Figure A. 26 and the yielding of steel occurred at 0.84 mm; see Figure A. 1.

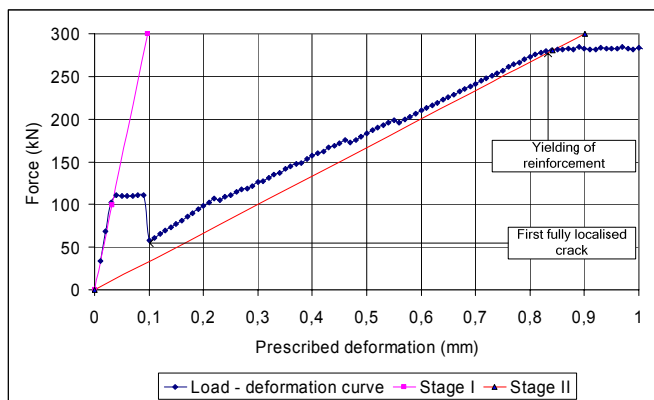


Figure A. 1 Load – Deformation curve

## The evolution of the crack pattern and propagation

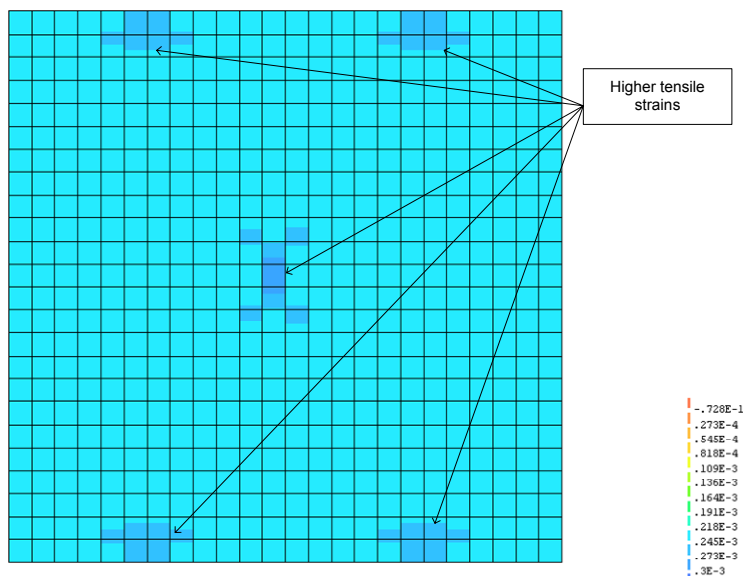


Figure A. 2 Crack localisation at deformation value 0.09 mm

On slowly increasing the prescribed deformation, tensile strain in weakened element and at the corner were higher than in other parts of the model; see Figure A. 2. The stress field from the weakened element propagated outwards and bifurcated to balance

with the high stress field near transverse reinforcement along free edge of the model; see Figure A. 2.

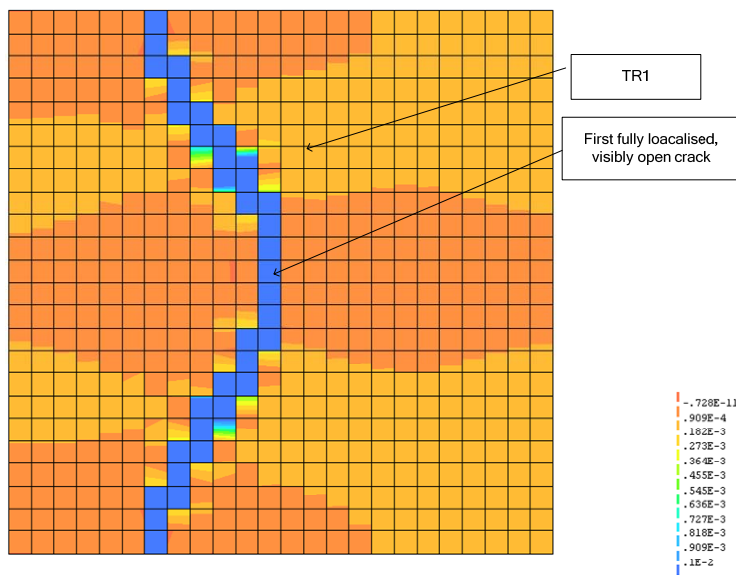


Figure A. 3 Fully localised first visible crack at deformation value 0.1mm

The first crack pattern was in the form of an arc; see Figure A. 3. When prescribed deformation was increased, tensile stress increased at free edges and slowly propagated inwards; when it reached near the longitudinal reinforcement the stress field was forced to turn 45 ° due to influence of the axial force in the longitudinal reinforcement. Tensile stress field from the weakened element propagated outwards from the weakened element. At prescribed deformation of 0.1 mm, the first crack occurred at which the force was high enough to cause the full localisation of micro cracks; see Figure A. 3.

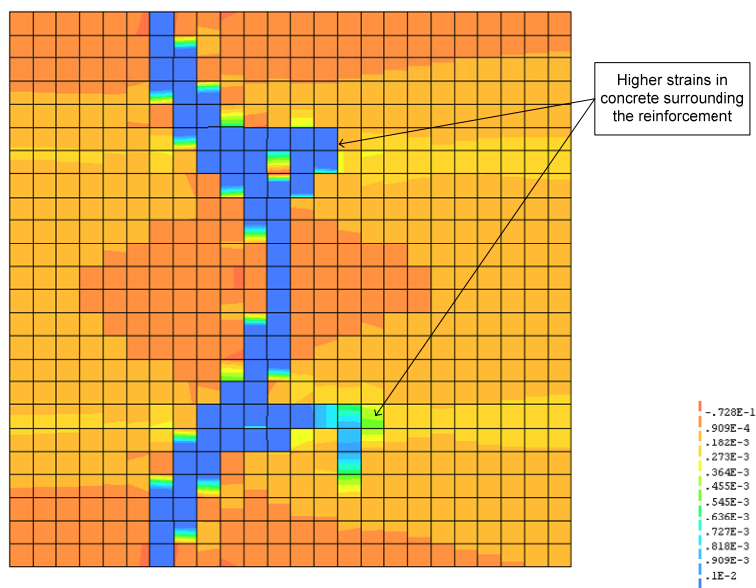


Figure A. 4 Propagation of crack at deformation value 0.45 mm

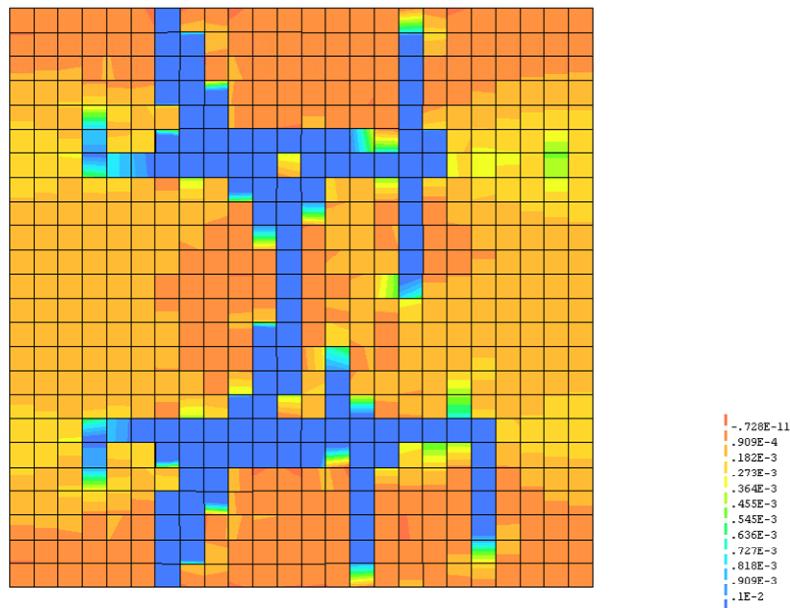


Figure A. 5 Development of new cracks and propagation of cracks at deformation value 0.56 mm

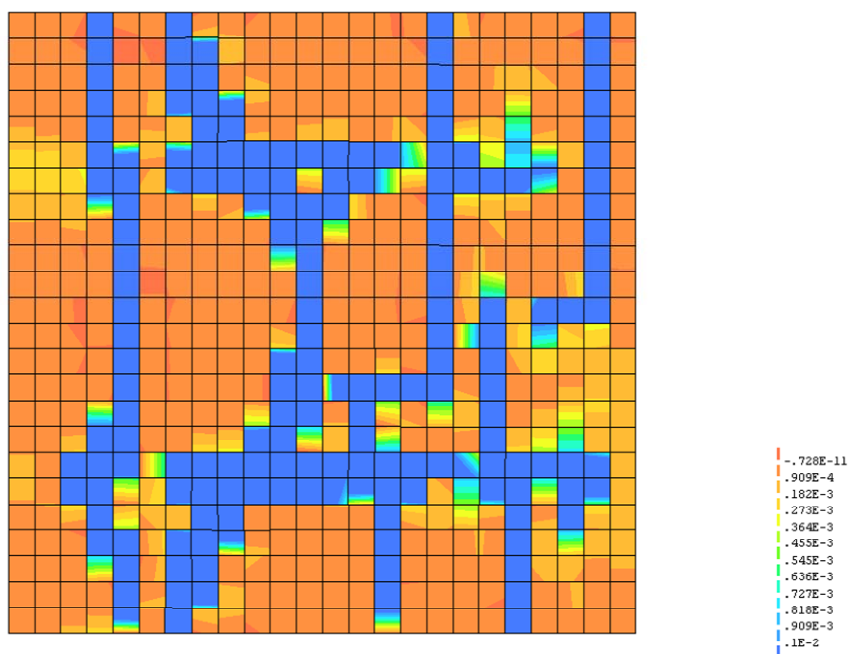
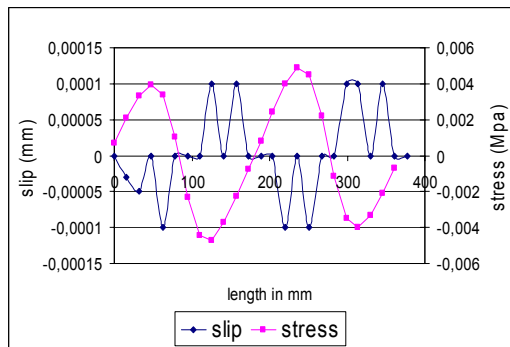


Figure A. 6 Fully stabilised cracked state at deformation value 0.83 mm

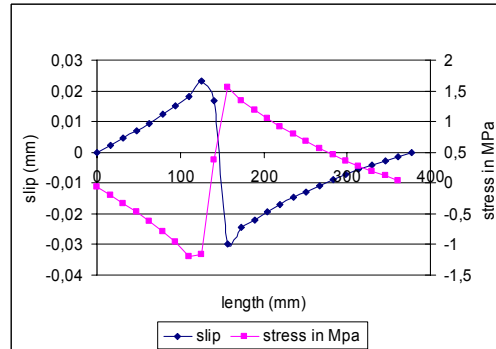
On increasing the prescribed deformation, the strains in concrete surrounding the longitudinal reinforcement started to increase; see Figure A. 4. New cracks started to generate from the region surrounding longitudinal reinforcements and propagated away from the reinforcements; see Figure A. 5. Reinforcements started to carry the entire tensile stresses and started to yield, the crack pattern at start of yielding was as shown; see Figure A. 6. At the stabilised cracked state there were four well developed connected cracks; see Figure A. 6

## Bond stress and Slip variation

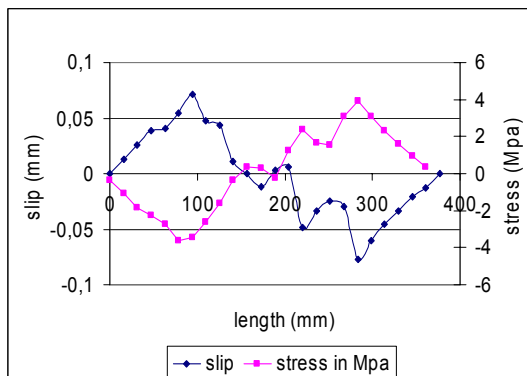
The bond stress and slip variation were calculated for different prescribed deformation value along reinforcement TR1 for all the tension test models; see Figure A. 7



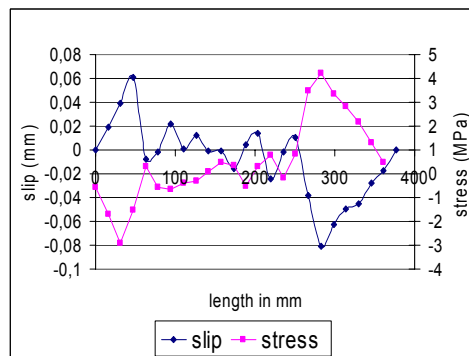
(a) 0.09 mm



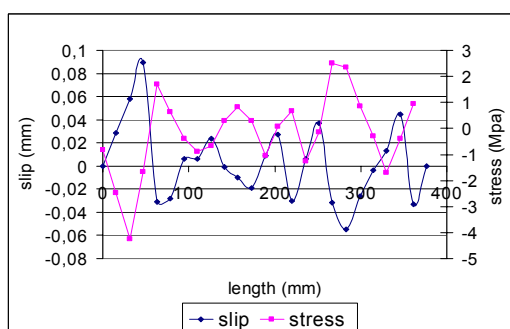
(b) 0.1 mm



(c) 0.45 mm



(d) 0.56 mm



(e) 0.83 mm

Figure A. 7 Bond stress and slip variation along reinforcement TR1 for different prescribed deformation values.

Bond stress and slip variation showed a direct proportional relationship. Slips were calculated at node points between concrete and reinforcement. Slip was obtained using the displacement of nodes in respective direction and bond stress was obtained as an average value of shear traction over each element obtained from Gaussian points in the interface element. The bond stress obtained from the model when compared with the bond slip curve for the confined good bond conditions in CEB (1993) was appropriate.

When the first crack occurred, bond stress and slip was higher at the region where the first crack crossed TR1; see Figure A. 3 and Figure A. 7(b), for the same step axial stress in the reinforcement was also higher in the same region; see Figure A. 9

At prescribed loading of 0.45 mm the crack propagated along the reinforcement line and hence bond stress and slip were higher; see Figure A. 7. Stress was higher at more points in the reinforcement when compared to previous prescribed deformation cases.

At stabilised crack stage (prescribed deformation value 0.84 mm) when more cracks cannot appear because most of concrete elements along TR1 were cracked; see Figure A. 6, reinforcement started to yield; see Figure A. 9 (*curve 0.83*). The stress – strain curve of the reinforcement from the analysis was as shown; Figure A. 8 which corresponded well with the material input for the reinforcement steel. Reinforcement started to yield at (0.0022, 446MPa) coordinates and started to harden from 0.011 strain values; see Figure A. 8.

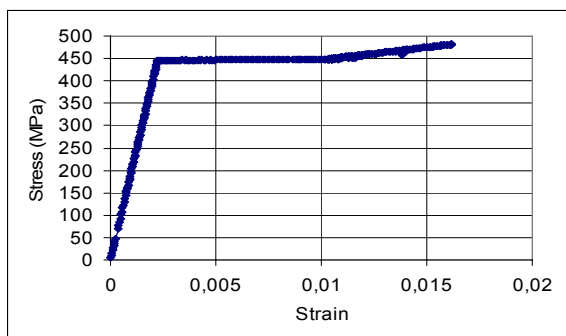


Figure A. 8 Stress – strain curve of reinforcement

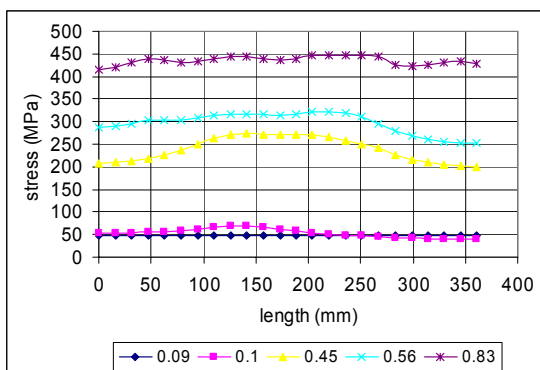


Figure A. 9 Stress variation along TR1 for various prescribed deformation values

The stress variation clearly indicated the activation of reinforcement at cracked regions; see Figure A. 9 which could be possible only if interface elements had the capacity to transfer the forces between concrete and reinforcement.

### Analysis Type 1b

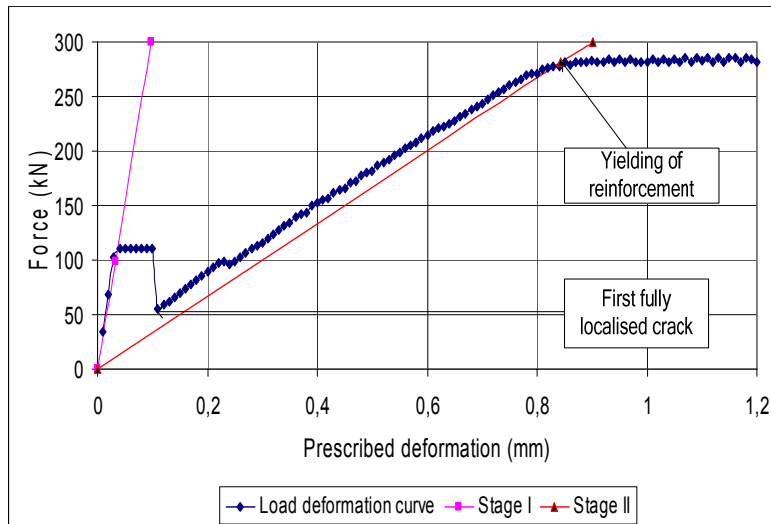


Figure A. 10 Load – Deformation curve with Stage I and II curves

First visible crack occurred at 0.11 mm and reinforcement yielded at 0.84 mm.

Crack initiated at 0.03 mm

### Evolution of the crack and its propagation of cracks

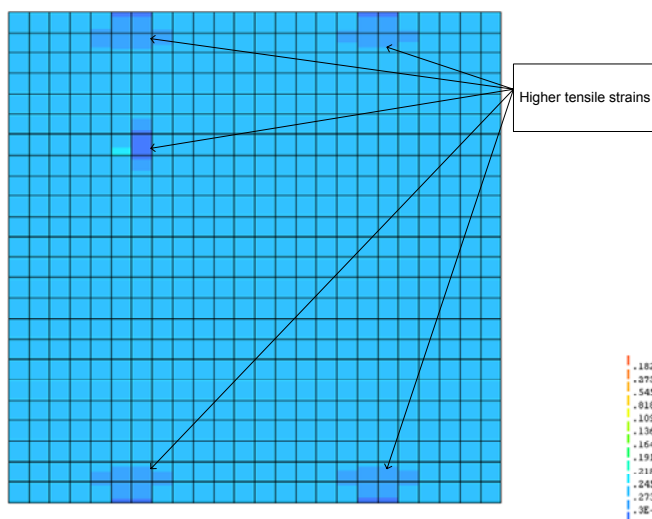


Figure A. 11 Crack localisation at a deformation value of 0.1 mm

The strains were higher in concrete elements near transverse reinforcements along free edge and in weakened element. The stress field propagated in the form of a bottle from free edges.

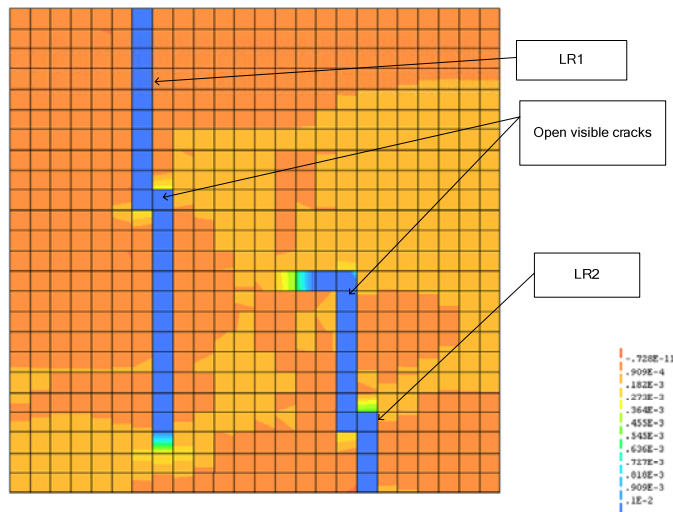


Figure A. 12 Visible open crack at deformation value 0.11 mm

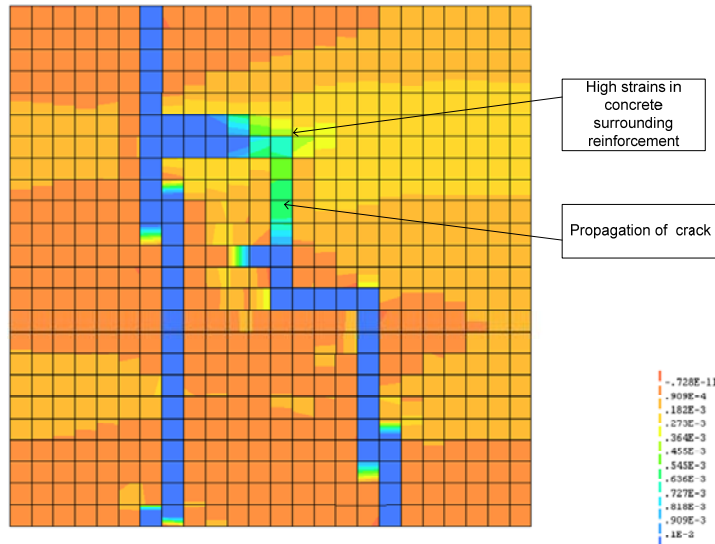


Figure A. 13 Propagation of crack at deformation value 0.23 mm

First visible crack occurred along the transverse reinforcements LR1 and propagated across the model. To satisfy the forced phenomenon of crack occurring along LR1 and to bring stable energy equilibrium a crack also occurred along line LR2 which had propagated through half the length of the model; see Figure A. 12. As the prescribed deformation increased the cracks started to localise and connect each other;

see Figure A. 13 and at the same time due to the increase in the axial stress in reinforcement the concrete elements surrounding the reinforcement had higher tensile strains; see Figure A. 13. New cracks developed from the region surrounding reinforcement and localised; see Figure A. 14. Reinforcement started to yield after the stabilised cracked stage; see Figure A. 15

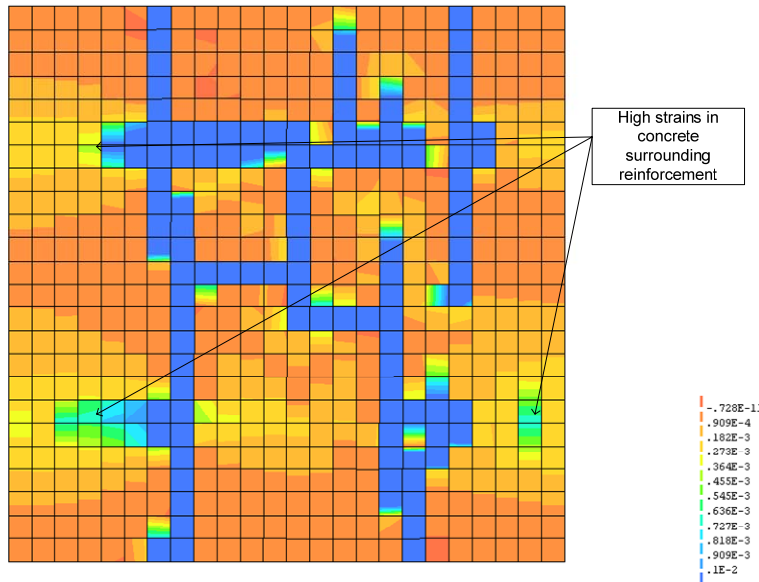


Figure A. 14 Propagation of crack at deformation value 0.55 mm

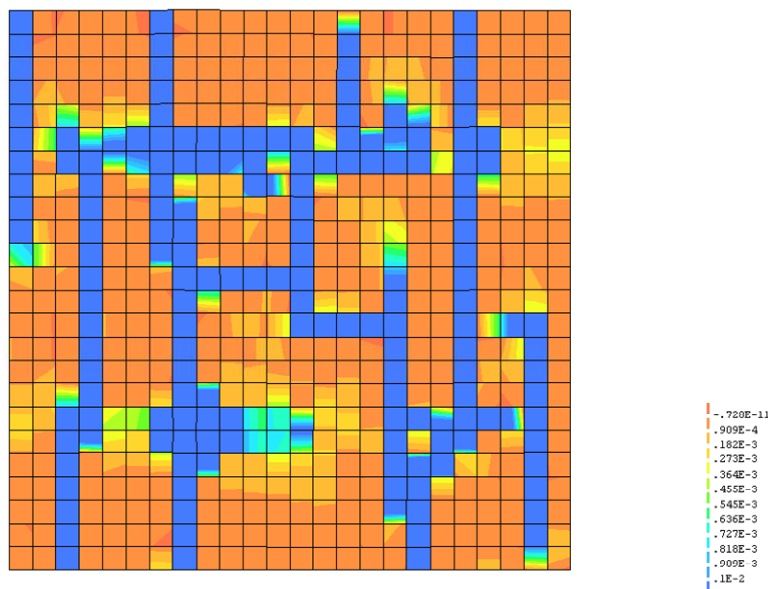
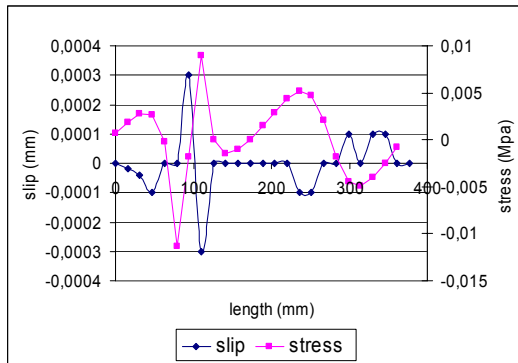


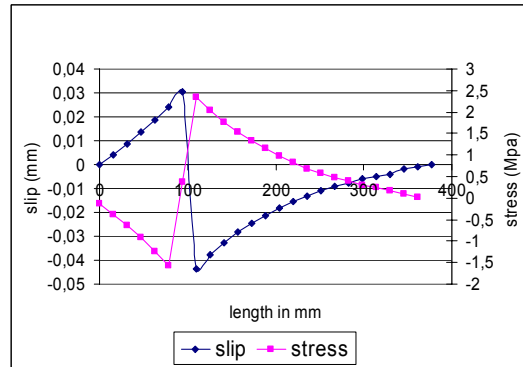
Figure A. 15 Fully stabilised cracked state at deformation value 0.84 mm

At the stabilised cracked state there were four well developed cracks; see Figure A. 6

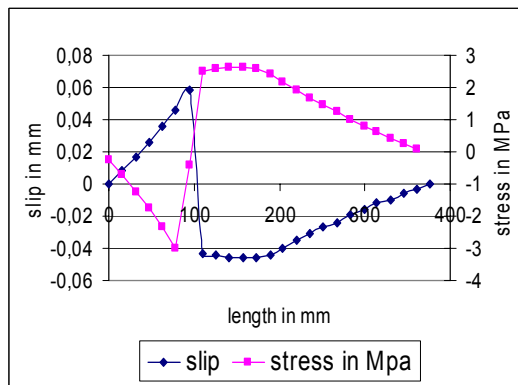
## Bond stress and slip variation along reinforcement TR1



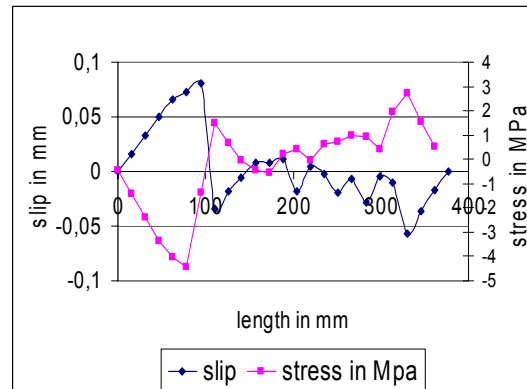
(a) 0.1 mm



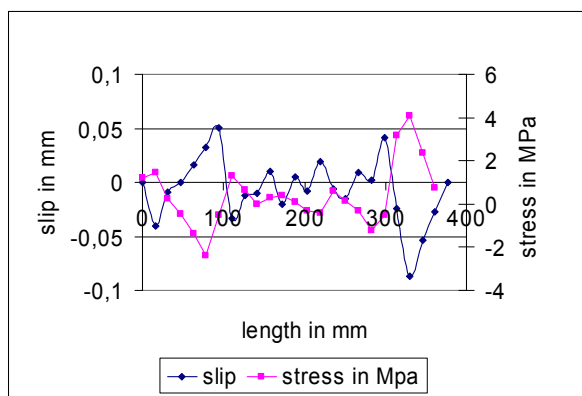
(b) 0.11 mm



(c) 0.23 mm



(d) 0.55 mm



(e) 0.84 mm

Figure A. 16 Bond stress and slip variation along reinforcement TR1 for different prescribed deformation values

Bond stress were higher were slip was higher. At the stage when first crack occurred the bond stress and slip was higher in the region where the crack crossed TR1; see Figure A. 16. Bond stress increased as the number of cracked concrete elements surrounding reinforcement increased; see Figure A. 16

The stress – strain curve of reinforcement from the analysis corresponded well with the material input data for reinforcement steel. Reinforcement yielded at (0.0022, 446 MPa) coordinate and started to harden from 0.011 strain value; see Figure A. 8

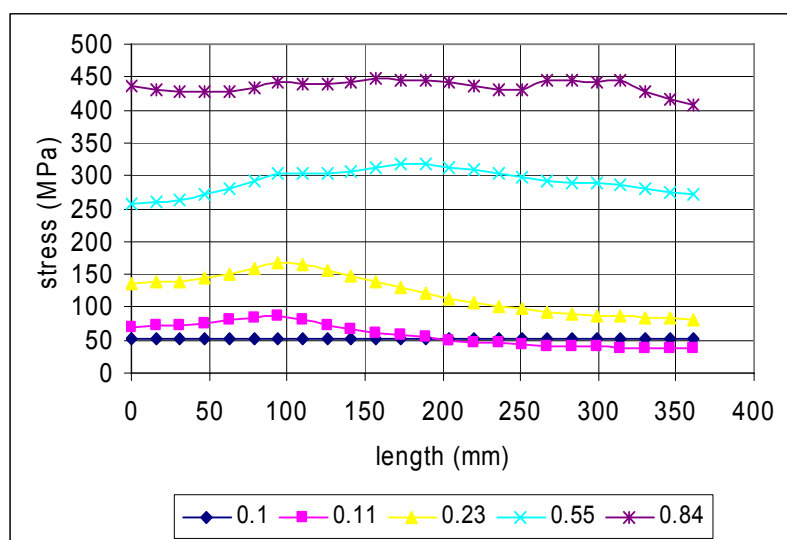


Figure A. 17 Stress variation along reinforcement TR1 for different prescribed deformation

Axial stress in reinforcement was higher at regions where concrete surrounding reinforcement was cracked. We can observe an increase in the stress in steel at region between 50 mm to 150 mm in which concrete cracked at a prescribed deformation value 0.11 mm; see Figure A. 12 and Figure A. 17 (curve 0.11). The yielding of reinforcement was clearly shown at prescribed deformation value 0.84 mm and at points where concrete was cracked; see Figure A. 17 (curve 0.84)

### Analysis Type 1c

The localisation of crack started when the principal tensile stress of the model was equal to  $f_{ct}$ ; see Figure A. 18. The crack initiates at a deformation value of 0,03 mm and was fully opened and visible at 0,25 mm at this point there was a drastic change in the stiffness of the model and the curve adopts a lesser slope compared to the slope of the stage I curve; see Figure A. 18

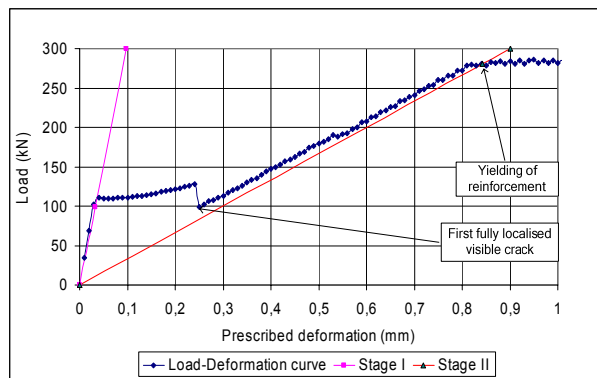


Figure A. 18: Comparison of Load-Deformation curve with Stage I and Stage II curves

### Evolution of the Crack and its propagation

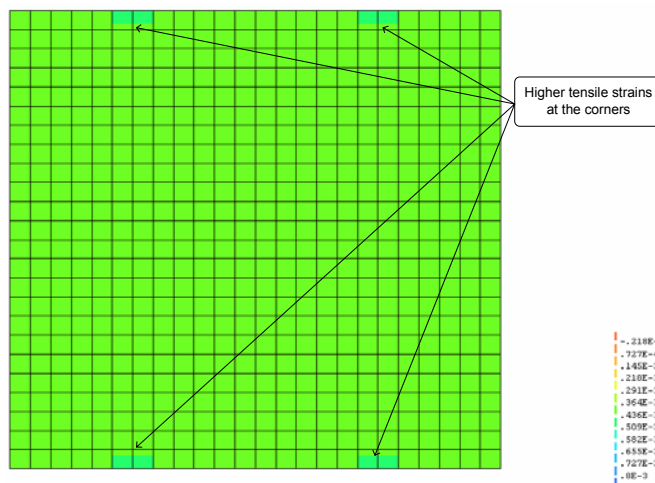


Figure A. 19: Tensile strains at prescribed deformation of 0.15 mm

When prescribed deformation was applied to the model, tensile stresses were higher in the concrete at the free edges near transverse reinforcement; this was due to the restraint provided by the transverse reinforcement against the shrinking of the cross section of the concrete due to Poisson's effect, normal to the direction of the applied deformation; see Figure A. 19. As the prescribed deformation increased, stresses in the concrete localised into a bottle shaped stress field; see Figure A. 21. The stress was symmetrical due to symmetrical loading and boundary conditions. The crack initiated at the free edge of the concrete due to high local stresses caused by transverse reinforcements, the crack propagated towards the inside and changed direction due to the change of inclination of the principal tensile stress direction. At the deformation value of 0.25 mm open visible cracks were observed; see Figure A.6.

On further increase in the prescribed deformation, cracks further developed and new cracks were obtained; see Figure A. 23. At a certain stage when the tensile stresses transferred from reinforcement to uncracked concrete in-between cracks cannot be equal to  $f_{ct}$  (tensile strength of concrete) due to unavailability of more length than the 'transfer length' reinforcement started to yield and no more cracks could be formed ;

see Figure A. 24. Transfer length is defined as the length needed for the complete transference of tensile stresses from the reinforcement to the concrete.

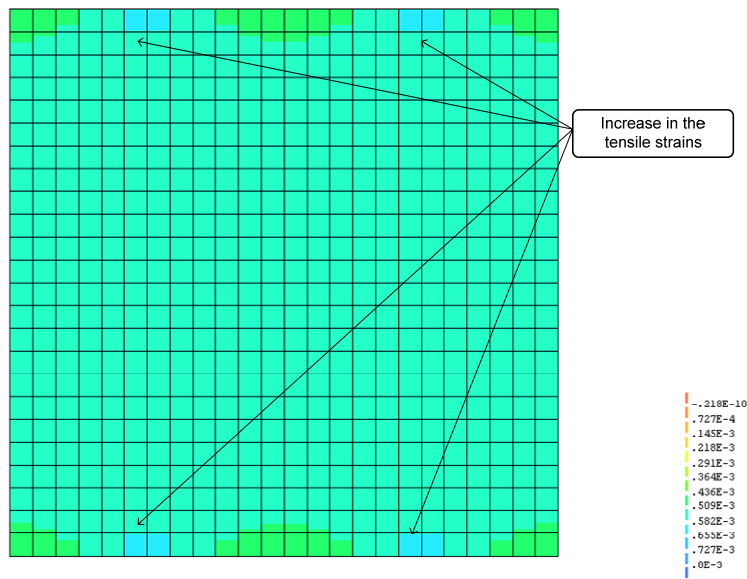


Figure A. 20: Tensile strains at prescribed deformation of 0.20 mm

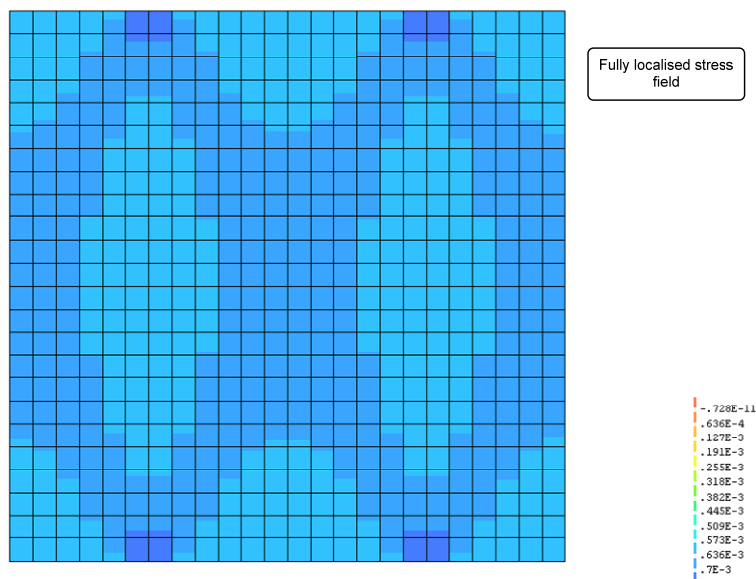


Figure A. 21 Tensile strains at prescribed deformation of 0.24 mm

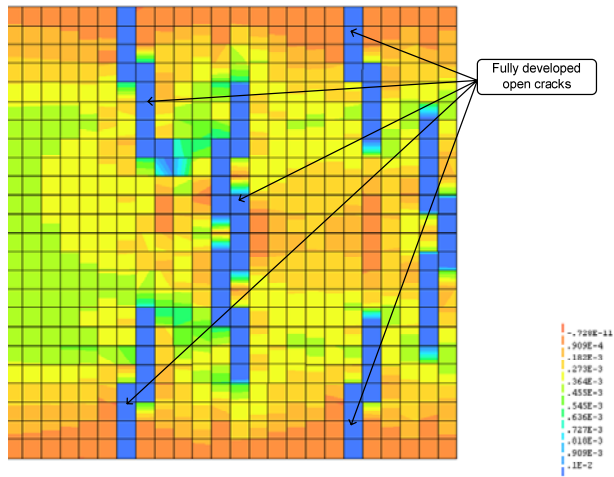


Figure A. 22 First open visible crack at prescribed deformation of 0.25 mm

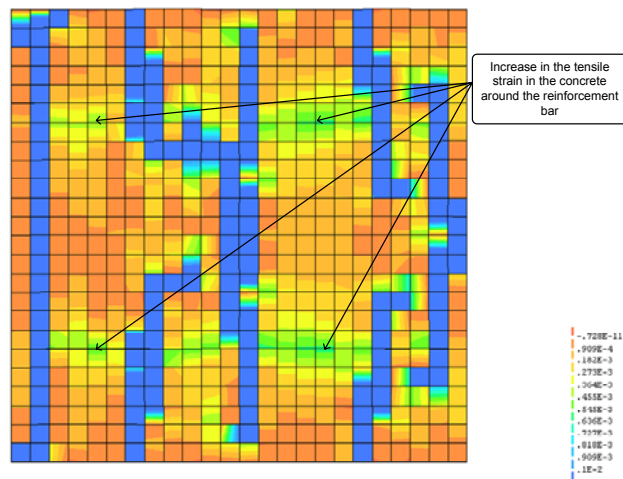


Figure A. 23 Visible cracks at prescribed deformation of 0.57 mm

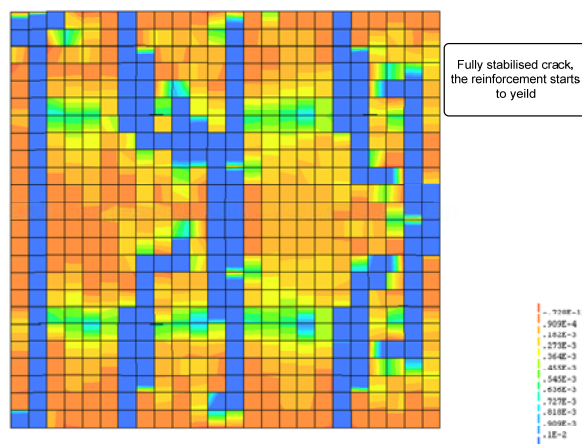
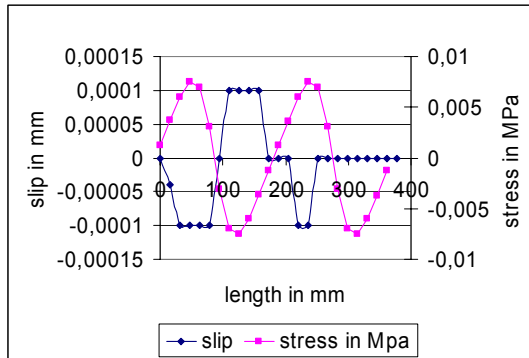
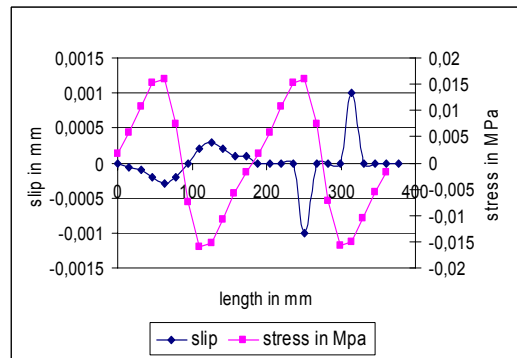


Figure A. 24 Fully stabilised cracked state at 0.83 mm

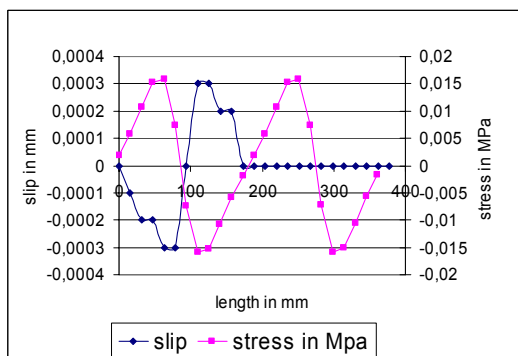
## Bond stress and slip variation



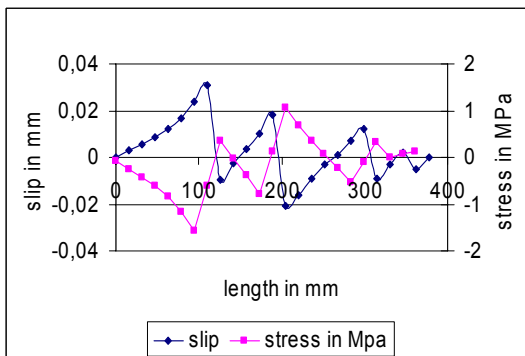
(a) 0.15 mm



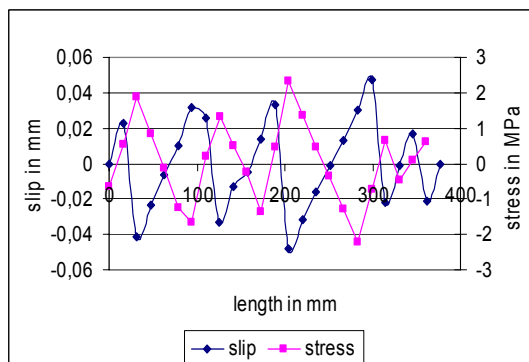
(b) 0.20 mm



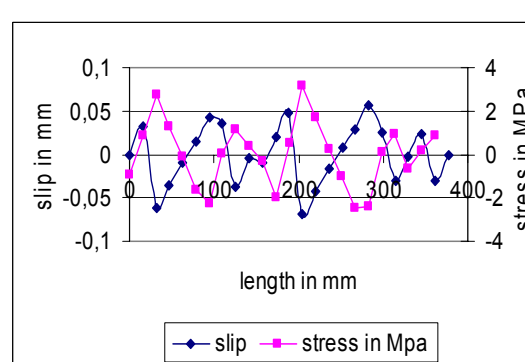
(c) 0.24 mm



(d) 0.25 mm



(e) 0.57 mm



(f) 0.83 mm

Figure A. 25 Bond stress and slip variation along reinforcement TR1 at different prescribed deformation values

The bond stress and slip were higher at regions where cracks developed; see Figure A. 25.

## Comparison of analyses type 1

Load – deformation curves for the Type 1 analyses were similar except at first crack stage. The difference was due to the forced cracking phenomenon that was induced by weakening a concrete element in analyses 1 a & b. In analyses 1 a & b after the formation of first crack the model starts to converge to its lowest natural equilibrium which has more probability to occur in reality compared to forced equilibrium thus we can find that after a certain deformation value around 0.3 mm all curves follow a similar path; see Figure A. 26

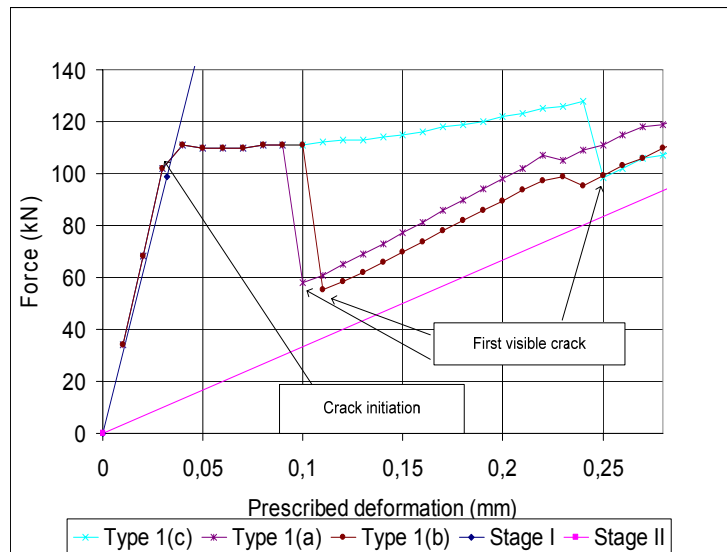


Figure A. 26 Comparison of analyses type 1

The crack initiated for the same force value i.e. the cracking force of concrete, but the first visible localised crack appeared at different force magnitude for analyses type 1c and type 1 a & b. The reason was that in analysis type 1c the model followed its own lowest natural energy equilibrium; the model consumed more energy to completely localise than in analyses 1 a & b; see Figure A. 26

# Appendix B: Tension analyses using higher order elements

## Analysis Type 2a

Crack initiated at deformation value 0.03 mm, first visible crack occurred at 0.19 mm and yielding of reinforcement at 0.84 mm; Figure B 1

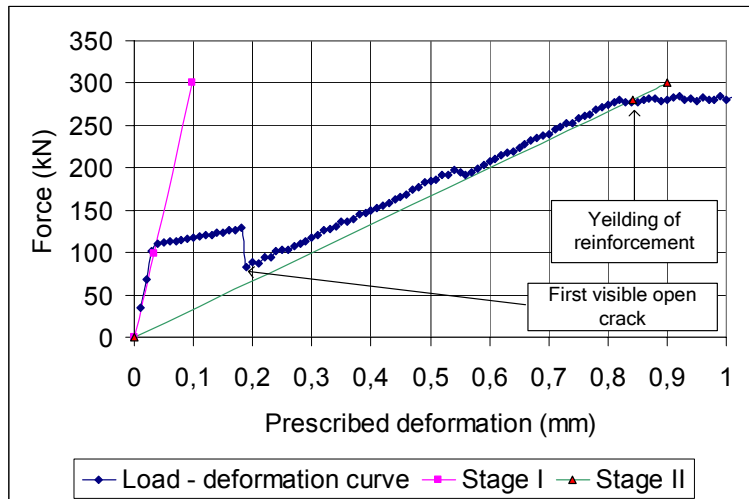


Figure B 1 Load – deformation curve with Stage I and II curves

## Crack evolution and propagation

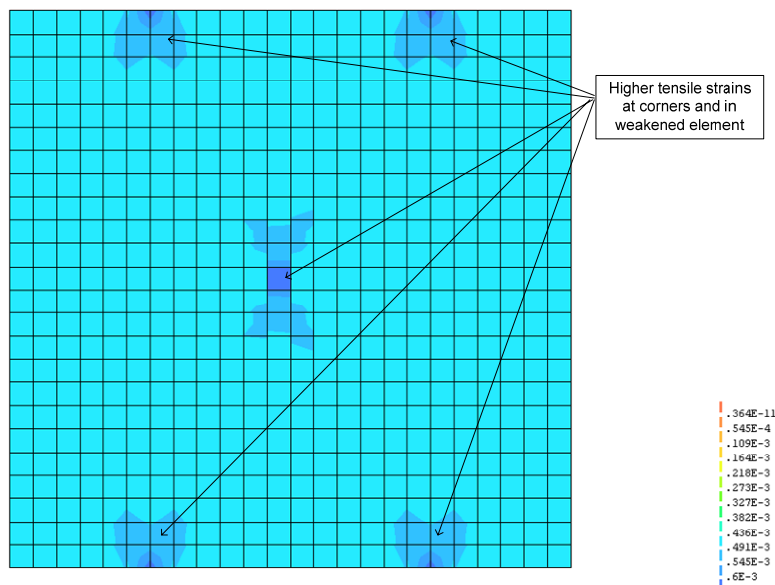


Figure B 2 Crack pattern at deformation value 0.18 mm

On slowly increasing the prescribed deformation, tensile strain in weakened element and at the corner were higher than in other parts of the model; see Figure B 2. The stress field from the weakened element propagated outwards and bifurcated to balance with the high stress field near transverse reinforcement along free edge of the model; see Figure B 2. When compared with analysis type1a it was observed that the stress field was similar at a step before a visible crack appeared. The contour plot of tensile strain field was finer and smoother when using higher order elements than when using lower order element due to presence of more number of nodes in higher order elements and since displacements at the nodes  $u_x$  and  $u_y$  are calculated using higher order polynomial; see Figure B 2 and Figure A. 2.

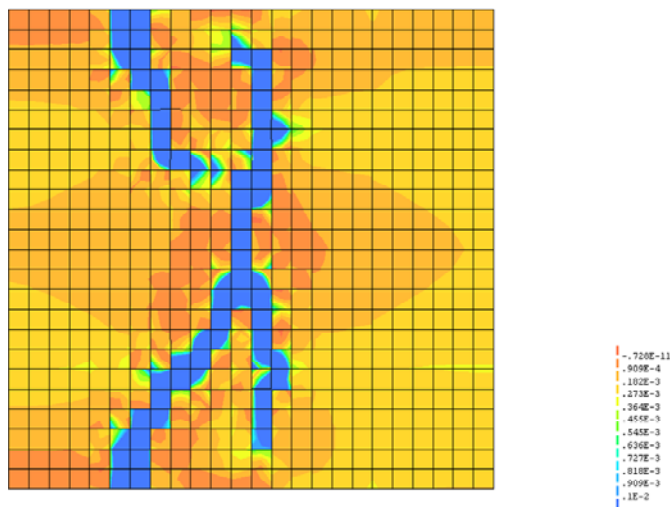


Figure B 3 Crack pattern at deformation value 0.19 mm

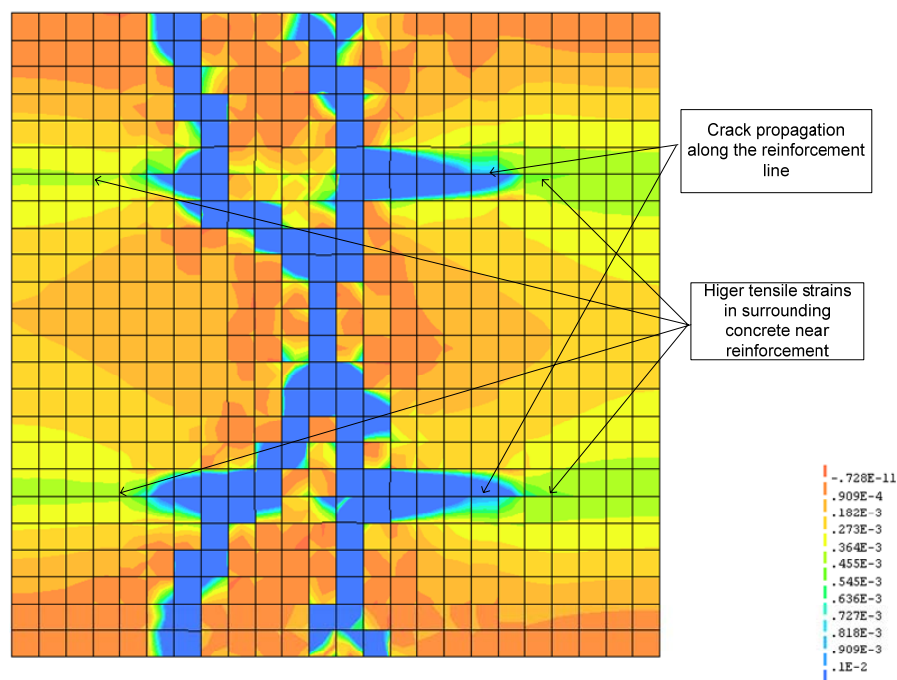


Figure B 4 Crack pattern at deformation value 0.36 mm

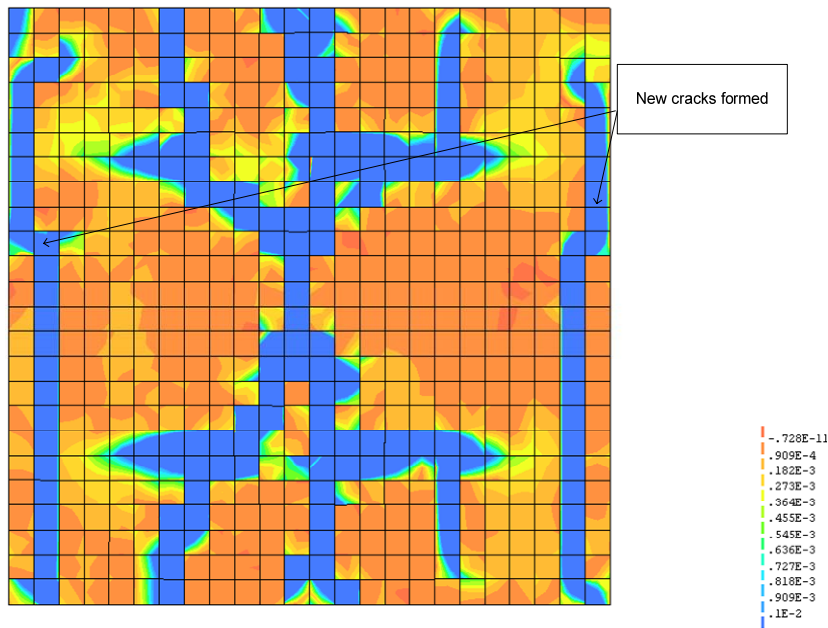


Figure B 5 Crack pattern at deformation value 0.56 mm

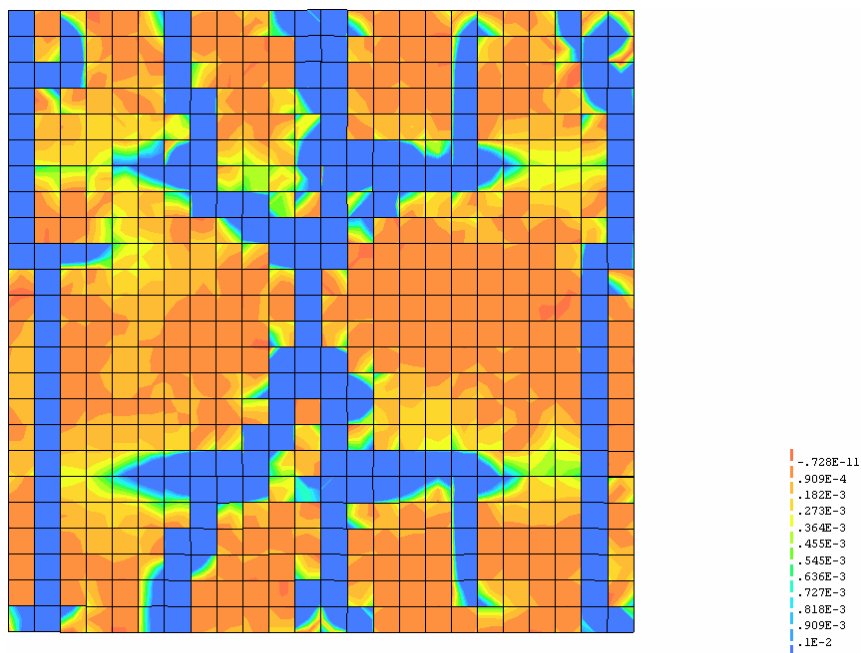


Figure B 6 Crack pattern at deformation value 0.74 mm

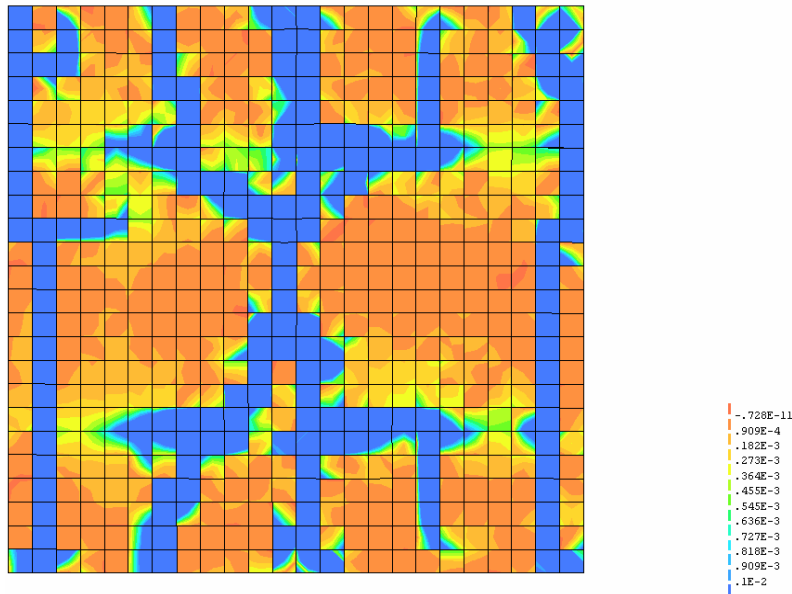
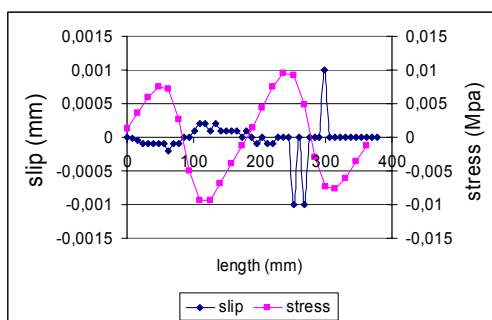


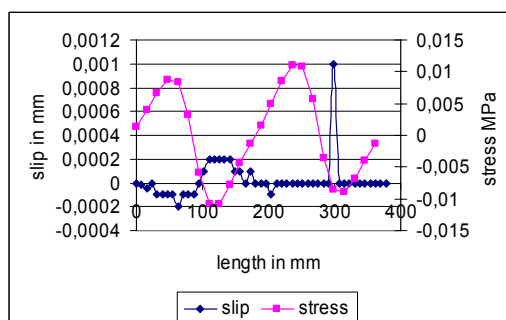
Figure B 7 Crack pattern at deformation value 0.84 mm

First crack occurred at prescribed deformation value of 0.19 mm; see Figure B 3. The first crack had a minor difference when compared to first crack pattern of same type of analysis with lower order elements; see Figure A. 3. Force needed to cause the first completely localised crack for a model with higher order elements was higher than force required to cause the first localised crack in a model with lower order elements; see Figure B 28. When prescribed deformation was increased the cracks propagated along reinforcements due to increase in tensile stress in concrete elements surrounding reinforcements; see Figure B 4 and Figure B 5. Reinforcement started to yield after at a prescribed deformation value 0.84 mm at which the cracking process stopped and model was in stabilised cracked state; see Figure B 7.

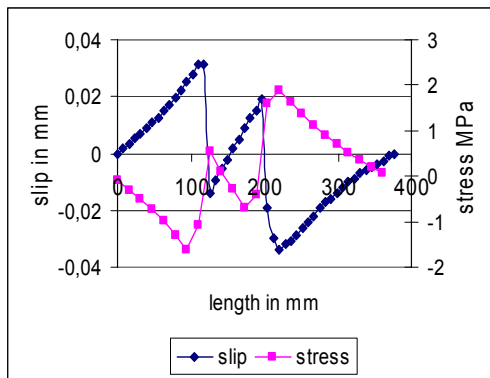
### Bond stress and slip variation along line TR1



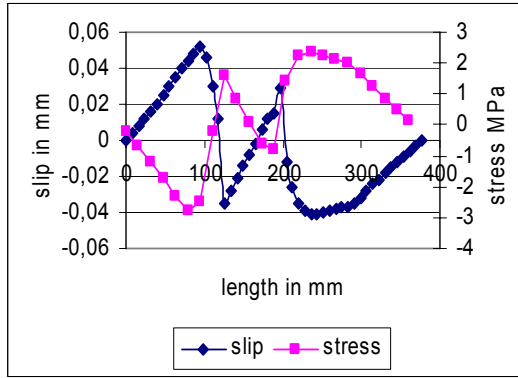
(a) 0.18 mm



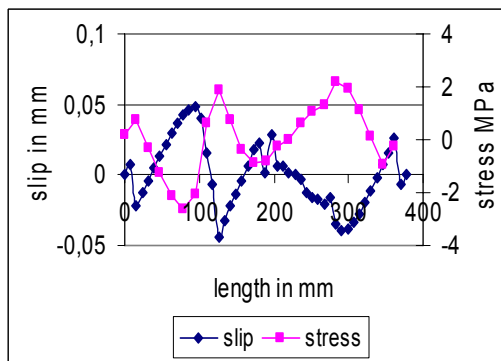
(b) 0.19 mm



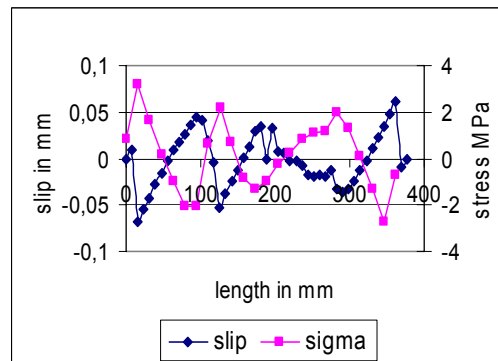
(c) 0.36 mm



(d) 0.56 mm



(e) 0.74 mm



(f) 0.84 mm

Figure B 8 Bond stress and slip variation along TR1 for different prescribed deformation

Bond stresses and slip was higher at regions where concrete was cracked, the behaviour of higher order interface elements was similar with lower order interface elements see Figure B 8. The stress – strain curve corresponded well with the material input data for reinforcement steel. Axial stress in reinforcement was higher at regions where concrete was cracked; see Figure B 9.

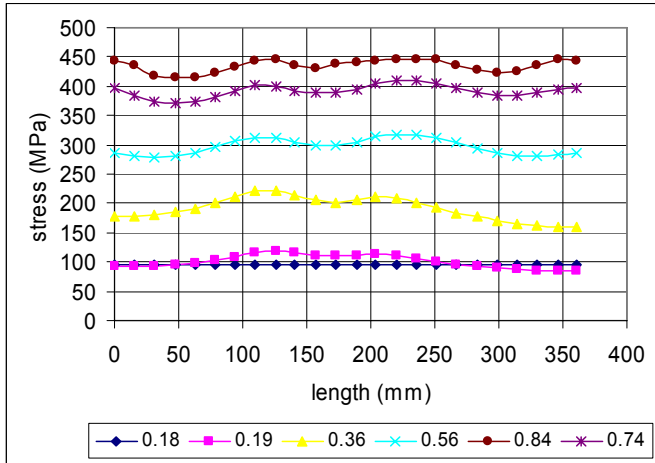


Figure B 9 Stress variation along TRI for different prescribed deformation

### Analysis Type2b

Crack initiated at deformation value 0.03 mm, first visible crack occurred at 0.2 mm and yielding of reinforcement at 0.84 mm

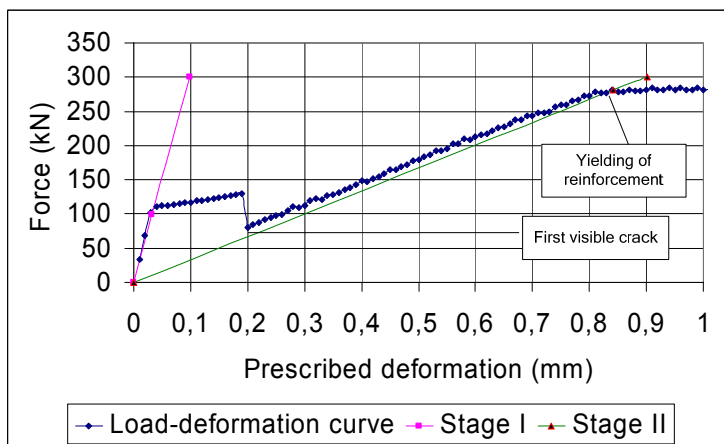


Figure B 10 Load – deformation curve analysis type 2(b)

### Evolution and propagation of crack

The stress field looked symmetrical but with minor distortion in the field due to presence of the weakened element; see Figure B 11, which would have localised into a symmetrical form if no element was weakened; see Figure B 21. The first crack occurred when the micro cracks fully localised

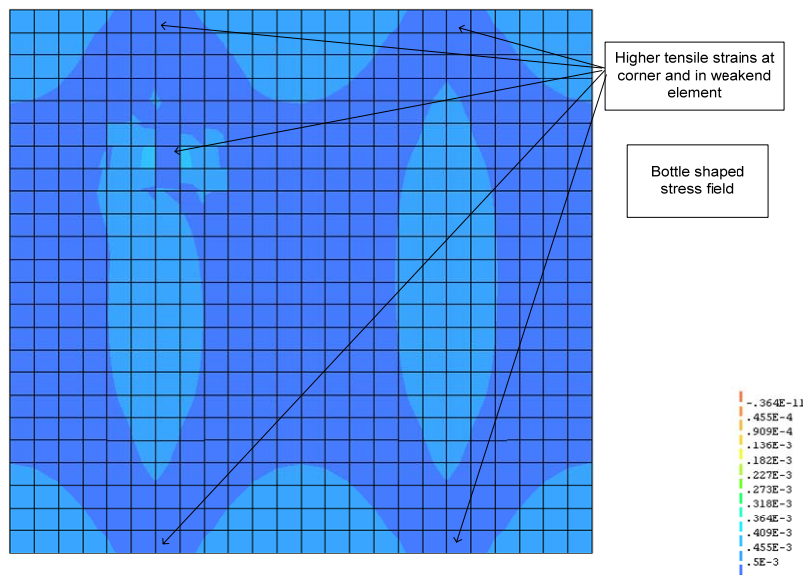


Figure B 11 Crack pattern at deformation value 0.19mm

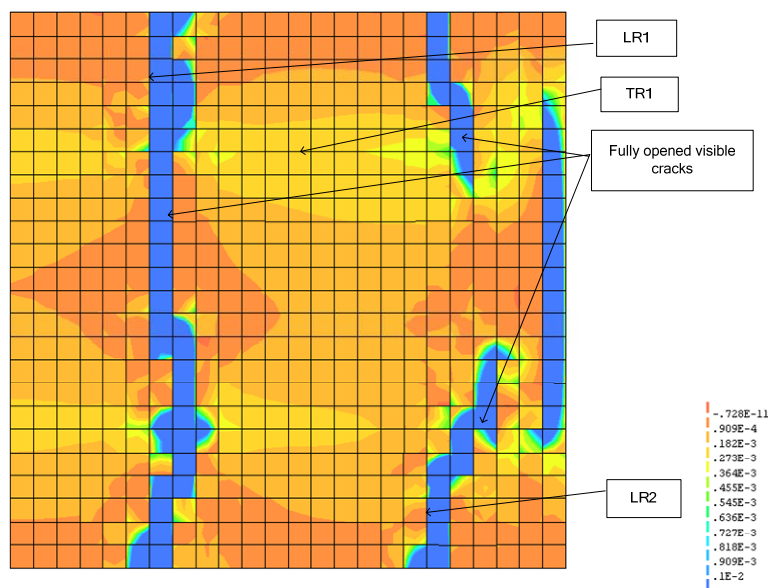


Figure B 12 Crack pattern at deformation value 0.2mm

First visible completely localised crack appeared at deformation value 0.2 mm. The crack propagated along reinforcement line LR1. Crack was forced to happen along LR1 by weakening a concrete element at an intersection of reinforcements; see Figure 4.22 to balance the forced cracking process and to satisfy stable energy equilibrium conditions, cracks also developed along LR2; see Figure B 12

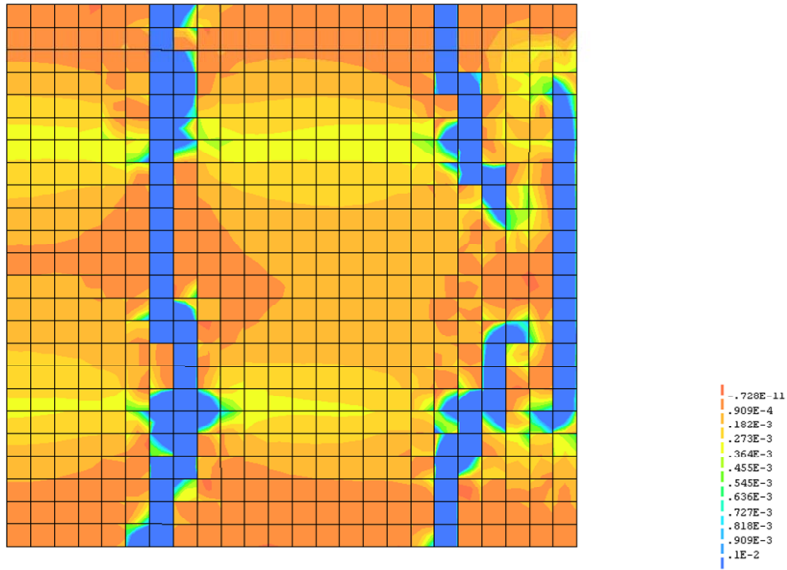


Figure B 13 Crack pattern at deformation value 0.3mm

After first crack formation, tensile stress started to increase along reinforcement line TR1. Stress field generated in the form of a bulb from reinforcements into concrete can be seen; see Figure B 13. Reinforcement started to yield after reaching a stabilised cracked state; see Figure B 16

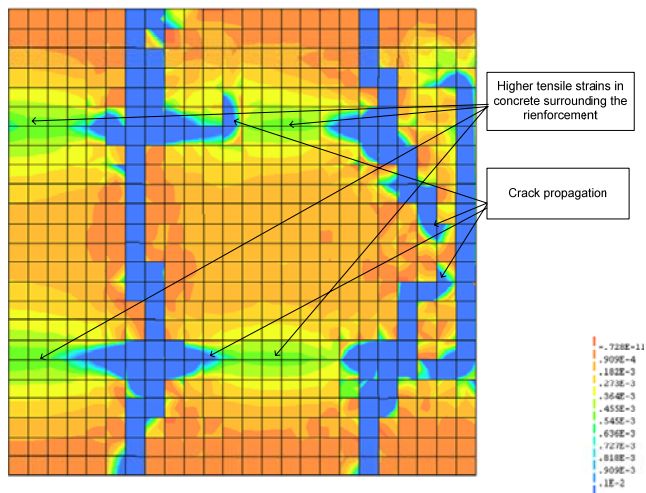


Figure B 14 Crack pattern at deformation value 0.56mm

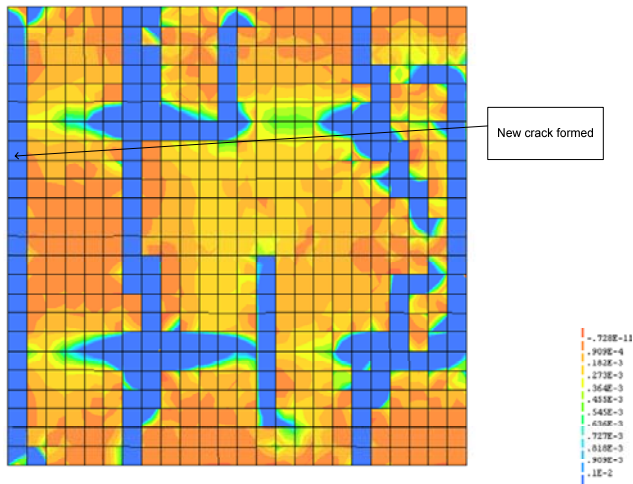


Figure B 15 Crack pattern at deformation value 0.75mm

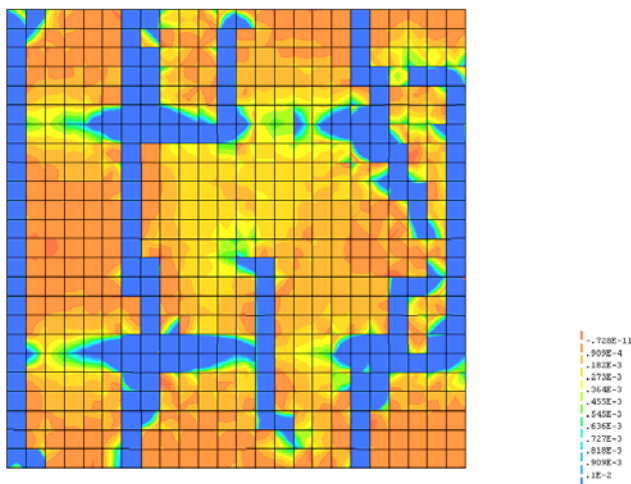
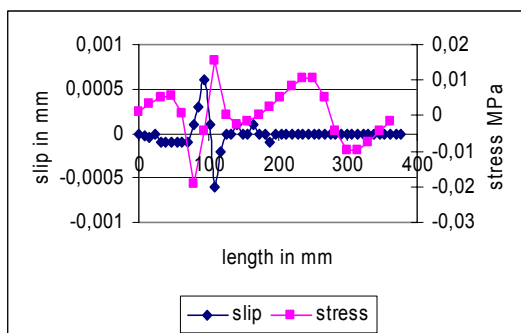


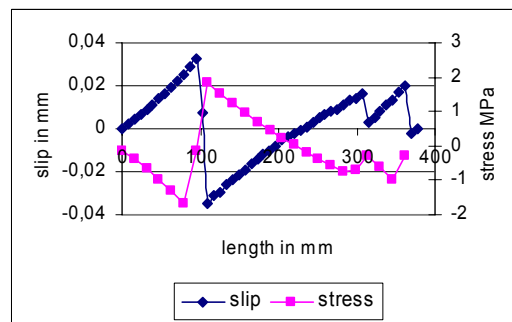
Figure B 16 Crack pattern at deformation value 0.84mm

### Bond stress and slip variation

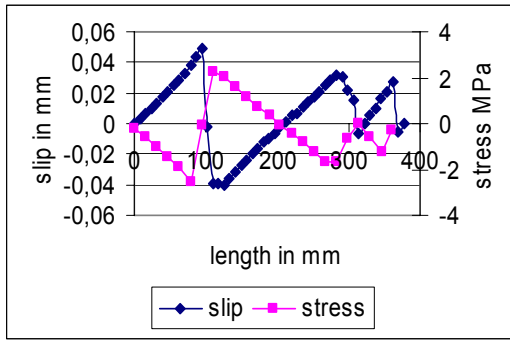
Bond stress and slip variation were calculated along reinforcement line TR1; see Figure B 17



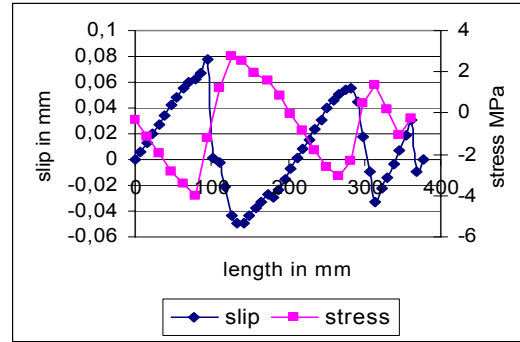
(a) 0.19 mm



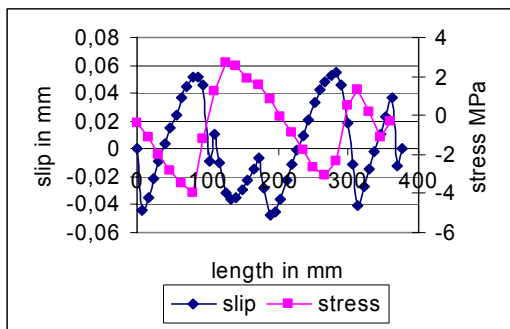
(b) 0.2 mm



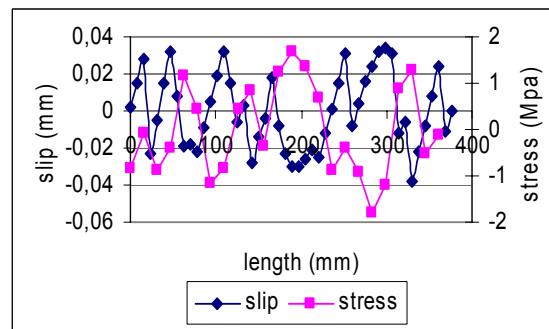
(c) 0.3 mm



(d) 0.56 mm



(e) 0.75 mm



(f) 0.84 mm

Figure B 17 Bond stress and slip variation along TR1 for different prescribed deformation

Stress – strain curve of the reinforcement corresponded well with the material input data for reinforcement steel. Axial stress in reinforcement was higher in regions where concrete elements surrounding reinforcement were cracked and entire tensile stress was carried by reinforcement; see Figure B 18

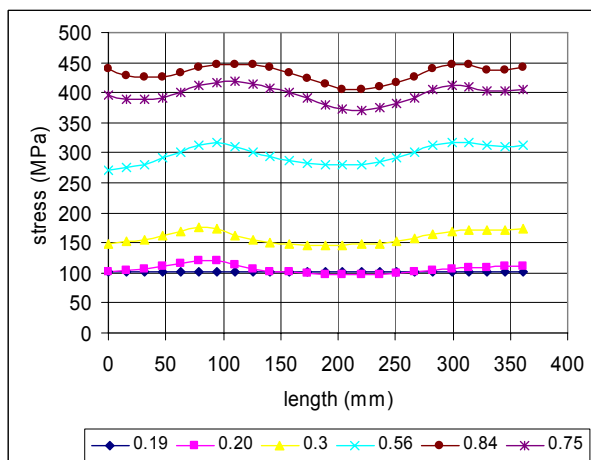


Figure B 18 Stress variation along TR1 for different prescribed deformation

## Analysis Type 2c

First visible crack occurred at prescribed deformation 0.26 mm, reinforcement yielded at 0.84 mm. The crack initiated at 0.03mm

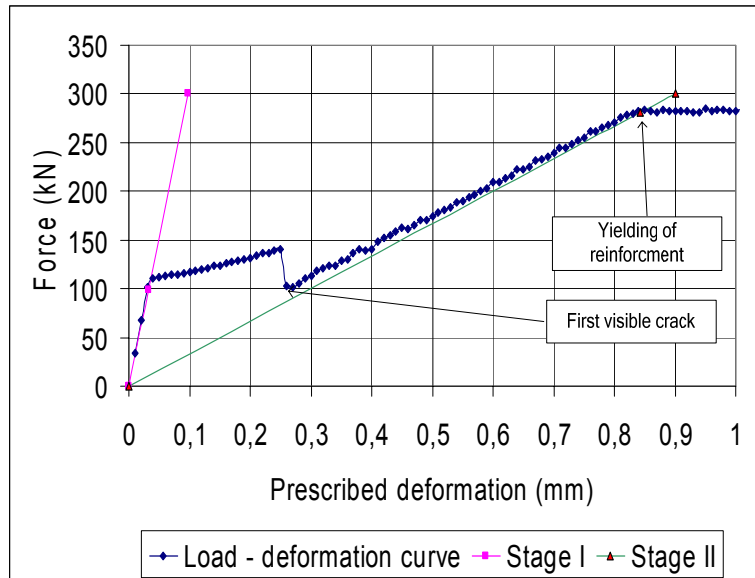


Figure B 19 Load – deformation curve

## Evolution of crack and propagation

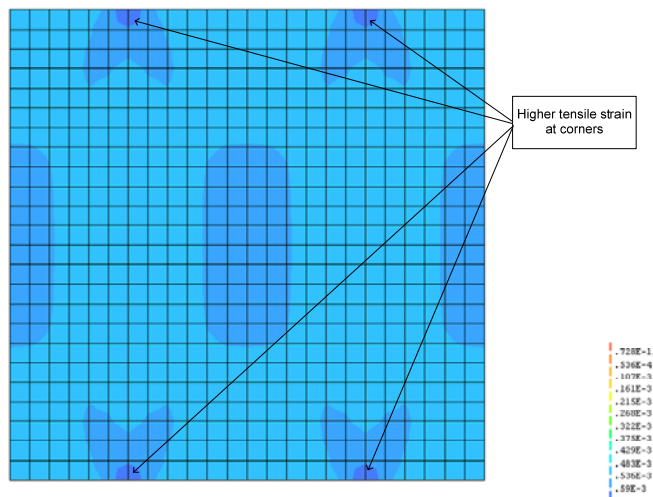
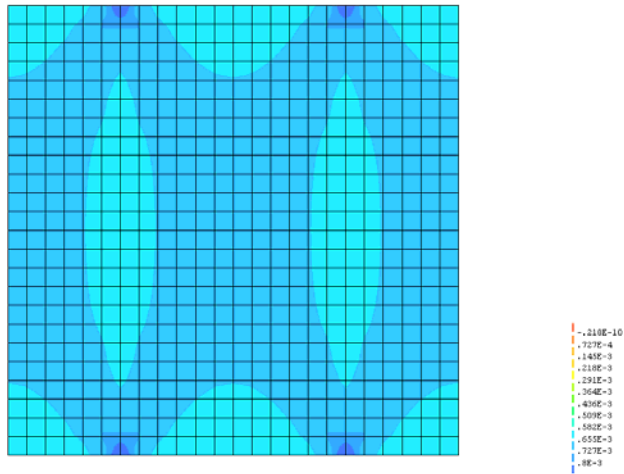
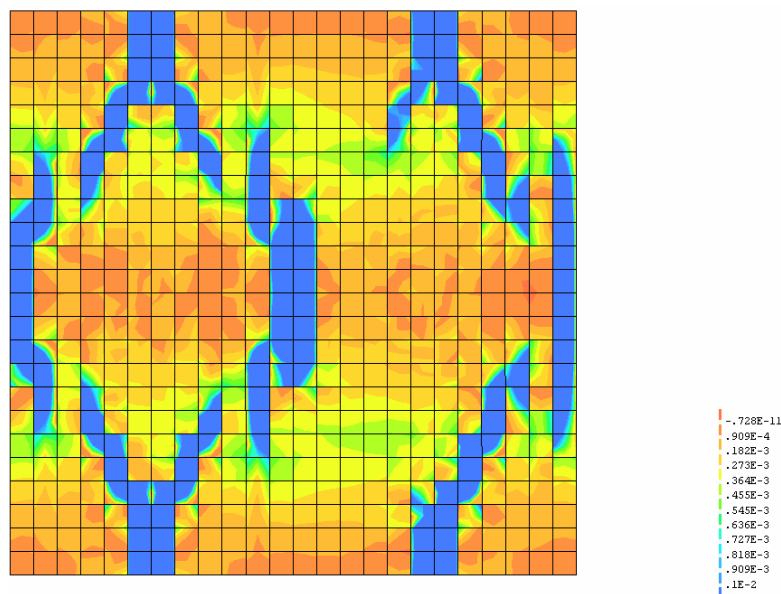


Figure B 20 Crack pattern at deformation value 0.20mm



*Figure B 21 Crack pattern at deformation value 0.25mm*

The stress field localised into a bottle shaped form with stress higher in concrete elements at the edges near transverse reinforcement; see Figure B 21. The first crack of analysis type2c; see Figure B 22 was similar but with minor difference to first crack of analysis type1c; see Figure A. 1



*Figure B 22 Crack pattern at deformation value 0.26mm*

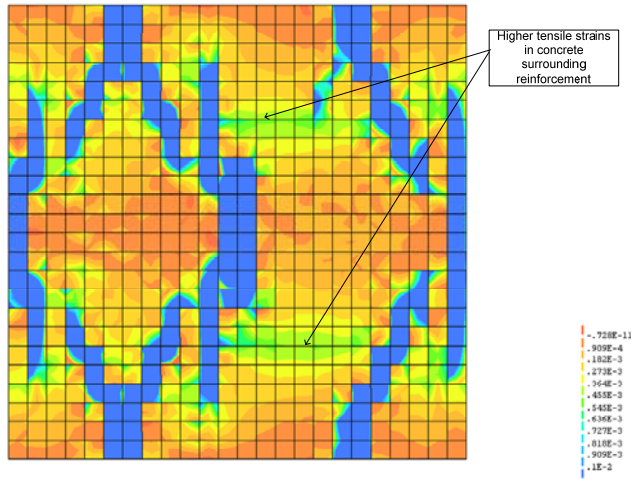


Figure B 23 Crack pattern at deformation value 0.39mm

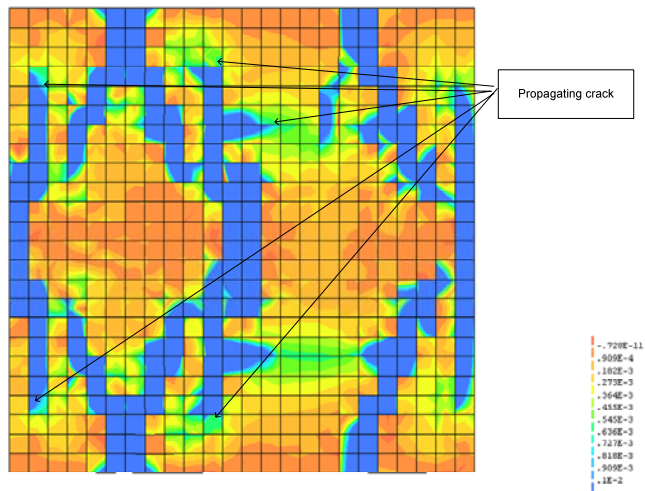


Figure B 24 Crack pattern at deformation value 0.57mm

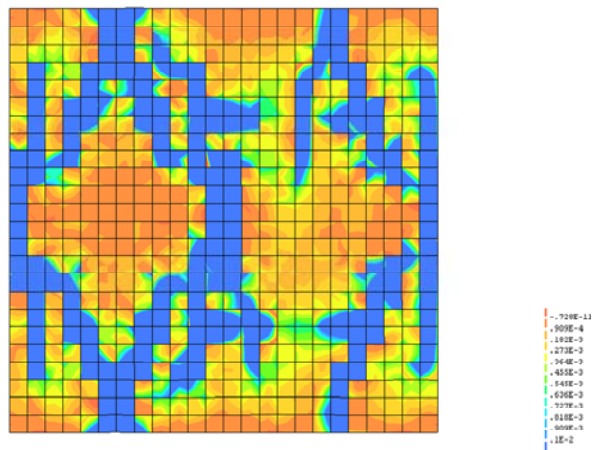
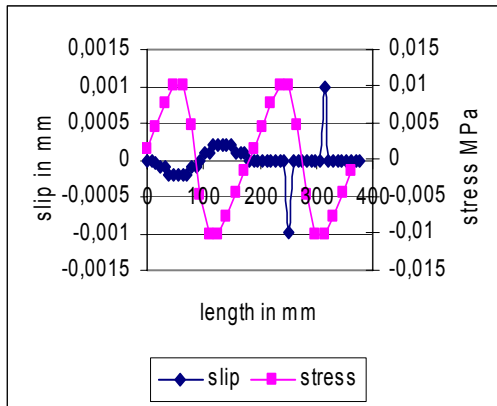
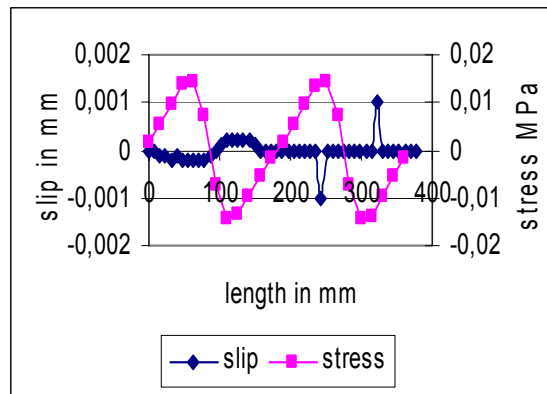


Figure B 25 Crack pattern at deformation value 0.84mm

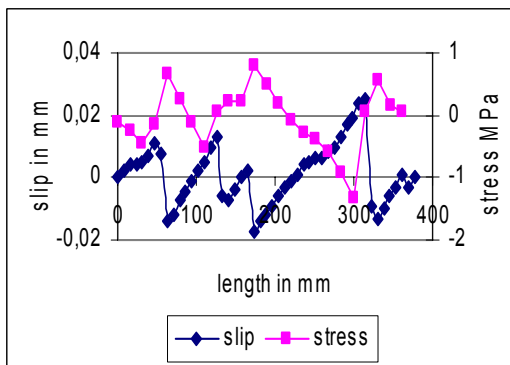
## Bond stress and slip variation



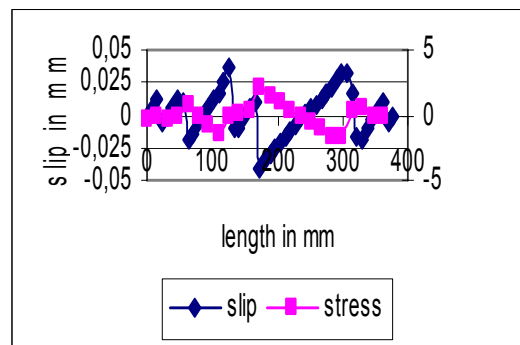
(a) 0.2 mm



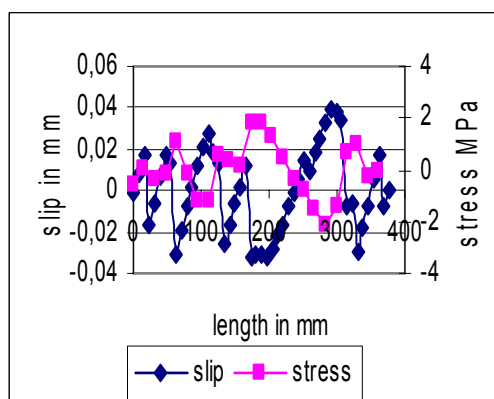
(b) 0.25 mm



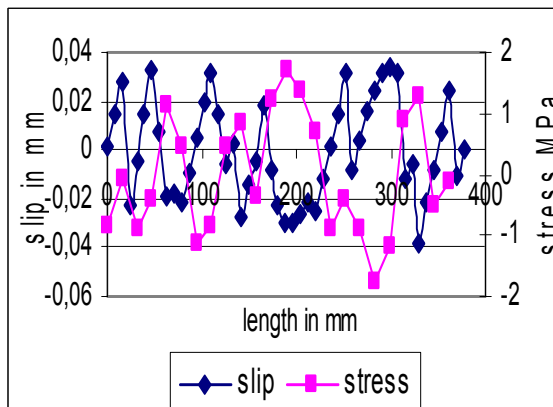
(c) 0.26 mm



(d) 0.39 mm



(e) 0.57 mm



(f) 0.84 mm

Figure B 26 Bond stress and slip variation along TRI for different prescribed deformation values

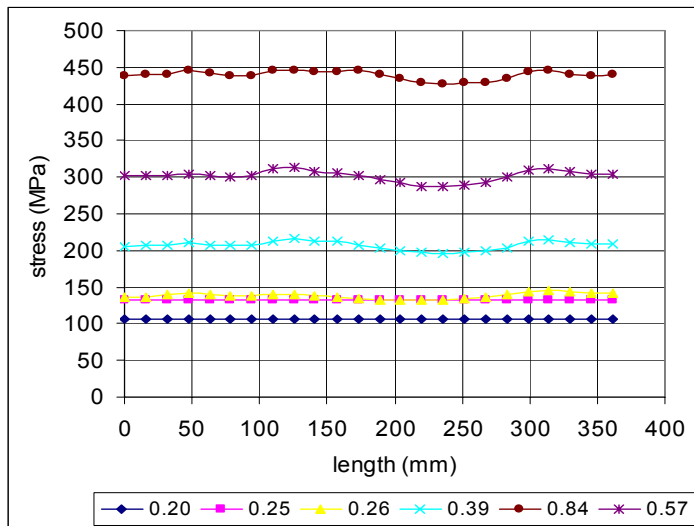


Figure B 27 stress variation along TR1 for different prescribed deformation

### Comparison of all analyses

Load – deformation curve of all analyses were similar but with minor difference at the first crack stage. The analyses type 2c and type 1c behaved similar but with negligible difference at first crack stage. The model made of higher order elements consumed more energy to crack and cracked at more places; see Figure B 22 compared to model with lower elements; see Figure A. 22. Crack initiated at the same value (0.03mm, 100kN); see Figure B 28. The tension stiffening effect in reinforced concrete is clearly shown by all models; see Figure 4.23

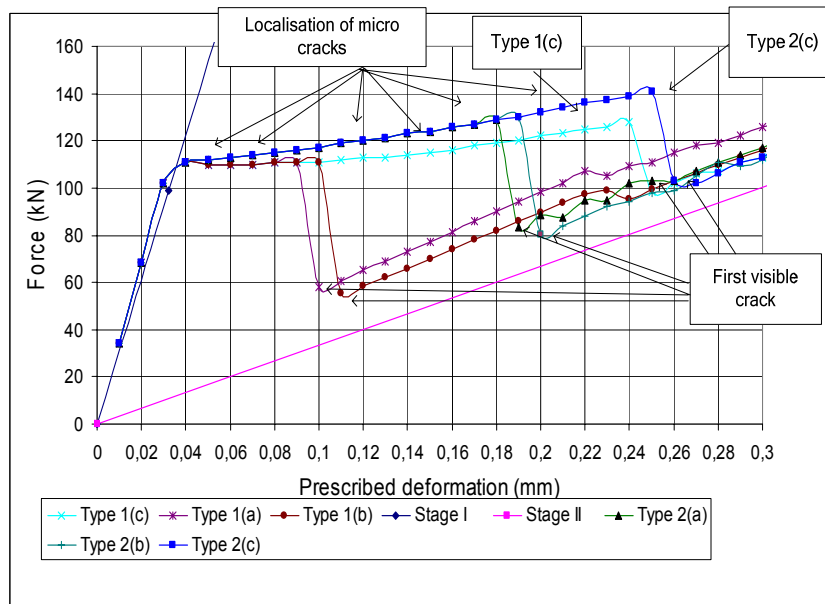


Figure B 28 Closer view of the Load – deformation curves

## Appendix C: Hand Calculation for verification analyses

### Cracking force

The force at which the first crack is formed and starts to localise

$$N_{cr} = f_{ct} * A_c$$

Where  $N_{cr}$  is the cracking force in kN

$f_{ct}$  is the concrete tensile stress in MPa

A is the cross sectional area of concrete in m

$$f_{ct} = 2.98 \text{ MPa}$$

$$A_c = 0.3772 \times 0.0889 \text{ m}^2$$

$$N_{cr} = 100 \text{ kN}$$

### Yielding force

The force at which reinforcement starts to yield

$$N_y = f_{st} * A_s$$

Where  $N_y$  is the yield force in kN

$A_s$  is the reinforcement steel area in m<sup>2</sup>

$f_{st}$  is the yield stress in MPa

$$A_s = 2 * 314.159 \text{E-}06 \text{ m}^2$$

$$F_{st} = 446.1275 \text{ MPa}$$

$$N_y = 280.31 \text{ kN}$$

### Deformation value at first cracking of concrete

$$\delta_l_c = \frac{N_{cr} \cdot l}{A_c \cdot E_c}$$

Where  $\delta_l_c$  is the deformation in mm

$N_{cr}$  is the cracking force in kN

l is the length of the model in m

$A_c$  is the cross sectional area of the model in m<sup>2</sup>

$E_c$  is the elastic modulus in GPa

$$E_c = 34.5 \text{ GPa}$$

$$L = 0.3772 \text{ m}$$

$$\delta_c = 32.28 \text{E-}03 \text{ mm}$$

**Deformation value at yielding of steel**

$$\delta_y = \frac{N_y \cdot l}{A_s \cdot E_s}$$

Where  $E_s$  is the elastic modulus of steel in GPa

$\delta_y$  is the deformation in mm

$$E_s = 199.8 \text{ GPa}$$

$$\delta_y = 0.8422 \text{ mm}$$

## Appendix D: Batch file (\*.BAT file) used for the generation of the input file.

\*if there is no full stop at the end of a comment it means the continuation of the sentence in the next line.

FEMGEN SHEARPANEL \*enter the name of the model, example SHEARPANEL.

PROPERTY FE-PROG DIANA STRUCT\_2D \*specify 2d or 3d model.

YES \*needed to run the program over and over again

\*close the opened idiana interface to run again in the same iDIANA interface.

\*\*\*\*\*note\*\*\*\*\*

\*LREIN means longitudinal reinforcement starting from left to right.

\*TREIN means transversal reinforcement starting from bottom to top.

\*CONC means concrete.

\*REIN means reinforcement.

\*INL.. means related to longitudinal interface elements.

\*INT.. means related to transversal interface elements.

\*ele: in the comment means elements.

\*\*\*\*\*defintion of the units\*\*\*\*\*

UTILITY SETUP UNITS LENGTH METER

UTILITY SETUP UNITS FORCE NEWTON

UTILITY SETUP UNITS TEMPERATURE CELSIUS

UTILITY SETUP UNITS MASS KILOGRAM

\*\*\*\*\*model creation speed\*\*\*\*\*

UTILITY SETUP ANI SPEED 100

\*\*\*\*\*monitor position\*\*\*\*\*

DRAWING CONTENTS MONITOR POSITION .10893E-1 .876906

\*\*\*\*\*definitions of the tranformations\*\*\*\*\*

\*the size of one grid in y direction

\*enter the spacing of the reinforcement in y dir.

CONSTRUCT TRANSFRM TRANSLATE TRY1 0 .1886 0

\*the size of 1 grid in the x direction

\*enter the spacing of the reinforcement in x dir.

CONSTRUCT TRANSFRM TRANSLATE TRX1 .1886 0 0

\*transformation used for sweeping conc points

\*to create interface elements and lrein elements

\*choose any arbitrary value.

CO TRANSFRM TRANSLATE TRZL 0 0 1

\*transformation used to sweep conc points

\*to create interface elements and trein elements

\*enter any arbitrary value different from the value

\*used for sweeping the longitudinal rein.

CO TRANSFRM TRANS TRZT 0 0 2

\*to move the top edge to half the reinforcement spacing.

CO TRANSFRM TRANS TEDGEM 0 -.0943 0

\*to move the left edge to half the reinforcement spacing.

CO TRANSFRM TRANS LEDGEM 0.0943 0 0

\*to move the bottom edge to half the reinforcement spacing.

CO TRANSFRM TRANS BEDGEM 0 0.0943 0

\*to move the right edge to half the reinforcement spacing.

CO TRANSFRM TRANS REDGEM -0.0943 0 0

\*used to copy the corner interface elements to other corner

\*in the longi dir.

CO TRANSFRM TRANS INLCOPY 0 0.2829 0

\*used to copy the corner interface elements to other corner

\*in the trans dir.

CO TRANSFRM TRANS INTCOPY 0.2829 0 0

\*\*\*\*\*

\*creation of conc elements.

GEOM POINT P1 0 0 0

\*sweeping the point in y direction.

GEOM SWEEP P1 TRY1 12 \*sweep command should be independant otherwise

\*the entire model will shift position rather than just moving the edge.

\*sweeping the line in x direction to create surface.

GEOM SWEEP L1 TRX1 12

\*\*number of copies based

\*on total number of grids - 1 in each direction in a row.

GEOM COPY S1 TRX1 2

\*\*creation of set of first row concrete elements.

CO SET FROW APPEND SURF ALL

\*\*copying the first row in y direction

\*number copies is equal to total number grids -1 in y dir in a row.

GEOM COPY FROW TRY1 2

\*creation of set for concrete elements.

CO SET CONSURF APPEND SURF ALL

\*creation of set for the edges.

\*left edge.

\*note: tol=0.02 (tol means tolerance)

CO SET LEDGE APPEND LINES LIMITS UMIN -0.0001 UMAX 0.0001 WMIN -0.0001 WMAX 0.0001

\*top edge, value of vmin is number of grids in a row\*spacing of rein-tol,vmax the same but +tol .

CO SET TEDGE APPEND LINES LIMITS VMIN 0.55 VMAX .57 WMIN -0.0001 WMAX 0.0001

\*right edge, value of umin is number of grids in a row\*spacing of rein-tol,umax same but +tol.

CO SET REDGE APPEND LINES LIMITS UMIN .55 UMAX .57 WMIN -0.0001 WMAX 0.0001

\*bottom edge.

CO SET BEDGE APPEND LINES LIMITS VMIN -0.001 VMAX 0.001 WMIN -0.0001 WMAX 0.0001

\*creation of set for interior lines.

CO SET OPEN INTCON

CO SET APPEND LINES ALL

CO SET REMOVE LEDGE TEDGE REDGE BEDGE

CO SET CLOSE

\*creation of sets which are helpful in tyings.

\*points of conc along the lrein 1.

CO SET CLP1 APPEND POINTS LIMIT UMIN 0.18 UMAX 0.19

\*points of conc along the lrein 2.

CO SET CLP2 APPEND POINTS LIMIT UMIN 0.36 UMAX 0.38

\*points of conc along the trein 1.

CO SET CTP1 APPEND POINTS LIMIT VMIN 0.18 VMAX 0.19

\* points of conc along the trein 2.

CO SET CTP2 APPEND POINTS LIMIT VMIN 0.36 VMAX 0.39

\*lines of conc along the lrein 1.

CO SET CLL1 APPEND LINES LIMIT UMIN 0.18 UMAX 0.19

\*lines of conc along the lrein 2.

CO SET CLL2 APPEND LINES LIMIT UMIN 0.36 UMAX 0.38

\*lines of conc along the trein 1.

CO SET CTL1 APPEND LINES LIMIT VMIN 0.18 VMAX 0.19

\*lines of conc along the trein 2.

CO SET CTL2 APPEND LINES LIMIT VMIN 0.36 VMAX 0.39

\*moving the corner grids to create corner grids of

\*half grid size (half of the rein spacing).

GEOM MO LEDGE LEDGEM

YES

GEOM MO REDGE REDGEM

YES

GEOM MO BEDGE BEDGEM

YES

GEOM MO TEDGE TEDGEM

YES

DRA DISP

\*\*changing the mesh division to half the main division

\*creation of set for corner conc surfaces.

CO SET CORSURF APPEND SURF S1 S2 S7 S9

MESH DIVI FACT CORSURF 0.5

\*\*\*\*\*

\*\*\*creation of the local axis\*\*\*\*\*

\*\*we have to fine the line to be spilt before entering

\*the name of the line to be broken, use matlab code to identify

GEOM SPLIT L5 Z1 0.5

GEOM SPLIT L17 Z2 0.5

GEOM COPY Z2 Z3 TRANS 0 0 0.1 \*to create the local z axis at z2.

GEOM COPY P1 Z4 TRANS 0 0 0.1 \*to creat local zaxis at z1.

GEOM COPY Z1 Z5 TRANS 0 -1E-5 0 \*to create dummy support beams.

GEOM COPY Z2 Z6 TRANS 1E-3 0 0 \*to create dummy support beams.

\*creation of local axis at z2.

CONSTRUCT COORDSYS RECTANGUL AXO Z2 Z3 Z1

\*creation of local axis at z1.

CO COORDSYS RECTANGUL OVERALL P1 Z4 P7

\*attaching the local axis.

PROP ATTACH Z6 COORDSYS AXO

\*attaching the local axis to conc elements to make sure

\*the oreintation of the axis of all the conc ele in the same dir.

PROP ATTACH CONSURF COORDSYS OVERALL

\*\*creation of dummy support beams\*\*\*\*

GEOM LINE DB1 Z1 Z5

GEOM LINE DB2 Z2 Z6

CO SET DUMBEAMS APPEND LINES DB1 DB2

\*mesh division for dummybeams

MESHING DIVISION LINE DUMBEAMS 2

\*\*\*\*\*

\*\*creation of the Irein\*\*\*\*

\*changing the names

CO NAME POINT PL 1

CO NAME LINE LR 1

CO NAME SURF INL 1

\*sweeping the conc points.

GEOM SWEEP P3 TRZL 1 DEPENDEN

\*sweeping the line to get interface element.

GEOM SWEEP LR1 LR2 BEDGEM 6 DEPENDEN \*mention half the main division.

GEOM SWEEP LR2 LR5 TRY1 12 DEPENDEN

\*here enter a copy command to create more interior interface elements in lre in dir

\*grids of try1 distance, below is the command; activate it.

\*GEOM COPY INL2 TRY1 2 DEPENDEN

\*copying the corner interface element to the other corner.

GEOM COPY INL1 INLCOPY

\*creation of the inl element set.

CO SET OPEN FRLREIN

CO SET APPEND SURF ALL

CO SET REMOVE CONSURF

CO SET CLOSE

\*copy in the x dir.

GEOM COPY FRLREIN TRX1 1 DEPENDEN

\*changing the eye view.

EYE ANG -60 45

\*creation of the entire lre in interface set.

CO SET OPEN INLREIN

CO SET APPEND SURF ALL

CO SET REMOVE CONSURF

CO SET CLOSE

\*\*\*\*\*

\*\*changing the names for creation of lre in.

CO NAME POINT PR 1

CO NAME LINE T 1

CO NAME SURF INTR 1

\* sweeping conc point.

GEOM SWEEP P2 TRZT 1 DEPENDEN

\*sweeping the line to creat interface ele in x dir.

GEOM SWEEP T1 LEDGEM 6 DEPENDEN

GEOM SWEEP T2 TRX1 12 DEPENDEN

\*enter the number of copies in the x dir; activate the command

\*to create more interior interface ele.

\*change the number of copies that u

\*need based on number of grids-2.

\*GEOM CO INTR2 TRX1 2 DEPENDEN

\*copying the corner interface ele to other corner.

GEOM CO INTR1 INTCOPY

\*\*creation of set of first row interface ele in trein dir

CO SET OPEN FTREIN

CO SET APPEND SURF ALL

CO SET REMOVE CONSURF INLREIN

CO SET CLOSE

\*change the number of copies that u

\*need based on number of grids-2.

GEOM COPY FTREIN TRY1 1 DEPENDEN

\*creation of interface element set in trein direction.

CO SET OPEN INTREIN

CO SET APPEND SURF ALL

CO SET REMOVE INLREIN CONSURF

CO SET CLOSE

\*\*\*\*\*

\*\*\*creation of the reinforcement sets\*\*\*

&

CO SET OPEN LREIN

CO SET APPEND LINES LIMITS WMIN 0.99 WMAX 1.11

CO SET CLOSE

\*trein set

CO SET OPEN TREIN

CO SET APPEND LINES LIMITS WMIN 1.99 WMAX 2.11

CO SET CLOSE

\*\*\*\*\*

\*creation of sets helpful for tyings

\*sets of points.

CO SET LREINP1 APPEND POINTS LIMIT UMIN 0.18 UMAX 0.19 WMIN 0.99 WMAX 1.11

CO SET LREINP2 APPEND POINTS LIMIT UMIN 0.36 UMAX 0.38 WMIN 0.99 WMAX 1.11

CO SET TREINP1 APPEND POINTS LIMIT VMIN 0.18 VMAX 0.19 WMIN 1.99 WMAX 2.11

CO SET TREINP2 APPEND POINTS LIMIT VMIN 0.36 VMAX 0.39 WMIN 1.99 WMAX 2.11

\*\*\*\*\*

\*sets of lines.

CO SET LREINL1 APPEND LINES LIMIT UMIN 0.18 UMAX 0.19 WMIN 0.99 WMAX 1.11

CO SET LREINL2 APPEND LINES LIMIT UMIN 0.36 UMAX 0.38 WMIN 0.99 WMAX 1.11

CO SET TREINL1 APPEND LINES LIMIT VMIN 0.18 VMAX 0.19 WMIN 1.99 WMAX 2.11

CO SET TREINL2 APPEND LINES LIMIT VMIN 0.36 VMAX 0.39 WMIN 1.99 WMAX 2.11

\*\*\*\*\*

\*moving the reinforcement back to the same height as the concrete elements to create

\*interface elements of zero area.

GEOM MO LREIN Z 0

YES

GEOM MO TREIN Z 0

YES

\*\*\*\*\*

\*\*\*creation of loaders made of beam elements

\*to load the corner nodes.

\*changing name.

CO NAME POINT Z 7

CO NAME LINE DB 3

GEOM SWEEP P1 TRANS -1E-3 0 0 DEPENDENT

GEOM SWEEP P7 TRANS 1E-3 0 0 DEPENDENT

GEOM SWEEP P16 TRANS 1E-3 0 0 DEPENDENT

GEOM SWEEP P13 TRANS -1E-3 0 0 DEPENDENT

GEOM SWEEP P1 TRANS 0 -1E-3 0 DEPENDENT

GEOM SWEEP P7 TRANS 0 -1E-3 0 DEPENDENT

GEOM SWEEP P16 TRANS 0 1E-3 0 DEPENDENT

GEOM SWEEP P13 TRANS 0 1E-3 0 DEPENDENT

\*creation of loader sets.

CO SET XTRUSS APPEND LINES DB3 DB4 DB5 DB6

CO SET YTRUSS APPEND LINES DB7 DB8 DB9 DB10

\*mesh division for the loaders.

MESHING DIVISION LINE XTRUSS 1

MESHING DIVISION LINE YTRUSS 1

\*\*\*\*\*

\*\*meshing type for the model.

MESH TYPE CONSURF Q8MEM \* 4 node plane stress ele.

MESH TYPE INLREIN L8IF \*4 node interface ele.

MESH TYPE INTREIN L8IF \* 4 node interfce ele.

MESH TYPE LREIN L7BEN \*2 node beam ele.

MESH TYPE TREIN L7BEN \*2 node beam ele.

MESH TYPE DUMBEAMS CL9BE \* 3 node beam e.le

MESH TYPE XTRUSS L7BEN \* 2 node beam ele.

MESH TYPE YTRUSS L7BEN \*2 node beam ele.

MESH TYPE LEDGE L7BEN \*2 node beam ele.

MESH TYPE REDGE L7BEN \*2 node beam ele.

MESH TYPE BEDGE L7BEN \*2 node beam ele.

MESH TYPE TEDGE L7BEN \*2 node beam ele.

```

*mesh generation.

MESH GEN

VIEW MESH

EYE ZOOM IN .519 .6440001 .751 .45

****creation of material properties panel a3****

*concrete material

PROP MAT CONC EX EX "A3CONC.DAT"

*reinforcement material

PROP MAT STEEL EX EX "20STAL.DAT"

*interface material

PROP MAT BONDS EX EX "BOCOGOOD.DAT"

****creation of physical properties*****

*half the test panel thickness.

PROPERTY PHYSICAL CONTHK GEOMETRY PLANSTRS THREGULR 0.0889

*dia of the rein.

PROPERTY PHYSICAL BARDIA GEOMETRY BEAM CLASSII PREDEFIN CIRCLE 20E-03

*cicumference of the rein bar.

PROPERTY PHYSICAL BTHIK GEOMETRY INTERFAC LINE BONDSL 62.832E-03

***assigning the material&physical properties to the elements***

PROP ATTACH CONSURF MAT CONC

PROP ATTACH LREIN MAT STEEL

PROP ATTACH TREIN MAT STEEL

PROP ATTACH LREIN PHY BARDIA

PROP ATTACH TREIN PHY BARDIA

PROP ATTACH CONSURF PHY CONTHK

PROP ATTACH INLREIN MAT BONDS

PROP ATTACH INTREIN MAT BONDS

PROP ATTACH INLREIN PHY BTHIK

PROP ATTACH INTREIN PHY BTHIK

***

```

\*\*\*\*\*creation of supports\*\*\*\*\*

PROP BOUNDARY CONSTRAINT BO1 Z5 123

PROP BOUNDARY CONSTRAINT BO2 Z6 23

\*creation of tyings

\*not exactly the tyings but they help us to pick the node pairs

\*of rein and conc nodes to tie the conc and the rein nodes

\*to slip in the rein direction only.

PROP BOUNDARY MPC RCONNECT PROXIMITY BO3 LREINL1 CLL1 2

PROP BOUNDARY MPC RCONNECT PROXIMITY BO4 LREINL2 CLL2 2

PROP BOUNDARY MPC RCONNECT PROXIMITY BO5 TREINL1 CTL1 1

PROP BOUNDARY MPC RCONNECT PROXIMITY BO6 TREINL2 CTL2 1

\*\*\*to view the points

VIEW GEOM +Z5

VIEW GEOM +Z6

\* to view the local coordinate system at the point

LABEL MESH CSYST Z6

VIEW MESH +LREIN RED

VIEW MESH +TREIN RED

\*\*\* generation of \*.dat file

UTI WRITE DIANA shearpanel

YES\*needed when data is overwritten to the same dat file 'shearpanel'.

U SET COL INV

\*\*\*please note that tyings are originally created using excel files due to

\*unavailibility of appropriate commands in iDIANA interface to create the wished tyings

\*please refer excel sheets for futher part of \*.dat file.

\*\*\*the bat file doesn't contain anything regarding the loading beam system

\*\* the loading beam system was created using excel.

## Appendix E: Batch file (\*.bat) used for the extraction of the results from the postprocessor.

\*inverting the colour of the screen.

U S COL INV

\*plotting the displacements of the four nodes used for

\*the calculation of shear strain.

RESULTS LOADCASE all

R N TDTX...G TDTX

P G N 638 725 329 224

U T P O xdisp.lst

P G N 638 725 329 224

U T P C

R N TDTX...G TDTy

P G N 638 725 329 224

U T P O ydisp.lst

P G N 638 725 329 224

U T P C

\*plotting the load deformation curve.

R N FRX...G RESFRX

P G N 80003

U T P O lodeform.lst

P G N 80003

U T P C

\*\*\*\*\*

\*transverse reinforcement 1.

CONSTRUCT LINE ELEMENTS TREIN1 LIST 147 TO 170

y

\*transverse reinforcement 1.

CONSTRUCT LINE ELEMENTS TREIN2 LIST 171 TO 194

y

\*longitudinal reinforcement 1.

CONSTRUCT LINE ELEMENTS LREIN1 LIST 99 TO 122

y

\*longitudinal reinforcement 1.

cONSTRUCT LINE ELEMENTS LREIN2 LIST 123 TO 146

y

\*nodes in the left edge

CONSTRUCT LINE nodes LEFTE LIST 1 2 3 4 5 6 7 27 28 29 30 :

31 32 33 34 35 36 37 38 39 40 41 42 43 44

y

\*nodes in the right edge

CO LINE nodes RIGHTE LIST 20 21 22 23 24 25 26 :

86 87 88 89 90 91 92 93 94 95 96 69 70 71 72 73 74 68

y

\*nodes in the top edge

CO LINE nodes TOPE LIST 44 45 46 47 48 49 50 51 52 53 54 55 :

56 57 58 59 60 61 62 63 64 65 66 67 68

y

\*nodes in the bottom edge

CO LINE nodes BOTTE LIST 1 8 9 10 11 12 13 75 76 77 :

78 79 80 81 82 83 84 85 14 15 16 17 18 19 20

y

\*concrete nodes under longitudinal reinforcement 1

CO LINE nodes CLL1 LIST 13 209 215 221 227 233 239 :

347 353 359 365 371 377 383 389 395 401 407 413 623 :

629 635 641 647 50

Y

\*concrete nodes under longitudinal reinforcement 2

CO LINE NODES CLL2 LIST 14 245 257 269 281 293 305 419 :

431 443 455 467 479 491 503 515 527 539 551 653 665 677 689 701 62

Y

\*concrete nodes under transverse reinforcement 1

CO LINE NODES CTL1 LIST 7 244 243 242 241 240 239 316 315 314 :

313 312 311 310 :

309 308 307 306 305 346 345 344 343 342 26

Y

\*concrete nodes under transverse reinforcement 1

CO LINE NODES CTL2 LIST 38 418 417 416 415 414 413 562 561 :

560 559 558 557 556 555 554 553 552 551 622 621 620 619 618 69

Y

\*nodes of longitudinal reinforcement 1

CO LINE NODES L1 LIST 101 TO 125

Y

\*nodes of longitudinal reinforcement 2

CO LINE NODES L2 LIST 126 TO 150

Y

\*nodes of transverse reinforcement 1

CO LINE NODES T1 LIST 151 TO 175

Y

\*nodes of transverse reinforcement 2

CO LINE NODES T2 LIST 176 TO 200

Y

\*\*\*\*\*

\*plotting local stress in x direction in the element

RESULTS ELEMENT EL.SXX.L SXX

r l lc2 578

P G LINE TREIN1

u t p o stresst1.lst

p g line trein1

u t p c

p g line trein2

u t p o stresst2.lst

p g line trein2

u t p c

p g line lrein1

u t p o stressl1.lst

p g line lrein1

u t p c

p g line lrein2

u t p o stressl2.lst

p g line lrein2

u t p c

\*\*\*\*\*

\*plotting the local stres in x direction at gaussian points

RESULTS GAUSSIAN EL.SXX.L SXX

r l lc2 578

P G LINE TREIN1

u t p o gstresst1.lst

p g line trein1

u t p c

p g line trein2

u t p o gstresst2.lst

p g line trein2

u t p c

p g line lrein1

u t p o gstressl1.lst

p g line lrein1

u t p c

p g line lrein2

u t p o gstressl2.lst

p g line lrein2

u t p c

\*to find whether lines r straight or not

\*plotting the x displacements along the edges

R N TDT TDTX

P G L TOPE

U T P O topx.lst

P G L TOPE

U T P C

P G L BOTTE

U T P O botx.lst

P G L BOTTE

U T P C

P G L RIGHTE

U T P O rightx.lst

P G L RIGHTE

U T P C

P G L LEFTE

U T P O leftx.lst

P G L LEFTE

U T P C

\*\*\*\*\*

\*plotting the y displacements along the edges

R N TDT TDTy

P G L TOPE

U T P O topy.lst

P G L TOPE

U T P C

P G L BOTTE

U T P O boty.lst

P G L BOTTE

U T P C

P G L RIGHTE

U T P O righty.lst

P G L RIGHTE

U T P C

P G L LEFTE

U T P O lefty.lst

P G L LEFTE

U T P C

\*\*\*\*\*

\*plotting the deformed shape of the model

V M

V O D U TDT RES 100

EYE FRAME

EYE ZOOM .233 .79 .197 .754

R L LC2 30

RESULTS ELEMENT EL.E1... E1

P C F 1E-3 T 0 L 10

L M CONS

E L

UTILITY SETUP PLOTTER FORMAT POSTSCRIPT COLOUR

DRAWING SAVE PLOTFILE 30

YES

STEP 30

\*\*\*\*\*

R L LC2 31

E L O

L M O

D D

L M CONS

E L

DRAWING SAVE PLOTFILE 31

YES

STEP 31

\*\*\*

R L LC2 130

E L O

L M O

D D

L M CONS

E L

DRAWING SAVE PLOTFILE 130

YES

STEP 130

\*\*\*\*\*

R L LC2 210

E L O

L M O

D D

L M CONS

E L

DRAWING SAVE PLOTFILE 210

YES

STEP 210

\*\*\*\*\*

R L LC2 310

E L O

L M O

D D

L M CONS

E L

DRAWING SAVE PLOTFILE 310

YES

STEP 310

\*\*\*\*\*

R L LC2 375

E L O

L M O

D D

L M CONS

E L

DRAWING SAVE PLOTFILE 375

YES

STEP 375

\*\*\*\*\*

R L LC2 578

E L O

L M O

D D

L M CONS

E L

DRAWING SAVE PLOTFILE 578

YES

STEP 578

\*\*\*\*\*

R N TDT TDTX

\*used for the calculation of dowel action and slip

r l lc2 30

p g line ctl1

u t p o 30ctl1x.lst

p g line ctl1

u t p c

p g line ctl2

u t p o 30ctl2x.lst

p g line ctl2

u t p c

\*\*\*\*\*

r l lc2 31

p g line ctl1

u t p o 31ctl1x.lst

p g line ctl1

u t p c

p g line ctl2

u t p o 31ctl2x.lst

p g line ctl2

u t p c

\*\*\*\*\*

r l lc2 130

p g line ctl1

u t p o 130ctl1x.lst

p g line ctl1

u t p c

p g line ctl2

u t p o 130ctl2x.lst

p g line ctl2

u t p c

\*\*\*\*\*

r l lc2 210

p g line ctl1

u t p o 210ctl1x.lst

p g line ctl1

u t p c

p g line ctl2

u t p o 210ctl2x.lst

p g line ctl2

u t p c

\*\*\*\*\*

r l lc2 310

p g line ctl1

u t p o 310ctl1x.lst

p g line ctl1

u t p c

p g line ctl2

u t p o 310ctl2x.lst

p g line ctl2

u t p c

\*\*\*\*\*

r l lc2 375

p g line ctl1

u t p o 375ctl1x.lst

p g line ctl1

u t p c

p g line ctl2

u t p o 375ctl2x.lst

p g line ctl2

u t p c

\*\*\*\*\*

r l lc2 578

p g line ctl1

u t p o 578ctl1x.lst

p g line ctl1

u t p c

p g line ctl2

u t p o 578ctl2x.lst

p g line ctl2

u t p c

\*\*\*\*\*

R L LC2 31

P G LINE T1

U T P O 31t1x.lst

P G LINE T1

U T P C

P G LINE T2

U T P O 31t2x.lst

P G LINE T2

U T P C

P G LINE L1

U T P O 3111x.lst

P G LINE L1

U T P C

P G LINE L2

U T P O 3112x.lst

P G LINE L2

U T P C

\*\*\*\*\*

R L LC2 30

P G LINE T1

U T P O 30t1x.lst

P G LINE T1

U T P C

P G LINE T2

U T P O 30t2x.lst

P G LINE T2

U T P C

P G LINE L1

U T P O 3011x.lst

P G LINE L1

U T P C

P G LINE L2

U T P O 30l2x.lst

P G LINE L2

U T P C

\*\*\*\*\*

R L LC2 130

P G LINE T1

U T P O 130t1x.lst

P G LINE T1

U T P C

P G LINE T2

U T P O 130t2x.lst

P G LINE T2

U T P C

P G LINE L1

U T P O 13011x.lst

P G LINE L1

U T P C

P G LINE L2

U T P O 130l2x.lst

P G LINE L2

U T P C

\*\*\*\*\*

R L LC2 210

P G LINE T1

U T P O 210t1x.lst

P G LINE T1

U T P C

P G LINE T2

U T P O 210t2x.lst

P G LINE T2

U T P C

P G LINE L1

U T P O 210l1x.lst

P G LINE L1

U T P C

P G LINE L2

U T P O 210l2x.lst

P G LINE L2

U T P C

\*\*\*\*\*

R L LC2 310

P G LINE T1

U T P O 310t1x.lst

P G LINE T1

U T P C

P G LINE T2

U T P O 310t2x.lst

P G LINE T2

U T P C

P G LINE L1

U T P O 31011x.lst  
P G LINE L1  
U T P C  
P G LINE L2  
U T P O 31012x.lst  
P G LINE L2  
U T P C  
\*\*\*\*\*  
R L LC2 375  
P G LINE T1  
U T P O 375t1x.lst  
P G LINE T1  
U T P C  
P G LINE T2  
U T P O 375t2x.lst  
P G LINE T2  
U T P C  
P G LINE L1  
U T P O 37511x.lst  
P G LINE L1  
U T P C  
P G LINE L2  
U T P O 37512x.lst  
P G LINE L2  
U T P C  
\*\*\*\*\*  
R L LC2 578  
P G LINE T1  
U T P O 578t1x.lst  
P G LINE T1

U T P C

P G LINE T2

U T P O 578t2x.lst

P G LINE T2

U T P C

P G LINE L1

U T P O 57811x.lst

P G LINE L1

U T P C

P G LINE L2

U T P O 57812x.lst

P G LINE L2

U T P C

\*\*\*\*\*

R N TDT TDTY

\*\*\*\*\*

R L LC2 31

P G LINE L1

U T P O 311ly.lst

P G LINE L1

U T P C

P G LINE L2

U T P O 3112y.lst

P G LINE L2

U T P C

P G LINE T1

U T P O 311ty.lst

P G LINE T1

U T P C

P G LINE T2

U T P O 31t2y.lst

P G LINE T2

U T P C

\*\*\*\*\*

R L LC2 30

P G LINE L1

U T P O 3011y.lst

P G LINE L1

U T P C

P G LINE L2

U T P O 3012y.lst

P G LINE L2

U T P C

P G LINE T1

U T P O 30t1y.lst

P G LINE T1

U T P C

P G LINE T2

U T P O 30t2y.lst

P G LINE T2

U T P C

\*\*\*\*\*

R L LC2 130

P G LINE L1

U T P O 13011y.lst

P G LINE L1

U T P C

P G LINE L2

U T P O 13012y.lst

P G LINE L2

U T P C

P G LINE T1

U T P O 130t1y.lst

P G LINE T1

U T P C

P G LINE T2

U T P O 130t2y.lst

P G LINE T2

U T P C

\*\*\*\*\*

R L LC2 210

P G LINE L1

U T P O 210l1y.lst

P G LINE L1

U T P C

P G LINE L2

U T P O 210l2y.lst

P G LINE L2

U T P C

P G LINE T1

U T P O 210t1y.lst

P G LINE T1

U T P C

P G LINE T2

U T P O 210t2y.lst

P G LINE T2

U T P C

\*\*\*\*\*

R L LC2 310

P G LINE L1

U T P O 31011y.lst  
P G LINE L1  
U T P C  
P G LINE L2  
U T P O 31012y.lst  
P G LINE L2  
U T P C  
P G LINE T1  
U T P O 310t1y.lst  
P G LINE T1  
U T P C  
P G LINE T2  
U T P O 310t2y.lst  
P G LINE T2  
U T P C  
\*\*\*\*\*  
R L LC2 375  
P G LINE L1  
U T P O 37511y.lst  
P G LINE L1  
U T P C  
P G LINE L2  
U T P O 37512y.lst  
P G LINE L2  
U T P C  
P G LINE T1  
U T P O 375t1y.lst  
P G LINE T1  
U T P C  
P G LINE T2

U T P O 375t2y.lst

P G LINE T2

U T P C

\*\*\*\*\*

R L LC2 578

P G LINE L1

U T P O 578l1y.lst

P G LINE L1

U T P C

P G LINE L2

U T P O 578l2y.lst

P G LINE L2

U T P C

P G LINE T1

U T P O 578t1y.lst

P G LINE T1

U T P C

P G LINE T2

U T P O 578t2y.lst

P G LINE T2

U T P C

\*\*\*\*\*

R L LC2 30

P G LINE CLL1

U T P O 30cll1y.lst

p g line cll1

u t p c

p g line cll2

u t p o 30cll2y.lst

p g line cll2

u t p c

\*\*\*\*\*

R L LC2 31

P G LINE CLL1

U T P O 31cll1y.lst

p g line cll1

u t p c

p g line cll2

u t p o 31cll2y.lst

p g line cll2

u t p c

\*\*\*\*\*

R L LC2 130

P G LINE CLL1

U T P O 130cll1y.lst

p g line cll1

u t p c

p g line cll2

u t p o 130cll2y.lst

p g line cll2

u t p c

\*\*\*\*\*

R L LC2 210

P G LINE CLL1

U T P O 210cll1y.lst

p g line cll1

u t p c

p g line cll2

u t p o 210cll2y.lst

p g line cll2

u t p c

\*\*\*\*\*

R L LC2 310

P G LINE CLL1

U T P O 310cll1y.lst

p g line cll1

u t p c

p g line cll2

u t p o 310cll2y.lst

p g line cll2

u t p c

\*\*\*\*\*

R L LC2 375

P G LINE CLL1

U T P O 375cll1y.lst

p g line cll1

u t p c

p g line cll2

u t p o 375cll2y.lst

p g line cll2

u t p c

\*\*\*\*\*

R L LC2 578

P G LINE CLL1

U T P O 578cll1y.lst

p g line cll1

u t p c

p g line cll2

u t p o 578cll2y.lst

p g line cll2

u t p c

\*\*\*\*\*

RESULTS ELEMENT EL.MX..L MZ

\*plotting the moments in the reinforcements

\*\*\*\*\*

R L LC2 30

P G LINE TREIN1

U T P O 30trein1.lst

P G LINE TREIN1

U T P C

P G LINE TREIN2

U T P O 30trein2.lst

P G LINE TREIN2

U T P C

P G LINE LREIN1

U T P O 30lrein1.lst

P G LINE LREIN1

U T P C

P G LINE LREIN2

U T P O 30lrein2.lst

P G LINE LREIN2

U T P C

\*\*\*\*\*

R L LC2 31

P G LINE TREIN1

U T P O 31trein1.lst

P G LINE TREIN1

U T P C

P G LINE TREIN2

U T P O 31trein2.lst

P G LINE TREIN2

U T P C

P G LINE LREIN1

U T P O 31rein1.lst

P G LINE LREIN1

U T P C

P G LINE LREIN2

U T P O 31rein2.lst

P G LINE LREIN2

U T P C

\*\*\*\*\*

R L LC2 130

P G LINE TREIN1

U T P O 130rein1.lst

P G LINE TREIN1

U T P C

P G LINE TREIN2

U T P O 130rein2.lst

P G LINE TREIN2

U T P C

P G LINE LREIN1

U T P O 130rein1.lst

P G LINE LREIN1

U T P C

P G LINE LREIN2

U T P O 130rein2.lst

P G LINE LREIN2

U T P C

\*\*\*\*\*

R L LC2 210

P G LINE TREIN1

U T P O 210trein1.lst

P G LINE TREIN1

U T P C

P G LINE TREIN2

U T P O 210trein2.lst

P G LINE TREIN2

U T P C

P G LINE LREIN1

U T P O 210lrein1.lst

P G LINE LREIN1

U T P C

P G LINE LREIN2

U T P O 210lrein2.lst

P G LINE LREIN2

U T P C

\*\*\*\*\*

R L LC2 310

P G LINE TREIN1

U T P O 310trein1.lst

P G LINE TREIN1

U T P C

P G LINE TREIN2

U T P O 310trein2.lst

P G LINE TREIN2

U T P C

P G LINE LREIN1

U T P O 310lrein1.lst

P G LINE LREIN1

U T P C

P G LINE LREIN2

U T P O 310rein2.lst

P G LINE LREIN2

U T P C

\*\*\*\*\*

R L LC2 375

P G LINE TREIN1

U T P O 375trein1.lst

P G LINE TREIN1

U T P C

P G LINE TREIN2

U T P O 375trein2.lst

P G LINE TREIN2

U T P C

P G LINE LREIN1

U T P O 375rein1.lst

P G LINE LREIN1

U T P C

P G LINE LREIN2

U T P O 375rein2.lst

P G LINE LREIN2

U T P C

\*\*\*\*\*

R L LC2 578

P G LINE TREIN1

U T P O 578trein1.lst

P G LINE TREIN1

U T P C

P G LINE TREIN2

U T P O 578trein2.lst

P G LINE TREIN2

U T P C

P G LINE LREIN1

U T P O 578lrein1.lst

P G LINE LREIN1

U T P C

P G LINE LREIN2

U T P O 578lrein2.lst

P G LINE LREIN2

U T P C

\*\*\*\*\*

\*interface elements along the longitudinal reinforcement 1

CO LINE ELEMENTS ILREIN1 LIST 784 783 782 781 780 779 796 795 794 :

793 792 791 790 789 788 787 786 785 802 801 800 799 798 797

Y

\*interface elements along the longitudinal reinforcement 2

CO LINE ELEMENTS ILREIN2 LIST 808 807 806 805 804 803 820 :

819 818 817 816 815 814 813 812 811 810 809 826 825 824 823 822 821

Y

\*interface elements along the transverse reinforcement 1

CO LINE ELEMENTS ITREIN1 LIST 832 831 830 829 828 827 844 843 :

842 841 840 839 838 837 836 835 834 833 850 849 848 847 846 845

Y

\*interface elements along the transverse reinforcement 2

CO LINE ELEMENTS ITREIN2 LIST 856 855 854 853 852 851 868 867:

866 865 864 863 862 861 860 859 858 857 874 873 872 871 870 869

y

\*\*\*\*\*

RESULTS GAUSSIAN EL.STX.L STY

\*plotting the shear traction in interface elements

\*\*\*\*\*

R L LC2 31

P G LINE ILREIN1

U T P O 31ilrein1.lst

P G LINE ILREIN1

U T P C

P G LINE ILREIN2

U T P O 31ilrein2.lst

P G LINE ILREIN2

U T P C

P G LINE ITREIN1

U T P O 31itrein1.lst

P G LINE ITREIN1

U T P C

P G LINE ITREIN2

U T P O 31itrein2.lst

P G LINE ITREIN2

U T P C

\*\*\*\*\*

R L LC2 30

P G LINE ILREIN1

U T P O 30ilrein1.lst

P G LINE ILREIN1

U T P C

P G LINE ILREIN2

U T P O 30ilrein2.lst

P G LINE ILREIN2

U T P C

P G LINE ITREIN1

U T P O 30itrein1.lst

P G LINE ITREIN1

U T P C

P G LINE ITREIN2

U T P O 30itrein2.lst

P G LINE ITREIN2

U T P C

\*\*\*\*\*

R L LC2 130

P G LINE ILREIN1

U T P O 130ilrein1.lst

P G LINE ILREIN1

U T P C

P G LINE ILREIN2

U T P O 130ilrein2.lst

P G LINE ILREIN2

U T P C

P G LINE ITREIN1

U T P O 130itrein1.lst

P G LINE ITREIN1

U T P C

P G LINE ITREIN2

U T P O 130itrein2.lst

P G LINE ITREIN2

U T P C

\*\*\*\*\*

R L LC2 210

P G LINE ILREIN1

U T P O 210ilrein1.lst

P G LINE ILREIN1

U T P C

P G LINE ILREIN2  
U T P O 210ilrein2.lst  
P G LINE ILREIN2  
U T P C  
P G LINE ITREIN1  
U T P O 210itrein1.lst  
P G LINE ITREIN1  
U T P C  
P G LINE ITREIN2  
U T P O 210itrein2.lst  
P G LINE ITREIN2  
U T P C  
\*\*\*\*\*  
R L LC2 310  
P G LINE ILREIN1  
U T P O 310ilrein1.lst  
P G LINE ILREIN1  
U T P C  
P G LINE ILREIN2  
U T P O 310ilrein2.lst  
P G LINE ILREIN2  
U T P C  
P G LINE ITREIN1  
U T P O 310itrein1.lst  
P G LINE ITREIN1  
U T P C  
P G LINE ITREIN2  
U T P O 310itrein2.lst  
P G LINE ITREIN2  
U T P C

\*\*\*\*\*

R L LC2 375

P G LINE ILREIN1

U T P O 375ilrein1.lst

P G LINE ILREIN1

U T P C

P G LINE ILREIN2

U T P O 375ilrein2.lst

P G LINE ILREIN2

U T P C

P G LINE ITREIN1

U T P O 375itrein1.lst

P G LINE ITREIN1

U T P C

P G LINE ITREIN2

U T P O 375itrein2.lst

P G LINE ITREIN2

U T P C

\*\*\*\*\*

R L LC2 578

P G LINE ILREIN1

U T P O 578ilrein1.lst

P G LINE ILREIN1

U T P C

P G LINE ILREIN2

U T P O 578ilrein2.lst

P G LINE ILREIN2

U T P C

P G LINE ITREIN1

U T P O 578itrein1.lst

P G LINE ITREIN1

U T P C

P G LINE ITREIN2

U T P O 578itrein2.lst

P G LINE ITREIN2

U T P C

## Appendix F: Input data file (\*.dat file)

The input data file for the panel A3 is shown.

FEMGEN MODEL : A3

ANALYSIS TYPE : Structural 2D

'UNITS'

LENGTH M

TIME SEC

TEMPER CELSIU

FORCE N

'COORDINATES' DI=2

: coordinates for the model of the panel

1	9.430000E-02	9.430000E-02
2	9.430000E-02	1.100167E-01
3	9.430000E-02	1.257333E-01
4	9.430000E-02	1.414500E-01
5	9.430000E-02	1.571667E-01
6	9.430000E-02	1.728833E-01
7	9.430000E-02	1.886000E-01
8	1.100167E-01	9.430000E-02
9	1.257333E-01	9.430000E-02
10	1.414500E-01	9.430000E-02
11	1.571667E-01	9.430000E-02
12	1.728833E-01	9.430000E-02
13	1.886000E-01	9.430000E-02
14	3.772000E-01	9.430000E-02
15	3.929167E-01	9.430000E-02
16	4.086334E-01	9.430000E-02
17	4.243500E-01	9.430000E-02

“ “ “

```

“      “      “
“      “      “
732  3.929167E-01  4.400667E-01
733  4.557833E-01  4.557833E-01
734  4.400667E-01  4.557833E-01
735  4.243500E-01  4.557833E-01
736  4.086334E-01  4.557833E-01
737  3.929167E-01  4.557833E-01

```

:for dummy beams used to make eccentric work (previously used but not for the present analysis

```

750  2.829000E-01  4.7675E-01
751  2.829000E-01  4.8200E-01
752  9.210000E-02  2.82900E-01
753  8.999000E-02  2.829000E-01

```

::::: dummy nodes for the guiders connected to the concrete nodes, to control the slip at the edges between reinforcement and the concrete nodes

: longitudinal direction

```

130001  1.886000E-01  9.420000E-02
140001  3.772000E-01  9.420000E-02
500001  1.886000E-01  4.725000E-01
620001  3.772000E-01  4.725000E-01

```

:transverse direction

```

700001  9.420000E-02  1.886000E-01
260001  4.725000E-01  1.886000E-01
380001  9.420000E-02  3.772000E-01
690001  4.725000E-01  3.772000E-01

```

: Nodes for the beam system (refer Appendix J)

: Elements

'ELEMENTS'

CONNECTIVITY

: edge beams

1 L7BEN 1 2

2 L7BEN 2 3

“ “ “

“ “ “

“ “ “

95 L7BEN 95 96

96 L7BEN 96 69

:dummy support beams

97 CL9BE 80 97 98

98 CL9BE 91 99 100

:reinforcements

99 L7BEN 101 102

100 L7BEN 102 103

“ “ “

“ “ “

“ “ “

192 L7BEN 197 198

193 L7BEN 198 199

194 L7BEN 199 200

:corner loaders (dummy beams loading corner nodes)

: x dir

195 L7BEN 1 201

196 L7BEN 20 202

197 L7BEN 68 203

198 L7BEN 44 204

:y dir

199 L7BEN 1 205

200 L7BEN 20 206

201 L7BEN 68 207

202 L7BEN 44 208

:concrete elements

203 Q8MEM 13 12 210 209

204 Q8MEM 12 11 211 210

205 Q8MEM 11 10 212 211

“ “ “

“ “ “

“ “ “

776 Q8MEM 735 736 64 65

777 Q8MEM 736 737 63 64

778 Q8MEM 737 701 62 63

: interface elements

779 L8IF 239 233 107 106

780 L8IF 233 227 106 105

781 L8IF 227 221 105 104

“ “ “

“ “ “

“ “ “

873 L8IF 621 622 196 195

874 L8IF 622 551 195 194

:creation of dummy beams for eccent

900 CL9BE 753 752 32

901 CL9BE 56 750 751

:guiders used for relative tyings between reinforcement and concrete

:longitudinal 1

902 L7BEN 13 130001

904 L7BEN 50 500001

:longi 2

903 L7BEN 14 140001

905 L7BEN 62 620001

:trans 1

906 L7BEN 7 700001

907 L7BEN 26 260001

:trans 2

908 L7BEN 38 380001

909 L7BEN 69 690001

: elements for the beam system refer Appendix F

: material properties

## MATERIALS

:dummy edge beams

/ 1-96 / 7

: concrete elements

/ 203-496 498-778 / 1

: reinforcements

/ 99-194 / 2

:interface elements

/ 779-874 / 3

: dummy support beams and dummy beam elements

/ 97 98 10001-80002 195-202 900-909 / 6

:no weak concrete element

/ 497 / 1

## GEOMETRY

:dummy edge beams

/ 2-6 8-17 20-41

44-65 67-71 73-96 / 8

:reinforcements

/ 99-194 / 2

:interface elements

/ 779-874 / 3

:concrete elements

/ 203-778 / 4

:beam systeme

/ 10001-80002 / 6

:dummy beam elements and dummy support beams

/ 97 98 900-909 / 7

/ 195-202 / 7

:hinge at the corner nodes

/ 1 7 19 43 / 9

/ 66 72 18 42 / 10

'MATERIALS'

:a3 concrete

1 YOUNG 3.458000E+10

POISON 2.000000E-01

DENSIT 2.400000E+03

TOTCRK ROTATE

TENCRV HORDYK

TENSTR 2.980000E+06

GF1 6.780000E+01

COMCRV THOREN

COMSTR 4.160000E+07

REDCRV VC1993

CNFCRV VECCHI

:20 mm dia bar reinforcement

2 YOUNG 1.998100E+11

POISON 3.000000E-01

DENSIT 7.800000E+03

YIELD VMISES

HARDIA 446.1275E+06 0

446.1325E+06 0.0089

624.9230E+06 0.0469

624.9280E+06 0.1969

HARDEN STRAIN

: interface elements (bond slip curve from MODEL code for confined good bond conditions)

3 DSTIF 5.769E+10 60E+10

BONDSL 3

SLPVAL 0 0

5.769E+06 .1E-03

7.612E+06 .2E-03

8.953E+06 .3E-03

10.045E+06 .4E-03

10.982E+06 .5E-03

11.813E+06 .6E-03

12.565E+06 .7E-03

13.254E+06 .8E-03

13.893E+06 .9E-03

14.491E+06 1.0E-03

14.491E+06 3.0E-03

14.057E+06 3.1E-03

13.622E+06 3.2E-03

13.187E+06 3.3E-03

12.752E+06 3.4E-03

11.013E+06 3.7E-03

10.579E+06 3.9E-03

9.709E+06 4.1E-03

7.101E+06 4.7E-03

6.231E+06 4.9E-03

5.797E+06 5.0E-03

5.797E+06 5.6E-03

: dummy support beams

6 DENSIT 0

YOUNG 200.0E+9

POISON 0.3  
 :for dummy edge beams  
 7 DENSIT 0  
 YOUNG 1.998100E+11  
 POISON 0.3  
 'GEOMETRY'  
 :dia of bar (reinforcement)  
 2 CIRCLE 2.000000E-02  
 :circumference of bar  
 3 THICK 6.283190E-02  
 CONFIG BONDSL  
 :thickness of the concrete elements with local x axis oriented along the global x axis  
 4 THICK 8.890000E-02  
 ZAXIS 0.000000E+00 0.000000E+00 0.100000E+01  
 : loading beam system  
 6 ZAXIS 0 0 1  
 RECTAN 1 1  
 : dummy support beams  
 7 RECTAN 1 1  
 ZAXIS 0 0 1  
 : edge beams  
 8 CIRCLE 0.1E-03  
 ZAXIS 0 0 1  
 : provision of hinges at the start node of the edge beams  
 9 CIRCLE 0.1E-03  
 ZAXIS 0 0 1  
 HINGE PHIZ1  
 : provision of hinges at the end node of the edge beams  
 10 CIRCLE 0.1E-03  
 HINGE PHIZ2

ZAXIS 0 0 1

:creation of groups helpful for easy identification

'GROUPS'

ELEMEN

1 FROW / 1-24 73-84 203-346 /

NODES

2 FROW\_N / 1-26 75-85 209-346 /

ELEMEN

3 SE1 / 37-72 635-778 /

NODES

4 SE1\_N / 38-74 413-418 551-562 618-737 /

ELEMEN

5 SE2 / 25-36 85-96 347-634 /

NODES

6 SE2\_N / 7 26-38 69 86-96 239-244 305-316 342-622 /

ELEMEN

:Concrete elements

7 CONSURF / 1-96 203-778 /

: concrete nodes

NODES

8 CONSURF\_N / 1-96 209-737 /

: left edge beams

ELEMEN

9 LEDGE / 1-6 25-42 /

NODES

10 LEDGE\_N / 1-7 27-44 /

:top edge beams

ELEMEN

11 TEDGE / 43-66 /

NODES

12 TEDGE\_N / 44-68 /

:right edge beams

ELEMEN

13 REDGE / 19-24 67-72 85-96 /

NODES

14 REDGE\_N / 20-26 68-74 86-96 /

:bottom edge beams

ELEMEN

15 BEDGE / 7-18 73-84 /

NODES

16 BEDGE\_N / 1 8-20 75-85 /

:interior concrete nodes

17 INTCON / 7 13 14 26 38 50 62 69 209 215 221 227 233 239-245

257 269 281 293 305-316 342-347 353 359 365 371 377

383 389 395 401 407 413-419 431 443 455 467 479 491

503 515 527 539 551-562 618-623 629 635 641 647 653

665 677 689 701 /

: concrete nodes along longitudinal reinforcement 1

18 CLP1 / 13 50 239 413 /

: concrete nodes along longitudinal reinforcement 2

19 CLP2 / 14 62 305 551 /

: concrete nodes along transverse reinforcement 1

20 CTP1 / 7 26 239 305 /

: concrete nodes along transverse reinforcement 2

21 CTP2 / 38 69 413 551 /

: concrete line elements along longitudinal reinforcement 1

22 CLL1 / 13 50 209 215 221 227 233 239 347 353 359 365 371 377

383 389 395 401 407 413 623 629 635 641 647 /

: concrete line elements along longitudinal reinforcement 2

23 CLL2 / 14 62 245 257 269 281 293 305 419 431 443 455 467 479

491 503 515 527 539 551 653 665 677 689 701 /

: concrete line elements along transverse reinforcement 2

24 CTL1 / 7 26 239-244 305-316 342-346 /

: concrete line elements along transverse reinforcement 2

25 CTL2 / 38 69 413-418 551-562 618-622 /

:corner concrete elements

ELEMEN

26 CORSURF / 1-24 37-48 61-72 203-238 311-346 635-670 743-778 /

NODES

27 CORSURF\_N / 1-26 38-50 62-74 209-245 257 269 281 293 305 317-346

413-418 551 618-653 665 677 689 701 713-737 /

:dummy support beams

ELEMEN

28 DUMBEAMS / 97 98 /

NODES

29 DUMBEAMS\_N / 80 91 97-100 /

ELEMEN

30 FRLREIN / 99-122 779-802 /

NODES

31 FRLREIN\_N / 13 50 101-125 209 215 221 227 233 239 347 353 359

365 371 377 383 389 395 401 407 413 623 629 635

641 647 /

ELEMEN

32 SE3 / 123-146 803-826 /

NODES

33 SE3\_N / 14 62 126-150 245 257 269 281 293 305 419 431 443 455

467 479 491 503 515 527 539 551 653 665 677 689 701 /

: interface elements along longitudinal direction

ELEMEN

34 INLREIN / 779-826 /

NODES

35 INLREIN\_N / 13 14 50 62 101-150 209 215 221 227 233 239 245  
257 269 281 293 305 347 353 359 365 371 377 383  
389 395 401 407 413 419 431 443 455 467 479 491  
503 515 527 539 551 623 629 635 641 647 653 665  
677 689 701 /

ELEMEN

36 FTREIN / 147-170 827-850 /

NODES

37 FTREIN\_N / 7 26 151-175 239-244 305-316 342-346 /

ELEMEN

38 SE4 / 171-194 851-874 /

NODES

39 SE4\_N / 38 69 176-200 413-418 551-562 618-622 /

: interface elements along transverse direction

ELEMEN

40 INTREIN / 827-874 /

NODES

41 INTREIN\_N / 7 26 38 69 151-200 239-244 305-316 342-346 413-418  
551-562 618-622 /

: longitudinal reinforcement

ELEMEN

42 LREIN / 99-146 /

NODES

43 LREIN\_N / 101-150 /

: transverse reinforcement

ELEMEN

44 TREIN / 147-194 /

NODES

45 TREIN\_N / 151-200 /

: nodes at points along the longitudinal reinforcement L1

46 LREINP1 / 101 107 119 125 /

: nodes at points along the longitudinal reinforcement L2

47 LREINP2 / 126 132 144 150 /

: nodes at points along the transverse reinforcement T1

48 TREINP1 / 151 157 169 175 /

: nodes at points along the transverse reinforcement T2

49 TREINP2 / 176 182 194 200 /

: elements along the longitudinal reinforcement L1

ELEMEN

50 LREINL1 / 99-122 /

NODES

51 LREINL1\_N / 101-125 /

: elements along the longitudinal reinforcement L2

ELEMEN

52 LREINL2 / 123-146 /

NODES

53 LREINL2\_N / 126-150 /

: elements along the transverse reinforcement T1

ELEMEN

54 TREINL1 / 147-170 /

NODES

55 TREINL1\_N / 151-175 /

: elements along the transverse reinforcement T2

ELEMEN

56 TREINL2 / 171-194 /

NODES

57 TREINL2\_N / 176-200 /

: x direction corner loaders

ELEMEN

58 XTRUSS / 195-198 /

NODES

59 XTRUSS\_N / 1 20 44 68 201-204 /

:y direction corner loaders

ELEMEN

60 YTRUSS / 199-202 /

NODES

61 YTRUSS\_N / 1 20 44 68 205-208 /

: dummy beams used for eccent command in past analysis when eccent tying type was used

62 DUMECC\_N / 32 750-753 56 /

ELEMEN

63 DUMECC / 900 901 /

: dummy guiders used for relative slip relationship between the concrete and reinforcement nodes at the edges of the model

64 GUIDERS / 902-908 /

NODES

65 GUIDERS\_N / 13 14 130001 140001 26 260001

69 690001 62 620001 50 500001

38 380001 7 700001 /

:support condition assigned to the dummy beams

'SUPPORTS'

:supports of the model

/ 98 / TR 1

/ 98 / TR 2

/ 98 100 / TR 3

/ 98 100 / RO 1 2 3

/ 100 / TR 4

: supports within the beam system

/ SPOINTS / TR 1

/ SPOINTS / RO 1

/ LPOINT / TR 1 2

:tyings

'TYINGS'

: Within the beam system

EQUAL TR 2

10003 20001

10013 20006

“ “ “

“ “ “

“ “ “

50028 60015

60008 70005

60013 80005

: Between the beam system and the model

FIX TR 1

: Connecting the corner nodes at the top edge to the beam system

203 10001 TR 2 1

204 10006 TR 2 1

: Connecting the corner nodes at the bottom edge to the beam system

201 10011 TR 2 -1

202 10016 TR 2 -1

: Connecting the ends of the beams system to the bottom edge

8 20011 TR 2 -1

9 20016 TR 2 -1

10 20021 TR 2 -1

11 20026 TR 2 -1

12 20031 TR 2 -1

13 20036 TR 2 -1

75 20041 TR 2 -1

76 20046 TR 2 -1

77	20051	TR 2 -1
78	20056	TR 2 -1
79	20061	TR 2 -1
80	20066	TR 2 -1
81	20071	TR 2 -1
82	20076	TR 2 -1
83	20081	TR 2 -1
84	20096	TR 2 -1
85	20086	TR 2 -1
14	20091	TR 2 -1
15	20101	TR 2 -1
16	20106	TR 2 -1
17	20111	TR 2 -1
18	20116	TR 2 -1
19	20121	TR 2 -1

: Connecting the top edge to the beam system

45	20126	TR 2 1
46	20131	TR 2 1
47	20136	TR 2 1
48	20141	TR 2 1
49	20146	TR 2 1
50	20151	TR 2 1
51	20156	TR 2 1
52	20161	TR 2 1
53	20166	TR 2 1
54	20171	TR 2 1
55	20176	TR 2 1
56	20181	TR 2 1
57	20186	TR 2 1
58	20191	TR 2 1

59 20196 TR 2 1  
60 20201 TR 2 1  
61 20206 TR 2 1  
62 20211 TR 2 1  
63 20216 TR 2 1  
64 20221 TR 2 1  
65 20226 TR 2 1  
66 20231 TR 2 1  
67 20236 TR 2 1

FIX TR 2

: Connecting corner nodes of the right edge to the beam system

206 10005 TR 2 1  
207 10010 TR 2 1

. Connecting the corner nodes of the left edge to the beam system

208 10015 TR 2 -1  
205 10020 TR 2 -1

: Connecting the right edge to the beam system

43 20015 TR 2 -1  
2 20020 TR 2 -1  
3 20025 TR 2 -1  
4 20030 TR 2 -1  
5 20035 TR 2 -1  
6 20040 TR 2 -1  
7 20045 TR 2 -1  
27 20050 TR 2 -1  
28 20055 TR 2 -1  
29 20060 TR 2 -1  
30 20065 TR 2 -1  
31 20070 TR 2 -1  
32 20075 TR 2 -1

33	20080	TR 2 -1
34	20085	TR 2 -1
35	20090	TR 2 -1
36	20095	TR 2 -1
37	20100	TR 2 -1
38	20105	TR 2 -1
39	20110	TR 2 -1
40	20115	TR 2 -1
41	20120	TR 2 -1
42	20125	TR 2 -1

: Connecting the right edge to the beam system

21	20130	TR 2 1
22	20135	TR 2 1
23	20140	TR 2 1
24	20145	TR 2 1
25	20150	TR 2 1
26	20155	TR 2 1
86	20160	TR 2 1
87	20165	TR 2 1
88	20170	TR 2 1
89	20175	TR 2 1
90	20180	TR 2 1
91	20190	TR 2 1
92	20195	TR 2 1
93	20200	TR 2 1
94	20205	TR 2 1
95	20210	TR 2 1
96	20215	TR 2 1
69	20220	TR 2 1
70	20225	TR 2 1

71 20230 TR 2 1  
72 20235 TR 2 1  
73 20240 TR 2 1  
74 20185 TR 2 1

::tyings within the panel

::slip for the transverse reinforcement

EQUAL TR 1

102 209  
103 215  
104 221  
105 227  
106 233  
107 239  
108 347  
109 353  
110 359  
111 365  
112 371  
113 377  
114 383  
115 389  
116 395  
117 401  
118 407  
119 413  
120 623  
121 629  
122 635  
123 641  
124 647

127	245
128	257
129	269
130	281
131	293
132	305
133	419
134	431
135	443
136	455
137	467
138	479
139	491
140	503
141	515
142	527
143	539
144	551
145	653
146	665
147	677
148	689
149	701

: slip for the longitudinal reinforcements

#### EQUAL TR 2

152	244
153	243
154	242
155	241
156	240

157	239
158	316
159	315
160	314
161	313
162	312
163	311
164	310
165	309
166	308
167	307
168	306
169	305
170	346
171	345
172	344
173	343
174	342
177	418
178	417
179	416
180	415
181	414
182	413
183	562
184	561
185	560
186	559
187	558
188	557

189 556  
 190 555  
 191 554  
 192 553  
 193 552  
 194 551  
 195 622  
 196 621  
 197 620  
 198 619  
 199 618

:tyings to keep the edge straight

:bottom edge

BETWEE TR 2

8 1 20 1.57167E-02 3.61483E-01  
 9 1 20 3.14333E-02 3.45767E-01  
 10 1 20 4.71500E-02 3.30050E-01  
 11 1 20 6.28667E-02 3.14333E-01  
 12 1 20 7.85833E-02 2.98617E-01  
 :101 1 20 7.85833E-02 2.98617E-01  
 13 1 20 9.43000E-02 2.82900E-01  
 75 1 20 1.10017E-01 2.67183E-01  
 76 1 20 1.25733E-01 2.51467E-01  
 77 1 20 1.41450E-01 2.35750E-01  
 78 1 20 1.57167E-01 2.20033E-01  
 79 1 20 1.72883E-01 2.04317E-01  
 80 1 20 1.88600E-01 1.88600E-01  
 81 1 20 2.04317E-01 1.72883E-01  
 82 1 20 2.20033E-01 1.57167E-01  
 83 1 20 2.35750E-01 1.41450E-01

84	1	20	2.51467E-01	1.25733E-01
85	1	20	2.67183E-01	1.10017E-01
:126	1	20	2.67183E-01	1.10017E-01
14	1	20	2.82900E-01	9.43000E-02
15	1	20	2.98617E-01	7.85833E-02
16	1	20	3.14333E-01	6.28667E-02
17	1	20	3.30050E-01	4.71500E-02
18	1	20	3.45767E-01	3.14333E-02
19	1	20	3.61483E-01	1.57167E-02
: top edge				
BETWEEN TR 2				
45	44	68	1.57167E-02	3.61483E-01
46	44	68	3.14333E-02	3.45767E-01
47	44	68	4.71500E-02	3.30050E-01
48	44	68	6.28667E-02	3.14333E-01
49	44	68	7.85833E-02	2.98617E-01
:125	44	68	9.43000E-02	2.82900E-01
50	44	68	9.43000E-02	2.82900E-01
51	44	68	1.10017E-01	2.67183E-01
52	44	68	1.25733E-01	2.51467E-01
53	44	68	1.41450E-01	2.35750E-01
54	44	68	1.57167E-01	2.20033E-01
55	44	68	1.72883E-01	2.04317E-01
56	44	68	1.88600E-01	1.88600E-01
57	44	68	2.04317E-01	1.72883E-01
58	44	68	2.20033E-01	1.57167E-01
59	44	68	2.35750E-01	1.41450E-01
60	44	68	2.51467E-01	1.25733E-01
61	44	68	2.67183E-01	1.10017E-01
:150	44	68	2.82900E-01	9.43000E-02

62	44	68	2.82900E-01	9.43000E-02
63	44	68	2.98617E-01	7.85833E-02
64	44	68	3.14333E-01	6.28667E-02
65	44	68	3.30050E-01	4.71500E-02
66	44	68	3.45767E-01	3.14333E-02
67	44	68	3.61483E-01	1.57167E-02

: right edge

BETWEE TR 1

21	20	68	1.57167E-02	3.61483E-01
22	20	68	3.14333E-02	3.45767E-01
23	20	68	4.71500E-02	3.30050E-01
24	20	68	6.28667E-02	3.14333E-01
25	20	68	7.85833E-02	2.98617E-01
:175	20	68	9.43000E-02	2.82900E-01
26	20	68	9.43000E-02	2.82900E-01
86	20	68	1.10017E-01	2.67183E-01
87	20	68	1.25733E-01	2.51467E-01
88	20	68	1.41450E-01	2.35750E-01
89	20	68	1.57167E-01	2.20033E-01
90	20	68	1.72883E-01	2.04317E-01
91	20	68	1.88600E-01	1.88600E-01
92	20	68	2.04317E-01	1.72883E-01
93	20	68	2.20033E-01	1.57167E-01
94	20	68	2.35750E-01	1.41450E-01
95	20	68	2.51467E-01	1.25733E-01
96	20	68	2.67183E-01	1.10017E-01
:200	20	68	2.82900E-01	9.43000E-02
69	20	68	2.82900E-01	9.43000E-02
70	20	68	2.98617E-01	7.85833E-02
71	20	68	3.14333E-01	6.28667E-02

72 20 68 3.30050E-01 4.71500E-02  
73 20 68 3.45767E-01 3.14333E-02  
74 20 68 3.61483E-01 1.57167E-02

: left edge

BETWEE TR 1

2 1 44 1.57167E-02 3.61483E-01  
3 1 44 3.14333E-02 3.45767E-01  
4 1 44 4.71500E-02 3.30050E-01  
5 1 44 6.28667E-02 3.14333E-01  
6 1 44 7.85833E-02 2.98617E-01  
:151 1 44 9.43000E-02 2.82900E-01  
7 1 44 9.43000E-02 2.82900E-01  
27 1 44 1.10017E-01 2.67183E-01  
28 1 44 1.25733E-01 2.51467E-01  
29 1 44 1.41450E-01 2.35750E-01  
30 1 44 1.57167E-01 2.20033E-01  
31 1 44 1.72883E-01 2.04317E-01  
32 1 44 1.88600E-01 1.88600E-01  
33 1 44 2.04317E-01 1.72883E-01  
34 1 44 2.20033E-01 1.57167E-01  
35 1 44 2.35750E-01 1.41450E-01  
36 1 44 2.51467E-01 1.25733E-01  
37 1 44 2.67183E-01 1.10017E-01  
:176 1 44 2.82900E-01 9.43000E-02  
38 1 44 2.82900E-01 9.43000E-02  
39 1 44 2.98617E-01 7.85833E-02  
40 1 44 3.14333E-01 6.28667E-02  
41 1 44 3.30050E-01 4.71500E-02  
42 1 44 3.45767E-01 3.14333E-02  
43 1 44 3.61483E-01 1.57167E-02

:tyings to prevent pull out failure

:and to allow slip between the reinforcements and the concrete nodes at the edges

:longitudinal slip control

FIX TR 2

:longi 1

101 130001 TR 2 1

500001 TR 2 -1

125 TR 2 1

:longi 2

126 140001 TR 2 1

150 TR 2 1

620001 TR 2 -1

:transverse slip control

:trans 1

FIX TR 1

151 700001 TR 1 1

260001 TR 1 -1

175 TR 1 1

:trans 2

176 380001 TR 1 1

690001 TR 1 -1

200 TR 1 1

:tying the rotational freedom of

:opposite edges to keep the edge parallel to each other

:the top and the bottom edge

EQUAL RO 3

/ 8-13 75-79 81-85 14-19

45-55 57-67 751 750 130001 140001

620001 500001 205 206 207 208 / 80

: the left and the right edge

/ 2-7 27-31 33-43 21-26 86-90 92-96

69-74 753 752 700001 380001

690001 260001 201 204 202 203 / 91

:loads

'LOADS'

:self weight

CASE 1

WEIGHT

4 9.83

: application of prescribed deformation at the beam system

CASE 2

DEFORM

/ LPOINT / TR 2 1E-3

:direction of the axes

'DIRECTIONS'

1 1.000000E+00 0.000000E+00 0.000000E+00

2 0.000000E+00 1.000000E+00 0.000000E+00

3 0.000000E+00 0.000000E+00 1.000000E+00

4 7.071068E-01 -7.071068E-01 0.000000E+00

'END'

## Appendix G: Command file (\*.COM file)

```
*FILOS  
  
INITIA  
  
*INPUT  
  
*NONLIN  
  
TYPE PHYSIC  
  
BEGIN OUTPUT FEMVIE BINARY  
  
BEGIN SELECT  
  
  STEPS 1-300(1) 300-600(1) 600-750(2) 750-2000(5)  
  
  NODES ALL  
  
  ELEMEN ALL  
  
  REINFO ALL  
  
END SELECT  
  
FI="A3"  
  
DISPLA TOTAL TRANSL GLOBAL  
  
DISPLA TOTAL ROTATI GLOBAL  
  
FORCE RESIDU TRANSL GLOBAL  
  
FORCE RESIDU ROTATI GLOBAL  
  
STRAIN TOTAL GREEN GLOBAL  
  
STRAIN TOTAL GREEN LOCAL  
  
STRAIN TOTAL GREEN PRINCI  
  
STRAIN TOTAL GREEN LOCAL INTPNT  
  
STRAIN TOTAL GREEN GLOBAL INTPNT  
  
STRESS TOTAL CAUCHY GLOBAL  
  
STRESS TOTAL CAUCHY PRINCI  
  
STRESS TOTAL CAUCHY LOCAL  
  
STRESS TOTAL CAUCHY PRINCI INTPNT  
  
STRESS TOTAL CAUCHY LOCAL INTPNT  
  
STRESS TOTAL CAUCHY GLOBAL INTPNT
```

```

STATUS CRACK INTPNT
END OUTPUT
BEGIN OUTPUT FEMVIE BINARY
  BEGIN SELECT
    STEPS 1-300(1) 300-600(1) 600-750(2) 750-2000(5)
    ELEMEN 779-874
  END SELECT
  FI="A3INT"
  STRESS TOTAL TRACTI LOCAL INTPNT
  STRESS TOTAL FORCE LOCAL INTPNT
  STRAIN TOTAL TRACTI LOCAL INTPNT
END OUTPUT
BEGIN OUTPUT FEMVIE BINARY
  BEGIN SELECT
    STEPS 1-300(1) 300-600(1) 600-750(2) 750-2000(5)
    ELEMEN 99-194
  END SELECT
  FI="A3MOM"
  STRESS TOTAL MOMENT LOCAL NODES
  STRESS TOTAL MOMENT LOCAL INTPNT
  STRESS TOTAL DISMOM LOCAL INTPNT
  STRESS TOTAL DISMOM LOCAL NODES
END OUTPUT
BEGIN EXECUT
  BEGIN LOAD
    BEGIN STEPS
      BEGIN EXPLIC
        SIZE 1.0(1)
        :   ARCLLEN UPDATE
      END EXPLIC

```

```

END STEPS

LOADNR=1

END LOAD

BEGIN ITERAT
:  METHOD NEWTON REGULA
    METHOD SECANT BROYDE
    MAXITE=100
    BEGIN CONVER
        ENERGY CONTIN TOLCON=0.0001
        FORCE OFF
        DISPLA OFF
    END CONVER
END ITERAT

SOLVE

END EXECUT

BEGIN EXECUT

BEGIN LOAD

BEGIN STEPS

BEGIN EXPLIC
    SIZE 0.001(600)
:  ARCLEN UPDATE
    END EXPLIC

END STEPS

LOADNR=2

END LOAD

BEGIN ITERAT
:  METHOD NEWTON REGULA
    METHOD SECANT BROYDE
    MAXITE=700
    LINESE

```

```
BEGIN CONVER
:  FORCE CONTIN TOLCON 0.01 TOLABT=1E+20
:  DISPLA CONTIN TOLCON=0.01 TOLABT=1E+20
ENERGY CONTIN TOLCON=0.0001 TOLABT=1E+20
FORCE OFF
DISPLA OFF
END CONVER
END ITERAT
SOLVE
END EXECUT
*END
*END
```

## Appendix H: Mat lab files and math cad file

The following files were mat lab files helpful in the generation of the input file

### Stress-Strain curve used for generation of material input for the reinforcement

```
%%stress strain curve%%  
  
%%input  
  
% fy-yeild stress  
  
% f0.05- stress at strain 0.05  
  
% epsy- yeild strain  
  
% epsh- upper yield strain  
  
%output  
  
%hardia- values of plastic strain and hardening stress of steel  
  
% data: stresses and strains stresses in MPa  
  
clear all  
  
close all  
  
clc  
  
format short  
  
b=input('bardia(mm)=')  
  
epsy=input('epsilony=')  
  
epsh=input('epsilonh(0 or appropriate value)=')  
  
fy=input('fy (in Ksi) =')  
  
f1=input('f0.05 (in Ksi)=')  
  
es=input('Es(Ksi)=')  
  
ep=input('Ep(Ksi)=')  
  
%values in MPa  
  
fy=6.89*fy;  
  
f1=6.89*f1;  
  
Es=6.89*es;  
  
Ep=6.89*ep;  
  
%the yeild plateau can cause unstable solutions
```

```

%to prevent this we need to increase the stress value by some small value

%upper yield stress
fy2=fy+0.005;

%to prevent unstable solutions
f2=f1+0.005;

%%%%%%%%%%

%%%%%%%%%elastic strains

epse1=epsy;

epse3=f1/Es;

%needed just to extend the curve to prevent the unstable solution
epse4=f2/Es;

%%%%%%%%%plastic strains

epsp1=epsy-epse1;

epsp3=0.05-epse3;

%note epsp4 can be any value
epsp4=0.2-epse4;

%%%%%%%%%%55

if epsh==0

    %stresses after yeild stress matrix

    sigma=[fy f1 f2];

    %plastic strain matrix

    epsp=[epsp1 epsp3 epsp4];

    %[stress;plasticstrain] matrix

    hardia=[sigma' epsp']

    %for the [stress;strain] curve

    stress=[0 fy f1 f2];

    strain=[0 epsy 0.05 0.2];

else

    %elastic strain

    epse2=fy2/Es;

```

```

%%%%%%%%%%

%plastic strain
epsp2=epsh-epse2;

%plastic strain matrix
epsp=[epsp1 epsp2 epsp3 epsp4];

%stresses after yeild stress matrix
sigma=[fy fy2 f1 f2];

%[stress;plasticstrain] matrix
hardia=[sigma' epsp']

%for the [stress;strain] curve
stress=[0 fy fy2 f1 f2];
strain=[0 epsy epsh 0.05 .2];

end

%%%%%%%%%%

Es_Mpa=Es
Ep_Mpa=Ep
data=[stress' strain']
figure(1)
plot(epsp,sigma,'r*--')
xlabel('plastic \epsilon')
ylabel('\sigma (MPa)')
if b==10
    title('\sigma vs plastic \epsilon 10M rebar')
elseif b==15
    title('\sigma vs plastic \epsilon 15M rebar')
elseif b==20
    title('\sigma vs plastic \epsilon 20M rebar')
elseif b==25
    title('\sigma vs plastic \epsilon 25M rebar')
else

```

```

        title(' \sigma vs plastic \epsilon ')
end
grid on
figure(2)
plot(strain,stress,'-*)
xlabel('\epsilon')
ylabel('\sigma (MPa)')
if b==10
    title(' \sigma vs \epsilon 10M rebar')
elseif b==15
    title(' \sigma vs \epsilon 15M rebar')
elseif b==20
    title(' \sigma vs \epsilon 20M rebar')
elseif b==25
    title(' \sigma vs \epsilon 25M rebar')
else
    title(' \sigma vs plastic \epsilon ')
end
grid on

```

**File used for find the value of Umax, Umin, Vmax, Vmin used in the batch file and to find out the name of the lines to be split or the points at which supports for the model should be created.**

```

clear all
close all
y=input('number of grids =');
z=input('no: of grids even or odd if even mention 1 else 0');
s=input('grid spacing=')
if z==0
    x=((y-1)/2)+1;
    lno1=4+3*(x-2)+1;

```

```

Ino2=(4+(3*(y-1)))x-(yx(x-1));

a=y*s-0.001;

b=y*s+0.001;

p.linenum1=Ino1;

p.linenum2=Ino2;

p.uminvmin=a;

p.umaxvmax=b;

elseif z==1

x=y/2+1;

Ino1=y+1;

Ino2=(y+1)x

p.pointnumber1=Ino1;

p.pointnumber2=Ino2;

a=y*s-0.001;

b=y*s+0.001;

p.uminvmin=a;

p.umaxvmax=b;

else

disp('error')

end

p

```

Math cad file used for calculating the values of material properties for the weakened element used in the verification of the model

$$\text{percentageofchange} := 90\%$$

$$\text{fctm} := 2.98 \text{ MPa}$$

$$\text{fck} := 10 \text{ MPa}$$

$$\Delta f := 8 \text{ MPa}$$

$$\text{fctk} := 1.8 \text{ MPa}$$

$$\text{Gf0} := 0.025 \frac{\text{N}}{\text{mm}}$$

$$\text{fcm0} := 10 \text{ MPa}$$

$$\text{Ec0} := 2.15 \times 10^4 \text{ MPa}$$

$$p := \text{percentageofchange}$$

$$\text{fct} := p \cdot \text{fctm}$$

$$\text{fcm} := (\text{fck} + \Delta f) \cdot \left( \frac{\text{fct}}{\text{fctk}} \right)^{\frac{1}{6}}$$

$$\text{Gf} := \text{Gf0} \left( \frac{\text{fcm}}{\text{fcm0}} \right)^{0.7}$$

$$\text{Eci} := \text{Ec0} \left( \frac{\text{fcm}}{\text{fcm0}} \right)^{\frac{1}{3}}$$

$$\text{fct} = 2.682 \times 10^6 \text{ Pa}$$

$$\text{fcm} = 3.499 \times 10^7 \text{ Pa}$$

$$\text{Eci} = 3.264 \times 10^{10} \text{ Pa}$$

$$\text{Gf} = 60.073 \frac{\text{N}}{\text{m}^2}$$

# Appendix I: Bond – slip curve data

The bond slip curve used in the project were based on the values for Confined good bond conditions

Input	<table border="1"> <tr> <td>f<sub>cm</sub></td> <td>41,6 Mpa or N/mm<sup>2</sup></td> </tr> <tr> <td>clear rib spacing of the bars</td> <td>5 mm</td> </tr> <tr> <td>f<sub>ck</sub></td> <td>33,6 Mpa or N/mm<sup>2</sup></td> </tr> </table>	f <sub>cm</sub>	41,6 Mpa or N/mm <sup>2</sup>	clear rib spacing of the bars	5 mm	f <sub>ck</sub>	33,6 Mpa or N/mm <sup>2</sup>	f <sub>ck</sub> =f <sub>cm</sub> -8(Mpa) according to Table3.1 EN1992-1-1:2003
f <sub>cm</sub>	41,6 Mpa or N/mm <sup>2</sup>							
clear rib spacing of the bars	5 mm							
f <sub>ck</sub>	33,6 Mpa or N/mm <sup>2</sup>							

Note!! the slip values are given in mm and the traction values are in Mpa

	Unconfined Concrete		Confined Concrete	
	Good bond conditions	All other bond conditions	Good Bond condition	All other bond conditions
s1	0,600	0,600	1,000	1,000
s2	0,600	0,600	3,000	3,000
s3	1,000	2,500	5,000	5,000
α	0,400	0,400	0,400	0,400
r <sub>max</sub>	11,593	5,797	14,491	7,246
r <sub>f</sub>	1,739	0,869	5,797	2,898

RIBBED BARS					
slip	Unconfined Concrete		Confined Concrete		
	Good Bond condition bond stress	All other bond conditions bond stress	Good Bond condition bond stress	All other bond conditions bond stress	
0,000	0,000	0,000	0,000	0,000	0,000
0,100	5,662	2,831	5,769	2,885	2,885
0,200	7,471	3,735	7,612	3,806	3,806
0,300	8,786	4,393	8,953	4,476	4,476
0,400	9,857	4,929	10,045	5,022	5,022
0,500	10,778	5,369	10,982	5,491	5,491
0,600	11,593	5,797	11,813	5,907	5,907
0,700	9,130	5,537	12,665	6,282	6,282
0,800	6,666	5,278	13,254	6,627	6,627
0,900	4,202	5,019	13,893	6,947	6,947
1,000	1,739	4,759	14,491	7,246	7,246
1,100	1,739	4,500	14,491	7,246	7,246
1,200	1,739	4,241	14,491	7,246	7,246
1,300	1,739	3,981	14,491	7,246	7,246
1,400	1,739	3,722	14,491	7,246	7,246
1,500	1,739	3,463	14,491	7,246	7,246
1,600	1,739	3,203	14,491	7,246	7,246
1,700	1,739	2,944	14,491	7,246	7,246
1,800	1,739	2,685	14,491	7,246	7,246
1,900	1,739	2,425	14,491	7,246	7,246
2,000	1,739	2,166	14,491	7,246	7,246
2,100	1,739	1,907	14,491	7,246	7,246
2,200	1,739	1,647	14,491	7,246	7,246
2,300	1,739	1,388	14,491	7,246	7,246
2,400	1,739	1,129	14,491	7,246	7,246
2,500	1,739	0,869	14,491	7,246	7,246
2,600	1,739	0,869	14,491	7,246	7,246
2,700	1,739	0,869	14,491	7,246	7,246
2,800	1,739	0,869	14,491	7,246	7,246
2,900	1,739	0,869	14,491	7,246	7,246
3,000	1,739	0,869	14,491	7,246	7,246
3,100	1,739	0,869	14,057	7,028	7,028
3,200	1,739	0,869	13,622	6,811	6,811
3,300	1,739	0,869	13,187	6,594	6,594
3,400	1,739	0,869	12,752	6,376	6,376
3,500	1,739	0,869	12,318	6,159	6,159
3,600	1,739	0,869	11,883	5,941	5,941
3,700	1,739	0,869	11,448	5,724	5,724
3,800	1,739	0,869	11,013	5,507	5,507
3,900	1,739	0,869	10,579	5,289	5,289
4,000	1,739	0,869	10,144	5,072	5,072
4,100	1,739	0,869	9,709	4,855	4,855
4,200	1,739	0,869	9,274	4,637	4,637
4,300	1,739	0,869	8,840	4,420	4,420
4,400	1,739	0,869	8,405	4,202	4,202
4,500	1,739	0,869	7,970	3,985	3,985
4,600	1,739	0,869	7,536	3,768	3,768
4,700	1,739	0,869	7,101	3,550	3,550
4,800	1,739	0,869	6,666	3,333	3,333
4,900	1,739	0,869	6,231	3,116	3,116
5,000	1,739	0,869	5,797	2,898	2,898
5,100	1,739	0,869	5,797	2,898	2,898
5,200	1,739	0,869	5,797	2,898	2,898
5,300	1,739	0,869	5,797	2,898	2,898
5,400	1,739	0,869	5,797	2,898	2,898
5,500	1,739	0,869	5,797	2,898	2,898
5,600	1,739	0,869	5,797	2,898	2,898

## Appendix J: Loading Beam system

The loading beam system was checked before it was used for loading the model. The ends of the beam system were connected to the truss elements which enabled the check of the 'fix' tying possible. Some of the truss elements were oriented in the y direction and some in the x direction so that when the trusses are loaded using the fix tying which connects the movements of the ends of the beam system in the y direction to the movement of the trusses in their corresponding direction of orientation.

### INPUT FILE

: Fulcrum points (means the points from which the beam is suspended or connected to: the endpoints of the beam at an immediate high level.

: The fulcrum points of the beams are based on the amount of reaction force that has : : to be transferred to the two end points

:level 1

10003 1.050000E+01 -1.000000E-01

10008 1.050000E+01 -2.000000E-01

10013 1.050000E+01 -3.000000E-01

10018 1.050000E+01 -4.000000E-01

:level2

20003 1.050000E+01 -5.000000E-01

20008 1.050000E+01 -6.000000E-01

“ “ “

“ “ “

“ “ “

20233 1.050000E+01 -5.100000E+00

20238 1.050000E+01 -5.200000E+00

:level 3

30003 1.050000E+01 -5.300000E+00

30008 1.050000E+01 -5.400000E+00

“ “ “

“ “ “

“ “ “

30113 1.050000E+01 -7.500000E+00

30118 1.050000E+01 -7.600000E+00

:level 4

40003 1.050000E+01 -7.700000E+00

40008 1.050000E+01 -7.800000E+00

“ “ “

“ “ “

“ “ “

40053 1.050000E+01 -8.700000E+00

40058 1.050000E+01 -8.800000E+00

:level 5

50003 1.050000E+01 -8.900000E+00

50008 1.050000E+01 -9.000000E+00

“ “ “

“ “ “

“ “ “

50023 1.050000E+01 -9.300000E+00

50028 1.050000E+01 -9.400000E+00

:level 6

60003 1.050000E+01 -9.500000E+00

“ “ “

“ “ “

60013 1.050000E+01 -9.700000E+00

:level 7

70003 1.050000E+01 -9.800000E+00

:level 8

80003 1.033333E+01 -9.900000E+00

:start points of each beam

: first level

10001 1.000000E+01 -1.000000E-01

10006 1.000000E+01 -2.000000E-01

10011 1.000000E+01 -3.000000E-01

10016	1.000000E+01	-4.000000E-01
: second level		
20001	1.000000E+01	-5.000000E-01
20006	1.000000E+01	-6.000000E-01
“	“	“
“	“	“
“	“	“
20226	1.000000E+01	-5.000000E+00
20231	1.000000E+01	-5.100000E+00
20236	1.000000E+01	-5.200000E+00
:third level		
30001	1.000000E+01	-5.300000E+00
30006	1.000000E+01	-5.400000E+00
“	“	“
“	“	“
“	“	“
30106	1.000000E+01	-7.400000E+00
30111	1.000000E+01	-7.500000E+00
30116	1.000000E+01	-7.600000E+00
:fourth level		
40001	1.000000E+01	-7.700000E+00
40006	1.000000E+01	-7.800000E+00
“	“	“
“	“	“
“	“	“
40051	1.000000E+01	-8.700000E+00
40056	1.000000E+01	-8.800000E+00
:fifth level		
50001	1.000000E+01	-8.900000E+00
50006	1.000000E+01	-9.000000E+00

“	“	“
“	“	“
“	“	“
50021	1.000000E+01	-9.300000E+00
50026	1.000000E+01	-9.400000E+00
:sixth level		
60001	1.000000E+01	-9.500000E+00
60006	1.000000E+01	-9.600000E+00
60011	1.000000E+01	-9.700000E+00
:seventh level		
70001	1.000000E+01	-9.800000E+00
.eighth level		
80001	1.000000E+01	-9.900000E+00
:end points of the beam		
:first level		
10005	1.100000E+01	-1.000000E-01
10010	1.100000E+01	-2.000000E-01
10015	1.100000E+01	-3.000000E-01
10020	1.100000E+01	-4.000000E-01
:second level		
20005	1.100000E+01	-5.000000E-01
20010	1.100000E+01	-6.000000E-01
“	“	“
“	“	“
“	“	“
20235	1.100000E+01	-5.100000E+00
20240	1.100000E+01	-5.200000E+00
:third level		
30005	1.100000E+01	-5.300000E+00

30010	1.100000E+01	-5.400000E+00
“	“	“
“	“	“
“	“	“
30115	1.100000E+01	-7.500000E+00
30120	1.100000E+01	-7.600000E+00
:fourth level		
40005	1.100000E+01	-7.700000E+00
40010	1.100000E+01	-7.800000E+00
“	“	“
“	“	“
“	“	“
40055	1.100000E+01	-8.700000E+00
40060	1.100000E+01	-8.800000E+00
:fifth level		
50005	1.100000E+01	-8.900000E+00
50010	1.100000E+01	-9.000000E+00
“	“	“
“	“	“
“	“	“
50025	1.100000E+01	-9.300000E+00
50030	1.100000E+01	-9.400000E+00
:sixth level		
60005	1.100000E+01	-9.500000E+00
60010	1.100000E+01	-9.600000E+00
60015	1.100000E+01	-9.700000E+00
:seventh level		
70005	1.100000E+01	-9.800000E+00
: eighth level		
80005	1.100000E+01	-9.900000E+00

:first mid points

:first level

10002 1.025000E+01 -1.000000E-01

10007 1.025000E+01 -2.000000E-01

10012 1.025000E+01 -3.000000E-01

10017 1.025000E+01 -4.000000E-01

:second level

20002 1.025000E+01 -5.000000E-01

20007 1.025000E+01 -6.000000E-01

20012 1.025000E+01 -7.000000E-01

“ “ “

“ “ “

“ “ “

20227 1.025000E+01 -5.000000E+00

20232 1.025000E+01 -5.100000E+00

20237 1.025000E+01 -5.200000E+00

:third level

30002 1.025000E+01 -5.300000E+00

30007 1.025000E+01 -5.400000E+00

“ “ “

“ “ “

“ “ “

30112 1.025000E+01 -7.500000E+00

30117 1.025000E+01 -7.600000E+00

:fourth level

40002 1.025000E+01 -7.700000E+00

40007 1.025000E+01 -7.800000E+00

“ “ “

“ “ “

“ “ “

40052	1.025000E+01	-8.700000E+00
40057	1.025000E+01	-8.800000E+00
:fifth level		
50002	1.025000E+01	-8.900000E+00
50007	1.025000E+01	-9.000000E+00
“	“	“
“	“	“
“	“	“
50022	1.025000E+01	-9.300000E+00
50027	1.025000E+01	-9.400000E+00
:sixth level		
60002	1.025000E+01	-9.500000E+00
60007	1.025000E+01	-9.600000E+00
60012	1.025000E+01	-9.700000E+00
:seventh level		
70002	1.025000E+01	-9.800000E+00
: eighth level		
80002	1.016667E+01	-9.900000E+00
:second midpoints		
:first level		
10004	1.075000E+01	-1.000000E-01
10009	1.075000E+01	-2.000000E-01
10014	1.075000E+01	-3.000000E-01
10019	1.075000E+01	-4.000000E-01
:second level		
20004	1.075000E+01	-5.000000E-01
20009	1.075000E+01	-6.000000E-01
20014	1.075000E+01	-7.000000E-01
“	“	“
“	“	“

	“	“	“
20229	1.075000E+01	-5.000000E+00	
20234	1.075000E+01	-5.100000E+00	
20239	1.075000E+01	-5.200000E+00	
:third level			
30004	1.075000E+01	-5.300000E+00	
30009	1.075000E+01	-5.400000E+00	
	“	“	“
	“	“	“
	“	“	“
30114	1.075000E+01	-7.500000E+00	
30119	1.075000E+01	-7.600000E+00	
:fourth level			
40004	1.075000E+01	-7.700000E+00	
40009	1.075000E+01	-7.800000E+00	
	“	“	“
	“	“	“
	“	“	“
40054	1.075000E+01	-8.700000E+00	
40059	1.075000E+01	-8.800000E+00	
:fifth level			
50004	1.075000E+01	-8.900000E+00	
50009	1.075000E+01	-9.000000E+00	
	“	“	“
	“	“	“
	“	“	“
50024	1.075000E+01	-9.300000E+00	
50029	1.075000E+01	-9.400000E+00	
:sixth level			
60004	1.075000E+01	-9.500000E+00	

60009 1.075000E+01 -9.600000E+00

60014 1.075000E+01 -9.700000E+00

:seventh level

70004 1.075000E+01 -9.800000E+00

:eighth level

80004 1.066667E+01 -9.900000E+00

:nodes for truss elements to check the load distribution

: nodes for trusses oriented in the x direction

1 0,000000E+00 0,000000E+00

2 0,000000E+00 2,000000E-01

3 0,000000E+00 4,000000E-01

4 0,000000E+00 6,000000E-01

“ “ “

“ “ “

47 0,000000E+00 9,200000E+00

48 0,000000E+00 9,400000E+00

49 0,000000E+00 9,600000E+00

50 0,000000E+00 9,800000E+00

: nodes for trusses oriented in the y direction

51 3,000000E+00 0,000000E+00

52 3,200000E+00 0,000000E+00

53 3,400000E+00 0,000000E+00

54 3,600000E+00 0,000000E+00

55 3,800000E+00 0,000000E+00

“ “ “

“ “ “

“ “ “

196 1,200000E+01 1,000000E+00

197 1,220000E+01 1,000000E+00

198 1,240000E+01 1,000000E+00

199 1,260000E+01 1,000000E+00  
200 1,280000E+01 1,000000E+00

: Elements for the beam system

:first half of the beam

:first level

10001	CL9BE	10001	10002	10003
10006	CL9BE	10006	10007	10008
10011	CL9BE	10011	10012	10013
10016	CL9BE	10016	10017	10018

:second level

20001	CL9BE	20001	20002	20003
20006	CL9BE	20006	20007	20008
20011	CL9BE	20011	20012	20013
20016	CL9BE	20016	20017	20018
20021	CL9BE	20021	20022	20023
“	“	“		
“	“	“		
“	“	“		
20226	CL9BE	20226	20227	20228
20231	CL9BE	20231	20232	20233
20236	CL9BE	20236	20237	20238

:third level

30001	CL9BE	30001	30002	30003
30006	CL9BE	30006	30007	30008
30011	CL9BE	30011	30012	30013
“	“	“		
“	“	“		
“	“	“		
30106	CL9BE	30106	30107	30108
30111	CL9BE	30111	30112	30113

30116	CL9BE	30116	30117	30118
:fourth level				
40001	CL9BE	40001	40002	40003
40006	CL9BE	40006	40007	40008
40011	CL9BE	40011	40012	40013
“	“	“		
“	“	“		
“	“	“		
40046	CL9BE	40046	40047	40048
40051	CL9BE	40051	40052	40053
40056	CL9BE	40056	40057	40058
:fifth level				
50001	CL9BE	50001	50002	50003
50006	CL9BE	50006	50007	50008
“	“	“		
“	“	“		
“	“	“		
50021	CL9BE	50021	50022	50023
50026	CL9BE	50026	50027	50028
:sixth level				
60001	CL9BE	60001	60002	60003
60006	CL9BE	60006	60007	60008
60011	CL9BE	60011	60012	60013
:seventh level				
70001	CL9BE	70001	70002	70003
:eighth level				
80001	CL9BE	80001	80002	80003
:second half beam				
:first level				
10002	CL9BE	10003	10004	10005

10007	CL9BE	10008	10009	10010
10012	CL9BE	10013	10014	10015
10017	CL9BE	10018	10019	10020
:second level				
20002	CL9BE	20003	20004	20005
20007	CL9BE	20008	20009	20010
20012	CL9BE	20013	20014	20015
“	“	“		
“	“	“		
“	“	“		
20232	CL9BE	20233	20234	20235
20237	CL9BE	20238	20239	20240
:third level				
30002	CL9BE	30003	30004	30005
30007	CL9BE	30008	30009	30010
“	“	“		
“	“	“		
“	“	“		
30112	CL9BE	30113	30114	30115
30117	CL9BE	30118	30119	30120
:fourth level				
40002	CL9BE	40003	40004	40005
40007	CL9BE	40008	40009	40010
“	“	“		
“	“	“		
“	“	“		
40052	CL9BE	40053	40054	40055
40057	CL9BE	40058	40059	40060
:fifth level				
50002	CL9BE	50003	50004	50005

50007	CL9BE	50008	50009	50010
50012	CL9BE	50013	50014	50015
50017	CL9BE	50018	50019	50020
50022	CL9BE	50023	50024	50025
50027	CL9BE	50028	50029	50030

Sixth level

60002	CL9BE	60003	60004	60005
60007	CL9BE	60008	60009	60010
60012	CL9BE	60013	60014	60015

seventh level

70002	CL9BE	70003	70004	70005
-------	-------	-------	-------	-------

eighth level

80002	CL9BE	80003	80004	80005
-------	-------	-------	-------	-------

truss elements to check the load distribution

1	L2TRU	1	101
2	L2TRU	2	102
3	L2TRU	3	103
4	L2TRU	4	104
5	L2TRU	5	105
6	L2TRU	6	106
“	“	“	“
“	“	“	“
“	“	“	“
95	L2TRU	95	195
96	L2TRU	96	196
97	L2TRU	97	197
98	L2TRU	98	198
99	L2TRU	99	199
100	L2TRU	100	200

:TYINGS

: Within the beam system

EQUAL TR 2

10003 20001

10013 20006

20003 30001

20013 30006

20023 30011

20033 30016

20043 30021

20053 30026

20063 30031

20073 30036

20083 30041

20093 30046

20103 30051

20113 30056

20123 30061

20133 30066

20143 30071

20153 30076

20163 30081

20173 30086

20183 30091

20193 30096

20203 30101

20213 30106

20223 30111

20233 30116

30003 40001

30013 40006  
30023 40011  
30033 40016  
30043 40021  
30053 40026  
30063 40031  
30073 40036  
30083 40041  
30093 40046  
30103 40051  
30113 40056  
40003 50001  
40013 50006  
40023 50011  
40033 50016  
40043 50021  
40053 50026  
50003 60001  
50013 60006  
50023 60011  
60003 70001  
70003 80001  
10008 20005  
10018 20010  
20008 30005  
20018 30010  
20028 30015  
20038 30020  
20048 30025  
20058 30030

20068 30035  
20078 30040  
20088 30045  
20098 30050  
20108 30055  
20118 30060  
20128 30065  
20138 30070  
20148 30075  
20158 30080  
20168 30085  
20178 30090  
20188 30095  
20198 30100  
20208 30105  
20218 30110  
20228 30115  
20238 30120  
30008 40005  
30018 40010  
30028 40015  
30038 40020  
30048 40025  
30058 40030  
30068 40035  
30078 40040  
30088 40045  
30098 40050  
30108 40055  
30118 40060

40008 50005  
40018 50010  
40028 50015  
40038 50020  
40048 50025  
40058 50030  
50008 60005  
50018 60010  
50028 60015  
60008 70005  
60013 80005

:note that the groups were created as follows

:SPOINTS- contain the start points of all the beams

: LPOINT- is the loading point for the beam system where the prescribed deformation is applied

:HLYINGTOP- start points of the truss elements oriented along the x direction

:HLYINGBOT – end points of the truss elements oriented along the x direction

:VLYINGTOP- start points of the truss elements oriented along the y direction

:VLYINGBOT- end points of the truss elements oriented along the y direction

'SUPPORTS'

/ SPOINTS / TR 1

/ LPOINT / TR 1 2

/ HLYINGTOP / TR 2

/ HLYINGBOT / TR 1 2

/ VLYINGTOP / TR 1

/ VLYINGBOT / TR 1 2

: To the structure

FIX TR 1

Connection between the beam system and the trusses oriented in the x direction

1 1001 TR 2 -1

2 1006 TR 2 -1

3	1011	TR 2 1
4	1016	TR 2 1
FIX TR 1		
5	1005	TR 2 -1
6	1010	TR 2 -1
7	1015	TR 2 -1
8	1020	TR 2 -1
9	2011	TR 2 -1
10	2016	TR 2 -1
11	2021	TR 2 -1
12	2026	TR 2 -1
13	2031	TR 2 -1
14	2036	TR 2 -1
15	2041	TR 2 -1
16	2046	TR 2 -1
17	2051	TR 2 -1
18	2056	TR 2 -1
19	2061	TR 2 -1
20	2066	TR 2 -1
21	2071	TR 2 -1
22	2076	TR 2 -1
23	2081	TR 2 -1
24	2086	TR 2 -1
25	2091	TR 2 -1
26	2096	TR 2 1
27	2101	TR 2 1
28	2106	TR 2 1
29	2111	TR 2 1
30	2116	TR 2 1
31	2121	TR 2 1

32	2126	TR 2 1
33	2131	TR 2 1
34	2136	TR 2 1
35	2141	TR 2 1
36	2146	TR 2 1
37	2151	TR 2 1
38	2156	TR 2 1
39	2161	TR 2 1
40	2166	TR 2 1
41	2171	TR 2 1
42	2176	TR 2 1
43	2181	TR 2 1
44	2186	TR 2 1
45	2191	TR 2 1
46	2196	TR 2 1
47	2201	TR 2 1
48	2206	TR 2 1
49	2211	TR 2 1
50	2216	TR 2 1

: Connection between the beam system and the trusses oriented in the y direction

FIX TR 2

51	2221	TR 2 -1
52	2226	TR 2 -1
53	2231	TR 2 -1
54	2236	TR 2 -1
55	2015	TR 2 -1
56	2020	TR 2 -1
57	2025	TR 2 -1
58	2030	TR 2 -1
59	2035	TR 2 -1

60	2040	TR 2 -1
61	2045	TR 2 -1
62	2050	TR 2 -1
63	2055	TR 2 -1
64	2060	TR 2 -1
65	2065	TR 2 -1
66	2070	TR 2 -1
67	2075	TR 2 -1
68	2080	TR 2 -1
69	2085	TR 2 -1
70	2090	TR 2 -1
71	2095	TR 2 -1
72	2100	TR 2 -1
73	2105	TR 2 -1
74	2110	TR 2 -1
75	2115	TR 2 -1
76	2120	TR 2 1
77	2125	TR 2 1
78	2130	TR 2 1
79	2135	TR 2 1
80	2140	TR 2 1
81	2145	TR 2 1
82	2150	TR 2 1
83	2155	TR 2 1
84	2160	TR 2 1
85	2165	TR 2 1
86	2170	TR 2 1
87	2175	TR 2 1
88	2180	TR 2 1
89	2185	TR 2 1

90	2190	TR 2 1
91	2195	TR 2 1
92	2200	TR 2 1
93	2205	TR 2 1
94	2210	TR 2 1
95	2215	TR 2 1
96	2220	TR 2 1
97	2225	TR 2 1
98	2230	TR 2 1
99	2235	TR 2 1
100	2240	TR 2 1

:application of prescribed deformation

'LOADS'

CASE 1

DEFORM

/ LPOINT / TR 2 1E-3

:direction of the axes

'DIRECTIONS'

1	1,000000E+00	0,000000E+00	0,000000E+00
2	0,000000E+00	1,000000E+00	0,000000E+00
3	0,000000E+00	0,000000E+00	1,000000E+00

'END'

The next page contains the load factors and the distance of the fulcrum points from the left end of the beams and the results of the check of the beam system. Note that the values of product of Load factor and Reaction force at each beam end may have negligible variation this was due to the fact of rounding up the values while processing the data obtained from Diana. The values of the product of the reaction force and load factor should be equal to residual force at the loading point i.e. at node 80003



Number of beams	Fulcrum distance from left side								
1	1/2	1/2	1/2	1/2	1/2	1/2	1/2	1/2	1/3
2	1/2	1/2	1/2	1/2	1/2	1/2	1/2	1/2	
3	1/2	1/2	1/2	1/2	1/2	1/2	1/2	1/2	
4	1/2	1/2	1/2	1/2	1/2	1/2	1/2		
5	1/2	1/2	1/2	1/2	1/2	1/2	1/2		
6	1/2	1/2	1/2	1/2	1/2	1/2	1/2		
7	1/2	1/2	1/2	1/2	1/2	1/2			
8	1/2	1/2	1/2	1/2	1/2				
9	1/2	1/2	1/2	1/2					
10	1/2	1/2	1/2	1/2					
11	1/2	1/2	1/2	1/2					
12	1/2	1/2	1/2	1/2					
13	1/2	1/2	1/2						
14	1/2	1/2	1/2						
15	1/2	1/2	1/2						
16	1/2	1/2	1/2						
17	1/2	1/2	1/2						
18	1/2	1/2	1/2						
19	1/2	1/2	1/2						
20	1/2	1/2	1/2						
21	1/2	1/2	1/2						
22	1/2	1/2	1/2						
23	1/2	1/2	1/2						
24	1/2	1/2	1/2						
25	1/2	1/2	1/2						
26	1/2	1/2	1/2						
27	1/2	1/2	1/2						
28	1/2	1/2	1/2						
29	1/2	1/2	1/2						
30	1/2	1/2	1/2						
31	1/2	1/2	1/2						
32	1/2	1/2	1/2						
33	1/2	1/2	1/2						
34	1/2	1/2	1/2						
35	1/2	1/2	1/2						
36	1/2	1/2	1/2						
37	1/2	1/2	1/2						
38	1/2	1/2	1/2						
39	1/2	1/2	1/2						
40	1/2	1/2	1/2						
41	1/2	1/2	1/2						
42	1/2	1/2	1/2						
43	1/2	1/2	1/2						
44	1/2	1/2	1/2						
45	1/2	1/2	1/2						
46	1/2	1/2	1/2						
47	1/2	1/2	1/2						
48	1/2	1/2	1/2						

```
;
; Model: BEAMSYS
; Nodal FRX,,,,G RESFRX
```

```
; Graph begins
```

Point no,	X	Y	Load in kN
0			
1	1	1,64E+07	1,64E+04
2	2	3,27E+07	3,27E+04
3	3	4,91E+07	4,91E+04
4	4	6,55E+07	6,55E+04
5	5	8,19E+07	8,19E+04
6	6	9,82E+07	9,82E+04
7	7	1,15E+08	1,15E+05
8	8	1,31E+08	1,31E+05
9	9	1,47E+08	1,47E+05
10	10	1,64E+08	1,64E+05

```
; Graph ends
```

0	1	2	3	4	5	6	7	8	9	10
1,64E+04	3,27E+04	4,91E+04	6,55E+04	8,19E+04	9,82E+04	1,15E+05	1,31E+05	1,47E+05	1,64E+05	

step truss number	xforce									
	1	2	3	4	5	6	7	8	9	10
1	-85,3	-171	-256	-341	-426	-512	-597	-682	-768	-853
2	-85,3	-171	-256	-341	-426	-512	-597	-682	-768	-853
3	85,3	171	256	341	426	512	597	682	768	853
4	85,3	171	256	341	426	512	597	682	768	853
5	171	341	512	682	853	1020	1190	1360	1540	1710
6	171	341	512	682	853	1020	1190	1360	1540	1710
7	171	341	512	682	853	1020	1190	1360	1540	1710
8	171	341	512	682	853	1020	1190	1360	1540	1710
9	171	341	512	682	853	1020	1190	1360	1540	1710
10	171	341	512	682	853	1020	1190	1360	1540	1710
11	171	341	512	682	853	1020	1190	1360	1540	1710
12	171	341	512	682	853	1020	1190	1360	1540	1710
13	171	341	512	682	853	1020	1190	1360	1540	1710
14	171	341	512	682	853	1020	1190	1360	1540	1710
15	171	341	512	682	853	1020	1190	1360	1540	1710
16	171	341	512	682	853	1020	1190	1360	1540	1710
17	171	341	512	682	853	1020	1190	1360	1540	1710
18	171	341	512	682	853	1020	1190	1360	1540	1710
19	171	341	512	682	853	1020	1190	1360	1540	1710
20	171	341	512	682	853	1020	1190	1360	1540	1710
21	171	341	512	682	853	1020	1190	1360	1540	1710
22	171	341	512	682	853	1020	1190	1360	1540	1710
23	171	341	512	682	853	1020	1190	1360	1540	1710
24	171	341	512	682	853	1020	1190	1360	1540	1710
25	171	341	512	682	853	1020	1190	1360	1540	1710
26	-171	-341	-512	-682	-853	-1020	-1190	-1360	-1540	-1710
27	-171	-341	-512	-682	-853	-1020	-1190	-1360	-1540	-1710
28	-171	-341	-512	-682	-853	-1020	-1190	-1360	-1540	-1710
29	-171	-341	-512	-682	-853	-1020	-1190	-1360	-1540	-1710
30	-171	-341	-512	-682	-853	-1020	-1190	-1360	-1540	-1710
31	-171	-341	-512	-682	-853	-1020	-1190	-1360	-1540	-1710
32	-171	-341	-512	-682	-853	-1020	-1190	-1360	-1540	-1710
33	-171	-341	-512	-682	-853	-1020	-1190	-1360	-1540	-1710
34	-171	-341	-512	-682	-853	-1020	-1190	-1360	-1540	-1710
35	-171	-341	-512	-682	-853	-1020	-1190	-1360	-1540	-1710
36	-171	-341	-512	-682	-853	-1020	-1190	-1360	-1540	-1710
37	-171	-341	-512	-682	-853	-1020	-1190	-1360	-1540	-1710
38	-171	-341	-512	-682	-853	-1020	-1190	-1360	-1540	-1710
39	-171	-341	-512	-682	-853	-1020	-1190	-1360	-1540	-1710
40	-171	-341	-512	-682	-853	-1020	-1190	-1360	-1540	-1710
41	-171	-341	-512	-682	-853	-1020	-1190	-1360	-1540	-1710
42	-171	-341	-512	-682	-853	-1020	-1190	-1360	-1540	-1710
43	-171	-341	-512	-682	-853	-1020	-1190	-1360	-1540	-1710
44	-171	-341	-512	-682	-853	-1020	-1190	-1360	-1540	-1710
45	-171	-341	-512	-682	-853	-1020	-1190	-1360	-1540	-1710
46	-171	-341	-512	-682	-853	-1020	-1190	-1360	-1540	-1710
47	-171	-341	-512	-682	-853	-1020	-1190	-1360	-1540	-1710
48	-171	-341	-512	-682	-853	-1020	-1190	-1360	-1540	-1710
49	-171	-341	-512	-682	-853	-1020	-1190	-1360	-1540	-1710
50	-171	-341	-512	-682	-853	-1020	-1190	-1360	-1540	-1710









51	-85,3	-171	-256	-341	-426	-512	-597	-682	-768	-853
52	-85,3	-171	-256	-341	-426	-512	-597	-682	-768	-853
53	85,3	171	256	341	426	512	597	682	768	853
54	85,3	171	256	341	426	512	597	682	768	853
55	171	341	512	682	853	1020	1190	1360	1540	1710
56	171	341	512	682	853	1020	1190	1360	1540	1710
57	171	341	512	682	853	1020	1190	1360	1540	1710
58	171	341	512	682	853	1020	1190	1360	1540	1710
59	171	341	512	682	853	1020	1190	1360	1540	1710
60	171	341	512	682	853	1020	1190	1360	1540	1710
61	171	341	512	682	853	1020	1190	1360	1540	1710
62	171	341	512	682	853	1020	1190	1360	1540	1710
63	171	341	512	682	853	1020	1190	1360	1540	1710
64	171	341	512	682	853	1020	1190	1360	1540	1710
65	171	341	512	682	853	1020	1190	1360	1540	1710
66	171	341	512	682	853	1020	1190	1360	1540	1710
67	171	341	512	682	853	1020	1190	1360	1540	1710
68	171	341	512	682	853	1020	1190	1360	1540	1710
69	171	341	512	682	853	1020	1190	1360	1540	1710
70	171	341	512	682	853	1020	1190	1360	1540	1710
71	171	341	512	682	853	1020	1190	1360	1540	1710
72	171	341	512	682	853	1020	1190	1360	1540	1710
73	171	341	512	682	853	1020	1190	1360	1540	1710
74	171	341	512	682	853	1020	1190	1360	1540	1710
75	171	341	512	682	853	1020	1190	1360	1540	1710
76	-171	-341	-512	-682	-853	-1020	-1190	-1360	-1540	-1710
77	-171	-341	-512	-682	-853	-1020	-1190	-1360	-1540	-1710
78	-171	-341	-512	-682	-853	-1020	-1190	-1360	-1540	-1710
79	-171	-341	-512	-682	-853	-1020	-1190	-1360	-1540	-1710
80	-171	-341	-512	-682	-853	-1020	-1190	-1360	-1540	-1710
81	-171	-341	-512	-682	-853	-1020	-1190	-1360	-1540	-1710
82	-171	-341	-512	-682	-853	-1020	-1190	-1360	-1540	-1710
83	-171	-341	-512	-682	-853	-1020	-1190	-1360	-1540	-1710
84	-171	-341	-512	-682	-853	-1020	-1190	-1360	-1540	-1710
85	-171	-341	-512	-682	-853	-1020	-1190	-1360	-1540	-1710
86	-171	-341	-512	-682	-853	-1020	-1190	-1360	-1540	-1710
87	-171	-341	-512	-682	-853	-1020	-1190	-1360	-1540	-1710
88	-171	-341	-512	-682	-853	-1020	-1190	-1360	-1540	-1710
89	-171	-341	-512	-682	-853	-1020	-1190	-1360	-1540	-1710
90	-171	-341	-512	-682	-853	-1020	-1190	-1360	-1540	-1710
91	-171	-341	-512	-682	-853	-1020	-1190	-1360	-1540	-1710
92	-171	-341	-512	-682	-853	-1020	-1190	-1360	-1540	-1710
93	-171	-341	-512	-682	-853	-1020	-1190	-1360	-1540	-1710
94	-171	-341	-512	-682	-853	-1020	-1190	-1360	-1540	-1710
95	-171	-341	-512	-682	-853	-1020	-1190	-1360	-1540	-1710
96	-171	-341	-512	-682	-853	-1020	-1190	-1360	-1540	-1710
97	-171	-341	-512	-682	-853	-1020	-1190	-1360	-1540	-1710
98	-171	-341	-512	-682	-853	-1020	-1190	-1360	-1540	-1710
99	-171	-341	-512	-682	-853	-1020	-1190	-1360	-1540	-1710
100	-171	-341	-512	-682	-853	-1020	-1190	-1360	-1540	-1710



